The Thesis Committee for Abhinav Sharma
Certifies that this is the approved version of the following thesis:

Assessment of Polymer Injectivity during Chemical Enhanced Oil Recovery Processes

APPROVED BY
SUPERVISING COMMITTEE:

Supervisor:

Gary Pope, Supervisor

Mojdeh Delshad, Co-Supervisor

Chun Huh, Co-Supervisor

Assessment of Polymer Injectivity during Chemical Enhanced Oil Recovery Processes

by

Abhinav Sharma, B.E.

Thesis

Presented to the Faculty of the Graduate School of

The University of Texas at Austin

in Partial Fulfillment

of the Requirements

for the Degree of

Master of Science in Engineering

The University of Texas at Austin

December 2010

Dedication

To my ever loving and devoting parents and my brother

Acknowledgements

I will always remain grateful to the Department of Petroleum and Geosystems Engineering at the University of Texas at Austin for giving me this unique opportunity to study and learn at this prestigious institution. I would like to thank my advisors Dr. Mojdeh Delshad, Dr. Gary Pope and Dr. Chun Huh for their guidance and encouragement during the course of this research. Under their supervision, I have gained extensive technical knowledge and developed valuable professional skills which will help me in all walks of life ahead.

I am extremely thankful to Dr. Chrissi King for her support and valuable suggestions during this research. I am also grateful to Dr. Do Hoon Kim for providing me with the updated laboratory data. I am also grateful for the financial support provided by the industrial sponsors of the chemical EOR research in the Center for Petroleum and Geosystems Engineering at the University of Texas at Austin, for the opportunity to serve as a summer intern with Rex Energy and for their permission to use valuable data from their ongoing field pilot.

I would like to thank my colleagues for their insightful discussions and suggestions, namely - Faiz Veedu, Vikram Chandrasekar, Ahra Lee, Nitish Koduru, Vinay Sahni, Hyuntae Yang, Dr. Hourshad Mohammadi and Dr. Ali Farhadinia. I would also like to thank Sahil Malhotra, Abhishek Goel, Furqan Gilani, Naveed Arsalan, Hariharan Ramachandran and Himanshu Yadav for their friendship.

Finally, I would like to thank my parents and my brother for their unconditional love. Without their support this could not have been possible.

December 2010

Abstract

Assessment of Polymer Injectivity during Chemical Enhanced Oil Recovery Processes

Abhinav Sharma, M.S.E.

The University of Texas at Austin, 2010

Supervisor: Gary A. Pope, Mojdeh Delshad and Chun Huh.

Polymers play a key role in several EOR processes such as polymer flooding, surfactant-polymer flooding and alkaline-surfactant-polymer flooding due to their critical importance of mobility control in achieving high oil recovery from these processes. Numerical simulators are used to predict the performance of all of these processes and in particular the injection rate of the chemical solutions containing polymer; since the economics is very sensitive to the injection rates. Injection rates are governed by the injection viscosity, thus, it is very important to model the polymer viscosity accurately. For the predictions to be accurate, not only the viscosity model must be accurate, but also the calculation of equivalent shear rate in each gridblock must be accurate because the non-Newtonian viscosity models depend on this shear rate. As the size of the gridblock increases, the calculation of this velocity becomes less numerically accurate, especially close to wells.

This research presents improvements in polymer viscosity model. Using the improvements in shear thinning model, the laboratory polymer rheology data was better matched. For the first time, polymer viscosity was modeled for complete range of velocity using the Unified Viscosity Model for published laboratory data. New models were developed for relaxation time, time constant and high shear viscosity during that match. These models were then used to match currently available HPAM polymer's laboratory data and predict its viscosity for various concentrations for full flow velocity range.

This research presents the need for injectivity correction when large grid sizes are used. Use of large grid sizes to simulate large reservoir due to computation constraints induces errors in shear rate calculations near the wellbore and underestimate polymer solution viscosity. Underestimated polymer solution viscosities lead to incorrect injectivity calculation. In some cases, depending on the well grid block size, this difference between a fine scale and a coarse simulation could be as much as 100%. This study focuses on minimizing those errors. This methodology although needs some more work, but can be used in accurate predictions of reservoir simulation studies of chemical enhanced oil recovery processes involving polymers.

Table of Contents

List of Tables

List of Figures

1 Introduction and Literature Review

Polymers play a key role in several EOR processes such as polymer flooding, surfactant-polymer flooding and alkaline-surfactant-polymer flooding due to the critical importance of mobility control in achieving high oil recovery from these processes. Polymer injection is generally carried as a tertiary flood as polymer flood or as surfactant polymer flood. Addition of water soluble polymer increases its viscosity, hence, decreases the mobility ratio.

Numerical simulators are used to predict the performance of the process. To accurately predict the field scale performance polymer rheology needs to be accounted accurately. This study focuses on improvements in modeling of polymer rheology, both shear thinning and shear thickening. A better fit to the laboratory data was obtained after those improvements. Later, those improvements were incorporated in UTCHEM.

In a chemical EOR process, the cost of chemicals account for major part of the expenses. Injectivity of chemicals like polymer is another important aspect for any field scale project as it drives the economics. Predicting the injectivity correctly is imperative for any projects success. Due to computational constraints, using large grid sizes to simulate large reservoirs is common in the petroleum industry. If the reservoir is heterogeneous, then the petrophysical properties are upscaled. However, even in a homogeneous reservoir model, just due to the use of large grid sizes, errors are introduced in flux calculations at the well grid block in comparison to a fine scale simulation. This generates erroneous shear rate and hence, incorrect viscosities at the well block. Erroneous viscosities lead to incorrect injectivity calculation. In some cases, depending on the well grid block size, this difference between a fine scale and a coarse simulation could be as much as 100%. This research presents a practical approach to

calculate the correct shear rate at the well block when large well grid sizes are used and hence, the correct injectivity.

Before presenting the research discussed above, the literature review on the topic is presented below.

1.1 CHEMICAL ENHANCED OIL RECOVERY

After the acceptance of waterflooding in the 1950's it became apparent that the displacement of oil by water was often detrimentally affected by heterogeneity and poor mobility ratio. Water soluble polymers were added in 1960's to the injection water to improve mobility ratio, improve areal sweep and fractional flow [Pope, 1980]. Later, chemicals like surfactants and alkali were added to mobilize the trapped oil.

Polymers are used for mobility control purposes not only in polymer flooding but also in other chemical floods like surfactant-polymer (SP) and alkali-surfactant-polymer floods etc. In the SP floods, as surfactants decrease the entry capillary pressure, they tend to finger. High molecular weight polymers like the hydrolyzed polyacrlamide polymer (HPAM) are used to maintain good mobility control. Polymers help to prevent fingering, channeling, and increase the sweep efficiency in heterogeneous reservoirs. [Sorbie,1991] This research focuses on the polymer flooding as a chemical enhanced oil recovery technique.

Polymer flooding has been applied commercially all around the world since about 4 decades. The economic viability of well designed polymer has been demonstrated earlier. Daqing (2002) and Chateaurenard (1988) are examples of large scale field polymer injection projects. A cumulative of over 300 million barrels of oil was produced during polymer flooding. Wang et al. (2002) reported an incremental of 12%-15% OOIP due to polymer flooding in Daqing oil field. Putz et al. (1988) reported that oil cut

increased to about as much as 60% in some wells in Chateaurenard field. Takagi et al. (1992) reported that Chateaurenard pilot was characterized by high oil recovery of 94.4% initial oil in place which was 4.1% more than the simulated results. They used UTCHEM, a compositional chemical simulator developed at The University of Texas at Austin for simulations. The pilot was economical with a cost of 1.5 bbls oil per lbm polymer.

An extensive literature is available pertaining to polymer for enhanced oil recovery. Some of the earlier studies on non-Newtonian fluids mostly focused on the rheology and transport of power law (shear thinning) fluids through the porous media. Bird, Stewart and Lightfoot did some work on non-Newtonian fluid transport in the 1960's. The rheological properties of polymers were studied by Yuan and Pope in 1981.

1.2 POLYMER RHEOLOGY AND ITS MODELING OVERVIEW

1.2.1 Polymer structure

Polymers are mainly used in the petroleum industry for their physical properties such as their viscosifying power. Sorbie (1991) explains that the physical properties of the polymer are very well related to their molecular structure. Bio-polymers (Xanthan) and synthetic polymers (polyacrlamide) are the major categories used in the petroleum industry for specific reasons. Bio-polymers like Xanthan are limited in their application as they are more susceptible to bio-degradation (Bragg et al., 1982) and can only be used below a temperature of 140^{o}C. Synthetic polymers like HPAM have a much wider application as they are less susceptible to bio-degradation and can be used in higher temperatures. HPAM is partially hydrolyzed form of polyacrlamide (PAM). Synthetic polymers like HPAM can better transport under reservoir conditions than the bio-polymers. To this day over 90% of the field applications have used HPAM.

HPAM molecule is a flexible chain structure is a known as a random coil in polymer chemistry. It is a synthetic straight-chain polymer of acrylamide monomers, some of which have been through partial hydrolysis. The degree of hydrolysis is an important parameter for HPAM as it affects various physical properties of HPAM like salinity/hardness tolerance, shear and thermal stability, and adsorption characteristics. Levitt et al. (2010) conducted various experiments and carefully observed the conditions in which the hydrolysis of both HPAM and PAM occurs. They observed that unhydrolyzed polyacrylamide (PAM) undergoes more hydrolysis than HPAM and that PAM's viscosity increases on hydrolysis. Hence, the idea of in-situ hydrolysis of PAM was proposed. This was a crucial observation as injecting a lower viscosity PAM solution was easier than injecting a higher viscosity HPAM solution.

1.2.2 Polymer rheology

The most important solution property of polymer which is of interest in polymer flooding is its viscosity. The study of the flow behavior of non-Newtonian fluids is called rheology. The viscometric behavior of polymer solutions is related to the molecular weight of the macro molecule which is related to key concepts like intrinsic viscosity.

The intrinsic viscosity is the limit of inherent viscosity or reduced viscosity as the solution concentration of polymer tends to zero. Intrinsic viscosity is the most fundamental measure of the molecular weight of the polymer and is independent of polymer concentration as shown below:

$$[\eta] = \underset{C_P \to 0}{Lim} \frac{\eta - \eta_s}{C_P \eta_s} = \underset{C_P \to 0}{Lim} \frac{\eta_r - 1}{C_p} \qquad [1\text{-}1]$$

where n_r is the relative viscosity and is given by $\eta_r = \frac{\eta}{\eta_s}$. Intrinsic viscosity was also related to inherent viscosity by Kraemer (1938). Since the intrinsic viscosity is only

related to molecular weight, Mark-Houwink equation presented an equation as shown below:

$$[\eta] = K'M^a \qquad [1\text{-}2]$$

where K' and a are constants for a given polymer in a particular solvent. Klein and Conard (1980) reported a K' = 7.19 x 10^{-3} and a = 0.77 for PAM of a molecular weight of about 5x10^6. In UTCHEM, polymer solution viscosity is modeled by the modified Flory-Huggins equation as mentioned below:

$$\mu_p^0 = \mu_w \left(1 + \left(A_{p1} C_{4\ell} + A_{p2} C_{4\ell}^2 + A_{p3} C_{4\ell}^3\right) C_{SEP}^{Sp}\right) \qquad [1\text{-}3]$$

The above equation is related to the intrinsic viscosity. The relative viscosity form the above equation can be deduced as:

$$\eta_r = \frac{\mu_o}{\mu_w} = 1 + \left(A_{p1} c_{4\ell} + A_{p2} c_{4\ell}^{\ 2} + A_{p3} c_{4\ell}^{\ 3}\right) C_{SEP}^{Sp} \qquad [1\text{-}4]$$

Hence, the intrinsic viscosity calculation can be related to Flory-Huggins by the following:

$$[\eta] = \underset{C_P \to 0}{Lim} \frac{\left[1 + \left(A_{p1} c_{4\ell} + A_{p2} c_{4\ell}^{\ 2} + A_{p3} c_{4\ell}^{\ 3}\right) C_{SEP}^{Sp}\right] - 1}{C_p} \qquad [1\text{-}5]$$

$$[\eta] = \underset{C_P \to 0}{Lim} \left(A_{p1} + A_{p2} c_{4\ell} + A_{p3} c_{4\ell}^{\ 2}\right) C_{SEP}^{Sp} \qquad [1\text{-}6]$$

$$[\eta] = A_{p1} C_{SEP}^{Sp} \qquad [1\text{-}7]$$

where $A_{p1} C_{SEP}^{Sp}$ represent the fundamental relationship between intrinsic viscosity and the Flory-Huggins model modeled in UTCHEM.

1.2.2.1 Pseudoplastic (Shear Thinning) Fluids

Since polymer is a non-Newtonian fluid, its solution viscosity is a function of shear rate. Most polymers present a shear thinning behavior as the shear rate increases. However, some show shear thickening behavior at high shear rates. Figure 1.1 presents

the viscosity versus shear rate behavior for Xanthan solution for a range of polymer concentrations at a salinity of 5g/l at 30^{o}C. As seen, the viscosity at low shear rate (or Newtonian viscosity) increases with increasing concentration of polymer. Moreover, as the shear rate increases, the polymer viscosity decreases. This decrease in viscosity is modeled by the power law model (Bird et al., 1960) and is given by the following expression:

$$\eta(\gamma_{.}) = K\gamma_{.}^{n-1} \qquad [1\text{-}8]$$

where $\gamma_{.}$ is the bulk shear rate, K and n are constants. However, Carreau equation models the complete shear thinning regime as given below:

$$\eta(\gamma_{.}) = \eta_{\infty} + (\eta_0 - \eta_{\infty})\left[1 + (\lambda\gamma)^2\right]^{\frac{(n-1)}{2}} \qquad [1\text{-}9]$$

where η_{∞}, η_0 are infinite shear and zero shear viscosities. λ and n are time constant and power law index.

1.2.2.2 Viscoelastic Polymers

Another subset of the behavior of non-Newtonian fluids is the shear thickening polymer solutions. Some of the shear-dependent fluids show a degree of elasticity. These elastic materials are deformed through a small displacement and tend to return to their original configuration. This elastic behavior is also associated to the memory of the material. Polymers molecules undergo flow field elongation and contractions when flow though pore throats and bodies in a porous media. As a result of this, polymer molecules stretch and recoil to adjust to the flow field. However, when the flow velocity is high, the polymer molecules do not have enough relaxation time to stretch and re-coil, adjusting to the flow. As a result of this elastic strain, the apparent viscosity of polymer increases. This increase in apparent viscosity of polymer is called shear thickening behavior. This is an extremely important property when polymer flows through the porous media.

Various researchers have studied the shear thickening behavior of polymers. Seright (2009) presented a study in which he injected Xanthan and HPAM polymers into Berea sandstone cores with a permeability of about 500 md and porosity of 21%. He reported Xanthan solutions showing shear thinning behavior only in the porous media. However, he further reported HPAM exhibiting only Newtonian and dilatant flow behavior at low and moderately high flow rates respectively.

Wang et al. (2001) reported that viscoelastic polymers could displace waterflood residual oil. They presented this observation based on the secondary recovery polymer floods performed in their laboratory. Huh and Pope (2008) presented possible mechanisms involving reduction in residual oil saturation from secondary polymer floods.

Chauveteau (1981) conducted various laboratory experiments to explain the flow of polymer in porous media. He presented the significance of both shear and elongation flow by flowing polymer through a capillary model with varying cross-sections. He injected various concentrations of a 7 million molecular weight polymer at a particular salinity and temperature. It was observed by Chauveteau that as the flow rate increases over a critical value, the apparent viscosity of polymer increases rapidly. The shear rate at this critical flow velocity is referred to as gamma star by Chauveteau. Figure 1.2 presents the polymer viscosity curve as a function of apparent shear rate as presented by Chauveteau.

He investigated various mechanisms involved at molecular level to explain polymer characteristics like dilatant behavior and permeability reduction. He suggested that dilatant behavior exhibited by polymer molecules is a result of coil stretch transition of macromolecules in elongation parts of flow. Furthermore, he mentioned that this stretching of molecules showed an increase in viscous friction and hence, dilatancy.

From his research, Chauveteau also suggested that the onset of dilatancy is a function polymer solution properties like polymer concentration, salinity and, molecular weight etc. He noticed that as the polymer concentration increases, the high shear polymer asymptotic viscosity increases. Furthermore, he suggested that as the molecular weight of the polymer increases, the gamma star decreases. Moreover, he also suggested that as the salinity decreases, the gamma star decreases. Also, as the polymer concentration increases, the high shear polymer viscosity increases. Like for example, the gamma star and high shear viscosity at 1360 ppm polymer concentration is about 500 sec^{-1} and 20 cp. Also, at 21 ppm polymer concentration, the gamma star and high shear viscosity are 3000 sec^{-1} and 2 cp.

He concluded his work suggesting that as a general trend the onset of dilatant behavior occurs when the product of shear rate and relaxation time is about equal to 10. Table 1.1 presents the data provided by Chauveteau on calculated product of gamma star and relaxation time representing the onset of dilatancy at about 10 for various concentrations of polymer at a particular salinity.

Many researchers have attempted to model in-situ polymer rheology to describe both shear thinning and thickening behavior. Hirasaki and Pope (1974) presented their study in which they modeled shear thinning fluids by power law and Blake-Kozeny models and, the dilatant behavior by Deborah number. The Deborah number is a function of relaxation time (a polymer characteristic) and characteristic deformation time of the flow field. Masuda et al. (1992) proposed a model to describe the shear thickening behavior of polymer solution in the porous media. From their laboratory study they proposed that the viscoelastic model was able to better match fractional flow curve, breakthrough time of polymer, the pressure drop and, oil recovery.

Recently, Delshad et al. (2008) presented a unified apparent viscosity model which accounts for the full range of velocity. This model has an advantage over the others as it accounts for the apparent polymer viscosity (both thinning and thickening) by using the bulk rheology data and porous media petrophysics only.

1.2.3 The Unified Viscosity Model

Delshad et al. (2008) presented the Unified Viscosity Model to model the full spectrum of Newtonian, shear thinning and shear thickening regimes of polymer viscosity. In this model, the polymer apparent viscosity is modeled as a function of effective shear rate which is correlated with Darcy velocity.

As observed by Chauveteau, the unified viscosity model assumes that polymer solution's apparent viscosity consists of two parts i.e. shear thinning and shear thickening. The shear thinning part (μ_{sh}) is the shear viscosity dominant part, and the polymer elongational-viscosity-dominant part is modeled as the shear thickening part (μ_{el}).

$$\mu = \mu_{sh} + \mu_{el} \qquad [1\text{-}10]$$

$$\mu_{app} = \mu_w + (\mu_p^0 - \mu_w)\left[1 + (\lambda\gamma_{eff})^2\right]^{(n-1)/2} + \mu_{max}\left[1 - \exp\left(-(\lambda_2\tau_r\gamma_{eff})^{n_2-1}\right)\right] \qquad [1\text{-}11]$$

The apparent polymer viscosity (μ_{app}) is a non linear model and a function of water viscosity (μ_w), polymer low shear viscosity (μ_p^0), in-situ effective shear rate (γ_{eff}), and empirical constants (λ,n,n_2). Relaxation time (τ_r) is the characteristic of a polymer and is measured in the laboratory by dynamic frequency sweep test. Polymer viscosity at very high shear rate (μ_{max}) is modeled as a function of polymer concentration and effective salinity as follows:

$$\mu_{max} = \mu_w\left(1 + \left(A_{p11}C_p + A_{p22}C_p^2\right)C_{SEP}^{S_p}\right) \qquad [1\text{-}12]$$

where AP_{11} and AP_{22} are model input parameters.

Kim et al. (2010) measured the relaxation time of HPAM for various concentrations of polymer, salinities, and temperature. They obtained the characteristic relaxation time by non-linear fitting of the G' and G" data into the generalized Maxwell model. They observed that relaxation time increases in with increasing polymer concentration and expressed the relationship as follows:

$$\tau_r = A_1 C_p^2 + A_2 C_p + \tau_0 \qquad [1\text{-}13]$$

where Cp is polymer concentration, and A1, A2 and τ0 are empirical constants. Table 1.2 presents the list of parameters and their correlation and values for the model.

Magbagbeola (2008) conducted laboratory corefloods at high velocities by injecting HPAM and other polymers to observe any shear thickening in-situ. He observed shear thickening and developed parameters for UVM for 1500 ppm of HPAM concentration. Later, his data was used to develop UVM parameters for HPAM.

1.2.4 Apparent Shear Rate

The bulk shear rate and the apparent shear rate are different. The shear rate at which the polymer viscosity measured in a viscometer is the bulk shear rate. The apparent shear rate is the shear rate observed by the non-Newtonian fluid in the porous media. It is computed by using the bundle of capillary tubes model for non-Newtonian fluids. Cannela et al. (1988) used the following equation to calculate the in-situ shear rate which is modeled by the modified Blake-Kozeny capillary bundle equation for multiphase flow:

$$\gamma_{eff} = C\left[\frac{3n+1}{4n}\right]^{n/(n-1)}\left[\frac{u_w}{\sqrt{kk_{rw}S_w\phi}}\right] \qquad [1\text{-}14]$$

where u_w is Darcy velocity of the polymer solution, k and K_{rw} are permeability and water relative permeability, S_w is water saturation, and ϕ is porosity. Canella et al. (1988) reported C = 6 after matching wide variety of corefloods. Wreath et al. (1990)

demonstrated the dependency of shear coefficient (C) on permeability for HPAM polymer solutions.

1.3 DESCRIPTION OF CHAPTERS

Chapter 1 presented a brief literature review about polymer flooding. In Chapter 2, the improvements in modeling of polymer rheology for both shear thinning and shear thickening are discussed. Using the enhancements in modeling polymer rheology presented in Chapter 2, Chapter 3 presents the effect of grid size on polymer injectivity and a practical correction for the same. Chapter 4 presents the effect of a transverse fracture and skin on polymer injectivity in horizontal well. Chapter 5 presents the design and optimization of a pilot scale surfactant-polymer flood. The results predicted by UTCHEM simulations were compared to field data. Finally, Chapter 6 summarizes the entire study and also presents conclusions of the present study. Moreover, recommendations for future work are also presented in Chapter 6. The appendix includes some input files for relevant cases of the present study.

Table 1.1: Product of gamma star and relaxation time at the onset of dilatancy for different polymer concentrations as observed by Chauveteau

C (ppm)	21	42	85	170	340	680	1360
$\tau_1 \times 10^{+3}$ (s)	4.4	4.6	4.7	5.4	6.4	8.7	14.3
$\dot{\gamma}^*$ (s^{-1})	3100	2900	2400	1850	1550	1160	610
$\dot{\gamma}^* \times \tau_1$	13.6	13.1	11.2	10	9.9	10.1	8.7

Table 1.2: Correlation parameters for relaxation time (Kim et al., 2010)

$$A_1 = a_0 + a_1\left(\frac{a_2C_1 + a_3}{C_1 + a_4}\right)\frac{(C_1 + \exp(a_5C_2)^{a6})^{a7}}{(C_1)^{a8}}$$

	a_0	a_1	a_2	a_3	a_4	a_5	a_6	a_7	a_8
FP3630S	5271.1	2.57	-116.06	2.79	0.00136	1000	-83.25	1	0.79
FP3330S	7215.3	1	-251.97	0.11	-0.00039	1000	-897.78	1	0.53
AN125	6173.8	1	-47.89	0.02	-0.00039	1000	-100.01	1	0.74

$$A_2 = b_0 + \left(\frac{b_1C_1 + b_2}{C_1 + b_3}\right)\frac{(C_1 + \exp(b_4C_2)^{b5})^{b6}}{(C_1)^{b7}}$$

	b_0	b_1	b_2	b_3	b_4	b_5	b_6	b_7
FP3630S	10	41.79	-0.847	0.001	1000	-6.46	1	0.026
FP3330S	-3.03	0.00218	-2.02×10^{-6}	0.011	1000	-11.05	1	1.821
AN125	3	2662.8	-2.362	0.02	1000	1	-1494.88	0.016

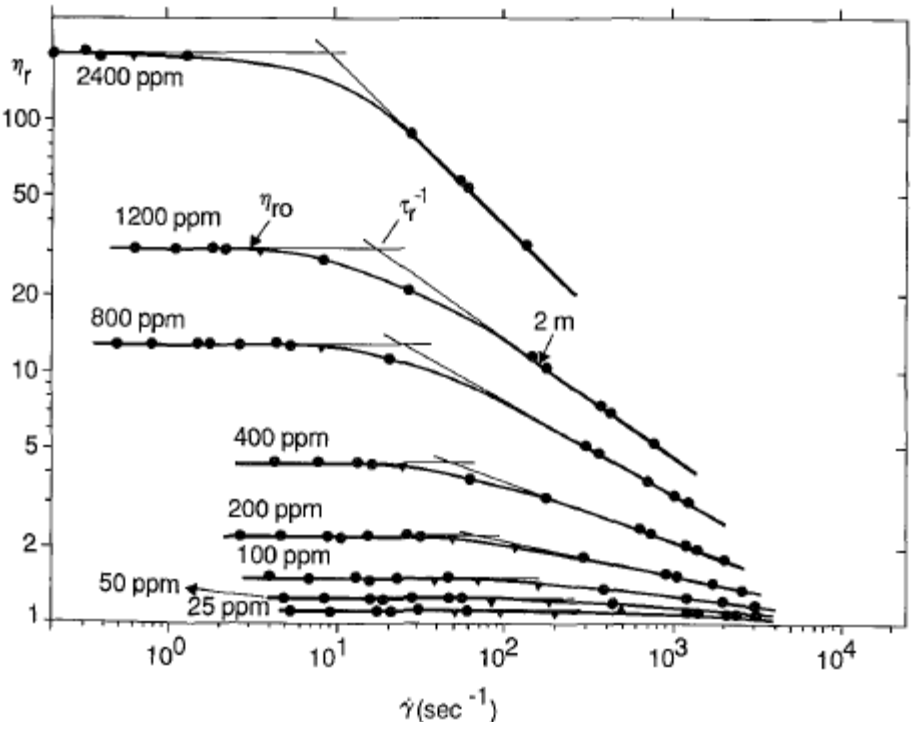

Figure 1.1: Shear thinning behavior of Xanthan solution at 5g/l, pH 7, 30°C (Sorbie 1991)

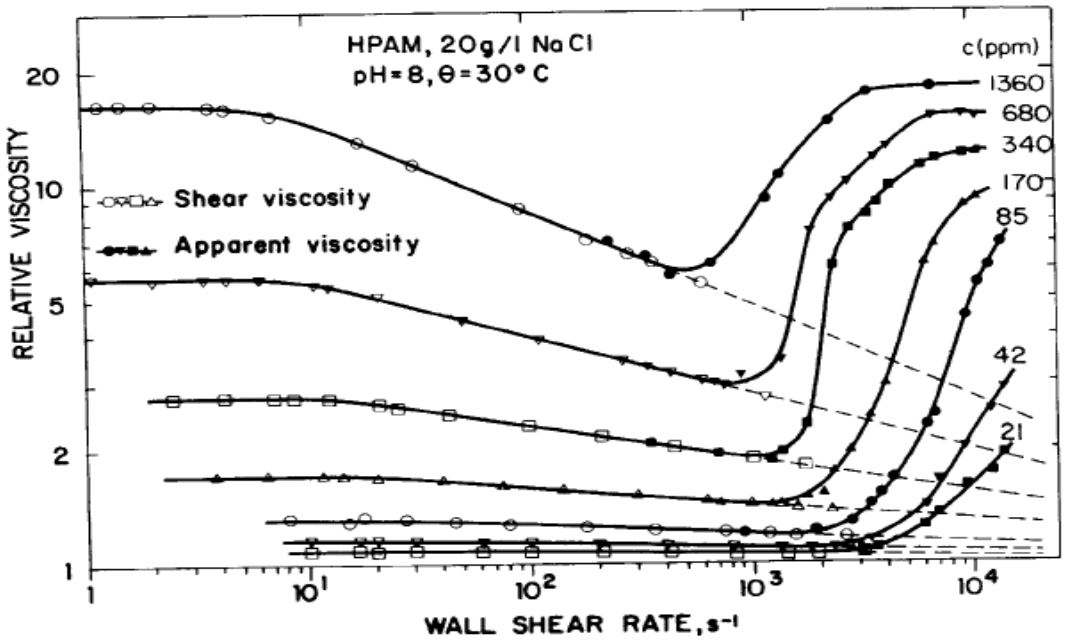

Figure 1.2: Full range polymer viscosity obtained by Chauveteau (1981)

2 Polymer viscosity model development

This chapter discusses new developments in polymer viscosity model for UTCHEM. Laboratory bulk and apparent viscosity measurements to develop a better fit to the data.

2.1 MODELING BULK POLYMER VISCOSITY

The viscosity of a polymer solution is a function of polymer concentration and solution salinity. The dependence of polymer viscosity on concentration and salinity is modeled in UTCHEM by modified Flory-Huggins equation as mentioned below:

$$\mu_p^0 = \mu_w \left(1 + \left(A_{p1} C_{4\ell} + A_{p2} C_{4\ell}^2 + A_{p3} C_{4\ell}^3\right) C_{SEP}^{S_p}\right) \qquad [1\text{-}2]$$

where, μ_p^0 is low shear polymer viscosity, μ_w is water viscosity, A_{P1}, A_{P2}, and A_{P3} are model parameters obtained by matching laboratory measurements. C_p is polymer concentration in water phase. $C_{SEP}^{S_p}$ are parameters used to model polymer viscosity dependence on salinity and hardness. The effective salinity C_{sep} is calculated by the following equation in meq/ml:

$$C_{SEP} = \frac{C_{51} + (\beta_P - 1) C_{61}}{C_{11}} \qquad [2\text{-}1]$$

where, C_{51}, C_{61} are anions and cations concentration in aqueous phase. β_p is an input parameter which represents the influence of divalent cations on the polymer properties as compared to monovalents. S_p is calculated by the slope of normalized polymer viscosity $\frac{(\mu_P - \mu_w)}{\mu_w}$ vs. C_{sep} on a log-log scale.

The effect of shear rate on polymer is modeled by Meter's equation (1964)

$$\mu_p = \mu_w + \frac{\mu_p^0 - \mu_w}{1 + \left(\frac{\dot{\gamma}_{eq}}{\dot{\gamma}_{1/2}} \right)^{P_\alpha - 1}} \qquad [2\text{-}2]$$

where $\dot{\gamma}_{1/2}$ is the shear rate at which viscosity is the average of μ_p^0 and μ_w. P_α is an empirical coefficient used to match the laboratory data.

Laboratory data was obtained at a particular salinity for Flopaam 3630S polymer. Figure 2.1 presents polymer viscosity vs. shear rate data obtained from the laboratory for various concentrations of polymer for a brine salinity B presented in Table 2.1. An attempt was made to model this data. First, the low shear polymer viscosity data was modeled by equation1 in UTCHEM. Figure 2.2 presents the match between laboratory low shear viscosity and UTCHEM model. The dots represent the laboratory and the curve represents UTCHEM model.

After matching the low shear viscosity data, polymer viscosity is calculated at various shear rates. A P_α of 1.7 and $\dot{\gamma}_{1/2}$ of 40 sec^{-1} is used for all concentrations of polymer to give the best match possible. Figure 2.3 presents the match between the laboratory data and UTCHEM model. Clearly, at high shear rates, the model fit deviates from the laboratory data.

In order to get a better match, $\dot{\gamma}_{1/2}$ was made a function of polymer concentration. So for each polymer concentration a different gamma half was used to match the data. The data points in Figure 2.4 are the $\dot{\gamma}_{1/2}$ which provide the best fit of polymer viscosity calculated from the UTCHEM model and the laboratory data. This gammahf was fit to an exponential function of polymer concentration as presented in Figure 2.4 and is now in UTCHEM:

$$\dot{\gamma}_{1/2} = \dot{\gamma}_{1/2(1)} \; e^{\dot{\gamma}_{1/2(2)} C_{4\ell}} \qquad [2\text{-}3]$$

where, $\dot{\gamma}_{1/2(1)}$ and $\dot{\gamma}_{1/2(2)}$ are the fitting parameters which provide the best fit. Using the above gammahf model, polymer viscosity was then plotted against shear rate and compared with the laboratory data. Figure 2.5 presents this comparison. Clearly, polymer viscosity modeled by using gammahf as a function of polymer concentration provides a better match. $\dot{\gamma}_{1/2(1)}$ and $\dot{\gamma}_{1/2(2)}$ are now a user input as gammahf1 and gammahf2.

2.2 POLYMER FULL VELOCITY RANGE MODELING

Apart from the shear thinning behavior, polymers exhibit the shear thickening behavior in the porous media as well.

Chauveteau (1981) conducted various laboratory experiments and reported observing dilatant behavior by the polymer. Dilatancy means increase in polymer viscosity at high flow velocity i.e. shear rate. Figure 1.2 presents the polymer viscosity curve as a function of apparent shear rate. The figure presented polymer viscosity curve at different polymer concentrations. The salinity and temperature were constant for all the cases. The molecular weight of the polymer studied by him was 7 million. It is seen that as the polymer concentration increases, the zero shear viscosity increases. This is a similar observation as seen in the section 2.1 of this chapter, even though the polymer was different. Also, as the shear rate increase, the polymer viscosity for all the concentrations decreases until the critical shear rate. It was observed by Chauveteau that as the flow rate increases over a critical value, the apparent viscosity of polymer increases rapidly. The shear rate at this critical flow velocity is referred to as gamma star by Chauveteau.

In the next section, we present the modeling of Chauveteau polymer data.

2.2.1 Modeling Chauveteau's polymer viscosity data

An attempt was made to model Chauveteau's polymer viscosity data presented in Figure 1.2. The unified viscosity model presented by Delshad et al. (2008) was used to model the data. The unified viscosity model covers the entire range of darcy velocity and accounts for both shear thinning and thickening behavior of polymer viscosity.

Chauveteau determined the bulk viscosities by using capillary viscometers especially designed to measure polymer viscosities for a wide range of shear rates. To measure the elongational behavior of polymer he flowed the polymer solutions through capillaries of different lengths which were separated by cylindrical expansions. The design of the above experimental setup is provided in his paper. We further our fit of his data assuming that the shear rate provided by Chauveteau is representative of the in-situ shear rate.

Chauvateau's viscosity data was digitized for our convenience and presented in Figure 2.6. To simplify our work, the shear thinning and thickening viscosity data are matched separately. The onset of dilatancy in his data was used to separate the thinning and thickening part of the viscosity data.

First, the shear thinning part of the data was fitted. The zero shear viscosities at different concentrations were read from Figure 2.6. The non-linear model for calculating low shear polymer viscosity was used to fit Chauveteau viscosity data. The fit of Chauveteau's low shear viscosity and UTCHEM's model is presented in Figure 2.7.

Next, the data was fitted by using λ as a fitting parameter. Also, the value of n was fixed at 0.78. To obtain the best fit of the shear thinning data, the empirical constant λ was made a function of polymer concentration. The red dots in Figure 2.8 represent empirical values of λ as a function of polymer concentration on a semi-log plot.

Furthermore, an exponential model was fitted to the empirical data and plotted in Figure 2.8. The model is as follows:

$$\lambda = \beta_{v1}\, e^{\beta_{v2}\, C_{4\ell}} \qquad [2\text{-}4]$$

where, β_{v1} and β_{v2} are user defined input parameters which provide the best fit to the data. The regression while matching Chauveteau's data with the exponential model is 99.78%, which is satisfactory. This model was then coded in UTCHEM.

Next, the shear thickening data provided by Chauveteau is fitted by using the elongational-viscosity dominant part of the UVM model. The parameters μ_{max} and product of λ and τ_r are used to match this shear thickening data.

First, the shear thickening viscosity i.e. plateau viscosity at high shear rate was read from Figure 2.6 for all polymer concentrations. This data is presented in Table 1.1. For modeling purposes, this high shear thickening viscosity is then subtracted from high shear thinning viscosity at the same shear rate. This viscosity is henceforth referred to as μ_{max} and is presented in Figure 2.9. As seen, μ_{max} varies with polymer concentration. μ_{max} increases with increase in polymer concentration and approaches a plateau at about 1340 ppm. To model this data, μ_{max} is modeled as logarithmic function of polymer concentration. The following model is used in UTCHEM:

$$\mu_{\max} = \mu_w \left[AP22\left(\ln C_{4\ell}\right) + AP11 \right] \qquad [2\text{-}5]$$

where, AP11 and AP22 are fitting parameters. Figure 2.9 presents the UTCHEM's model fit to the high shear viscosity of Chauveteau's data.

After matching the high shear viscosity with UTCHEM model, the second step was to fit the product of relaxation time and empirical constant λ_2 and develop a UTCHEM model for it. First, the digitalized shear thickening part of Chauveteau's data was extracted and subtracted from the shear thinning data at respective shear rates. Then,

the subtracted data was fitted with the product of τ_r and λ_2. Figure 2.10 presents the product plotted against the polymer concentration. Clearly, the product of τ_r and λ_2 increase with increasing polymer concentration.

Next, a constant value ofλ_2 of 0.01 is assumed to calculate the relaxation time. The calculated relaxation time now presented in Figure 2.12. One of the reasons for making this assumption is to allow us to calculate the value of relaxation time which is a characteristic property of a polymer and can be measured in the laboratory by the dynamic frequency sweep test. Another reason for this assumption that the value of τ_r now calculated for Chauveteau was in the range of 10^{-2}. Magbagbeola (2008) presented the measured laboratory values of relaxation time for various polymers. He showed that the relaxation time of 1500ppm Flopaam 3630S, AN125, and, HJ63020 were about 0.05 sec. The molecular weight (as listed by manufacturers) of AN125, Flopaam™ 3630S and, Hengfloc® 63020 are 8 million, 20 million, and 26 million Daltons respectively. For Chauveteau's polymer, the molecular weight was 7million and τ_r now calculated at 1340 ppm is about 0.05sec. Although, the molecular weight of all the above mentioned polymers are different but it certainly gives certain degree of confidence.

Next, the calculated τ_r is modeled as linear function of polymer concentration. The following model is used in UTCHEM as well:

$$\tau = \tau_0 C_{4\ell} + \tau_1 \qquad [2\text{-}6]$$

It should be noted that since the relaxation time for the polymer being studied is not available, hence, it is just used as a fitting parameter as for now. Figure 2.11 presents the UTCHEM's model fit with the calculated relaxation time from Chauveteau's data.

After fitting the models of the empirical constant (λ_2) and relaxation time (τ_r) with their calculated data, polymer viscosity curve was constructed for a complete flow velocity range using Unified Viscosity Model presented in equation3-6. Figure 2.12

presents the comparison between the viscosity data presented by Chauveteau and viscosity calculated using UVM. Dots in figure represent the digitized data by Chauveteau and curves represent the UVM predicted viscosity.

Overall, the match seems satisfactory. As seen, the shear thinning part of the data is a great match. Both, the curves and dots are well placed over each other. The shear thickening part of the viscosity curves present a decent match with Chauveteau data in dots. One of the interesting points between the match is that the onset of dilatancy of both the UVM curves and Chauveteau's dots decrease with increasing polymer concentration. Another interesting comparison is that the shear thickening part of 1360 ppm, 170 ppm, and 85 ppm match very well with Chauveteau data. The match of viscosity curves of 680 ppm and 340 ppm polymer concentration have some scope of improvement. However, it is interesting to see that the high shear viscosity of 680ppm curve plateau's at the approximately the same shear rate as shown by Chauveteau. One of the reasons for the mismatch could be experimental errors which inevitably occur while laboratory work. Table 2.2 provides best fit UVM parameters developed to match Chauveteau's data.

2.2.2 Modeling Flopaam HPAM™ 3630S complete range viscosity data

After successfully modeling Chauveteau's polymer viscosity data, Flopaam 3630S complete range viscosity data was attempted to model. Flopaam 3630S is a hydrolyzed polyacrylamide polymer which is widely used in many EOR processes in petroleum industry. The molecular weight of this polymer is 20 million Daltons. Both the bulk and relaxation time data were measured by Kim et. al (2010) at the University of Texas laboratory. The apparent polymer viscosity data was measured by Magbagbeola (2008) by doing various corefloods.

The bulk data set which is matched using the shear thinning part of UVM is presented in Figure 2.13. For simplicity, the polymer concentrations until 2000ppm were modeled. First, the low shear viscosity is modeled by using modified Flory Huggins equation modeled in UTCHEM as presented earlier. The matching parameters are presented in Table 2.2. Next, similar to methodology followed while modeling Chauveteau's data, the empirical constant (λ) is modeled by matching the rest of the data. The best fit match as obtained by making λ a function of polymer concentration presented as dots in Figure 2.14. Then, the UTCHEM exponential model fit of λ is modeled to that obtained by matching the laboratory data. This exponential fit is presented as a curve in Figure 2.14. The parameters β_{v1} and β_{v2} are also listed in the Table 2.2.

After the shear thinning data set is modeled, the shear thickening apparent data set was modeled. The low shear viscosity was modeled similar to the methodology adopted to model Chauveteau's dataset. Magbagbeola (2008) obtained high shear viscosity of 1500 ppm polymer concentration by doing various corefloods. He observed that the high shear viscosity of 1500 ppm polymer concentration 3630S polymer is 65 cp. Next, we assumed the high shear viscosity of polymer for 500 ppm polymer concentration so as to fit the UTCHEM's logarithmic high shear viscosity model. This was done since no other high shear viscosity data was available. The value assumed is 43 cp. Figure 2.15 presents UTCHEM model fit to the high shear viscosity data.

The next step to model the shear thickening is to model relaxation time. Relaxation time was used as a fitting parameter to obtain a good fit to Chauveteau's polymer dataset. However, the relaxation time for Flopaam 3630S is available in the literature. Based on a lot of measured data of relaxation time Kim et al. developed a model to calculate the relaxation time. Using their model parameters (Table 1.2), the

relaxation time was calculated for 3630S polymer at salinity B at 30.7 deg C. The dots in Figure 2.16 represent the relaxation time calculated at various polymer concentrations by their model. This data was then modeled by using UTCHEM's relaxation time model presented earlier. The curve presented in Figure 2.16 is represents the model fit to the data. Also, λ_2 was assumed as 0.01 as earlier. As seen earlier for Chauveteau's polymer data match, the relaxation time of 3630S polymer increases with polymer concentration.

Next, all the parameters and models developed for 3630S were combined into the unified viscosity model to construct polymer viscosity for full range of shear rate and hence, the in-situ velocities. It was assumed that the bulk shear rate is representative of the apparent shear rate. Figure 2.17 presents the UVM curves for the complete range of shear rate and data points represent the lab data. Clearly, a good match was obtained between the laboratory data and UVM model in the shear thinning regime. In the shear thickening regime, a better fit could be obtained. The predicted viscosity for 1500 ppm polymer concentration at high shear rates is slightly higher than the lab data.

To get a better fit between the lab data and UVM model data, a value of 0.003 was used for λ_2. Figure 2.18 presents the UVM curves when λ_2 was used. Clearly, a better fit is obtained. Now, the UVM polymer viscosity curve matches much better than before. All the UVM model input parameters are presented in Table 2.2.

2.3 CONCLUSIONS AND SUMMARY

This chapter presented the new developments in modeling polymer viscosity with the available. Gamma half was made a function of polymer concentration to obtain a better match with the bulk data measured in the laboratory. Polymer shear thickening data presented in the literature was modeled for the first time using the Unified Viscosity Model. Polymer viscosity measured by Chauveteau for a polymer was matched and new

models for relaxation time and other parameters were developed and implemented in UTCHEM. Then, by using those developed models, Flopaam 3630S viscosity was modeled for full velocity range. Further confidence was obtained when the relaxation time model developed by using Chauveteau's data fit fitted very well with Kim et al. correlation for Flopaam 3630S polymer data.

Table 2.1: Brine salinity of polymer solution (Salinity B)

Anion	conc., mg/lt	MW	charge	conc., meq/ml
Cl	11500	36	1	0.3239
SO4	0	98	2	0
HCO3	500	61	1	0.0082
CO3	0	60	2	0
Br	0	80	1	0
I	0	127	1	0
total anion	12000			0.323
Divalent Cation				
Mg	260	24.3	2	0.0214
Ca++	640	40	2	0.032
Sr	160	87.62	2	0.0037
Ba	80	137.327	2	0.0012
total divalents	1240	48.2		0.0534

Table 2.2: UVM parameters which provide best fit to the available data

Parameters names	Chauveteau model fit parameters	Flopaam 3630 S model fit parameters
betav1 ($\beta v1$)	0.0185	0.0133
betav2 ($\beta v2$)	17.298	14.2154
expn1 (n_1)	0.78	0.73
tetav (λ_2)	0.01	0.003
tau0 (τ_0)	0.300018	0.2394
tau1 (τ_1)	0.00768	0.0416
expn2 (n_2)	3.5	2.3
AP11	2.7406	121.2695
AP22	17.116	22.49356
Ap1	34.91541	23.26394
Ap2	435.1163	327.3245
Ap3	1054.952	60.70658
Sp	0	0
visw (μ_w)	0.798	0.798

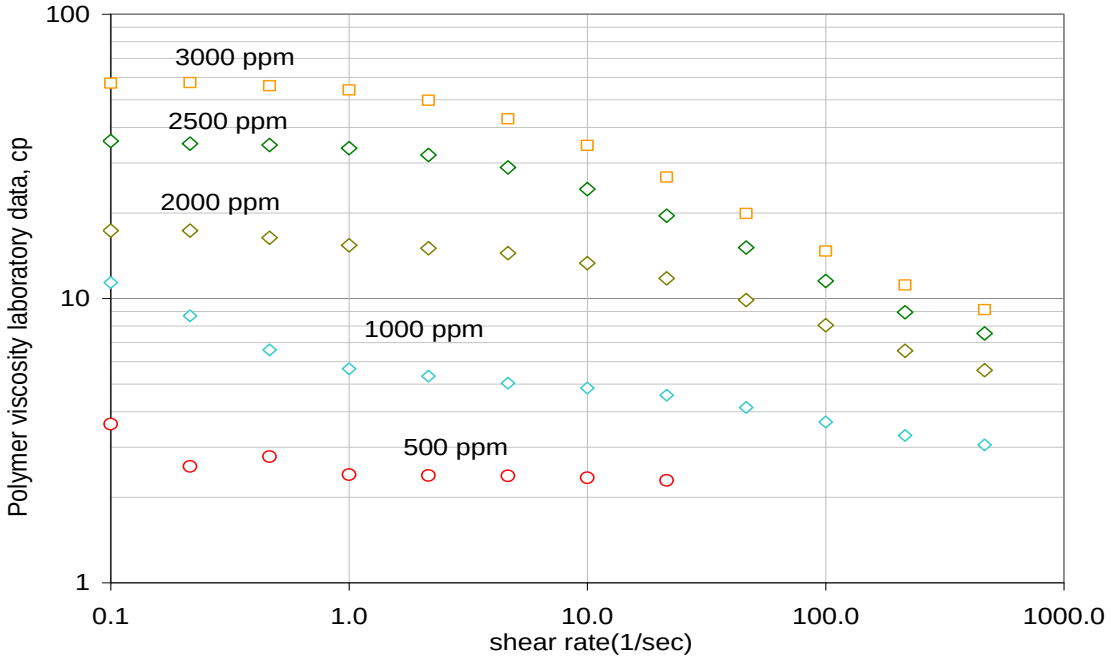

Figure 2.1: Laboratory bulk data for 3630 S at salinity B at 30.7 ^{o}C

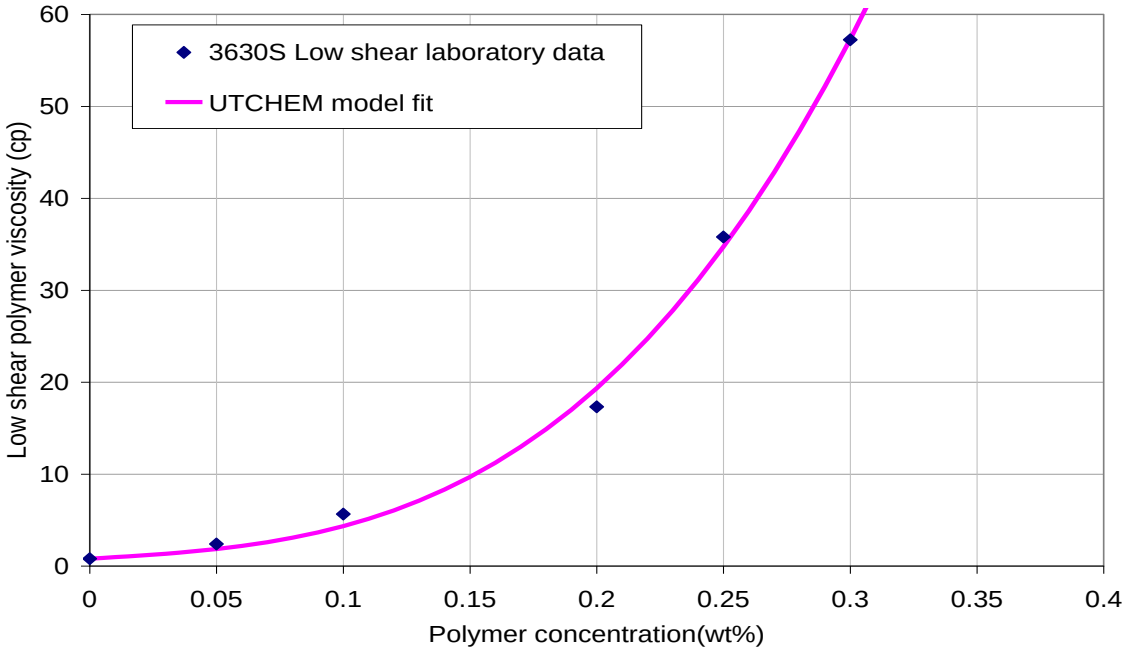

Figure 2.2: UTCHEM model fit to measured lab. data for Flopaam 3630S polymer viscosity vs. concentration (salinity B, 30.7 ^{o}C)

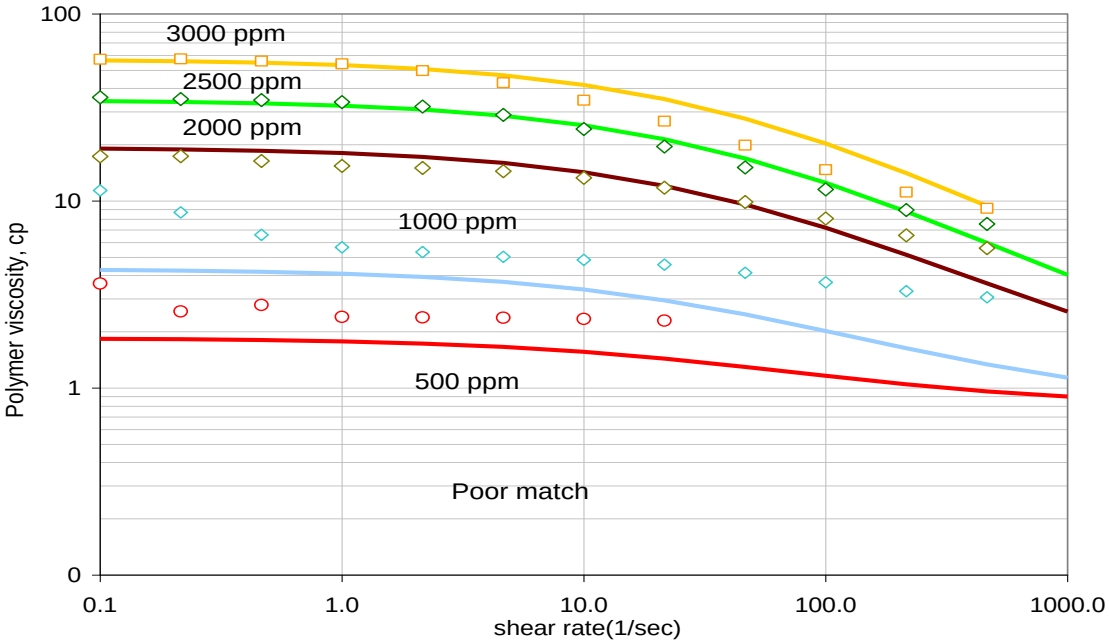

Figure 2.3 UTCHEM model fit to measured lab. data for Flopaam 3630S polymer viscosity vs. shear rate (Salinity B; 30.7 ^{o}C), when same gamma half is used for all polymer concentrations

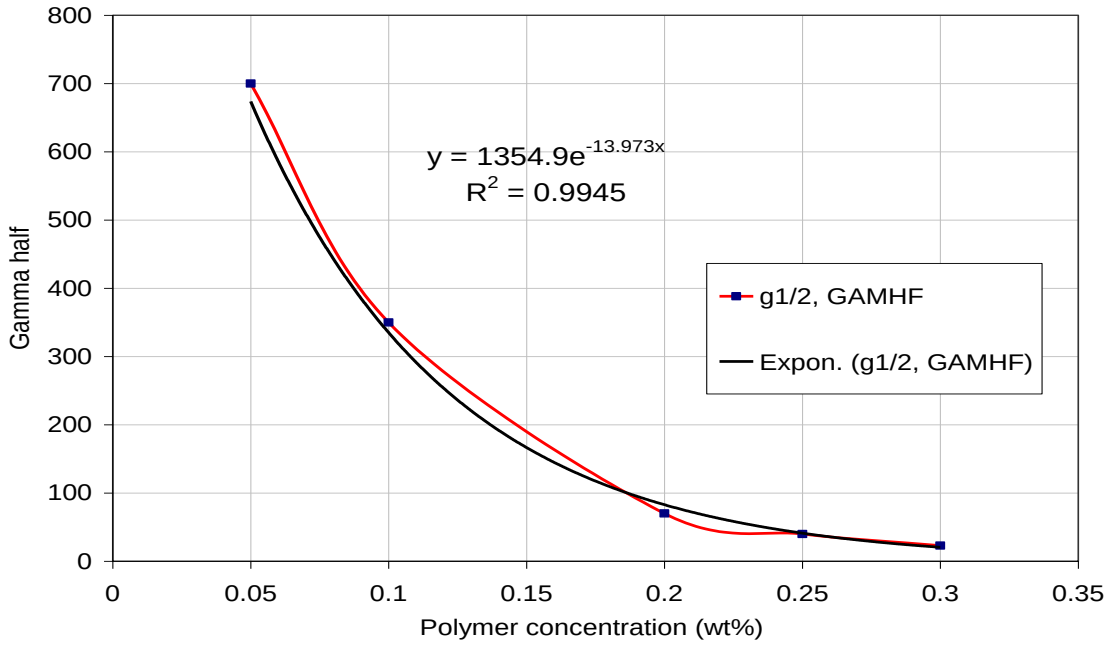

Figure 2.4: Variable GAMHF as a function of polymer concentration

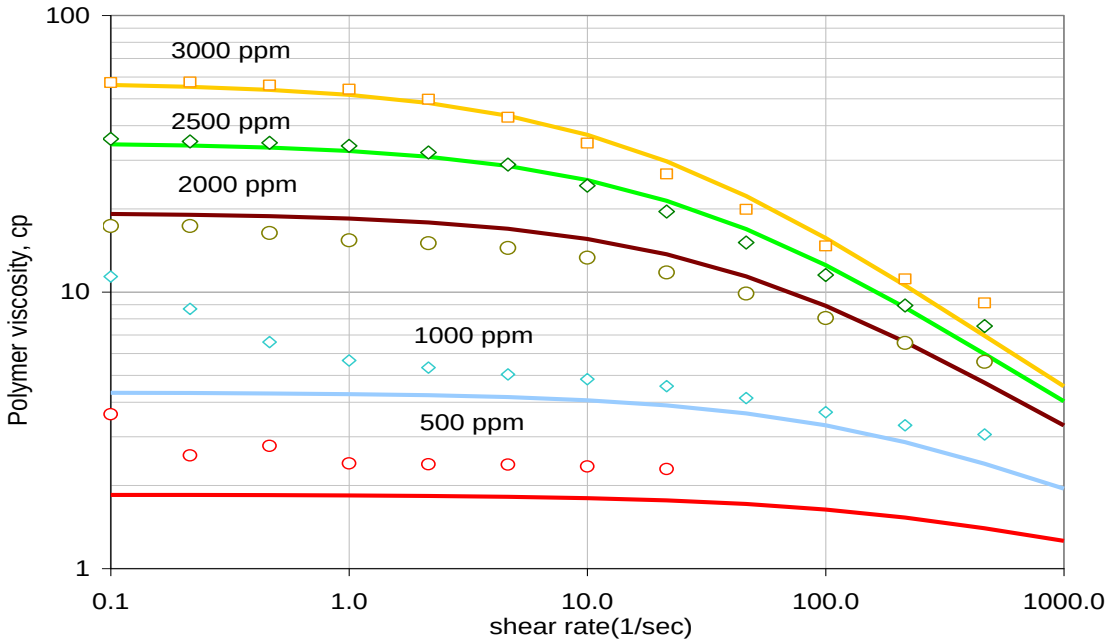

Figure 2.5: UTCHEM model fit to measured lab. data for Flopaam 3630S polymer viscosity vs. shear rate (Salinity B; 30.7 oC), when same gamma half is used for all polymer concentrations

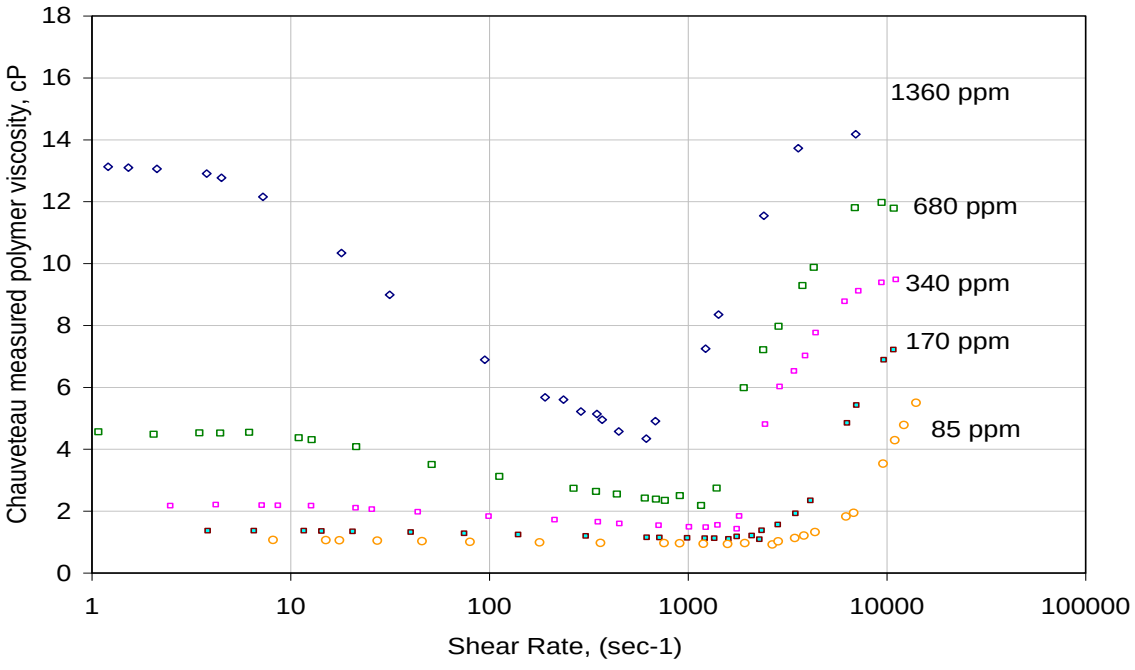

Figure 2.6: Digitalized Chauveteau data in Figure 1.2

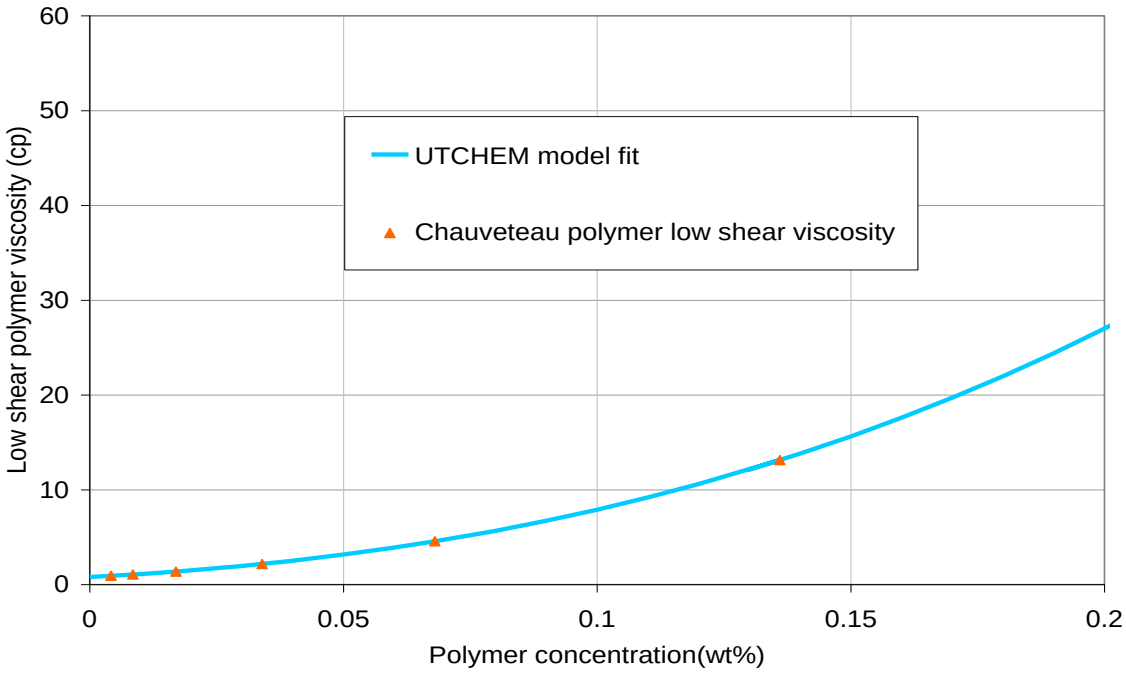

Figure 2.7: UTCHEM model fit to low shear viscosity of Chauveteau's data

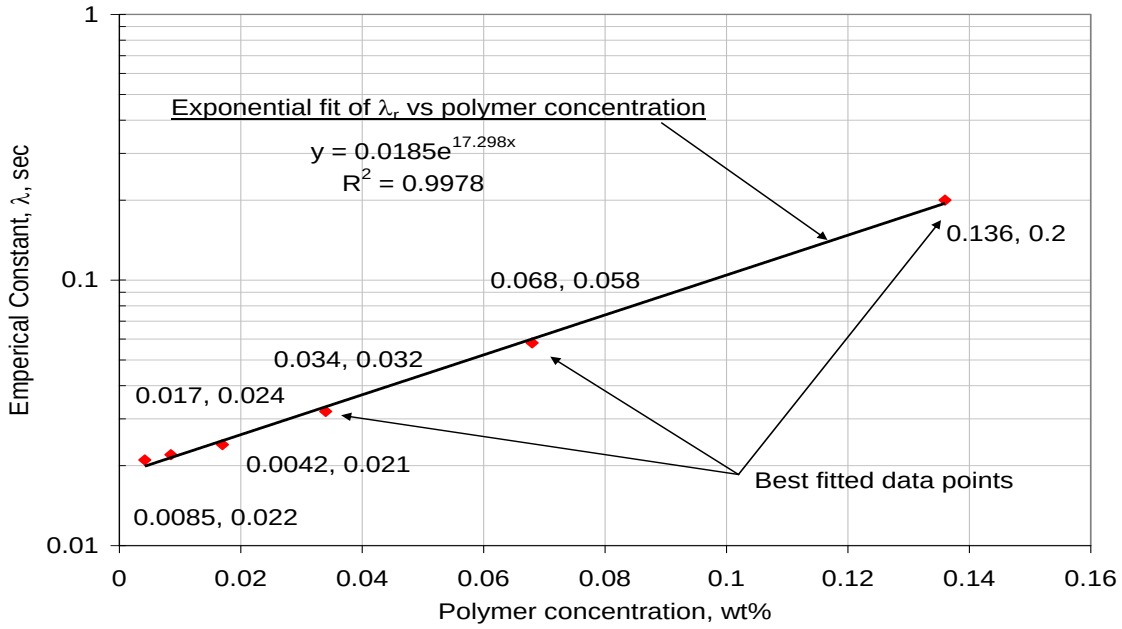

Figure 2.8: UTCHEM model fit to λ obtained by matching Chauveteau's data

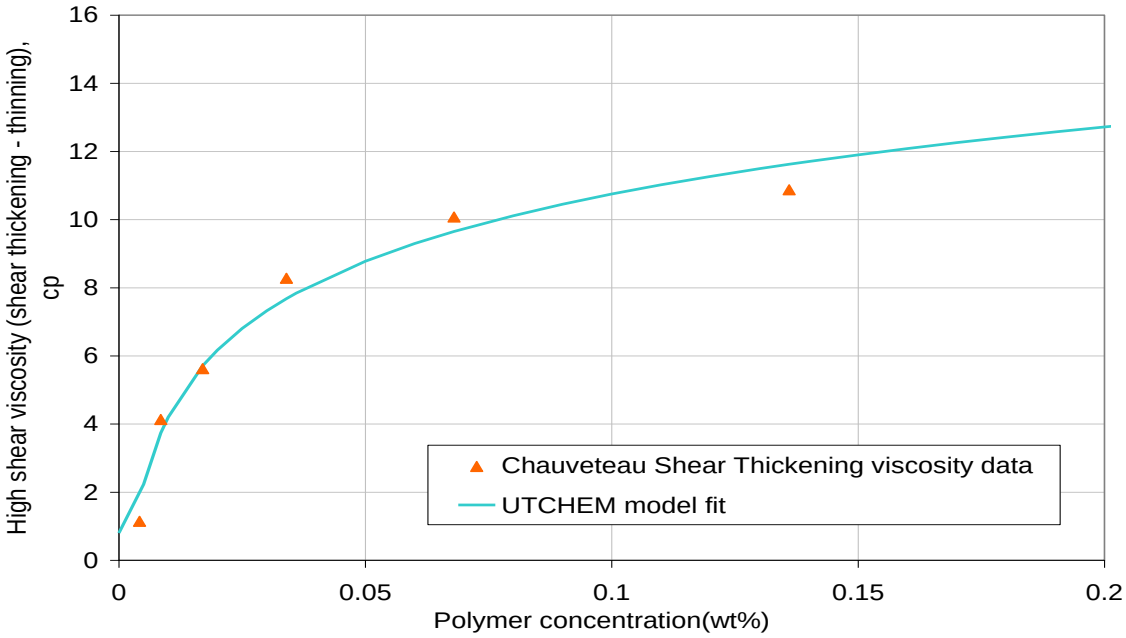

Figure 2.9: UTCHEM model fit the high shear viscosity of Chauveteau's polymer data

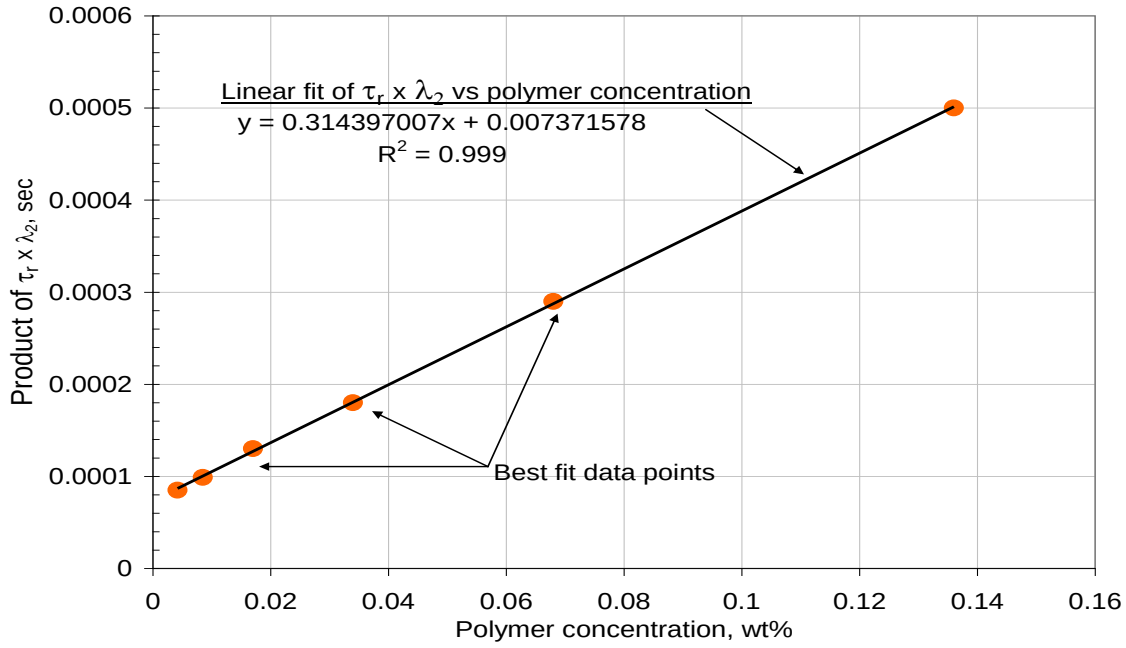

Figure 2.10: UTCHEM model fit to the product of λ_2 and τ_r obtained by matching Chauveteau's data

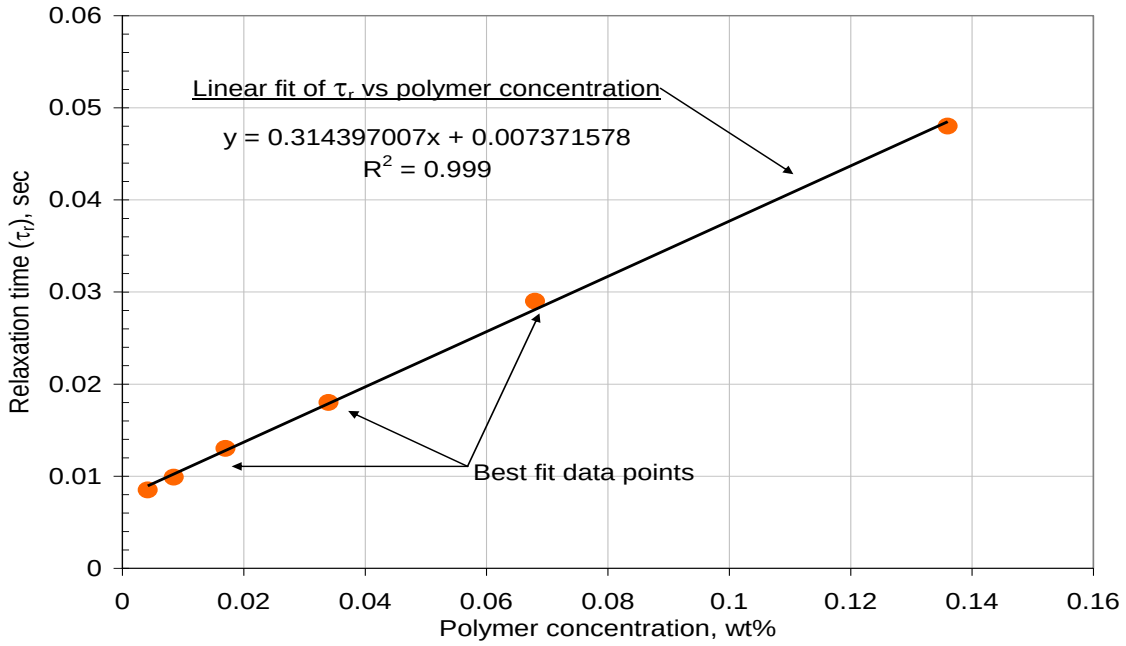

Figure 2.11: UTCHEM model fit to τ_r obtained by matching Chauveteau's data assuming λ_2 as 0.01

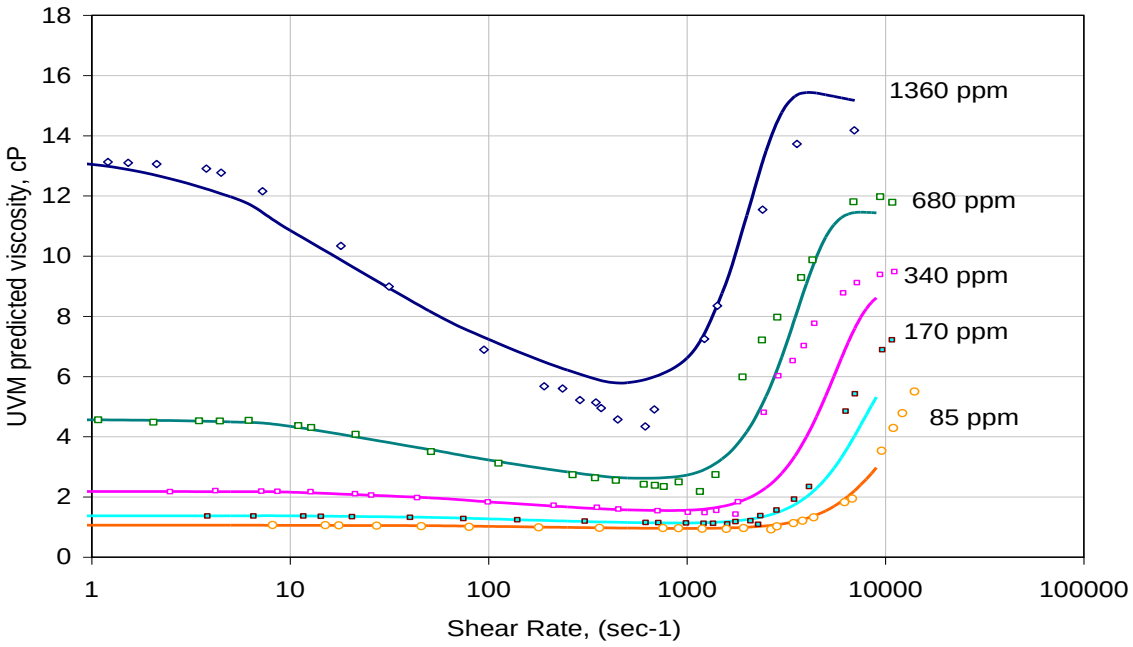

Figure 2.12: UVM model fit to Chauveteau's data

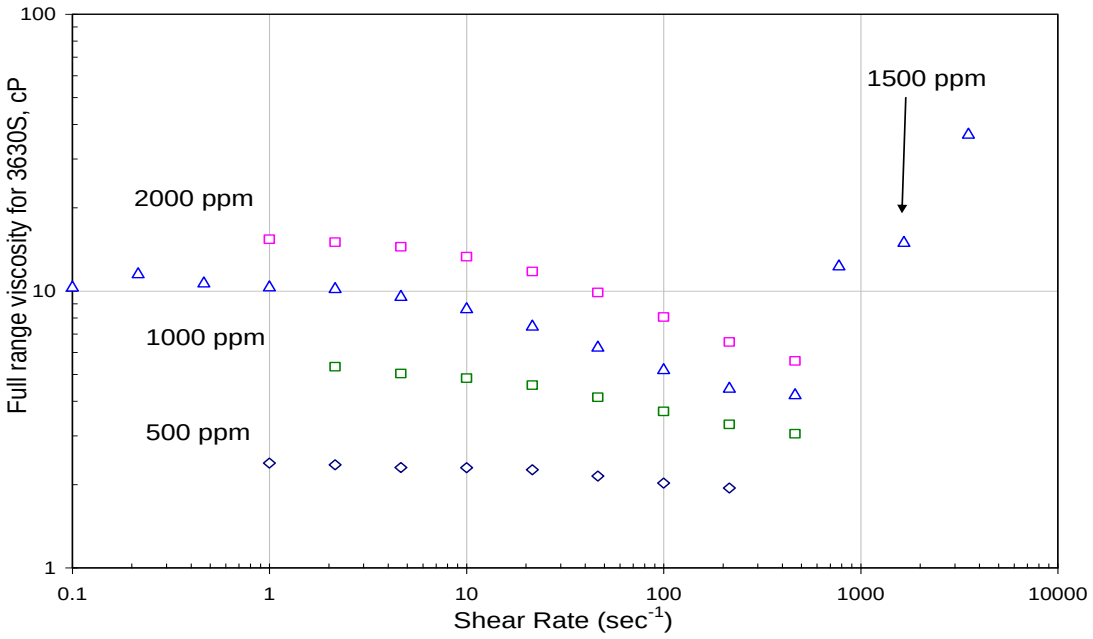

Figure 2.13: Laboratory data of Flopaam 3630S at Salinity B

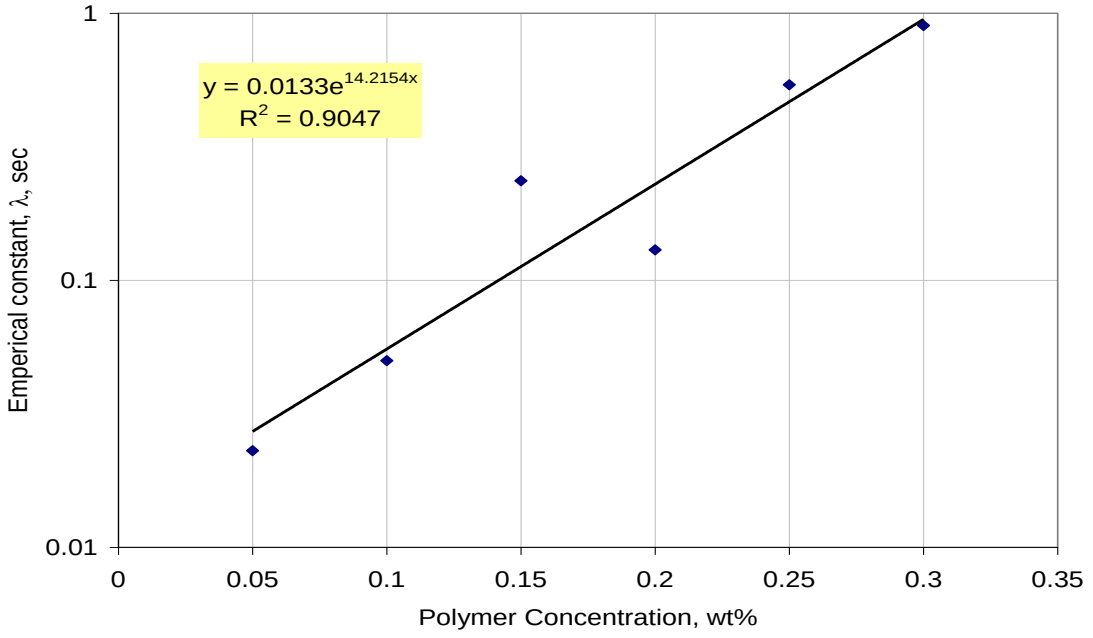

Figure 2.14: UTCHEM fit of λ obtained by matching laboratory data

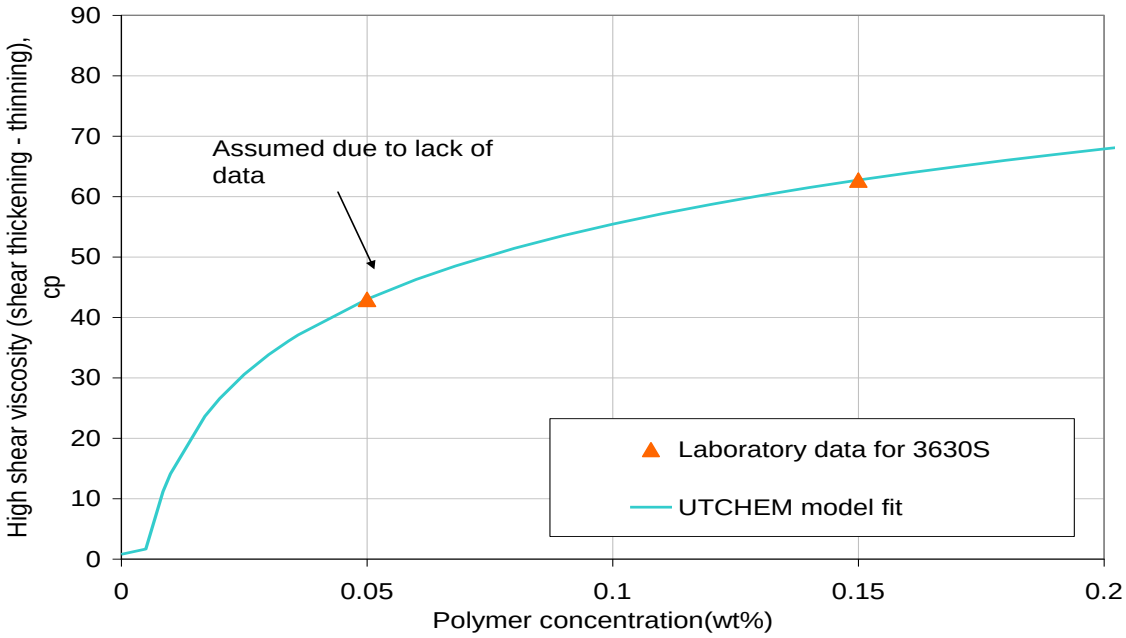

Figure 2.15: UTCHEM fit of high shear viscosity obtained by matching laboratory data

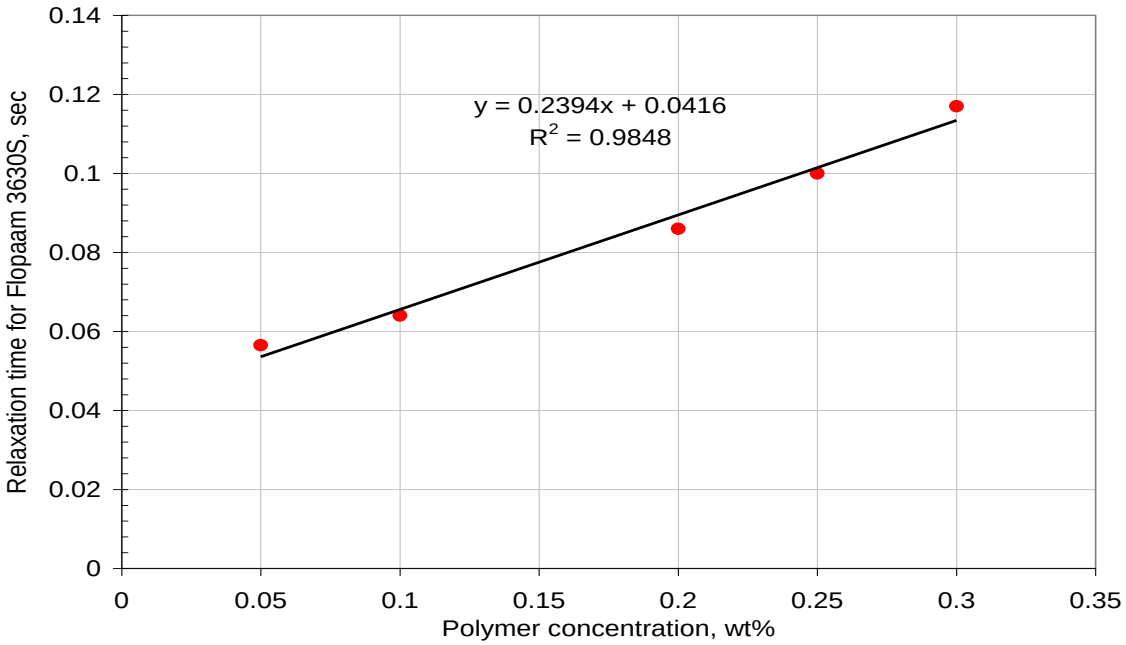

Figure 2.16: UTCHEM fit to relaxation time obtained by using correlation by Kim et al. (2010)

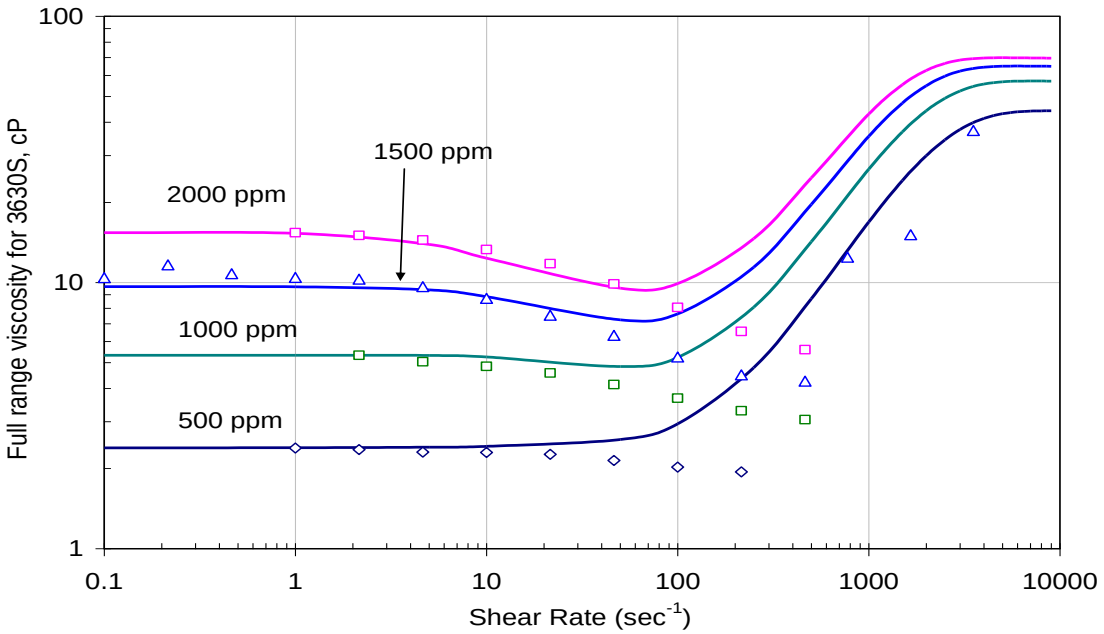

Figure 2.17: UTCHEM fit to full range polymer viscosity of 3630S polymer when λ_2 was 0.01

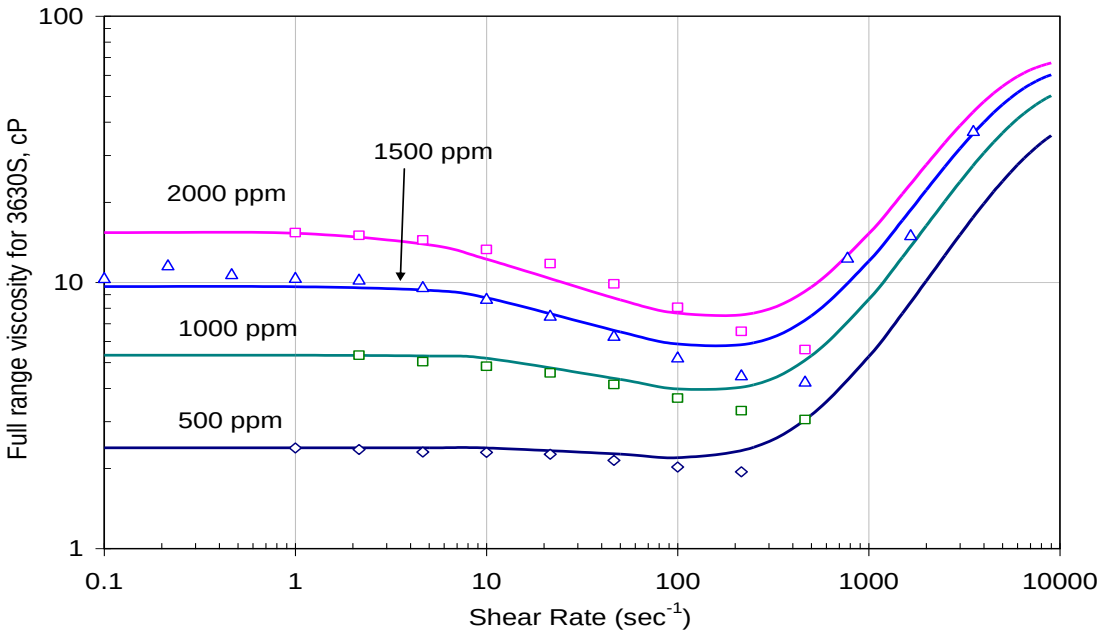

Figure 2.18: UTCHEM fit to full range polymer viscosity of 3630S polymer when λ_2 was 0.003

3 Polymer injectivity dependence on grid size

This chapter presents the effect of grid size on polymer injectivity. Very often the simulation models are large and hence, large grid sizes are used to save computational time. However, use of large well grid sizes together with conventional injectivity calculation scheme (Peaceman) significantly misrepresents the injectivity, especially for polymer. A systematic study was carried out to define the problem for injectivity correction when large grid sizes are used and, to find a possible correction for it. Simulations were done using very fine grid sizes and coarse grids for a single model to present the need for injectivity correction.

3.1 NEED FOR INJECTIVITY CORRECTION WITH DIFFERENT GRID SIZES

To conduct this numerical experiment correctly, a simplified five-spot pattern simulation model was set up. This homogeneous model is 2700 ft x 2700 ft x 4 ft. The permeability of the reservoir is 1 Darcy and the porosity is 20%. A five spot is simulated with the injector in the middle which is equidistance from four corner producers. Since the objective is to present the change in injectivity due to grid size change, all the wells are pressure constrained to allow maximum possible injection. The injector is constrained at a maximum of 2000 psi and the producers at a minimum of 200 psi. We assume water saturated model; hence, polymer injected displaces only water. All the physical dispersion parameters are negelected (set to zero). Other input details about the model and polymer rheology are provided in Table 3.1. It should be noted that Peaceman well radius and Darcy law was used to calculate injectivity in all the cases at the well grid block and the flag ISHEAR was input as 0.

Firstly, the model was meshed into 300' x 300' grid sizes (Figure 3.2) and a polymer was injected for 2 pore volume. Next, the same model was meshed in 180'x180',

100' x 100', 60'x60', 36'x36', and 12' x 12' (Figure 3.3) grids in Table 3.2. Since the grid sizes in all the models have the same x and y dimensions lengths, so henceforth for simplicity, a 300' x 300' model will be referred as 300' grid size model. Similarly, for all the other grid sizes model as well. The polymer injection rate is plotted against pore volume in Figure 3.4 for all the above cases. The legend of Figure 3.4 and all the other figures in this chapter represents [<grid size>, <ISHEAR>, <effective well radius>]. For example, for a simulated result of 12' x 12' grid size model having ishear set as 0 and rweff as 0, is presented as 12.0.0.

It is observed in Figure 3.4 that for all grid size cases, the injection rate decreases as the time of injection increases. This is due to an increase in polymer volume to be pushed in the reservoir. Since the well conditions are pressure constrained and the pressure drop increases with increasing polymer front size, the injection rate drops. Moreover, after 1 PV injection, the injection rate stops decreasing and it stabilizes because the polymer front has broken though.

Another interesting fact that can be seen in Figure 3.4 is that after 1 PV, the injection rate of the 12' model decreases much more sharply injection in comparison to coarser cases. This can be attributed to numerical dispersion. As seen in Figure 3.6, the polymer production curve becomes sharp for the finer-grid cases. For the coarsest-grid case, the polymer breakthrough occurs at about 0.5 PV and for the finest-grid case, it occurs at 0.9 PV. The occurrence of dispersion is further confirmed by the inspection of areal view of both the cases. Figure 3.7 and Figure 3.8 present the areal of the finest-grid and coarsest-grid cases. After 0.5 PV injection, clearly polymer is closer to the producer in the coarser case than in comparison to the finer case.

It is also interesting to observe that as the grid size increases, the polymer injectivity decreases. For example, after 0.4 PV polymer injection, the coarsest model

(300' grid size) has an injection rate of 180 Bbl/day and finest case (12' grid size) shows an injection rate of 400 Bbl/day. The injectivity difference between the coarsest model and the fine model is more than 200 Bbl/day. This is a staggering difference since all the input parameters in all the above simulated cases are the same, and the only difference is the grid size. Moreover, the time (in days) required to inject 2 PV of polymer for 12 ft grid model and 300 ft grid model is 8745 and 13934 days respectively. This means that the error in the simulations just by changing the grid sizes from 12' to 300' is about 5200 days or 14 years. Injectivity is very critical in calculating the economics for any project; hence, it is important to correct lower injectivity of coarser-grid models to match closer to those fine-grid models.

3.1.1 Explanations for Injectivity Difference at Different Grid Sizes

Earlier, the injection rate dependence on grid size is illustrated. This can be attributed to two reasons. One is that the calculated shear rate at the wellbore is not correct. The other reason expected is dispersion.

One of the main reasons for this injectivity change is shear rate. Polymer viscosity is a function of concentration, salinity, and shear rate, which is a function of fluid flux in the porous media. As the grid size increases, the shear rate decreases, polymer viscosity increases; hence, injection rate decreases. The shear rate at the well block as printed from the UTCHEM's Prof Output files is plotted with grid block size in a log-log scale in Figure 3.9. It is seen that the shear rate vs. grid size is a straight line on a log plot which gives further confidence on the results of the simulation. It is worthwhile noting that the shear rate at 300' and 36' well grid block sizes are 15 sec^{-1} and 243 sec^{-1}. This difference in shear rate prompts a big change in polymer viscosity as can be seen in the Figure 3.1, since the HPAM 3630 polymer at 3000 ppm is highly shear thinning. At 15 sec^{-1} and 240

sec^{-1}, the polymer viscosity is 35 cP and 10 cP. Furthermore, if we fit a trend line to this graph, then at injector well grid size of 1.5 ft, the shear rate is in the range of 15000 sec^{-1}. The case of 1.5 ft grid size was not simulated because the simulation time was extremely huge.

Another reason for this difference in injectivity could be numerical dispersion, since the physical dispersion parameters are zero. To illustrate this point, the polymer concentration from concentration output file was plotted for the gridblocks directly connecting an injector and producer. Figure 3.10 and Figure 3.11 compare the concentration profiles at various times for 36ft, 100 ft, and 300 ft grid sizes. In the above figures, the left most first point represents the injector and the right most point represents the producer, assuming that the wells are in the center of the grid. It is clear that the concentration front goes much further into the formation due to dispersion when a large gird size of 300 ft is simulated. For example in Figure 3.10 (after 0.5 pore volume injection), for all the cases the concentration of polymer at about 800 ft is 0.3 wt%. This is the same as injected concentration of polymer. But after 800 ft, the coarsest-grid case (300 ft) shows a concentration decrease to 0.05 wt% at 1500 grid mid point suggesting a dispersed front. However, for the finest-grid case, we note that the concentration front is sharper. This suggests the presence of polymer until 1650 ft from the injector for the coarsest-grid case and 1200 ft for the finest-grid case. This implies that in the 300 ft grid size simulation, the viscous polymer front is much farther into the formation, hence affecting the pressure profile between the injector and the producer.

It is difficult to determine the individual effects of both numerical dispersion and shear rate on injectivity. A simulation run was made in an attempt to differentiate the effect of shear rate and dilution. The polymer viscosity was made independent of shear rate, i.e. polymer was forced to behave like a newtonian fluid. To make this possible

gammahf1 was put as 10000 and gammahf2 was put to 0, hence, making polymer viscosity independent of shear rate. Polymer viscosity behavior with shear rate at various concentrations is presented in Figure 3.12, clearly showing a Newtonian behavior for low shear rates with the above mentioned gammhf input set. Now, the polymer viscosity is only a function of its concentration, hence, only dilution (and/or dispersion) effects are prominent. This simulation was done only for the coarsest case to quantify the contribution of dilution and shear rate. Figure 3.13 compares the injection rate of 300 ft grid size case for base case (in which both dispersion and shear rate have contributions, curve 300.0.0 in graph) and dispersion contribution only. It is seen that the injection rate decreases from 110 bbl/day to 77 bbl/day when newtonian polymer is modeled. This illustrates that the effect of both shear rate and dilution are prominent.

The pressure profiles between injector and producer were also plotted for the cases mentioned above at various injected pore volumes. As expected the pressure drops in the viscous front are slightly higher for the coarsest case, however, the differences are not great. For example, after 0.5 PV injection, at a center-point distance of 600ft, all the cases have 0.3 wt% polymer concentration (Figure 3.14). But the coarsest case has the most pressure drop. This could be attributed to the viscosity difference of 3 cP (Figure 3.16) between coarsest-grid and finest-grid model where the coarsest grid size shows a higher viscosity. Similar behavior is seen in Figure 3.15 and Figure 3.17 which presents the pressure profile at 0.9 PV. This difference in viscosity intern refers to shear rate calculation difference.

The next section explains the ways by which injectivity difference can be corrected.

3.2 INJECTIVITY CORRECTION USING EFFECTIVE WELL RADIUS FOR 1DARCY RESERVOIR

In the above section, the need for injectivity correction is illustrated. Assuming that the finest-grid case is closest to reality, polymer injectivity for the coarser-grid models should be corrected. In this section, the injectivity of the coarser models are corrected by using an effective well radius approach (ishear =1).

Effective well radius (henceforth rweff) is an input parameter in UTCHEM. The basic idea behind the use of rweff is to alter the shear rate of the well block. By introducing rweff, the flux is calculated based on the surface area of the well and the radius is considered to be rweff input.

$$u_\ell = \frac{Q}{2\pi R_{weff} h}$$

where, Q is the injection flow rate, h is well height in the grid block and Rweff is an input parameter. The shear rate is then calculated using this forced velocity which is a function of rweff. As the rweff increases the calculated flux decreases, hence, injection rate should decrease. As seen in Figure 3.9, the calculated shear rate is widely different for each grid size. An attempt is presented below to correct this issue.

For the coarsest case of 300 ft grid size, when ishear =0 is used, the calculated injectivity was in the lower range (Figure 3.4:) because the shear rate was 15 sec^{-1}. The injection rate can be increased by increasing the shear rate at the well block. This was done by using rweff (ishear =1). Figure 3.18 presents an attempt to increase the injectivity by using various rweff. For example, at 0.4 PV, the injection rate by using ishear =0 is about 180 bbl/day. When rweff of 5 ft, 30 ft is used, the injection rate changes to 810 bbl/day and 370 bbl/day. This is extremely useful, because this allows us to have a tool to alter the injection rates even though the injection well is pressure constrained. Moreover, it is seen that as the rweff increases, the injection rate decreases.

This is expected as the increase in rweff decreases the flux, which decreases the shear rate, hence, the viscosity increases. This causes the calculated injection rate to decrease. Similar behavior is observed for a 100ft well grid size model as presented in Figure 3.19. For all the other mentioned models mentioned in Table 3.2, the injectivity decreases with increasing rweff.

The main objective of rweff introduction is to match the injection rate of the coarse grids match to that of finest grid. Next step was to find the rweff at which the coarse case injectivity matches to that of finest case. Consider the injectivity curve for the coarsest case (300'x 300' grid size) presented in Figure 3.4 by using ishear = 0. For this 1 Darcy reservoir, the coarsest case (300ft) almost overlaps the finest case when a rweff of 26 is used (Figure 3.24). For the 20ft grid size, the rweff required to match the injection rate of the finest case of 12 ft was found to be 7ft. Figure 3.20 presents the match of the injection rates using the rweff of 7 ft. It is encouraging to see the match of injection rate by using rweff of 7 ft. Injection rates matches of rweff simulation runs for 36ft, 60ft, 100ft models are presented in Figure 3.21 to Figure 3.23, respectively.

Figure 3.25 presents the chart of rweff vs. well grid size. It is interesting to see the change in the slope of rweff between 60 ft and 100 ft grid size. This behavior of rweff vs. well grid size suggests that when the simulation well grid size is about 300 ft, then the rweff is about 30, 1/3rd of the grid size.

3.3 RWEFF SENSITIVITY TO RESERVOIR PERMEABILITY

Similar to the above methodology, a sensitivity of rweff to various reservoir permeabilities was done. In addition to the 1-Darcy case, 500md and 5000md reservoir permeability cases were also simulated. As before, the injection rates of the coarse cases were matched to that of the finest-grid case (12ft). The variation of matched rweff vs.

well grid sizes is presented in Figure 3.26. It is encouraging to see that for all the other permeabilities, rweff shows similar behavior. As seen in 1000 md case, a change of slope rweff vs. well grid size is observed after about 80 ft grid size.

3.4 SUMMARY

To conclude, the use of effective well radius can be an effective tool to correct the errors caused by both shear and numerical dilution during a numerical simulation. Injection rates for a wide range of coarse grid sizes were matched to that of the finest-grid case. A sensitivity analysis was also done to see the behavior of rweff vs. grid size. It should be kept in mind that all the simulations were done for a single phase flow. Some of the future work can be done on (i) multiphase-flow (oil displacement cases), (ii) injecting polymer slug instead of continuous injection; and (iii) injecting different polymer concentrations.

Table 3.1: Reservoir specifications and fluid properties

Reservoir Volume, ft x ft x ft	2700 x 2700 x 4
Number of grid blocks in X, Y, Z	Refer Table 3.2
Initial Reservoir Pressure, psi	1200
Average porosity	0.2
Permeability, md	500, 1000, 5000
Initial water saturation, fraction	1
Reservoir Salinity, meq/ml	0.33
Water viscosity, cp	0.85
Water Compressibility, psi^{-1}	0
Oil Compressibility, psi^{-1}	0
Parameters to calculate polymer viscosity at zero shear rate ((AP1, AP2 , AP3), $wt\%^{-1}$	20.3, 0 , 2390.7
Shear Coefficient(Gamma C), dimensionless	24
Parameter for salinity dependence of polymer viscosity (SSLOPE), dimensionless	-0.33
Parameter for shear rate dependence of polymer viscosity(POWN, GAMMAHF1,GAMMAHF2)	1.7, 1354.9, -13.97
Permeability reduction factors, (BRK , CRK)	100 , 0.03
Residual water saturation, fraction	0
Residual oil saturation, fraction	0
Endpoint relative permeability of water	1
Endpoint relative permeability of oil	1
Relative permeability exponent of water	2
Relative permeability exponent of oil	2
Physical Dipersion Coefficients for Water	0
Pressure Contraint: Injector and Producer	Injector: 2000 psi, Producers: 200 psi

Table 3.2: Details of simulation runs

Model Name	Short Name in Text	Number of Grids	Nx	Ny	Nz	Dx	Dy	Dz
12' x 12'	12 ft model	50625	225	225	1	12	12	4
20' x 20'	20 ft model	18225	135	135	1	20	20	4
36' x 36'	36 ft model	5625	75	75	1	36	36	4
60' x 60'	60 ft model	2025	45	45	1	60	60	4
100' x 100'	100 ft model	729	27	27	1	100	100	4
180' x 180'	180 ft model	225	15	15	1	180	180	4
300' x 300'	300 ft model	81	9	9	1	300	300	4

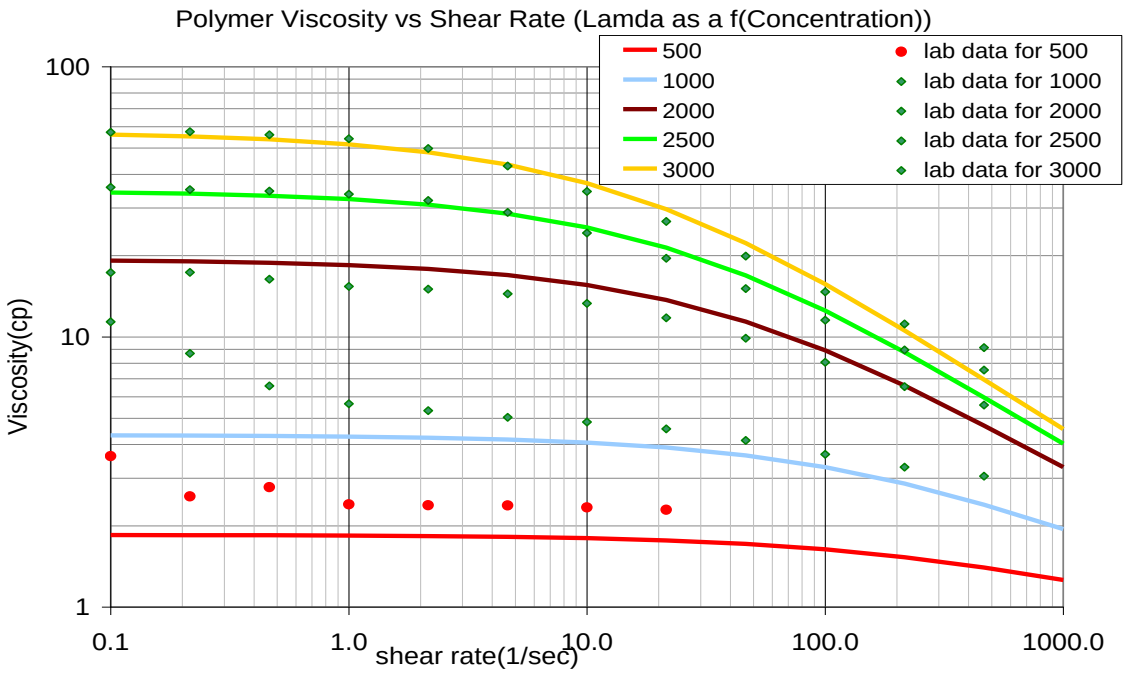

Figure 3.1: Polymer viscosity as a function of shear rate at different polymer solution concentrations

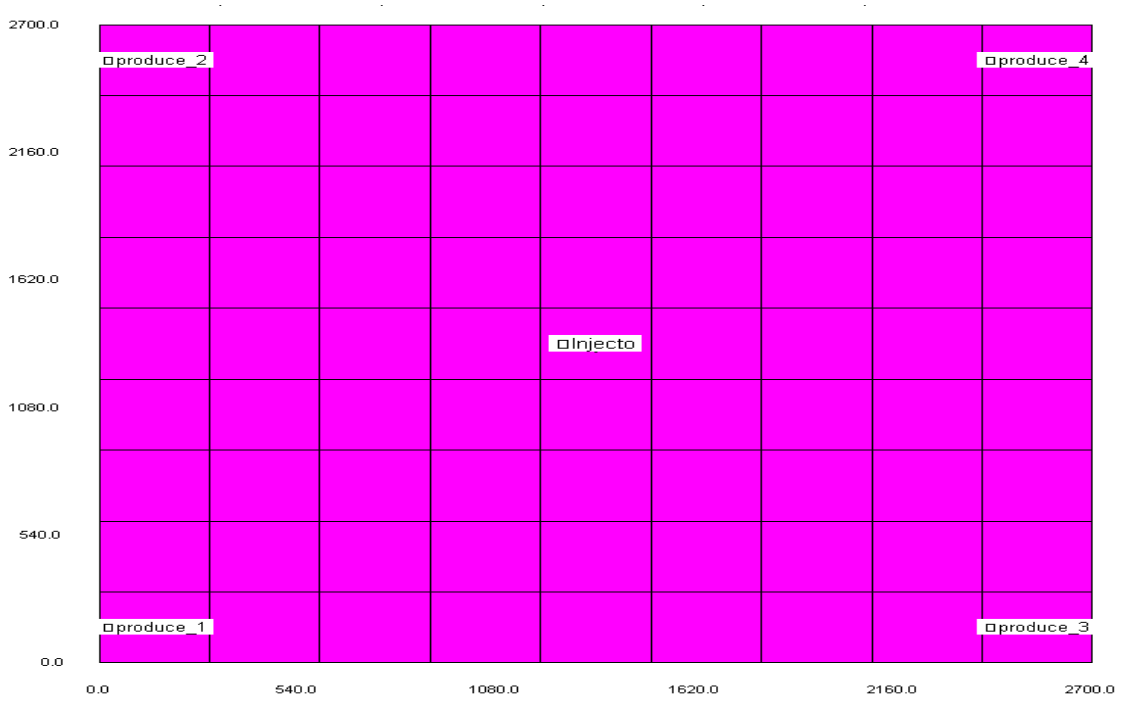

Figure 3.2: Areal view of reservoir for 300' x 300' grid size

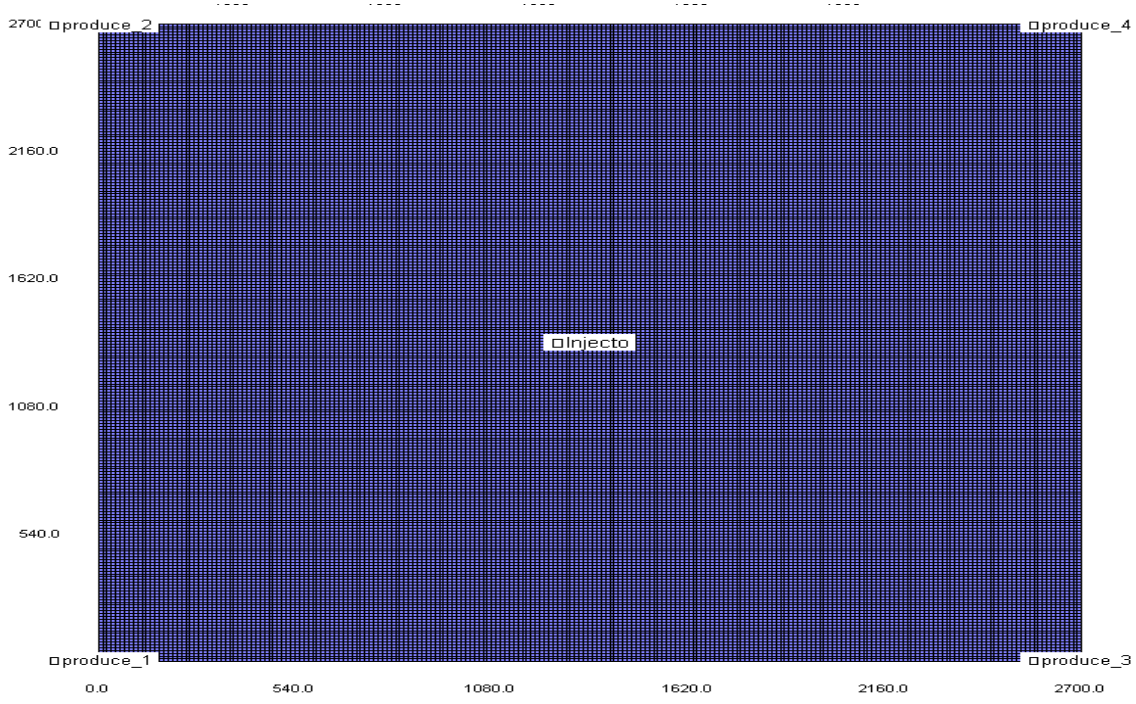

Figure 3.3: Areal view of reservoir for 300' x 300' grid size

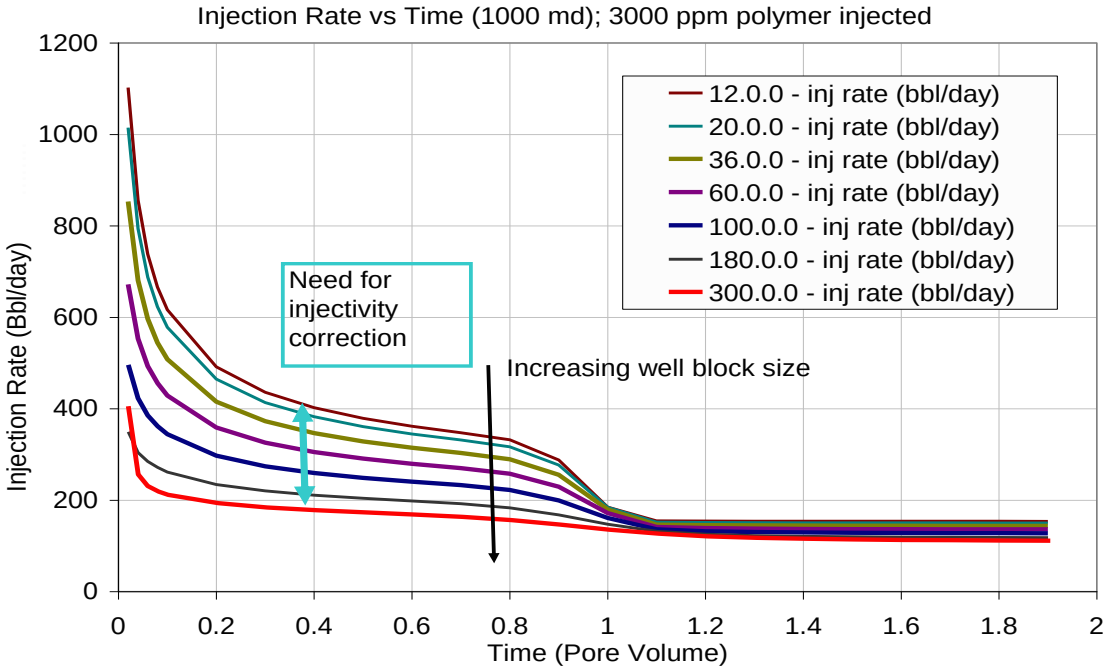

Figure 3.4: Injection rates for various grid sizes (time in pore volumes)

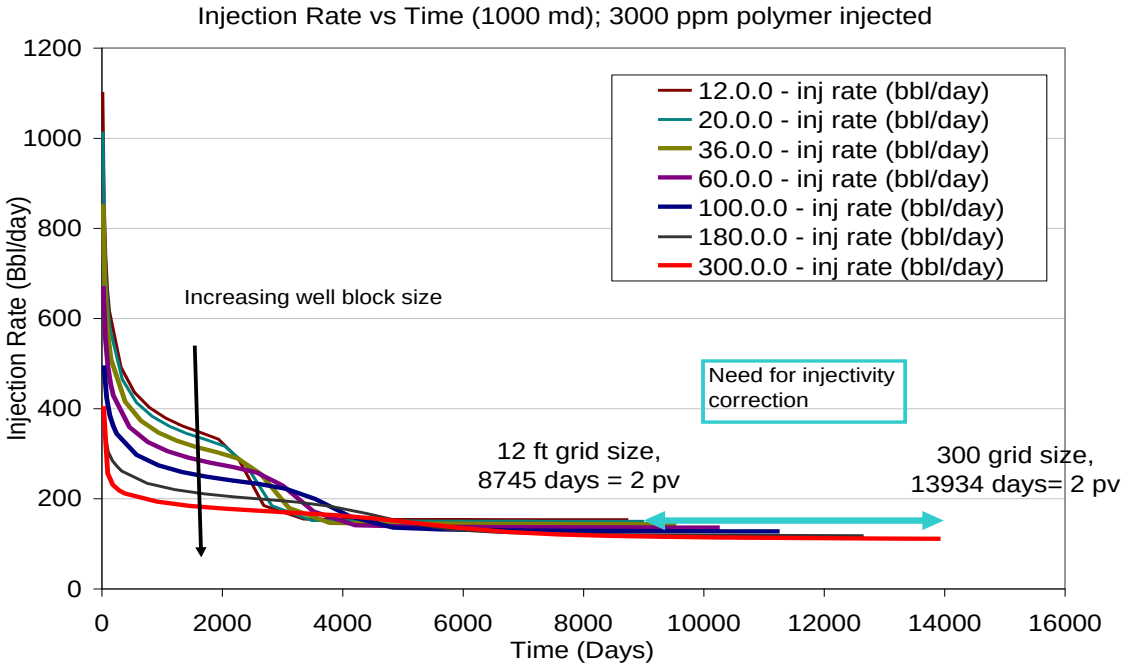

Figure 3.5: Injection rates for various grid sizes (time in days)

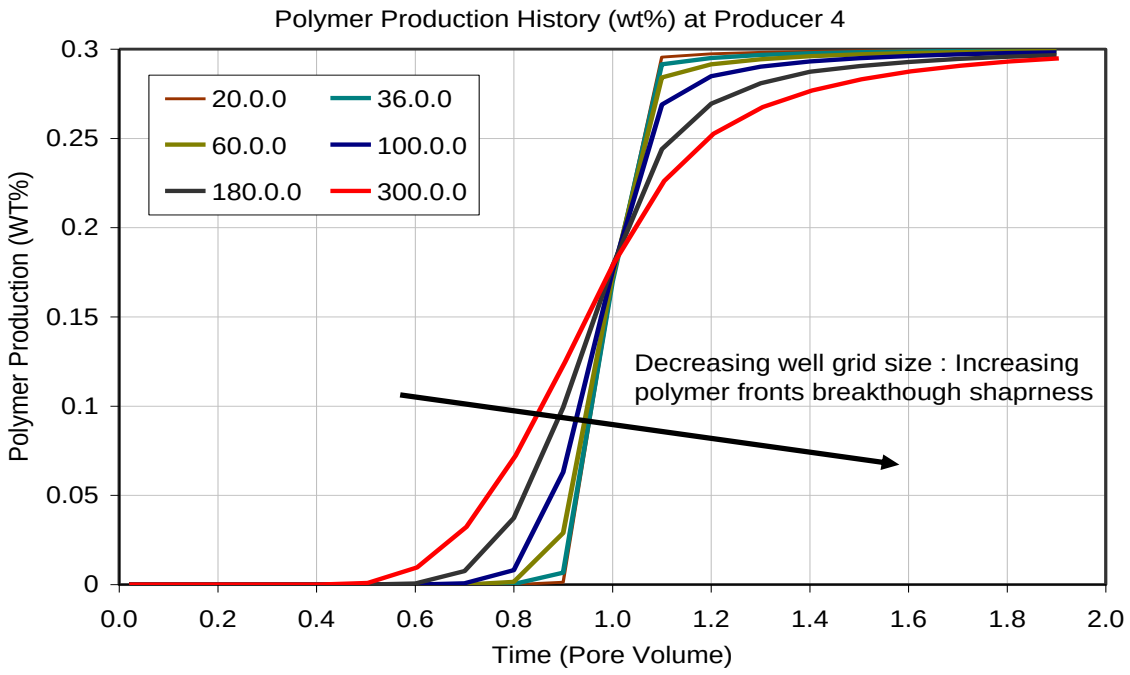

Figure 3.6: Polymer production at producer 4 for various grid sizes

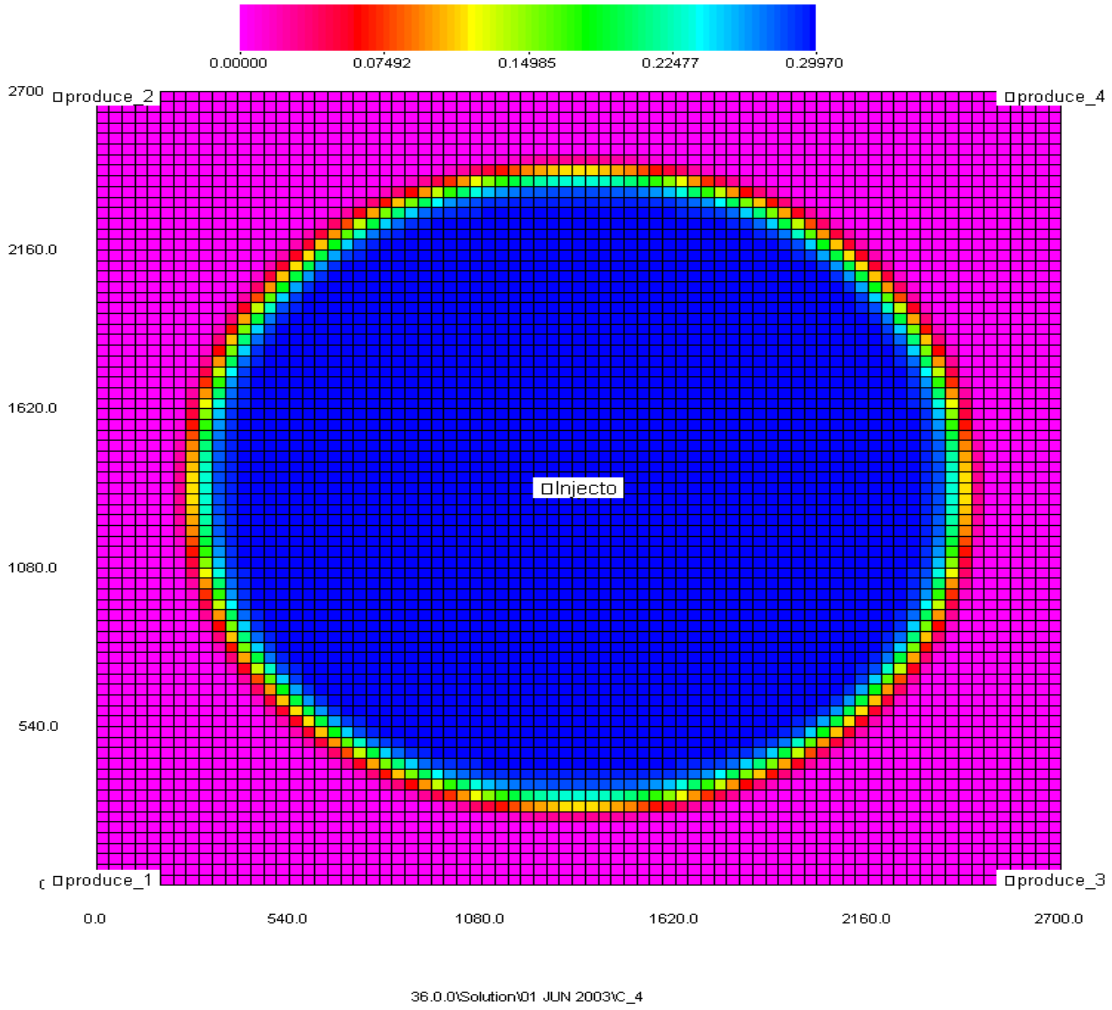

Figure 3.7: Polymer concentration front after 0.5 PV polymer injection for 12ft model

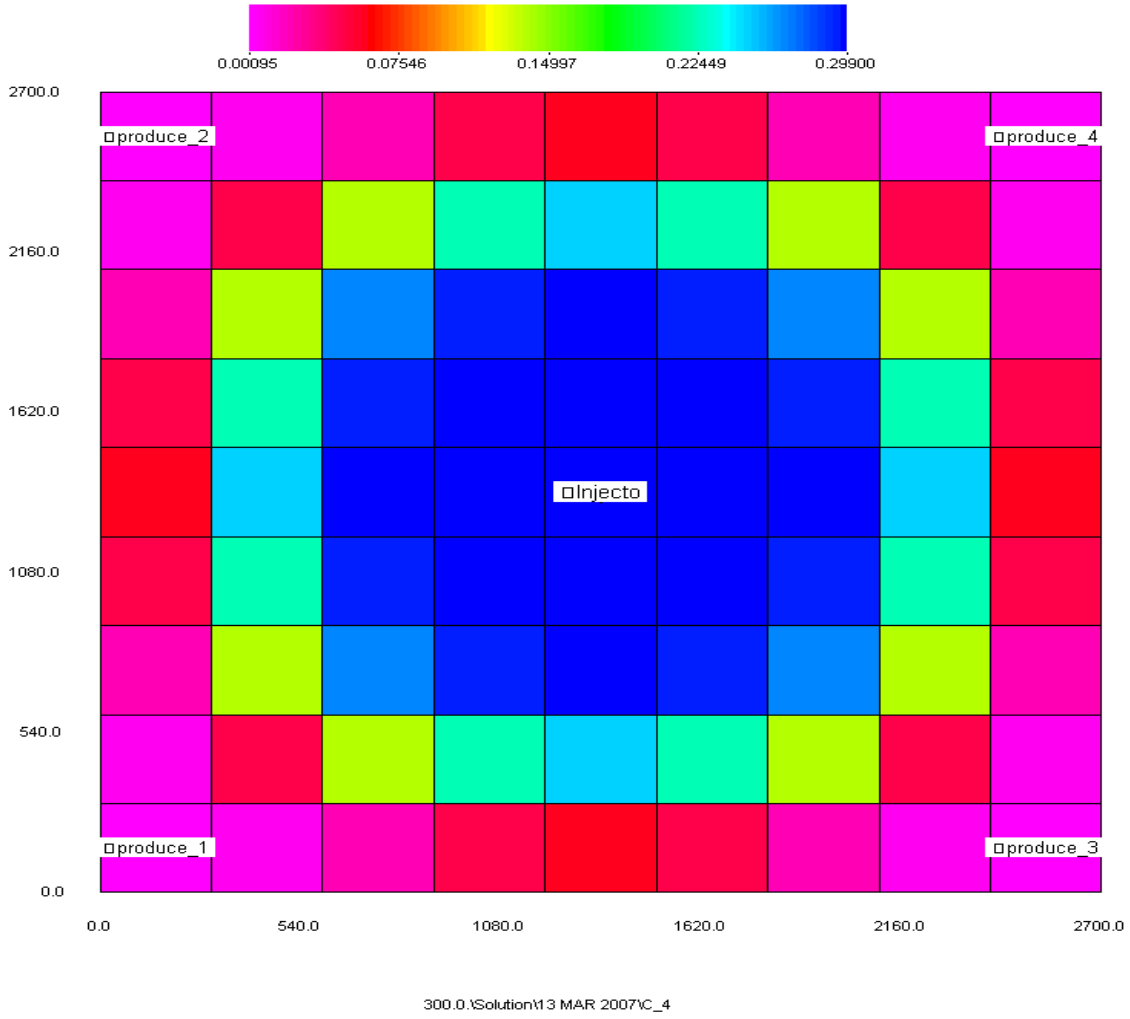

Figure 3.8: Polymer concentration (in wt %) front after 0.5 PV polymer injection for 300ft model

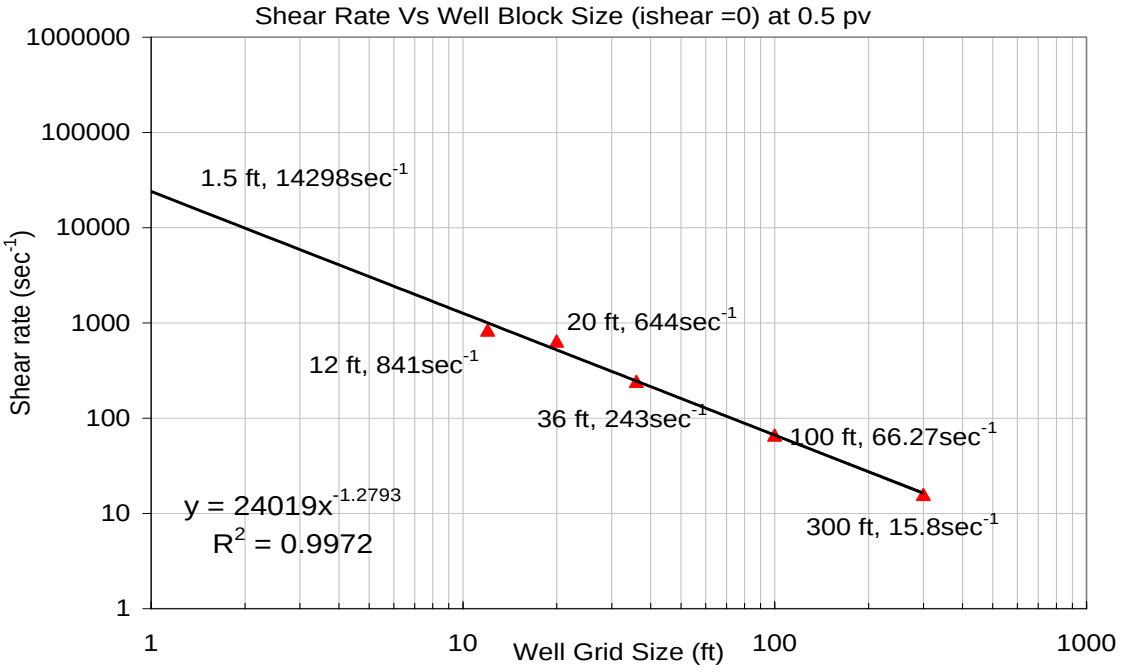

Figure 3.9: Shear rates from UTCHEM output file for various well grid sizes (ishear =0)

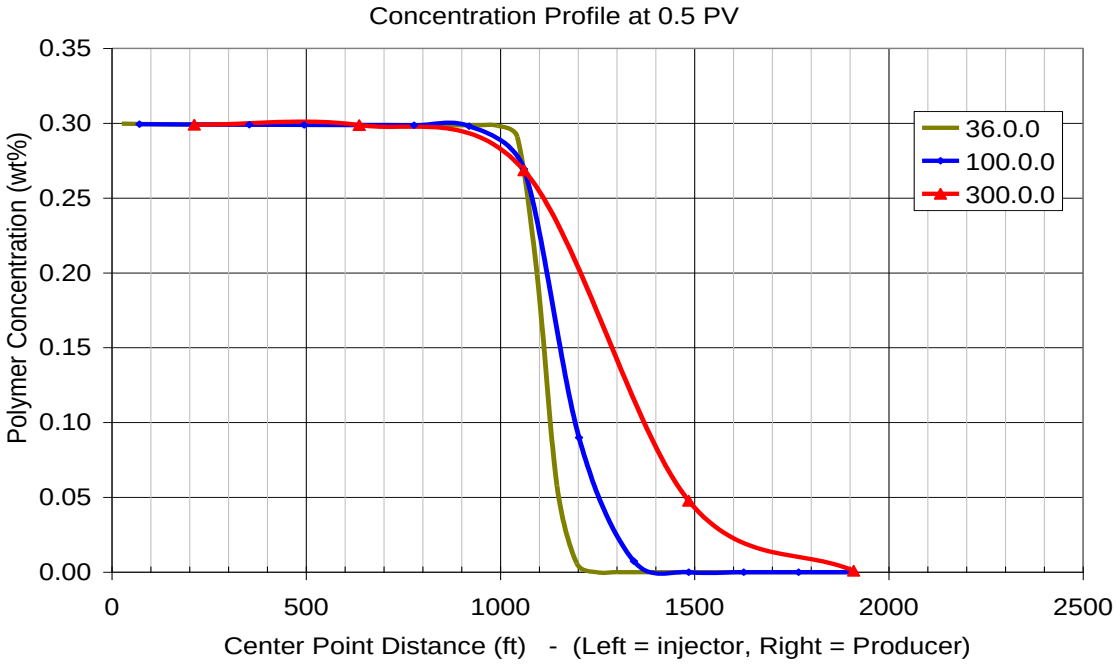

Figure 3.10: Polymer concentration profile between injector and producer at 0.5 PV

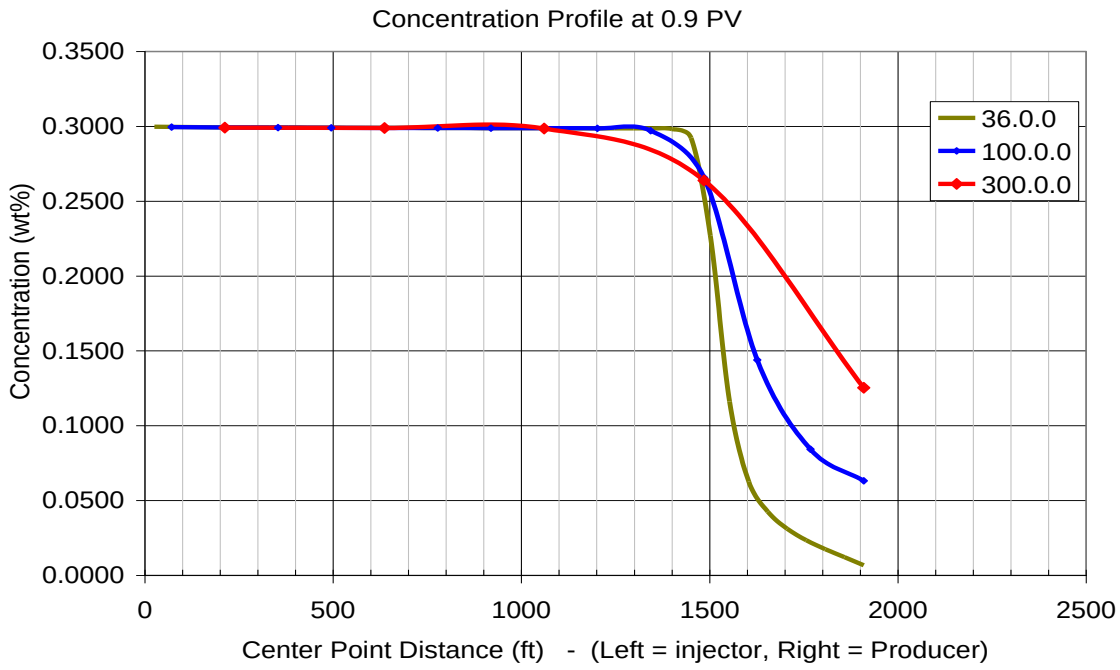

Figure 3.11: Polymer concentration profile between injector and producer at 0.9 PV

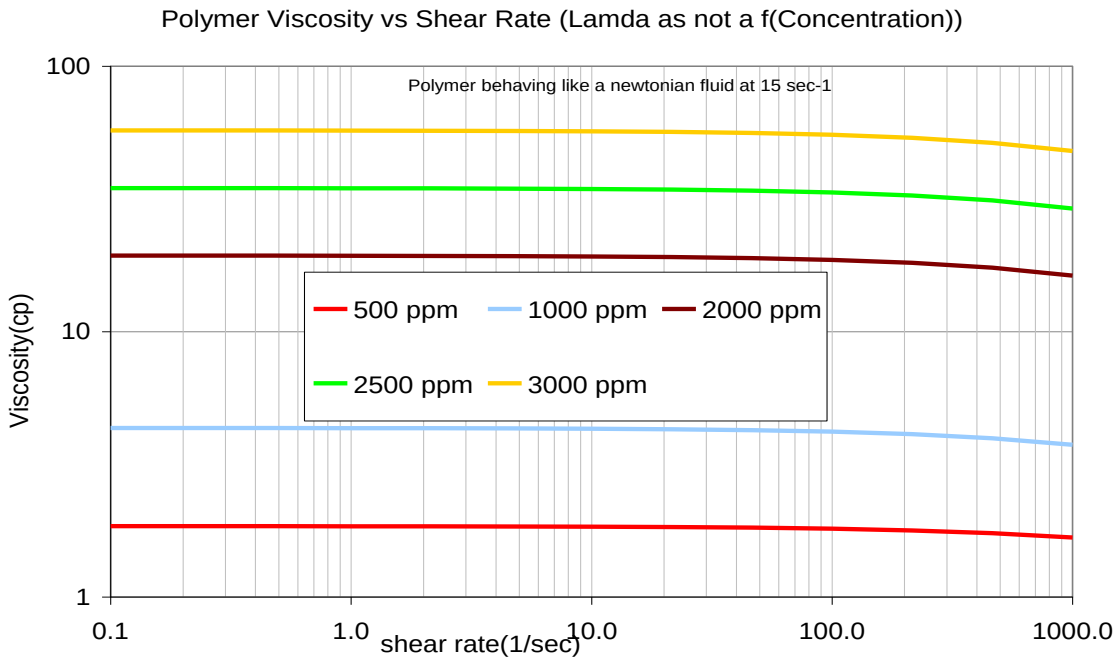

Figure 3.12: Newtonian polymer viscosity when gammahf1 = 10000

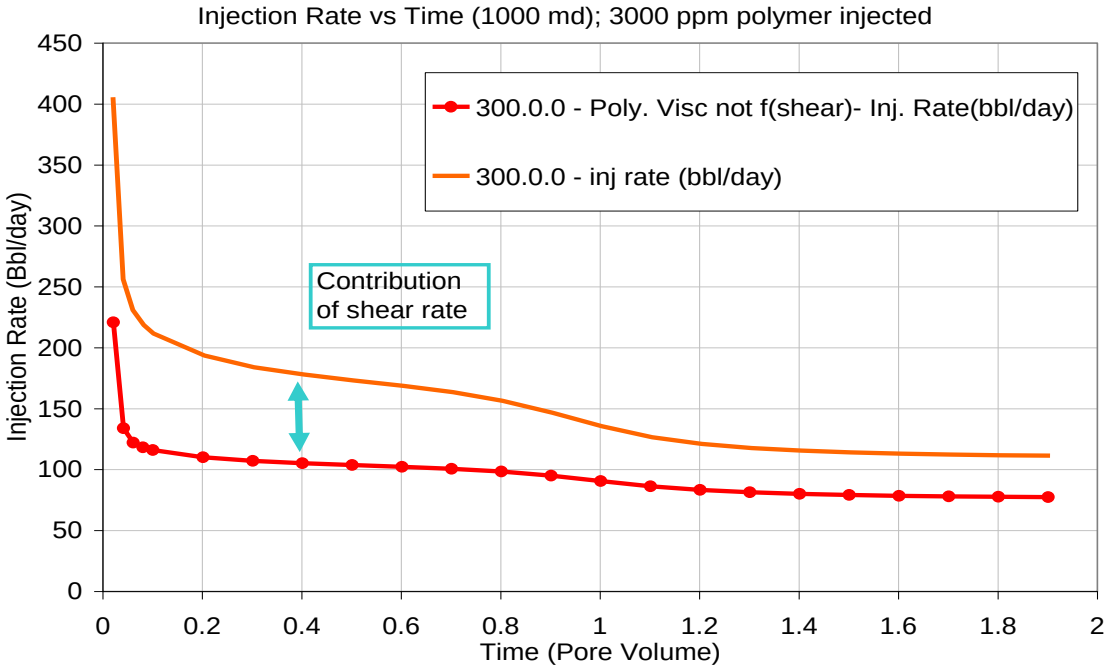

Figure 3.13: Injection rate contributions due to shear rate and dilution

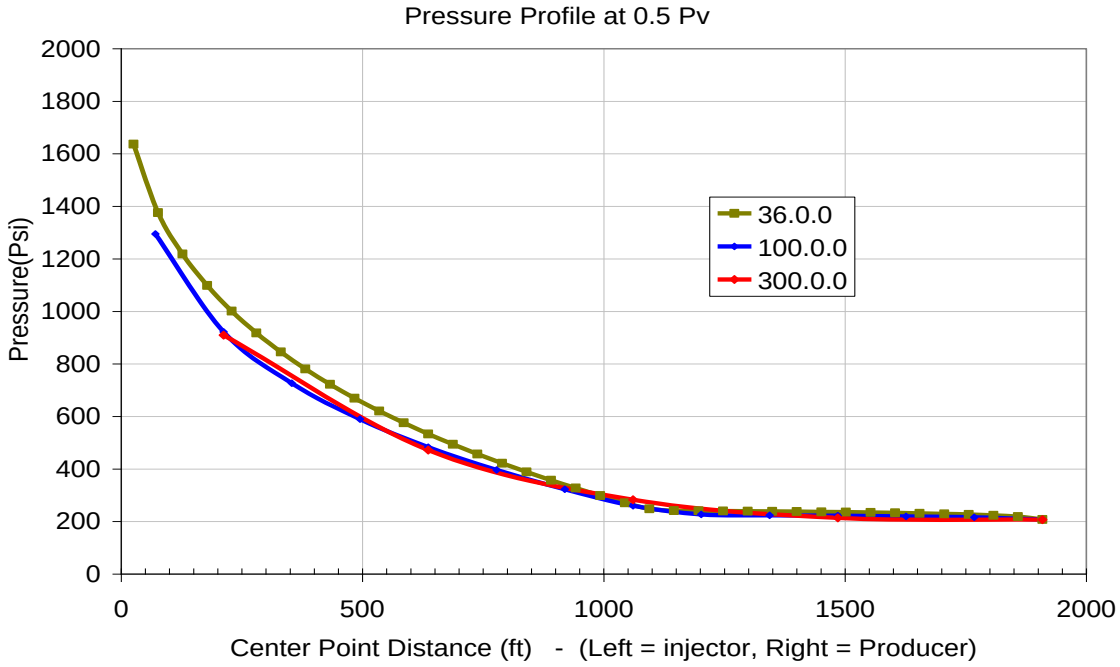

Figure 3.14: Pressure profile between injector and producer at 0.5 PV

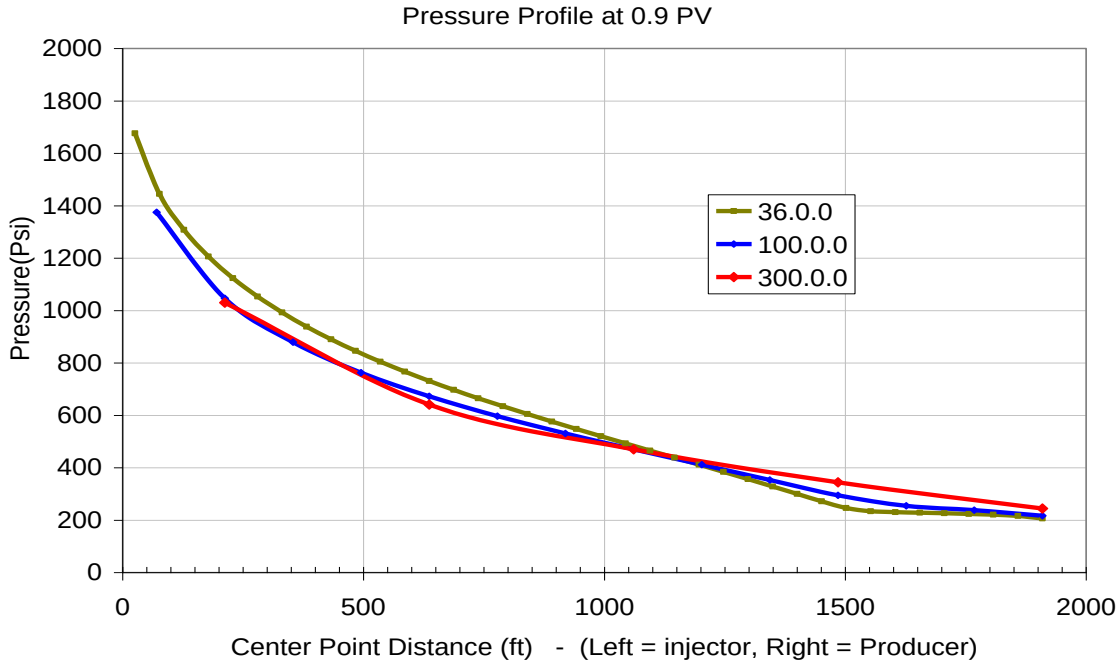

Figure 3.15: Pressure profile between injector and producer at 0.9 PV

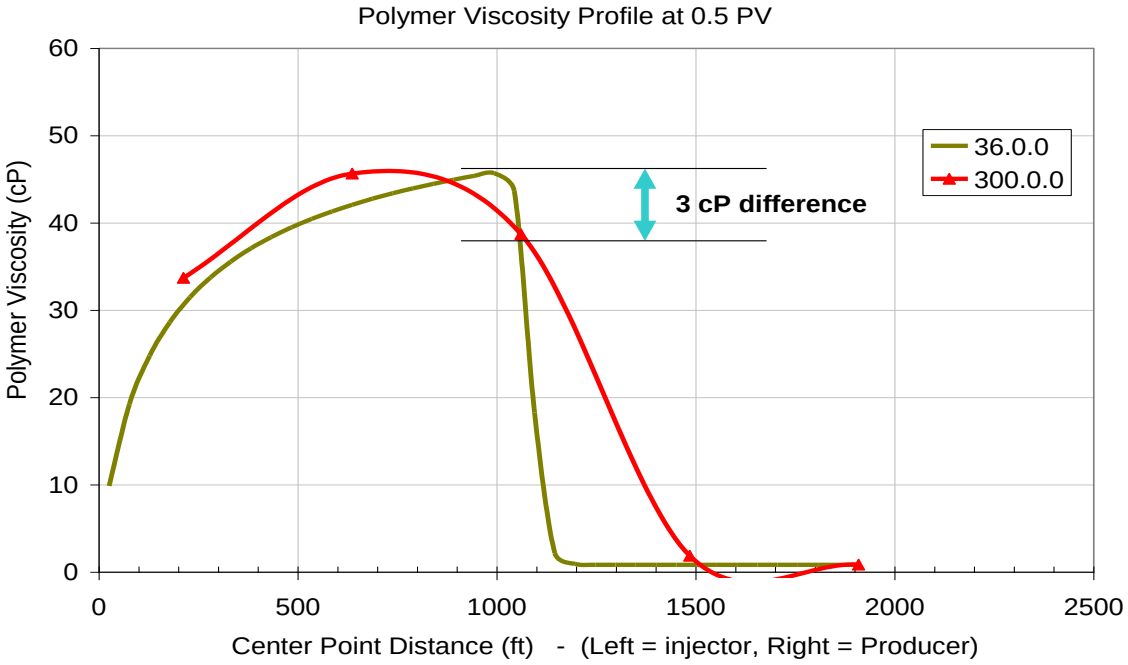

Figure 3.16: Viscosity profile between injector and producer at 0.5 PV

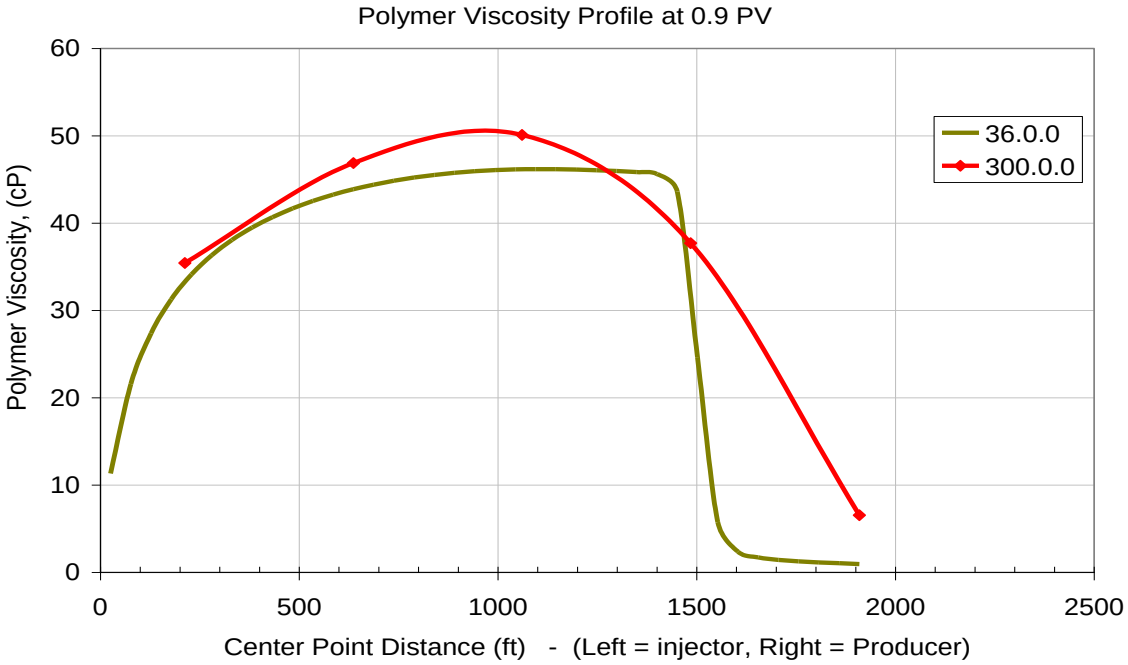

Figure 3.17: Viscosity profile between injector and producer at 0.9 PV

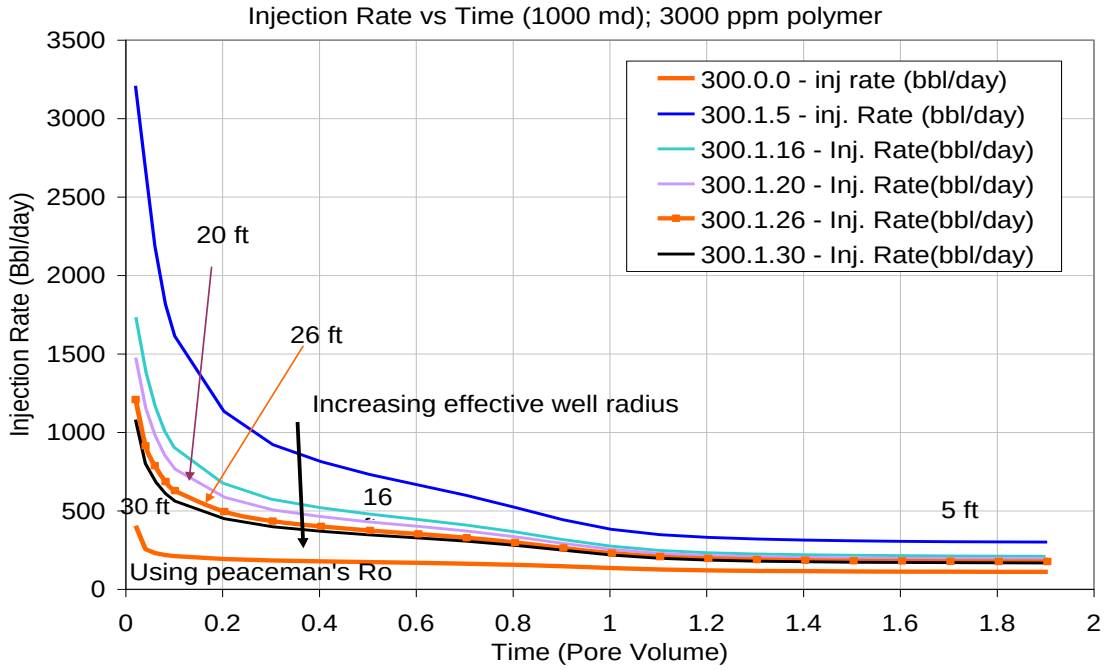

Figure 3.18: Rweff effect on injection rate using ishear =1 for 300 ft well grid size model

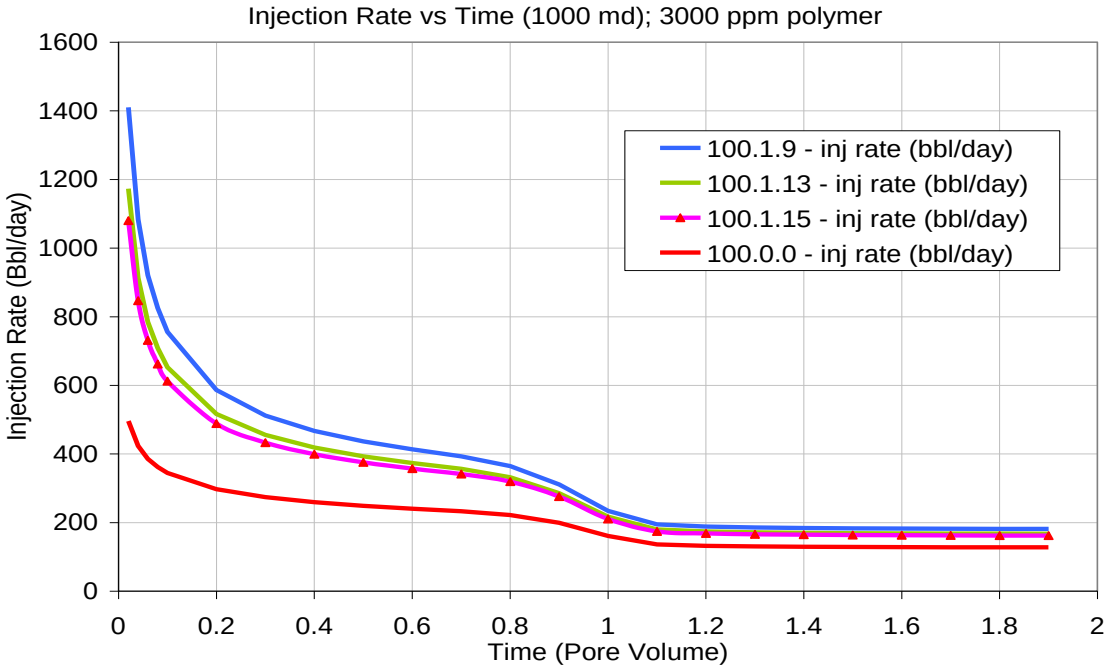

Figure 3.19: Rweff effect on injection rate using ishear =1 for 100 ft well grid size model

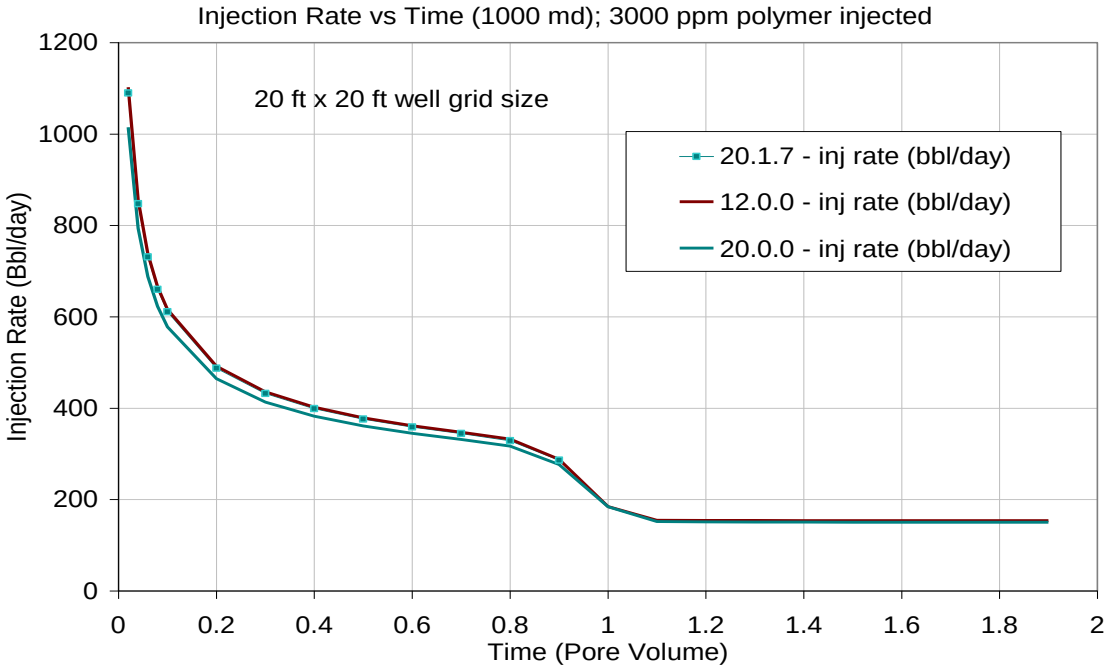

Figure 3.20: Injection rate match between 12 ft and 20 ft model using rweff of 7 ft

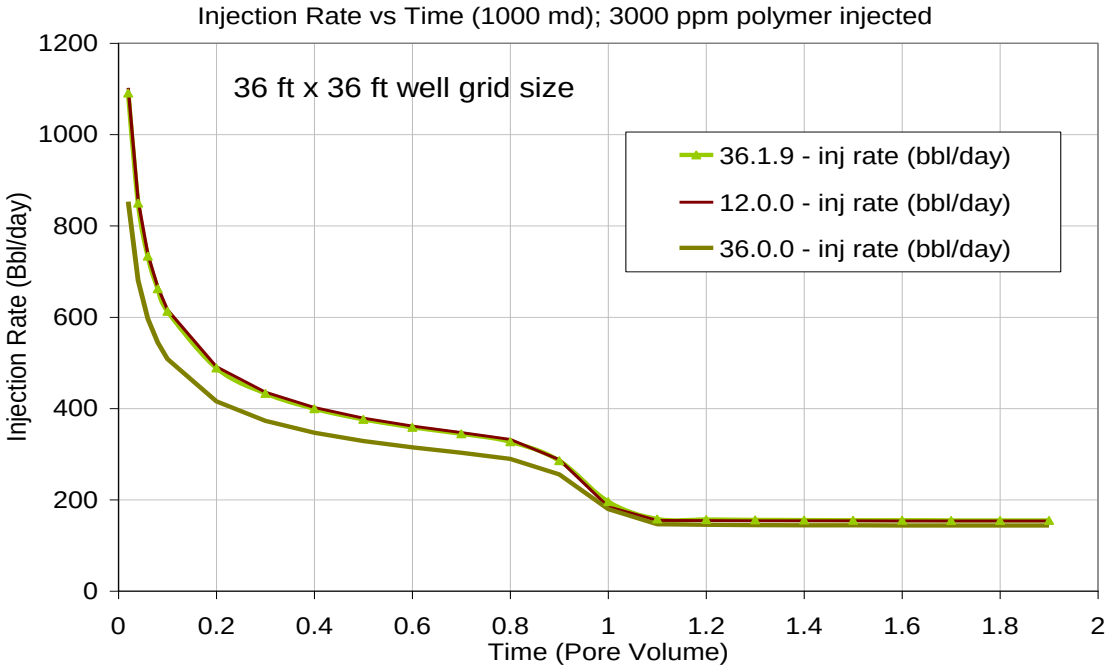

Figure 3.21: Injection rate match between 12 ft and 36 ft model using rweff of 9 ft

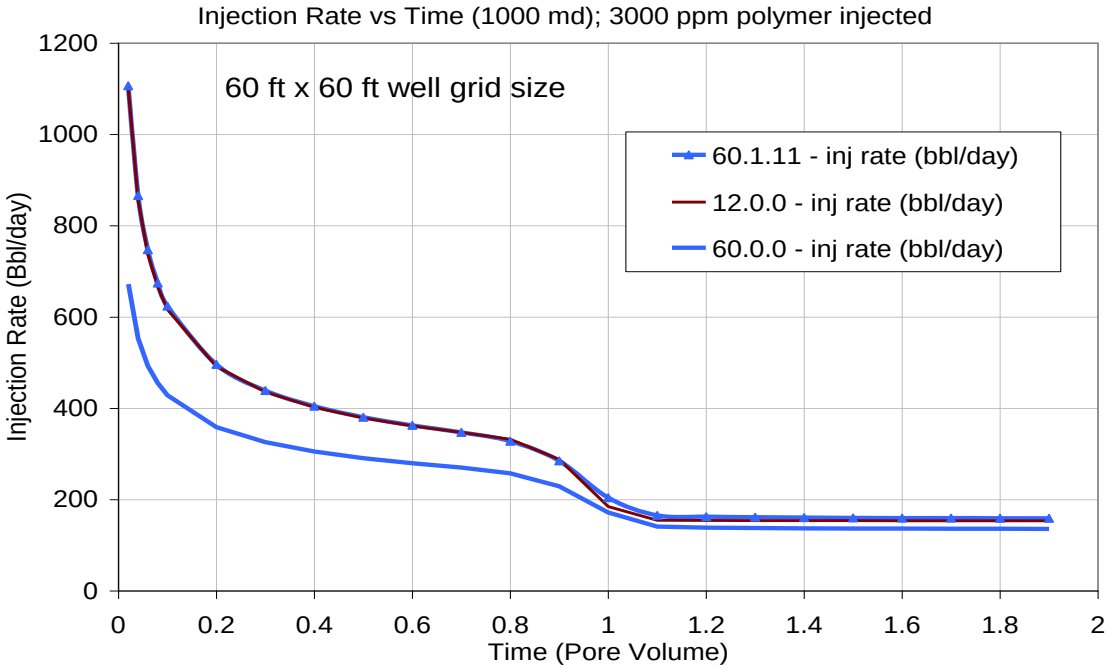

Figure 3.22: Injection rate match between 12 ft and 60 ft model using rweff of 11 ft

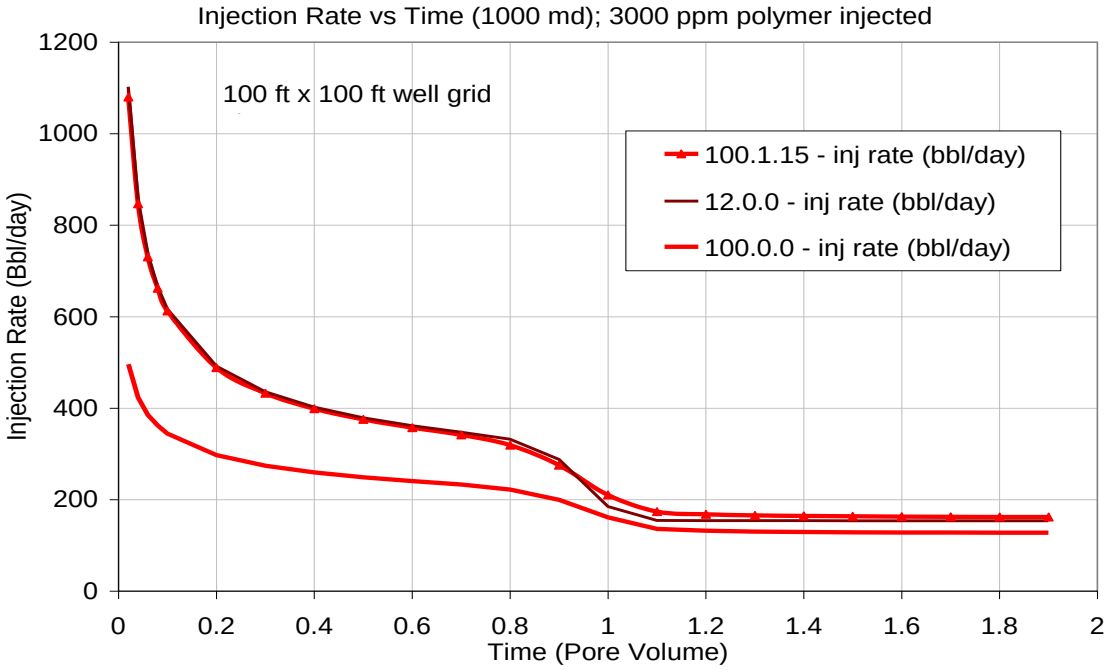

Figure 3.23: Injection rate match between 12 ft and 100 ft model using rweff of 15 ft

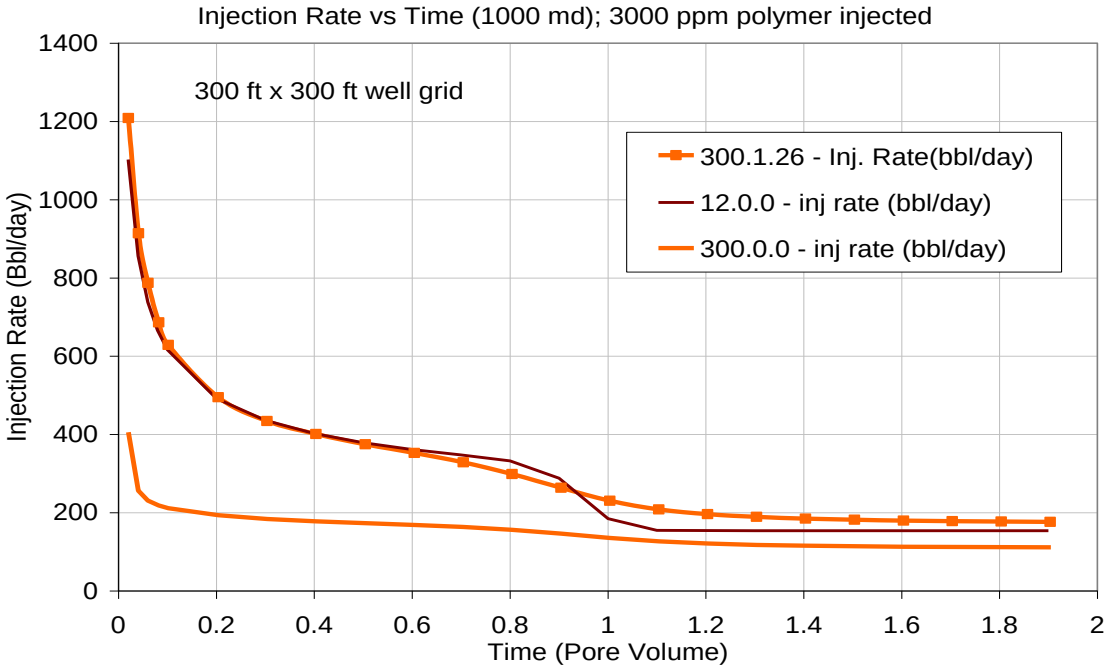

Figure 3.24: Injection rate match between 12 ft and 300 ft model using rweff of 26 ft

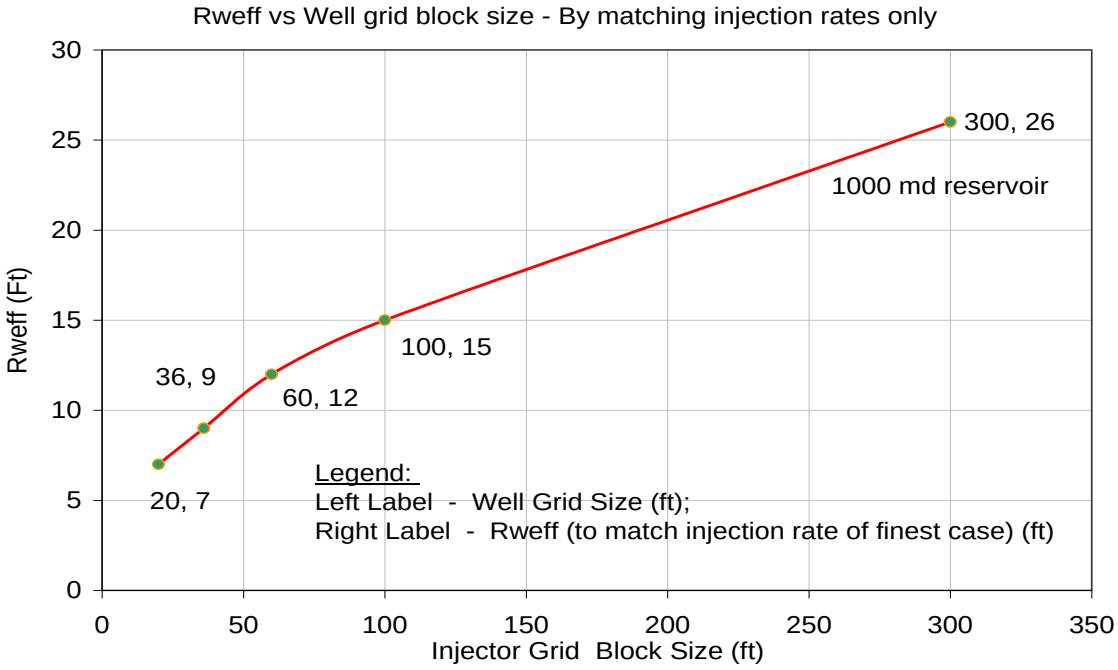

Figure 3.25: Rweff behavior vs. well grid size for 1000 md simulation model

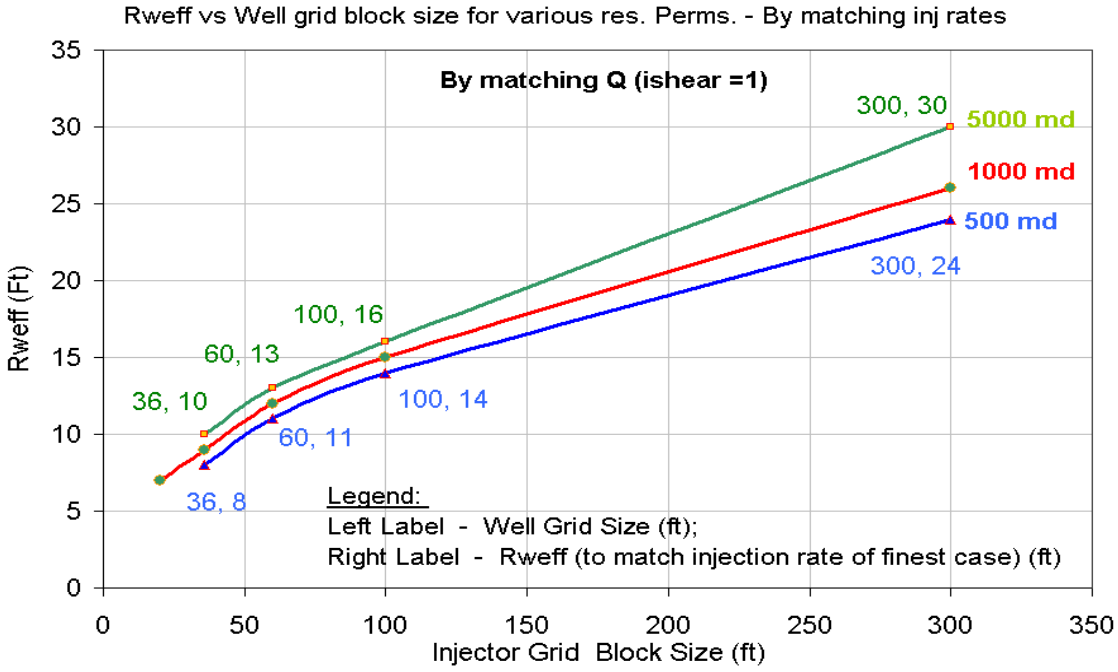

Figure 3.26: Rweff behavior vs. well grid size for 0.5D, 1D & 5D simulation model

4 Effect of Fracture and Near Wellbore Skin on Polymer Injectivity

We present a summary of simulation case studies for polymer flooding in the presence of fracture and skin for an offshore sandstone reservoir with very viscous crude oil. This reservoir is a sandstone formation with a porosity of 0.31 and high permeability of about 7 Darcy. Only a pair of horizontal wells is considered.

4.1 SIMULATION MODEL

4.1.1 Original Model

The original simulation model involved 1 injector and 3 producers. The distance between the 1st injector and 1st Producer was 984 ft. The injector is in the 12th layer and the producers are in the 1st layer as shown by the diagram below in Figure 4.1. The finest mesh in this model is: 82 ft in x direction, 65 ft in y direction, 8 ft in z direction. The simulated well length is 1300 ft (1/3rd of actual well length) and is completed parallel to simulated Y direction. There are 16 layers in the reservoir, each have different initial water saturation. The bottom most 4 layers is the aquifer.

4.1.2 Modified Simulation Model

Considering the vastness and the symmetry of the original model, a new model was prepared involving only 1 injector and the 1 producer as shown in the Figure 4.2. This simplified geological model saves a lot of simulation time.

The distance between the injector and the 1st producer was kept the same as the original model. Considering the symmetry of this homogeneous model, the 1 injector and 1 producer model is further modified. Instead of a 1300 ft simulated well length as in the original model, a 32.8 ft well length is being simulated which is about 1/120th of the actual well completed length. Even though the simulated well length in the modified simulation model is 32.8 ft, but all the results of this model will be presented for the

complete well length. This modified model is refined with the finest mesh of 2 ft, hence, allowing us to capture near wellbore fractures and skin damage.

To investigate polymer injectivity sensitivity a series of simulation were done on the above model. Polymer rheological data was obtained from the UT laboratory as a function of shear rate, salinity, polymer concentration at the reservoir temperature (Table 4.1) provides the input parameters for simulation).

4.2 MODIFIED MODEL SIMULATION

This reservoir is a high permeability reservoir with unconsolidated sand with 7 Darcy in the horizontal plane and 4.9 Darcy in the vertical direction. The salinity of reservoir brine presented in table 3.1. The injected water and polymer have the same salinity as the reservoir. The details of the reservoir input parameters are provided in Table 4.1.

Water flooding was performed for 12.25 years (4474 days) prior to polymer flooding. During water flooding the injector is constrained by rate injection of 75.9 bbl/day (3000bbl/day for 1300ft well). Water cones towards the production well during water flooding and large pockets of unswept oil still exist after the waterflood. Also, in the base case simulation the skin is zero.

After water flooding, polymer was injected into the reservoir for 10,500 days. Polymer concentration of 2000 ppm was injected during that time period. In contrast to water flooding, there is no injection rate limitation on polymer injection. This is done to see the maximum injection possible during polymer flooding. Polymer concentration of 2000 ppm is injected which yields about 15 cP viscosity. It is seen that a large amount of polymer is lost to the aquifer (bottom four layers). Simulation results also indicate the role of polymer in creating favorable mobility ratio and enhancing sweep efficiency,

where oil is pushed from the unswept zones towards the producer. A comparison of oil recovery between polymer flood and an extended water flood is presented in Figure 4.3. It is clear that cumulative oil recovery increases from 25.5% to 68.5% OOIP due to polymer flooding. Additional oil cut is also seen when polymer is injected as shown in Figure 4.4. This simulation case is henceforth referred to as the base case simulation.

4.3 ACCOUNTING FOR SKIN AS NEAR WELLBORE PERMEABILITY DAMAGE

It is very well known that near wellbore region is critical to predict a reservoir's performance. Introducing skin in the model is a means to model increased pressure difference near wellbore due to partial completion, inadequate number of perforations, turbulence, and most importantly, damage to natural reservoir permeability. It is estimated that near wellbore skin for the above reservoir is very high. This could be due to formation damage during drilling from mud and cuttings which is difficult to clean up. We simulate this high skin as mechanical skin and as near wellbore permeability damage to simulate reservoir performance.

4.3.1 Near wellbore mechanical skin

Considering a mechanical skin of 100, simulations were performed to see the effect on injection rates and cumulative oil recovery. Mechanical skin decreases the productivity index of the well and hence, decreases injection rate for the same injection pressure as shown by the equation below.

When the wellbore is parallel to Y direction, the productivity index is given by:

$$PI_l = \frac{2\pi\sqrt{kxkz}\,\Delta x}{0.15802\left[\ln\left(\frac{ro}{rw}\right)+s\right]} \quad \text{where,} \quad ro = \frac{\left[\left(\frac{kx}{kz}\right)^{0.5}\Delta z^2+\left(\frac{ky}{kx}\right)^{0.5}\Delta x^2\right]^{0.5}}{\left[\left(\frac{kx}{kz}\right)^{0.5}+\left(\frac{ky}{kx}\right)^{0.5}\right]}$$

This causes the decrease in cumulative oil recovery and a late oil recovery response as shown in Figure 4.5 and Figure 4.6 respectively. The injection rate reduces from 29,000 bbl/day (base case) to 12,000 bbl/day as shown in Figure 4.8.

The reason to introduce mechanical skin is to account for the additional pressure drop in near wellbore formation damage. The formation damage leads to the permeability in the damage zone. Since polymer is a non-Newtonian fluid, its viscosity is a function of the shear rate, hence, a function of permeability. In the above case, shear rate at the injector grid block is about 20 s^{-1}. This is a low shear rate considering a damaged zone around the injector. Hence, to introduce a higher shear rate, the permeability at the injector grid block can be altered by modeling skin and honoring the P.I. in both cases.

The next section accounts for the skin as near wellbore effective permeability.

4.3.2 Effective near wellbore permeability for skin

In the above section, skin was modeled as the mechanical skin to account for the formation damage. Skin can also be introduced by modifying the permeability at the injection grid blocks, honoring P.I. in the former case, hereafter referred to as effective skin permeability. Due to lower permeability, the near wellbore shear rate will be high. Introduction of the mechanical skin alone can not account for this important phenomenon. Since the injected fluid is polymer, its rheology needs to be coupled with near wellbore permeability damage. The only way to do so is to calculate an effective near wellbore permeability which is equivalent to the same skin by honoring the productivity index.

To account for a skin of 100, the effective permeability in near wellbore region decreased from 7 D to 0.089 D in the horizontal plane as shown in Figure 4.7. This is a large permeability contrast considering the injectivity prospects of polymer. Simulation

results clearly indicate a drop in polymer injection rate from 12,000 bbl/day (mechanical skin = 100) to about 6500 bbl/day (Figure 4.9). This decrease in injection rate is attributed to the low permeability around the wellbore. At the same pressure injection, we could only inject 6500 bbl/day of polymer with this lowered permeability. The above methodology clearly shows that modeling permeability damage by mechanical skin may over-predict the injection flow rate.

This decrease in injection rate increases the time required to obtain the same cumulative oil recovery as the base case. It is interesting to see that if the production oil cut is plotted with injected pore volume, all the curves collapse over one another Figure 4.10 and Figure 4.11). This shows that cumulative oil recovery is a function of injection rate only.

4.4 SIMULATION SENSITIVITY ANALYSIS

A sensitivity analysis was performed to understand the effect of fracture and reservoir permeability on various parameters such as cumulative oil recovery, oil cut, and injection rate.

4.4.1 Hypothetical Fracture introduction

A hypothetical fracture was introduced to the base case to see its effect on cumulative oil recovery and injection rate (Figure 4.12). The fracture is depicted as the red colored grid blocks in Figure 4.13. Dimension of fracture is 0.2' in all the directions in each grid block. It is assumed that the fracture length covers five cells in the X direction from the well block. The fracture permeability is assumed to be 1000 D x 7 D x 1000 D. A sample calculation for the effective grid block permeability in the presence of fracture is shown below.

$$k_x = \frac{1.8(7) + 0.2(1000)}{2} = 106.3\,Darcy$$

$$k_z = \frac{8.0021(4.9) + 0.2(1000)}{2} = 119.6\,Darcy$$

As presented in Figure 4.14, the change in cumulative oil recovery remains virtually insignificant at 0.36%. Moreover, the increase in injection rate remains is about 5% as well. This is attributed to high overall reservoir permeability of 7 Darcy. A localized permeability contrast of 106 Darcy did not produce any change in oil recovery. This point will be elaborated in the next section when the reservoir permeability is decreased systematically to observe cumulative oil sensitivity to reservoir permeability in presence of a fracture at the wellbore.

4.4.2 Presence of skin along with fracture

Next, we try to show the effect of fracture in presence of high skin around the wellbore. In the presence of skin being modeled as effective near wellbore permeability it is interesting to see its effect on polymer injectivity and cumulative oil recovery. The fracture permeability is assumed to be 1000 D in the horizontal plane. Accounting for the new decreased near wellbore permeability along with fracture, the grid block permeability is calculated to be about 1.74 D (Figure 4.15). It should be noted that the productivity index is honored to calculate the same. Figure 4.16 and Figure 4.17 present a comparison of cumulative oil recovery and polymer injection rate for the base case with and without fracture and base case with skin (effective perm.) with and w/o fracture. The fracture in the presence of skin increases the cumulative oil recovery from 62% to 66.8% and injection rate to a 197% increase. Clearly, in the presence of skin the fracture makes a big difference in oil recovery and injection rates.

4.4.3 Reservoir Permeability Sensitivity

The objective of this sensitivity is to understand that under which conditions the fracture impact be more significant. As shown in the previous section, presence of fracture to the base case (without the skin) does not show a significant impact on polymer injectivity and hence, on oil recovery.

To investigate this insignificant impact, simulations were performed for cases where the reservoir permeability was lowered from 7 Darcy to a hypothetical 4 Darcy and 0.5 Darcy. Both with and without fracture (no skin) cases were simulated for both the hypothetical reservoir permeabilities. It is seen that oil recovery decreases with decreasing the reservoir permeability in the same time period (Figure 4.18). The reason for this decrease can be explained by the decrease in the injection rate due to reservoir permeability as shown in Figure 4.19. Following the decrease in injectivity, a late oil bank break through is expected (Figure 4.20). It is interesting to see that as the permeability decreased, the impact of fracture becomes more significant. For reservoir permeability of 0.5 Darcy, the fracture introduction causes an increase in the injection rate by more than 11% as compared to 5% when the reservoir permeability was 7 Darcy. Moreover, the cumulative oil recovery in presence of fracture is increased by 15% for 0.5 D hypothetical formation permeability.

In the presence of fracture the relative increase in the injection rate is higher for a lower permeability reservoir. This clearly indicates that fracture response becomes more prominent for lower permeability formations.

4.5 SUMMARY

We investigated the impact of high skin in the presence of explicit fracture during polymer flooding under reservoir conditions. The sandstone formation has a porosity of 0.31 and a permeability of 7 D. A summary of the results are listed below.

1. For this 7 D reservoir, fracture around the wellbore does not enhance oil recovery during polymer flooding.
2. Fracture impact on injection rate and cumulative oil recovery decreases as the reservoir permeability increases.
3. Modelling skin as effective permeability around the wellbore accounts for polymer rheology. Hence, may be a better way of modelling skin.
4. Modelling effective skin permeability around the wellbore decreases the cumulative injection and oil recovery than if skin is modeled as mechanical skin.

Table 4.1: Summary of Simulation input parameters

Number of grid blocks in x,y,z directions	18, 5, 16
Cell Dimensions in X direction, ft	2,3.5,6.5,9,18,33,58,76, 19 x 82
Cell Dimensions in Y direction, ft	12.3, 9, 6, 3.5, 2
Cell Dimensions in Z direction, ft	8.021
Average porosity	0.31
Permeability (md) in X, Y, Z direction	7000, 7000, 4900 md
Initial water saturation	0.075
Residual water saturation	0.075
Residual oil saturation	0.25
End point relative permeability of water	0.3
End point relative permeability of oil	1
Relative permeability exponent of water	3.8
Relative permeability exponent of oil	1.9
Water viscosity, cp	0.8
Oil viscosity, cp	80
Reservoir salinity (meq/ml)	0.33
Injected water salinity (meq/ml)	0.33
Parameters to calculate polymer viscosity at zero shear rate (AP1, AP2, AP3), wt%-1	10, 0, 1600
parameter for salinity dependence of polymer viscosity (SSLOPE), dimensionless	-0.325
Parameter for shear rate dependence of polymer viscosity (GAMMAC, GAMMAHF, POWN)	3.97, 100, 1.7
Permeability Reduction factors, (BRK, CRK)	100, 0.04
Polymer adsorption parameters, (AD41, AD42)	1.4, 0
Longitudinal, Transverse dispersivity (ft)	0.16, 0.04
ISHEAR, Rweff (ft)	1, 0.35

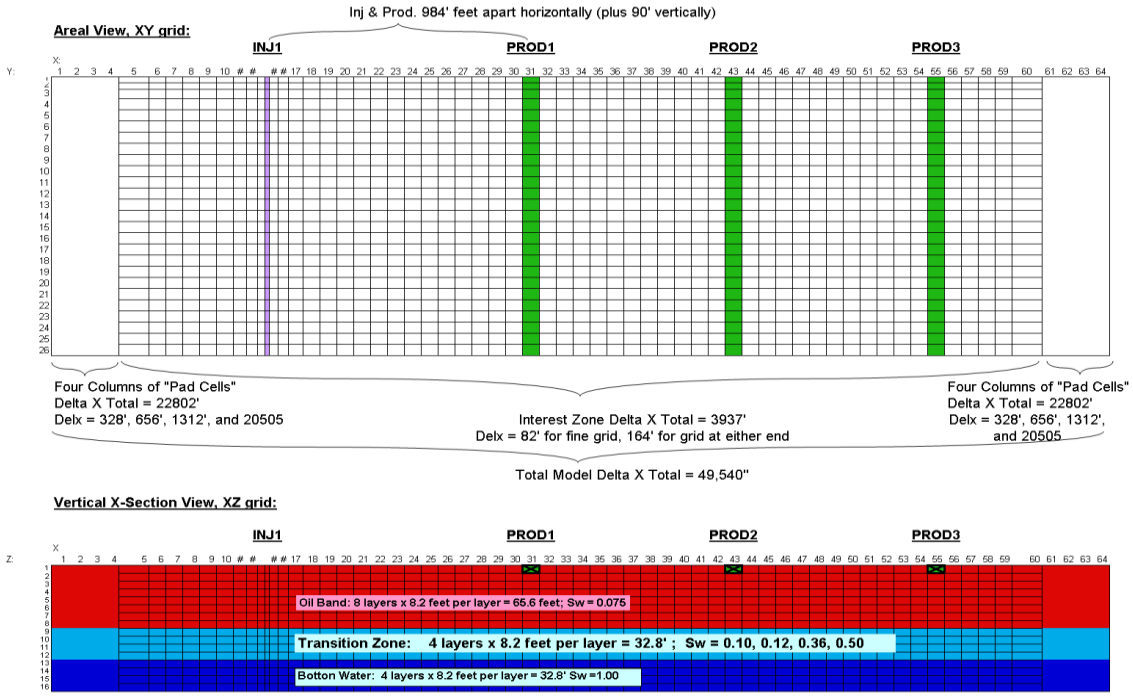

Figure 4.1: Reservoir original model

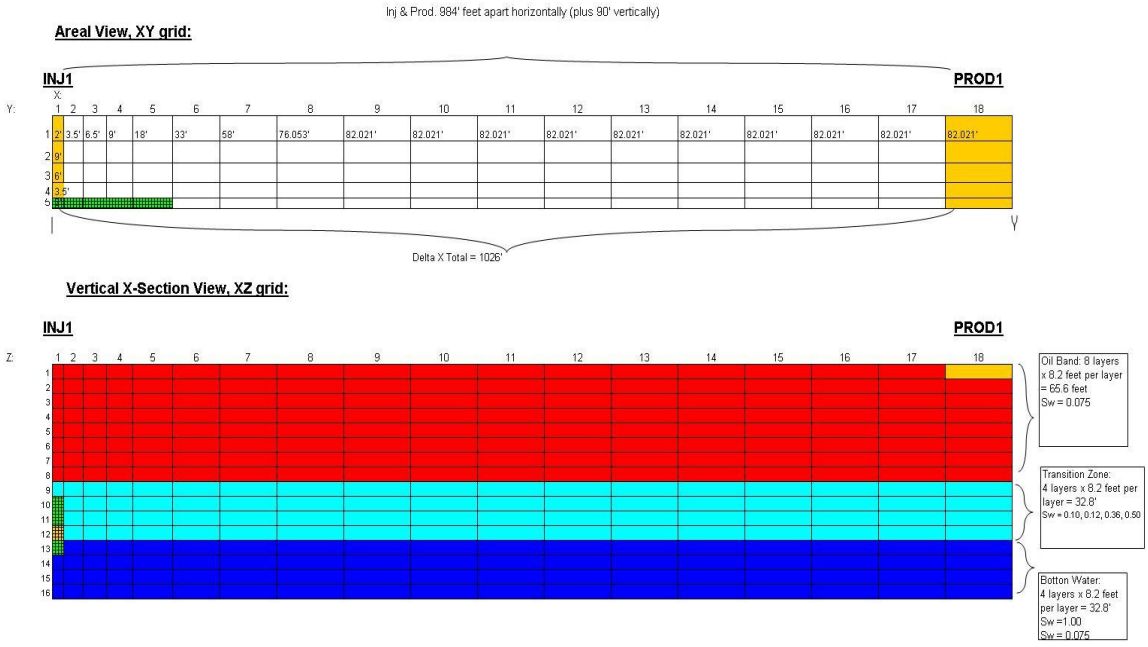

Figure 4.2: Modified simulation model; green grid blocks represent fractures

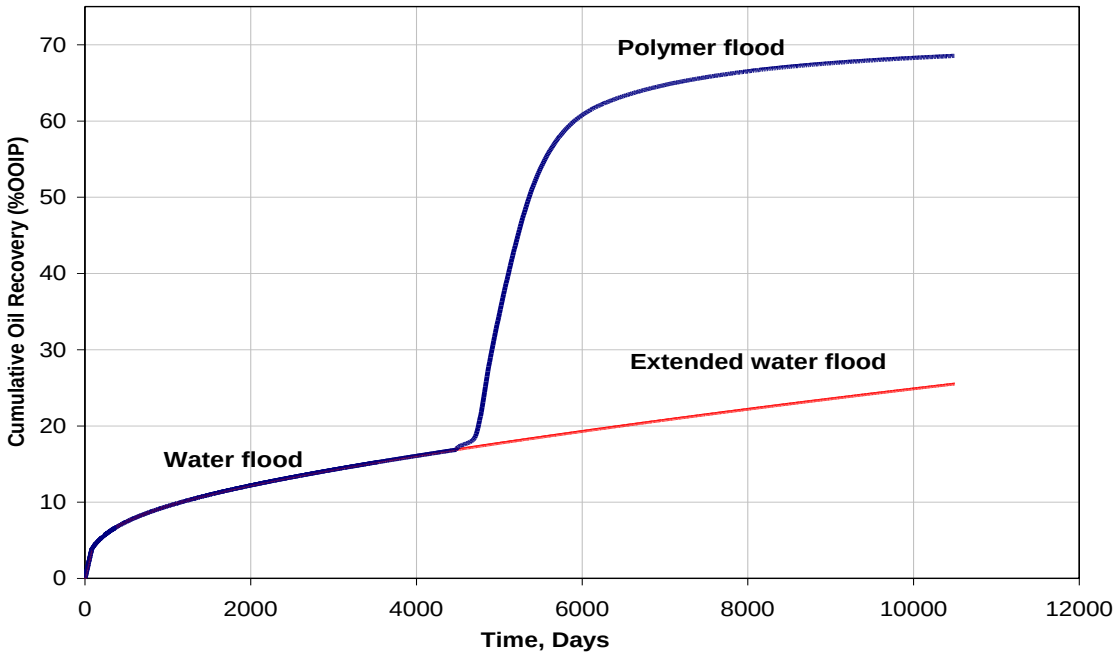

Figure 4.3: Comparison between extended water flooding and polymer flooding

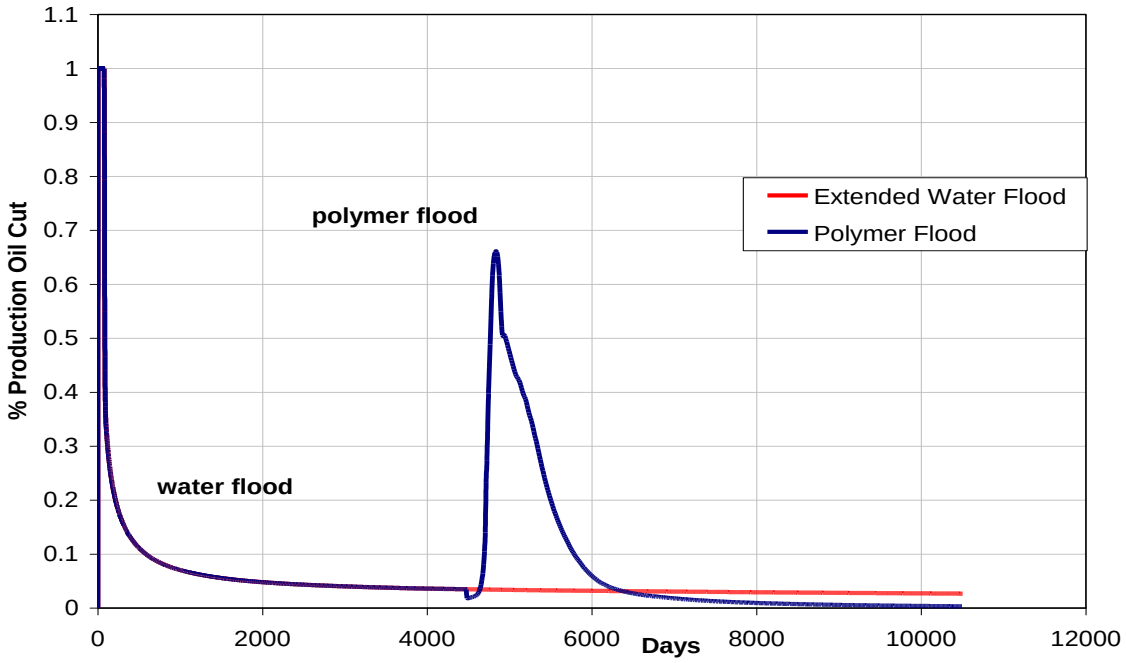

Figure 4.4: Comparison of oil cut between extended water flooding and polymer flooding

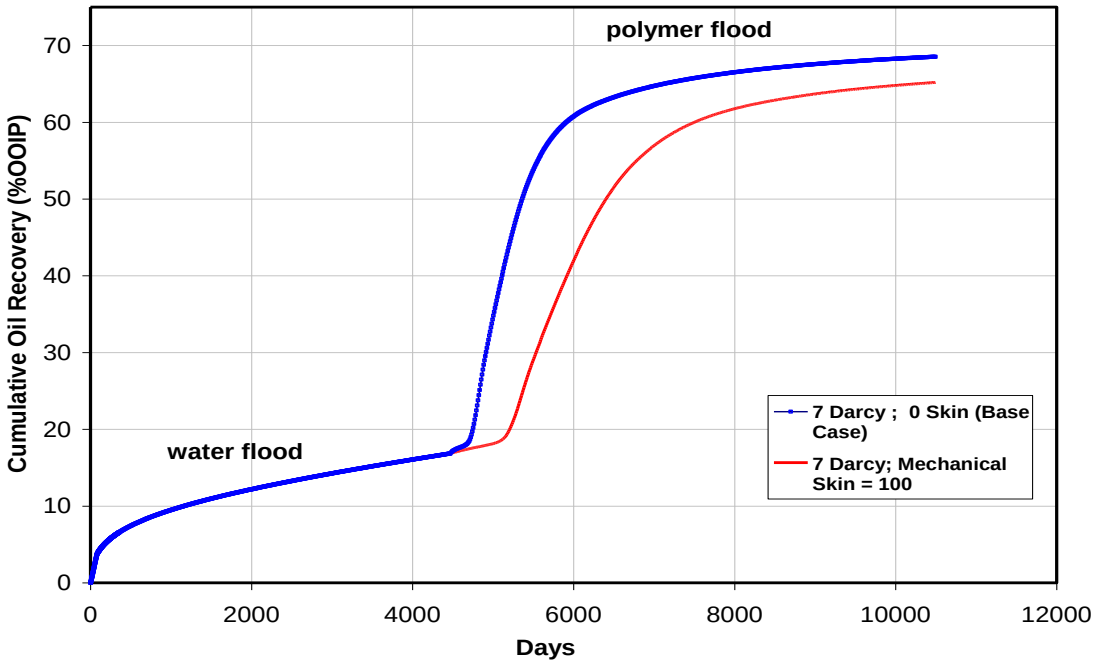

Figure 4.5: Oil recovery with mechanical skin included

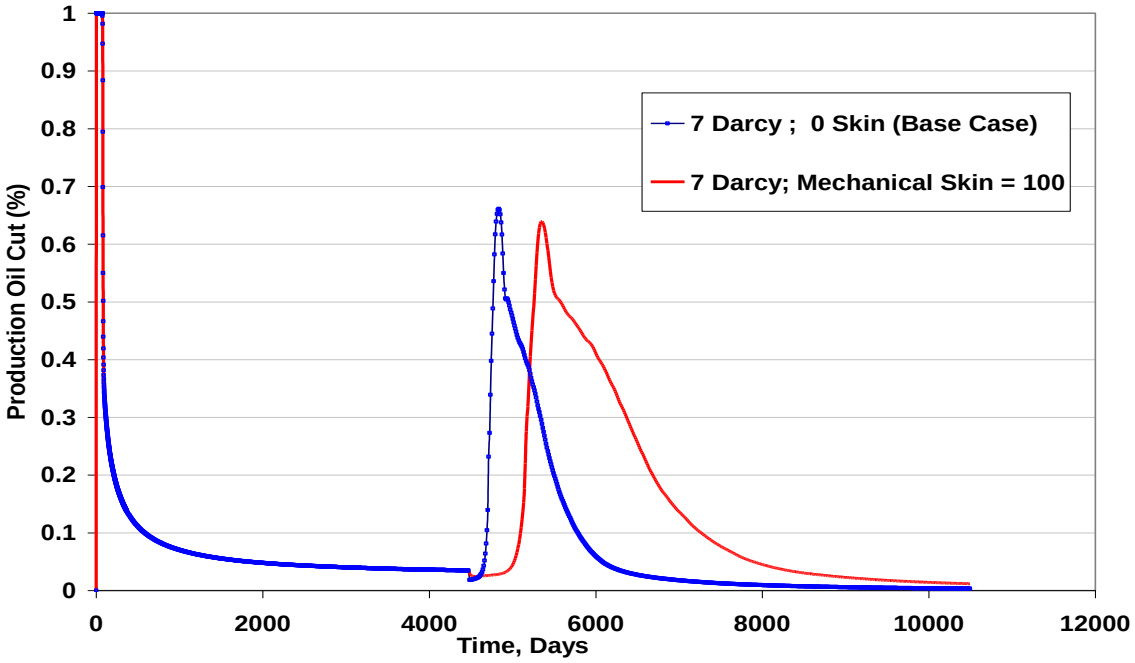

Figure 4.6: Oil cut response with mechanical skin in PI

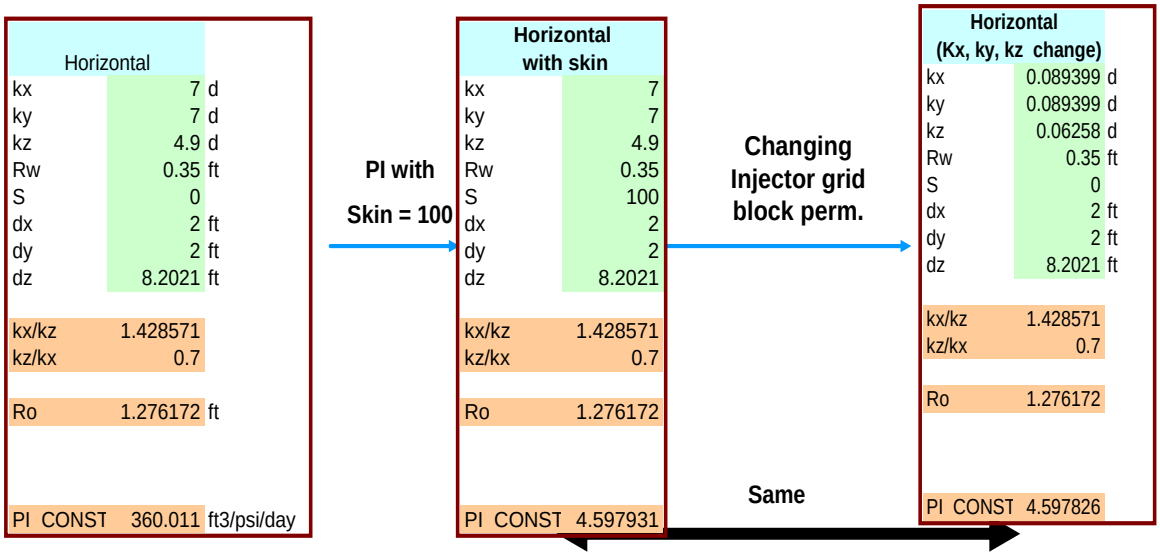

Figure 4.7: Calculation of near wellbore effective permeability in the presence of skin

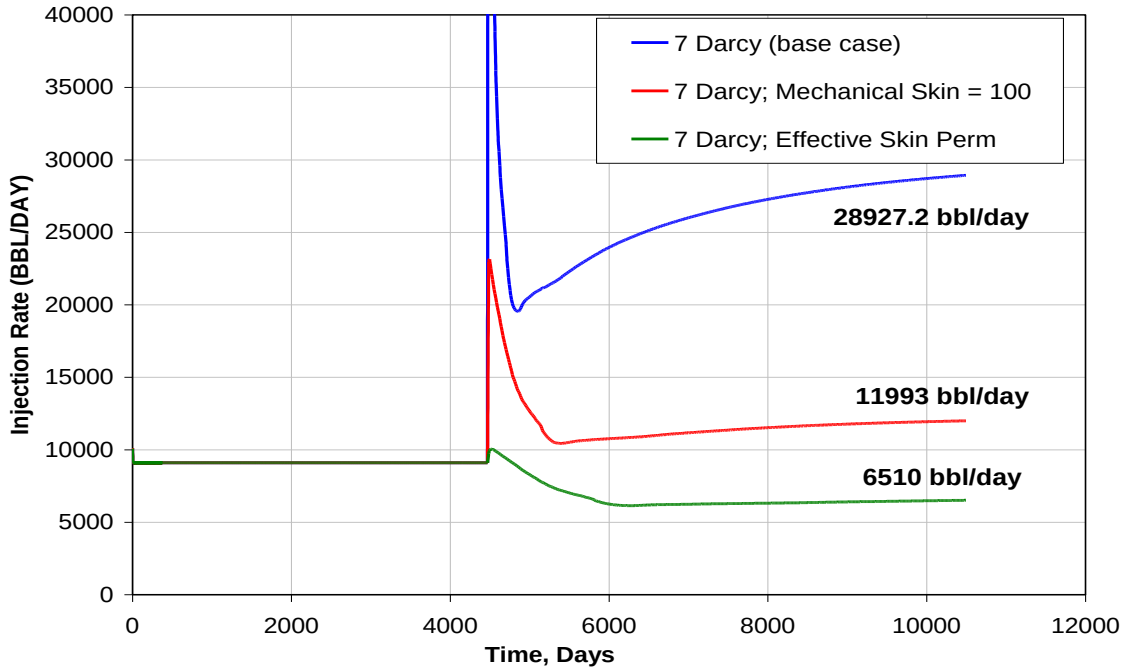

Figure 4.8: Lower injection rate when skin is modeled as effective permeability

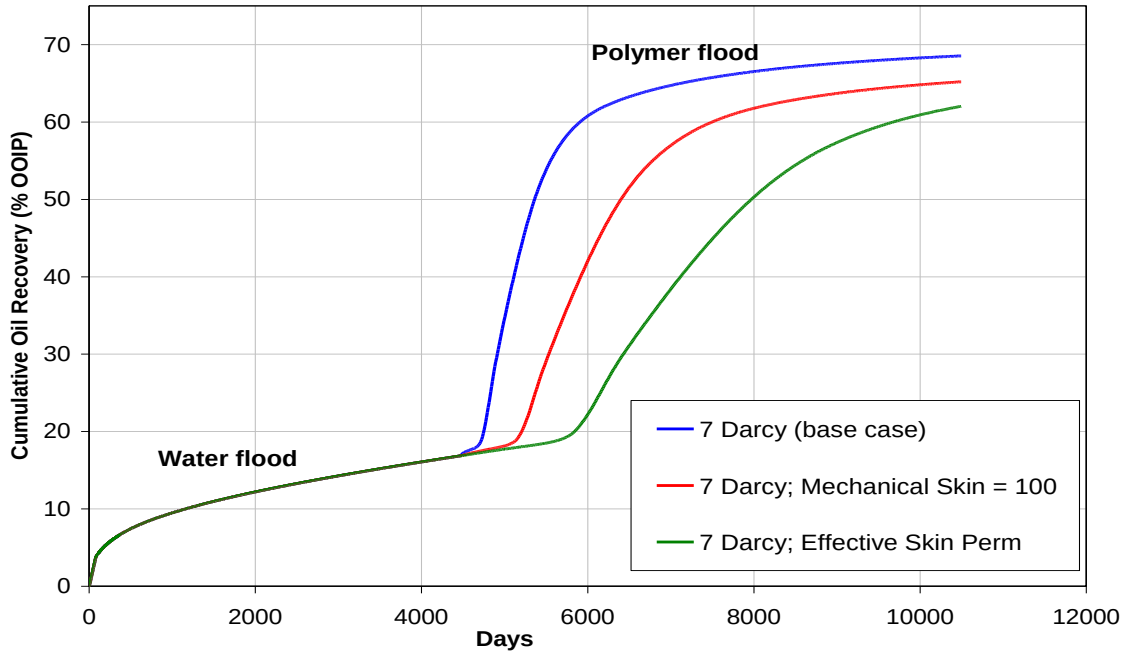

Figure 4.9: Lower oil recovery when skin is modeled as mechanical skin in PI and as effective permeability

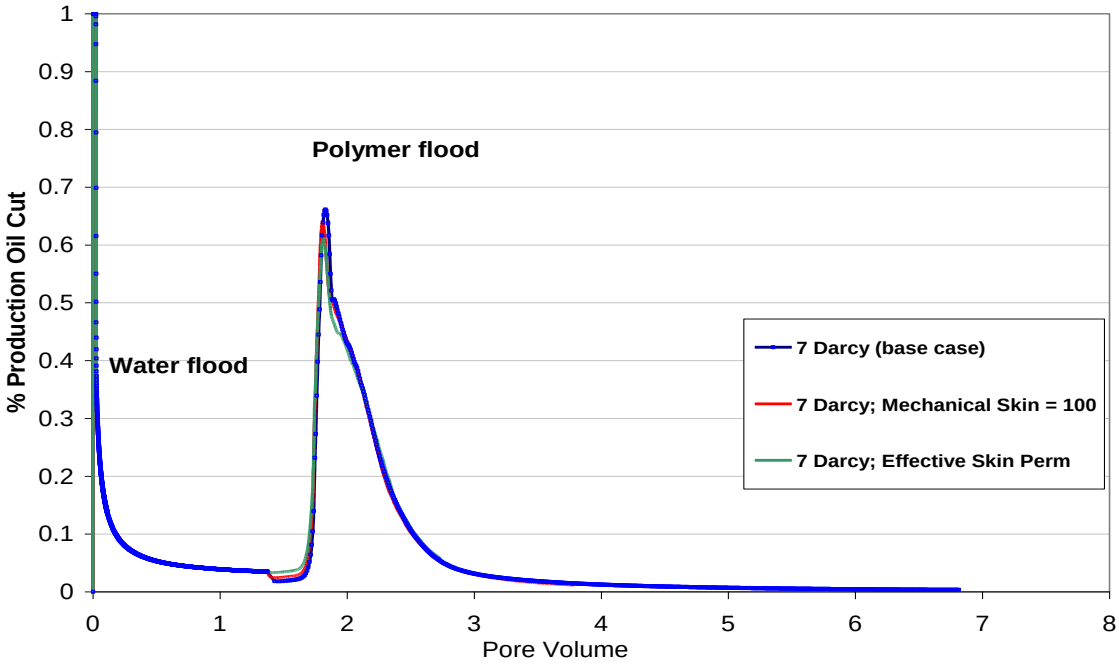

Figure 4.10: Oil cut response when skin is modeled as effective permeability.

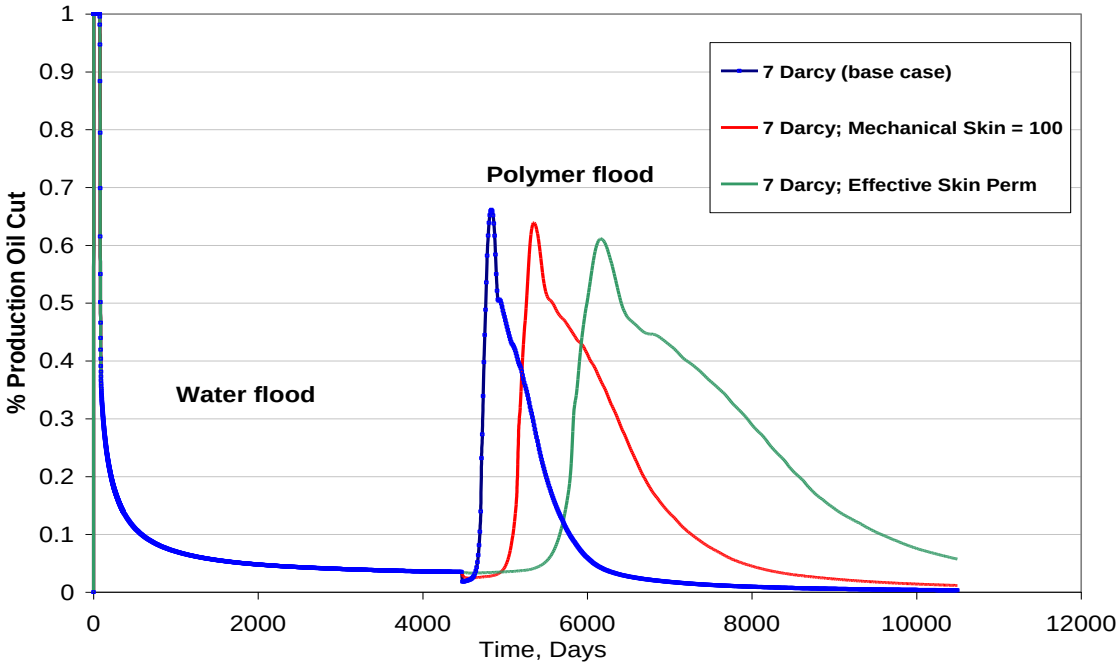

Figure 4.11: Late oil cut response when skin is modeled as effective permeability.

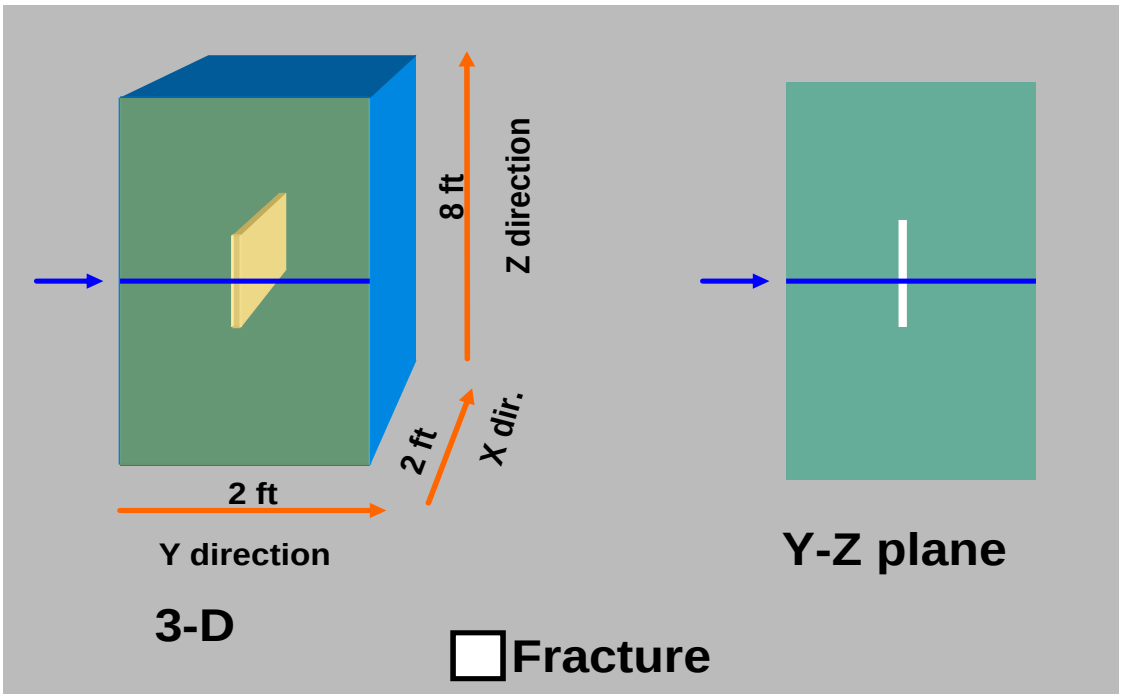

Figure 4.12: Fracture visualization

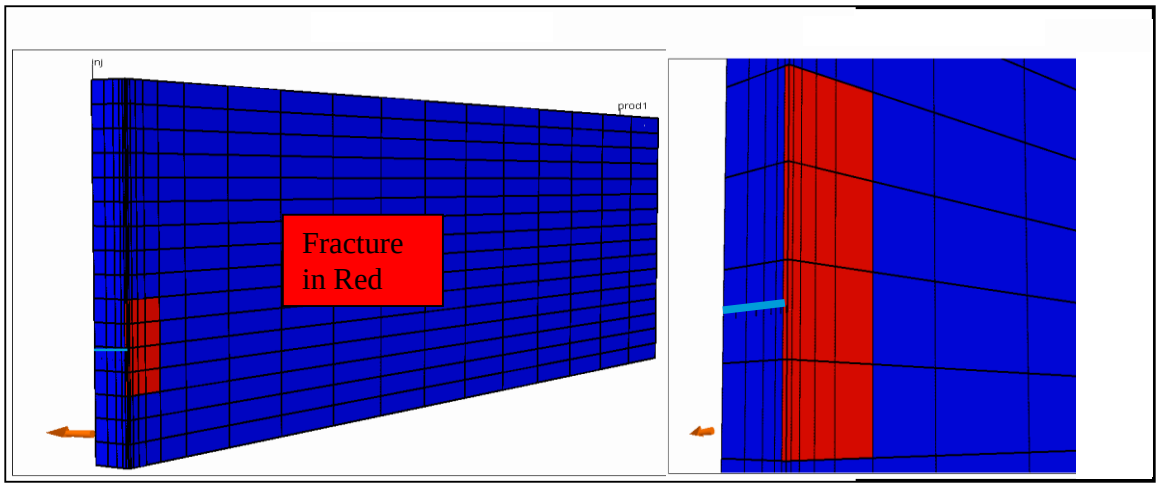

Figure 4.13: Simulated hypothetical fracture introduced in modified simulation model

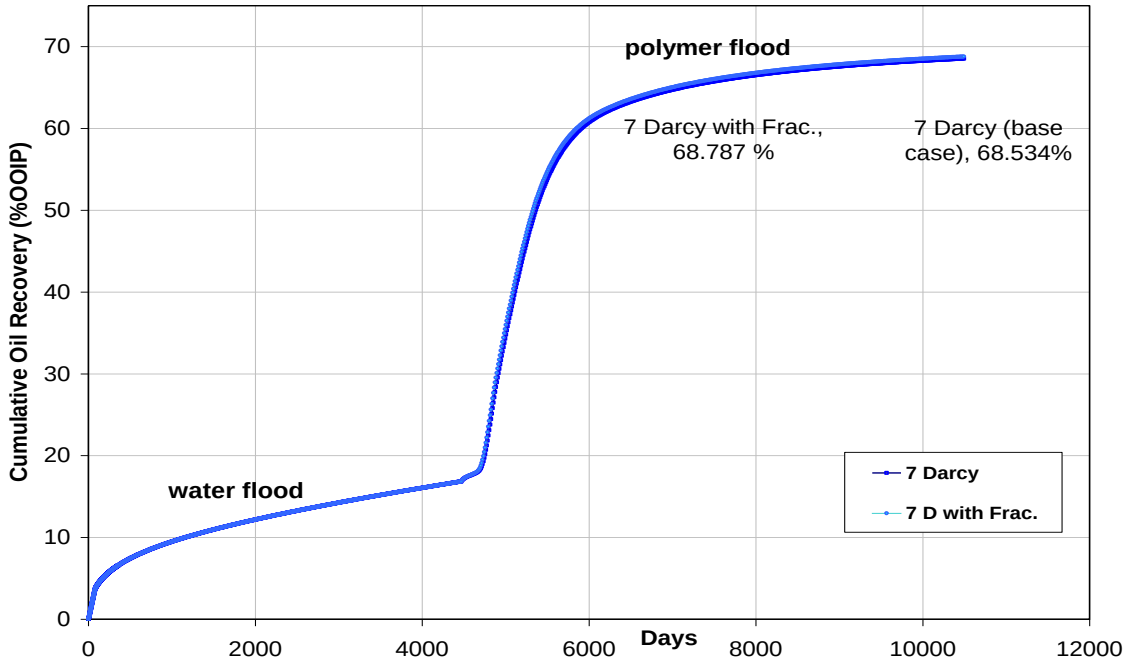

Figure 4.14: Cumulative oil recovery comparison with and without fracture

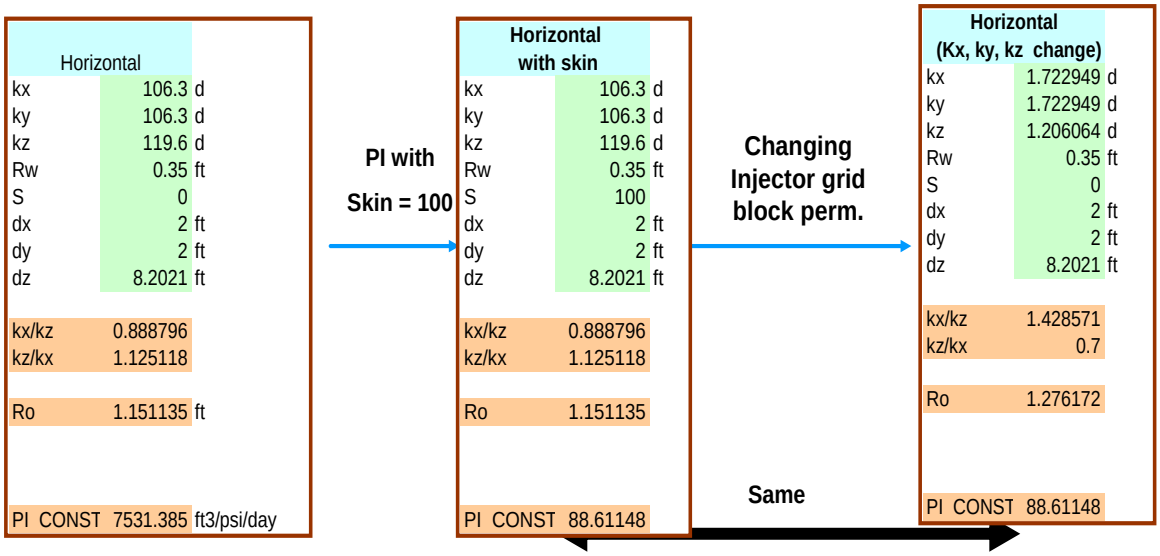

Figure 4.15: Near wellbore effective permeability in the presence of skin and fracture

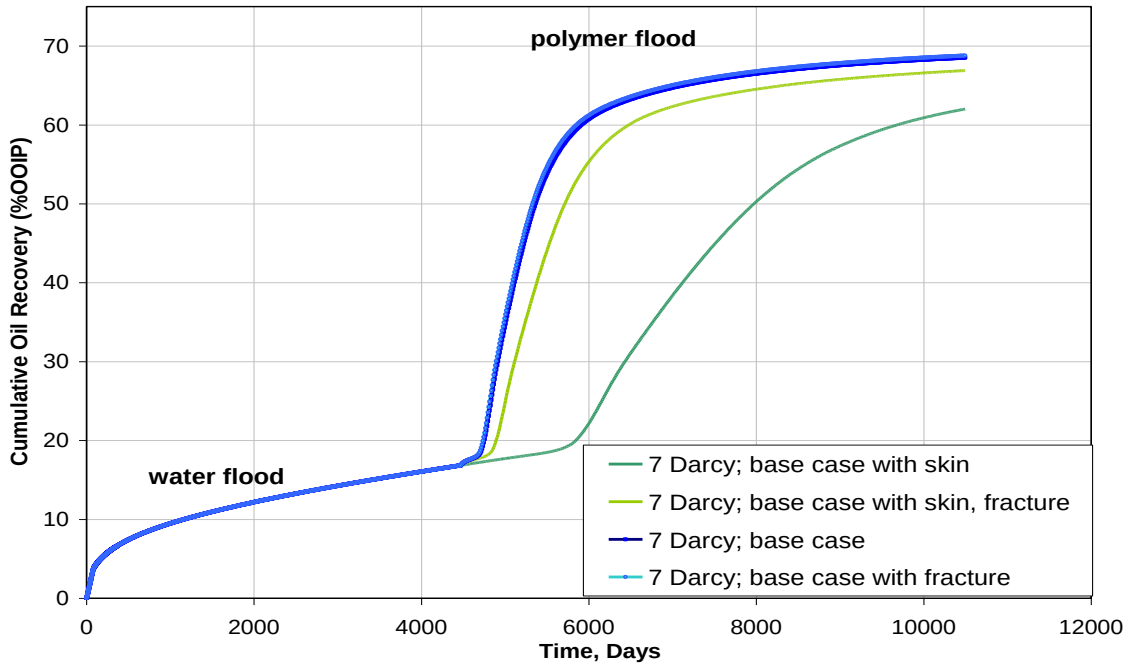

Figure 4.16: Cumulative oil recovery comparison in presence of fracture and skin

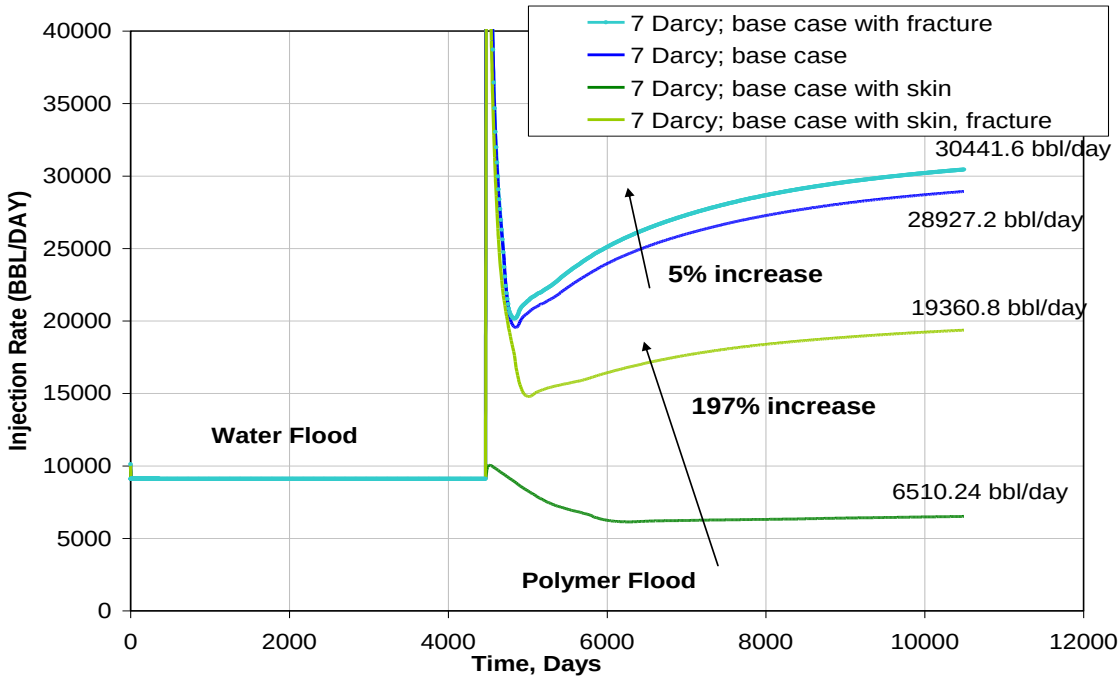

Figure 4.17: % injection rate change in presence of fracture and skin

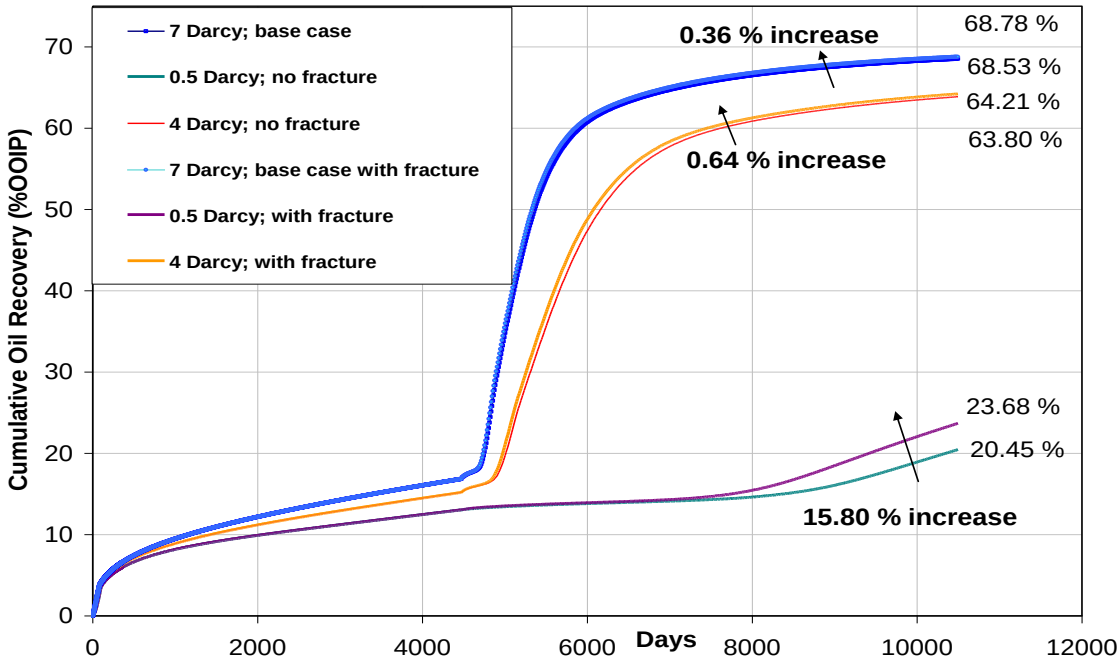

Figure 4.18: Cumulative Oil Recovery versus days with decreasing reservoir permeabilities

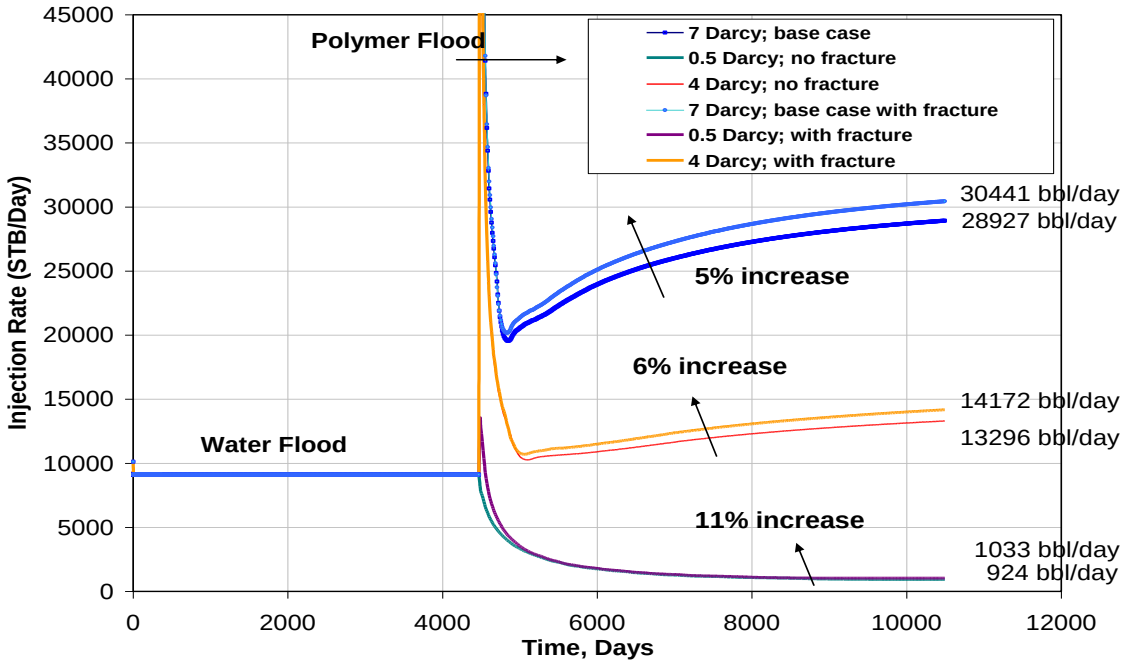

Figure 4.19: % injection rate increase in presence of fracture for different permeabilities

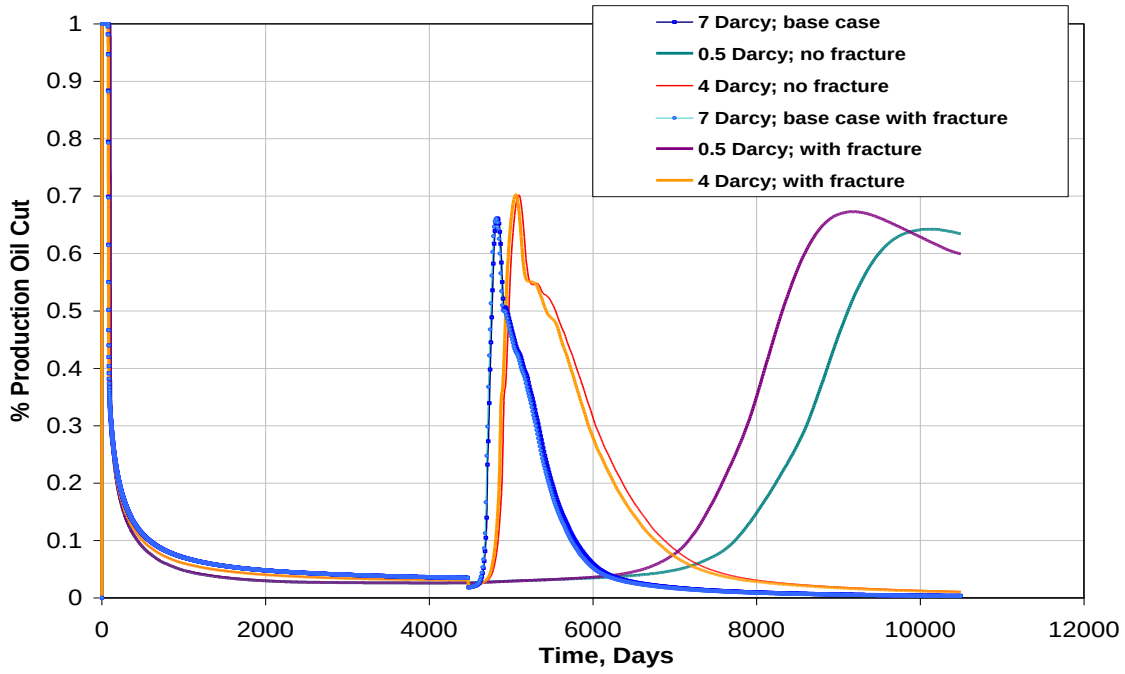

Figure 4.20: Oil cut comparison for different permeabilities

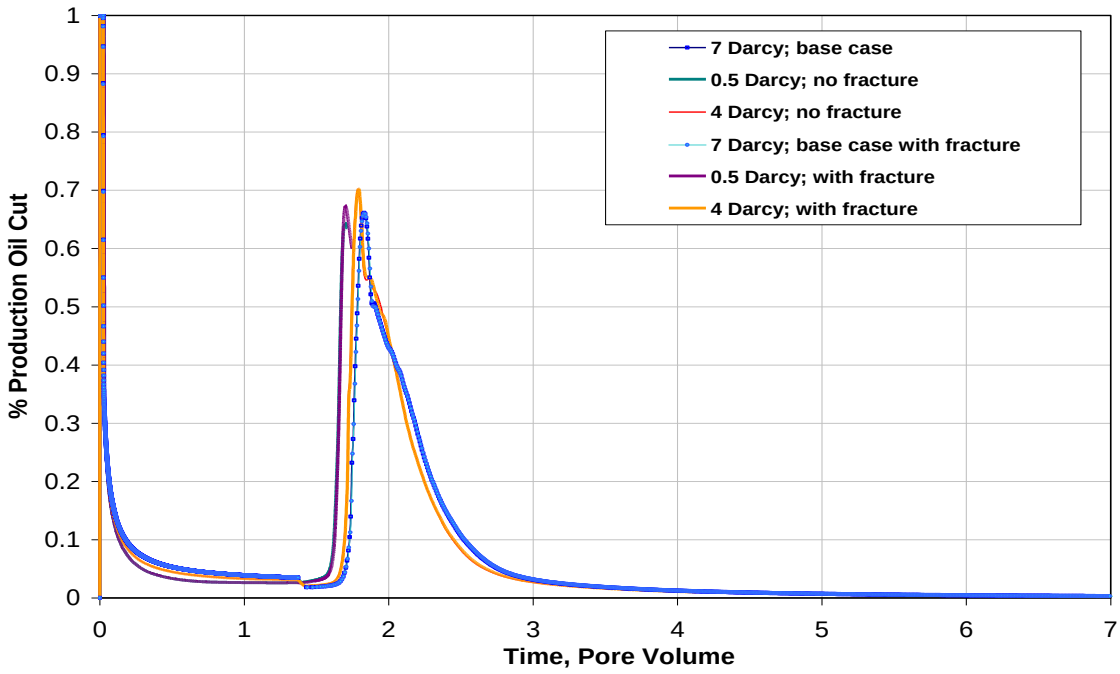

Figure 4.21: Oil cut comparison for different permeabilities

5 Design and Optimization of a Pilot Scale Surfactant/Polymer Flood

In this chapter, we present modeling and simulation of a pilot scale surfactant-polymer flood. Furthermore, we try to optimize the field scale performance by simulating various sensitivity cases. We use the lab data to predict the field scale performance of this sandstone reservoir. Then, the available field data is used to fine-tune the simulated results.

5.1 LABORATORY PHASE BEHAVIOR AND CORE FLOOD MODELING

Before the pilot simulations were started, phase behavior and laboratory core flood data were used to estimate as many process parameters as possible. Various surfactant-polymer-cosolvent-alkali-NaCl combinations were tested in the laboratory to observe both the aqueous and microemulsion phase behavior using the field crude oil and the best formulation (based on economics and solubilization ratio) was selected for testing in core floods. These experiments and corefloods were done by Robert Matt Dean and Chris Britton. Sodium carbonate was added to a fresh water source called JLSW. The composition of JLSW is presented in Table 5.1 and the formation brine composition is given in Table 5.2. The sodium carbonate was added to reduce the surfactant adsorption, but it also adds ionic strength along with the NaCl to bring the salinity up to its optimum value. The ASP formulation consisted of 0.75% TDA-13PO-SO4, 0.25% C2024 IOS with 0.75% IBA as cosolvent and sodium carbonate alkali. Figure 5.2 is a plot of the trends in the solubilization ratios as a function of salinity (total NaCl and Na2CO3). The optimum salinity observed from the surfactant phase behavior was 1.5% NaCl and 1% Na_2CO_3 in JLSW (total 0.455 meq/ml anions). The CSEL and CSEU were estimated to be 0.37 meq/ml and 0.541 meq/ml, respectively. Also, the optimum solubilization ratio is 30. The aqueous solutions with polymer were clear at optimum salinity.

The basic idea of adding polymer is to provide a viscosity of about 20 cP in the surfactant-polymer slug and polymer drive. To obtain this viscosity in the slug at 0.455 meq/ml, 2200 ppm HPAM (SNF's FP 3330S) polymer concentration was needed. Moreover, for the polymer drive, 2100 ppm polymer concentration was required to provide 20 cP viscosity at 0.266 meq/ml. Figure 5.5 through Figure 5.7 present a comparison of polymer lab data along with the UTCHEM model under reservoir conditions at various concentrations, salinity, and shear rate.

The ASP formulation was then tested in core floods. About 95% of the waterflood residual oil was recovered in the final coreflood. This core flood was simulated to estimate various process parameters needed to simulate the ASP pilot. The UTCHEM model parameters for phase behavior data, surfactant, relative permeability (Figure 5.1), capillary desaturation curve (Figure 5.3), surfactant adsorption (Figure 5.4), polymer viscosity dependence on salinity, polymer concentration, and shear rate are listed in Table 5.3.

5.2 BASE CASE SIMULATION

Before the simulation results are presented, it is imperative to discuss the reservoir and the simulation model. This reservoir is a 15 acre sandstone reservoir with 6 five-spots, henceforth, called the pattern. The pattern represents the area of interest and is a part of 103 acre simulation model, henceforth, referred to as the pod. Figure 5.8 presents the areal view of the simulation model including the pattern. The pattern is confined by geological boundary at north and south presented in pink in Figure 5.8. However, the pattern remains unconfined on the east and west side of the pattern.

The reservoir model consists of 9 layers. The top four layers represent a upper layer with similar geological characteristics such as porosity and permeability. Similarly,

the bottom five layers have similar geological properties. In general, within the pattern, the top four layers have lower porosity and permeability compared the bottom layers. The top four layers have an average porosity of 0.17 compared to 0.20 for the bottom five layers within the pattern. Moreover, the average permeability of the top four layers is 137 md compared to 203 md for the bottom five layers within the pattern. Also. it is interesting to see that in each layer individually, the porosity and permeability within the pattern is higher towards the middle. The thickness of the layers varies along the pattern. This change in the thickness is compensated by using a net-to-gross (NTG) factor in UTCHEM. The NTG factor for the bottom five layers is more than the top four layers.

The field was already water flooded at the start of the ASP pilot. Hence, some of the layers are already at residual oil saturation, especially the bottom most layers. Although, some mobile oil is still present in the reservoir, the main idea of this pilot is to recover the water flood residual oil. The oil saturation of layer 1 and layer 9 is presented in Figure 5.9 and Figure 5.10. The pink color represents zero oil saturation and blue represents maximum oil saturation. The top 4 layers have the most mobile oil. One of the reasons for higher initial oil saturation in the top 4 layers is lower permeability. Since the bottom layers are more permeable than the top layers, they were preferentially water flooded.

Figure 5.11 presents the pore volume of each layer in each five spot. Pore volume of all the five spot are listed from left to right in increasing order from 1 to 6 are listed from left to right. The pore volumes in the two middle five spots are more as compared to others because of more porosity and NTG. For example, the second and the fourth five spots have a pore volume of 108,110 bbls and 103,663 bbls. The sixth five spot has the lowest pore volume of 84,000 bbls.

The calculated pore volume (PV) for all 6 five-spots in the UTCHEM model is 523,968 bbls. As presented in Table 5.4 the initial oil present in the pattern is 178,226 bbls. Since the pattern is unconfined and the injectors are in the periphery of the pattern, some of the injected ASP slug is expected to be lost outside the pattern. The lost fluid is expected to be about 25%. Hence, for all the volumetric analysis, the adjusted pattern pore volume (PPV) is considered to be 655,000 bbls.

The pattern consists of 12 injectors and 6 producers. All the injectors are named as BCF 1-12. All the wells within the pattern are rate constrained which is guided by the field rates. For the base case, all the injectors inject at 125 bbls/day and all the producers produce at 250 bbls/day. A balanced injection/production profile is maintained within the pattern. In the field, the injectors BCF01, 05, 06, 10 have been hydraulically fractured and the other injection wells have been stimulated using a gas gun technique. The permeability of all injection well grid blocks was increased by a factor of 50.

The pattern is unconfined, hence, has the potential for fluid loss outside the pattern. The top four layers are confined by a natural barrier in the north and south. However, the bottommost five layers are confined in the north and unconfined in the southern part of the pattern. The east and west side of the pattern are mostly unconfined for all the layers. As seen in Figure 5.9, the pink color represents the boundary in layer 1 beyond which the flow is restricted. Figure 5.10 presents no or very little physical boundary in the north and south of the pattern in layer 9. Hence, more fluid can be expected to go off-pattern in bottommost layers than in top four layers.

To minimize the potential fluid loss outside the pattern, three peripheral injectors are located to the west (D7, DD6) and east (GG7) of the pattern. Also, three peripheral producers are present to the north (pM32) and south (pM23, pM28) to attempt to capture some of the mobilized oil outside the pattern. All the peripheral injectors inject water

from 0th day at a constant rate until the end of the pilot. However, for the base case, the peripheral producers are shut off. Later, sensitivity simulations will be presented to discuss the optimum time for opening them. The injection and production rate constraints for all the wells in the base case are presented in Table 5.6. In addition to the peripheral injectors and producers, six hypothetical hydraulic control wells were included in the model. WB1, WB2, WB3 and EB1, EB2, EB3 are the hydraulic control wells along the west and east boundaries. The purpose of these wells is to maintain the reservoir pressure.

0.35 PPV water preflood was injected. 3.5% NaCl was added to the softened fresh well water. The total salinity of the preflood was 0.522 meq/ml. One of the main reasons for having a preflood is to help to provide a favorable salinity gradient to the surfactant slug injected later. A controlled higher salinity before the surfactant slug helps in increasing the duration of the type-III mixing zone, which has ultra low IFT. Moreover, the preflood was used to displace the Ba++ ions in the formation brine to prevent the Ba++ from mixing with the sulfate ions in slug and possibly causing scaling at the production wells. The preflood also causes the divalent cations on the clays to unload and be replaced by Na+ ions by cation exchange. However, this was not necessary since the surfactant can tolerate high concentrations of divalent cations in the presence of oil. The simulated water injection results in an oil cut of 31 bbl/day as presented in Figure 5.12. Moreover, water injection results in an increase in reservoir pressure from 75 psi to about 400 psi (Figure 5.13).

Then, surfactant-polymer (SP) slug was injected for 234 days or about 0.25 PPV. The polymer concentration of 2200 ppm in the SP slug provides a viscosity of 20 cp at 0.455 meq/ml salinity. An increase in the oil cut is seen at about 230 days which is about 100 days since the start of slug injection. Figure 5.15 and Figure 5.16 show the pattern oil

saturation at 234th day for layer 1 and layer 9. A decrease in the oil saturation (pink color) can be clearly seen around the injector wells.

0.75 PPV polymer drive was injected after the SP slug until 550 days. Water post flush was conducted after the polymer drive. The size of the polymer drive is sufficient to push the SP slug towards the producer. The salinity of the polymer drive is 0.266 meq/ml, which is lower than the SP slug salinity. This type of salinity gradient allows effective salinity to pass through Type-II, Type-III and finally, Type-I and hence provides a favorable salinity gradient.

The cumulative oil recovery and oil production rate of the base case simulation is shown in Figure 5.12. The cumulative oil recovery is 117,930 bbls. The maximum oil production rate (purple color) predicted by UTCHEM is about 450 bpd. As a result of the water preflood, the mobile oil is pushed out of the reservoir. The oil cut before the oil bank is produced is about 31 bpd. At about 240 days, the oil bank break through occurs. The maximum oil cut occurs at about 400 days. It should be noted that the oil bank is still produced even after the polymer drive is injected. At about 680 days since the start of the preflood injection, the water cut goes below 1%. Hence, no more incremental oil recovery is counted after that.

Figure 5.14 presents the production rate of oil and surfactant in bpd. Clearly, phase 3 production rate starts at about 400 days and peaks at about 650 days and then stops at about 850 days. What is interesting to see is that oil and surfactant are together produced as microemulsion phase between 400 days and 700 days. After the fluid is produced from wellhead it passes through surface equipment that may result in emulsions forming and this part of the process is not modeled in this work. Emulsion breakers are required to break any emulsions and need to be planned beforehand.

A simulation was run to see the effectiveness of injecting ASP over a polymer flood. In the above base case, instead of the surfactant slug, polymer was injected from 128 days until 1400 days. Figure 5.17 presents the oil recovery curve of both the base case and only the polymer flood. Clearly, an additional recovery of 75,000 bbls is seen due to surfactant injection.

5.3 SENSITIVITY SIMULATIONS FOR CHEMICAL FLOODING

5.3.1 Chemical Slug Injection Scheme

Various cases were simulated with different surfactant-polymer slug and polymer drive sizes. Then the simulation results were compared with an empirical correlation published earlier.

5.3.1.1 Surfactant Mass Sensitivity

Surfactant is expensive and accounts for a major part of the expense during a chemical flood; hence, optimizing the surfactant mass is crucial. In the base case simulation 1% surfactant concentration was simulated in 0.25 PPV surfactant slug. For all the sensitivities below, injection and production rates were the same as the base case. The only change is the surfactant slug size, hence, the injected surfactant mass.

A sensitivity study for pore volume of surfactant injected was done. The slug sizes were varied from 0.1 PPV to 0.5 PPV. Figure 5.18 presents the oil recovery curve for all the cases. As observed that increase in injected surfactant mass increases the oil recovery. Since the most important parameter of a surfactant flood is its mass, all the sensitivity cases were normalized to base case - PV x Concentration. For example, the normalized effective surfactant mass for case1 in which 0.5 PV x 1% surfactant concentration is injected is (0.5x1)/(0.25x1) = 2.

Table 5.5 summarizes all sensitivity cases performed on the injected surfactant mass. As the injected surfactant mass increases, the oil recovery increases. The oil recovery increment due to addition of surfactant is observed in Figure 5.19. Even though the oil recovery increases with injected surfactant mass, but only 0.25 PPV of surfactant mass is injected in the field due economic constraints.

5.3.1.2 Polymer Drive Mass Sensitivity

Importance of a chase polymer drive cannot be underestimated. Polymer drive provides good mobility control and hence, decreases the chances of fingering. Moreover, it also provides salinity gradient to the surfactant slug which is the most important factor for the success of a surfactant flood. Lake et. al published a correlation between recovery efficiency and polymer drive by using actual field data. The study showed a strong correlation between recovery efficiency and mobility buffer size, hence, a correlation was developed by using data from 14 field five spot cases. A comparison of this correlation with simulated results will be presented.

Sensitivity to various polymer drive sizes was done. The base case contained 0.75 ppv polymer drive with 2100 ppm polymer concentration. The following sensitivities were based on the base case; the only change was polymer drive size. The sensitivities were done on polymer drive size ranging from 0.5ppv to 2 ppv. Figure 5.20 presents the recovery efficiency comparison for all the simulated cases. The pink curve represents the recovery efficiency in the presence of mobile oil. The blue curve below represents the recovery efficiency without mobile oil. Clearly, as the polymer drive size is increased, the recovery increases. This is attributed the better mobility control due to increased polymer drive size. However, only a 5% increase in recovery efficiency is seen when the polymer drive size is increased from 0.5 to 2 ppv.

Next, we compare the field data with the simulated results. Correlation developed by Lake et. al was used and the results are plotted with the simulated data. Figure 5.20 presents this comparison. The slope of recovery efficiency of field data is much greater than the simulation results. Another important observation is that clearly the recovery efficiency of the simulated results (in the presence of mobile oil) is higher than the field recovery efficiency. In the presence of mobile oil, the correlation and simulated results intersect at 2 ppv. However, when the mobile oil contribution is removed from the simulated data, the field data correlation and simulated curve (w/o mobile oil) intersect at about 1.3 ppv. The field data shows a much higher dependence on polymer mass than the simulated results. One of the reasons for smaller simulated slope could be viscous fingering. The phenomenon of viscous fingering is not very well captured by the simulators. Hence, even with smaller polymer drive size, a lot more oil is recovered than in comparison to field data. Furthermore, some of the other key reasons for this inconsistency could be surfactant mass injected prior to polymer drive, interfacial tension between oil and surfactant, and salinity. Moreover, unlike simulated cases, polymer drive was tapered in some of the field cases. Although, the conditions of each of the field case are unique, the qualitative comparison gives a good idea of the field response in comparison to simulated data.

5.3.2 Injection rate adjustment

The base case was simulated based on equal injection rates in all the 12 injectors. However, each of the 6 five-spots have different pore volumes. As presented in Figure 5.11, the second and the fifth five-spot have the maximum pore volume in all the layers. Clearly, each pattern should have different injection rates to balance the injection rate per unit PV. Moreover, the off pattern fluid loss in the cornermost injectors could also be

minimized by optimizing the injection rates. Hence, two injection rate sensitivities were performed. In the first sensitivity, the injection rates were calculated based on quarter-wise injector contribution. Based on the results of the first sensitivity, some changes in the injection rates were made in the field. The field rates were also simulated.

5.3.2.1 Injection rate quarter-wise contribution of each injector

Let us consider the quarter wise contribution of the injectors in the pattern and divide the individual injection rates based on a cumulative flow rate of 1500 bpd. For a homogeneous reservoir properties case, the corner-most injectors BCF 01, 04, 09, 12 contribute to only 1 quarter within the pattern and, hence, can be attributed 62.5 bpd each as their injection rates. BCF 02, 03, 05, 08, 10, 11 contribute to two quarters in the pattern, hence, are attributed 125 bpd injection rate each. Finally, BCF 06, 07 contribute to all four quarters of the pattern. Hence, both were attributed 250 bpd injection rates. Table 5.6 presents the list of injection rate for all the wells. A simulation run was done based on the rates mentioned above. The result of this run is compared with the base case in Figure 5.21. It is seen that 4350 bbls of additional oil is recovered when the unequal injection rates are simulated. As seen in Figure 5.21, the oil cut is greater when unequal rates are simulated.

Figure 5.22 through Figure 5.27 present a comparison of oil recovered by individual producers due to change in injection rates. It is interesting to note that all the producers present a higher rate of recovery. This is attributed to doubled injection rates at the middle injectors. Moreover, it can be noticed that the four corner five-spot producers contribute to the increased oil recovery than the middle five spots. This is because, BCF 06, 07 divert higher flow rate towards the producers other than pM 42, pM 45. To provide a quantitative estimate about the oil saturation, on an average in all the layers at

792nd day, the variable injection rate moves 6% more oil in the quarters around the injectors BCF 06, 07. Moreover, the corner injectors push 6.98% less oil in the unequal injection rate case in comparison to equal injection. This should be expected as in unequal rate case, the corner injectors inject half (62.5 bpd) as much being injected in equal injection case (125 bpd).

5.3.2.2 Field injection rates

The above study reflects that higher injection rate in the middle injectors has the potential to increase the overall oil recovery. As a cause of the above result, the field injection rates were modified at the time of slug injection i.e. 128th day. Injection rates of the middle injectors were increased, and the corner injectors were decreased. However, the rates are not drastically changed as like in the above case. The field injection rates of the middle injector rates was increased from 125 bpd to 150 bpd. The corner injectors were injecting at 110bpd (approx.). The complete list of field injection rates of each injector is provided in Table 5.6.

The field rates were not changed as drastically as presented in the above sensitivity because of the risk to fracture the formation near wellbore. The change of injection rates in the field is marginal in comparison to the base case. A simulation was done to compare the oil recovery of the new field rate and the base case. The result is presented in Figure 5.27. The oil recovery increases from 118,000 bbls (base case) to 120,000 bbls when the field rates are simulated. This is a marginal increase in oil recovery. However, it is still extremely important to have the correct rates in the simulator to capture the fluid flow in the reservoir correctly. All the further work will be done based on the field rates.

Figure 5.29 through Figure 5.38 present areal view oil saturation snapshots for layer 1 and layer 9 at various times for the above case. The times selected to present oil saturation are at the start of slug injection, & polymer drive injection, 100 days after drive injection, start of water drive injection and, after 1PPV water drive injection. This helps in visualizing the fluid transport in the porous media.

Layer 1 areal view snapshots at various times are presented from Figure 5.29 to Figure 5.33. As expected, oil is being displaced away from all the injectors. The emerging pink color around the injectors represents irreducible oil saturation to slug. It is also clearly seen that as time increases, more injected fluid is being pushed off pattern by the periphery injectors. Figure 5.34 through Figure 5.38 present oil saturation for layer 9 at various injection times. As seen earlier in layer1 profiles, the oil is being pushed away from the injectors with increasing injection times. Furthermore, it is interesting to see oil bank being pushed away from the peripheral injectors. Consider Figure 5.37; clearly, after 100 days of polymer drive injection a lot of fluid is being pushed away in north east, north west and south east and south west direction. The pink color represents the swept area by the slug, and the green color at the periphery of pink color is the oil bank. To minimize the loss of oil and injected fluid, it is imperative to open the peripheral producers at strategic times. This is presented in the next section.

5.3.3 Optimizing time for opening peripheral producers

In above simulations, the peripheral producers were shut off at all times. It is clear from Figure 5.37 that some of the oil is pushed off the pattern in the north west and south east direction. Hence, the peripheral producers can be helpful in producing the oil that is pushed off the pattern. The three peripheral producers are present at the north (pM32) and south (pM23, pM28).

Two sensitivities were done to optimize the time for opening the peripheral producers. Both the sensitivities were done based on the simulation results of field rates presented in Section 5.3.2.2. All the three peripheral producers were opened at the same time depending on the sensitivity and at the same rate of 50 bpd. The production rate of all the wells is presented in Table 5.6. In the first sensitivity, all the peripheral producers were opened at 234th day i.e. the last day of surfactant slug injection. In the second sensitivity, the peripheral producers were opened on the 334th day i.e. 100 days after polymer drive was first injected.

Results of both the sensitivities are presented in Figure 5.39. The oil recovery curve of both the runs is compared to the base case. For both the sensitivity cases, the cumulative oil recovery at 1400th day is about 128,000 bbls. Hence, this sensitivity does not show any difference in the time at which the peripheral producers should be opened. An incremental oil recovery of about 10,000 bbl over the base case is observed. Another, important thing is to notice is that the oil recovery is still increasing in both the cases at the 1400th day.

It is also interesting to see the individualistic contribution of each of the peripheral producers. Figure 5.40 presents the oil recovery of pM22, pM23, pM32 respectively for the case when the peripheral producers are opened at 334th day. The producer pM22 shows a sharp increase in the cumulative oil recovery since the time it is opened. However, it stabilizes at about 1500 bbls on 850th day i.e after 500 days it is opened. pM23 and pM32 are observed to produce after about 750 days. The oil produced in pM23, pM32 is about 4500 and 2500 bbls respectively. Figure 5.41 presents the oil cut of the peripheral producers. pM 23 shows the highest oil cut of 33 bpd at 900 days after which the oil rate decreases. It should be noted that at 1400th day, all the peripheral

producer observe a oil production decline. Hence, we should expect the oil recovery curve of pM23 and pM 32 soon after 1400 days.

5.4 TRACER STUDY: A FIELD DATA AND SIMULATION RESULTS COMPARISON

Tracers are used to estimate swept pore volume swept by the tracer, and to get a better idea about reservoir characterization & the geology of the reservoir. 12 unique conservative tracers were injected each injectors in reservoir B field to monitor the flood's performance. The tracers were unique fluorinated benzoic acids (FBA) and were injected with water. Since the tracers are conservative, the partitioning coefficient of all the tracers is inputted as zero in simulation.

250 grams of each unique tracer was injected in its respective injector on 69th day water of pre-flush. This was simulated in UTCHEM by injecting 50 ppm of each tracer for 0.25 days at 125 bpd injection rate. Fluid samples from all the 6 producers within the pattern were tested to detect every tracer. As of now, not all the tracers have broken through in the field. The tracers that have broken though are still in the initial stages of the concentration curve. None the less, the breakthrough times and the initial concentration points are still compared with the simulated results as it provides a good idea about any inconsistency between the simulation model and the field.

Figure 5.42 through Figure 5.47 present a comparison between the tracer concentration history of the field and UTCHEM. The dots represent the field data and the curve represents UTCHEM simulation output. The field data is noisy. Also, it is clearly seen that in some cases match is not very good. Below, the field tracer data at each producer is compared to that with the simulation model.

Figure 5.42 presents the tracer concentration history plot for the producer well pM31. As expected BCF 01,02,05,06 show up in pM31. However, a mismatch between

the field data and the simulation data is clearly visible. The breakthrough times of BCF01 and BCF05 are similar to that predicted by UTCHEM. It is encouraging to see that as predicted by UTCHEM BCF01 is one of the first wells to show up at pM31. BCF02 did not breakthrough in pM31 in the field yet, however, UTCHEM simulation clearly predicts its earlier breakthrough. This is clearly an inconsistency with the field data. BCF05 data is presented in the blue colored dots and curve. Although, the field breakthrough time of BCF05 is similar to that predicted by UTCHEM, its field concentration rises rapidly with time. Clearly, this is another inconsistency between the field data and simulation prediction. Perhaps the most inconsistent data set is seen in BCF 06 tracer concentration data. Clearly, its field breakthrough time is much shorter than simulated result. Moreover, the field concentration curve is rising rapidly. This could be due to the field hydraulic fracture in BCF06 well which may not be modeled very well in simulation model at present. Similar behavior of BCF06 is observed in all the wells in which it shows up.

Figure 5.43 presents tracer concentration history for producer well pM44. BCF02 is not seen to have broken through in the field, unlike predicted by UTCHEM output. It is encouraging to see that the field and simulation breakthrough time of BCF 03 are similar. However, the field concentration history increases rapidly. BCF06 and 07 both breakthrough much before than predicted in simulation.

Figure 5.44 presents tracer concentration history plot for producer pM44. Similar to the way seen in pM42, the breakthrough time of the field and simulation are similar for BCF03. However, the concentration curve for BCF03 rises rapidly in the field. BCF04 presents a satisfactory match with the field data. BCF07 breaks through earlier than predicted from the simulation model. BCF08 concentration rises rapidly as can be seen in the figure. This is inconsistent and needs to be somehow corrected.

Figure 5.45 presents the concentration plot for producer pM45. Tracer concentration from injector wells BCF 05,06,09,10 are observed in this well. As seen, the field breakthrough time and tracer concentration of injector well BCF05 matches with the simulated result. Similar behavior is observed for tracer from BCF09 to pM45. As observed in pM42,44, the BCF06 tracer breaks through earlier than expected. The tracer from BCF10 is also seen about 50 days earlier than expected.

Figure 5.46 presents the tracer concentrations for well pM46. Tracer from the injector wells BCF06, 07, 10, 11 are observed to be breaking through in this producer. The field breakthrough times of BCF06, 07, 11 are shorter than predicted from the simulated results. Interestingly, an early decline in the field concentration of BCF06 is observed in the field data. BCF10 shows up slightly slower than as predicted in UTCHEM. Although, more field data points are required to understand things better.

Lastly, Figure 5.47 presents the tracer concentration seen in the producer well pM47. BCF07,11 did not breakthrough yet in pM47. However, BCF08 field breakthrough time is more than as predicted by simulation results. BCF12 breakthrough is similar in the field as compared to the simulated results. However, the concentration curve of BCF12 increases rapidly in the field.

One of the good points from the above comparison is that no big surprises have been seen. Like no unexpected injectors have broken through to a producer. Although, some of the inconsistencies like BCF 02 not showing up on any producers requires some consideration. To summarize the above comparison, some adjustment to the reservoir properties is required to match the field data. After the match is obtained, adjustment to injection flow rate could be made to enhance sweep efficiency and optimize oil recovery. A few of the important reasons for this inconsistency between the field data and simulated data is fractures, reservoir characterization.

5.5 COMPARISON BETWEEN FIELD DATA AND SIMULATION RESULTS

The main objective of this section in this chapter is to compare model predictions to latest actual reservoir performance data. Latest injection and pressure data from the field is compared with simulated results. This section brings about the scope of future work required to better predict future reservoir behavior.

First, the injector field data for rate and pressures were compared with the simulated results. Figure 5.48 through Figure 5.59 compare both rate and pressure for all the injectors from BCF 01 to BCF 12. In all the figures, the curves containing dots are the field data. The smooth curves represent the predictive simulated results. The blue color curves represent pressures and, the pink color curves represent the injection rates. Field rates were simulated (Section 5.3.2.2) and compared with the available field data.

5.5.1 Comparison during water pre-flush

In all the figures, the first thing to notice is a lot of variation in the field data. Both the pressure and injection rates are noisy. Hence, a qualitative comparison of the field data with simulated results is done. It may be noticed that at certain times, the injection pressure and rate drastically dip to a zero. This sudden decrease of field data happens due to any production related issue. Once, the issue is resolved, the well starts again. For example, on 106th day, the injection pressure and rate of well BCF11 suddenly dipped to zero. This was done because the well was stimulated using the gas gun technique. This well was stimulated because prior to the 106th day the field pressure was about 800 psi which is considered on the higher side during water preflush. Clearly, after the well was gas gunned, the pressure soared to about 620 psi. This release in pressure after gas gun represent near well skin damage which was remedied.

During water preflush (until 128th day), the field injection pressure of all the injectors except BCF 05, 06 and, 10 are much higher than the simulated results.

Interestingly, BCF01, 05, 06, 10 are fractured wells in the field and their simulated bottom hole pressures are close for to the field pressures. Although, BCF01 field injection pressure is consistently 100psi higher than the simulated values, but it is still much closer to than the other non-fractured injector wells. Similar behavior of higher field injection pressure is observed in many other wells. BCF 08 shows the maximum difference in the field and simulated pressure of about 300psi at 125th day as seen in Figure 5.55 during water pre-flush.

5.5.2 After surfactant slug injection

More observations can be made by comparing data after the surfactant slug injection. One important observation is an increase in the field pressure after the surfactant slug injection at 134th day. Since the viscosity of the slug is about 20 cP, as expected, the injection pressure increases. For example, the field bottomhole pressure of BCF11 well is about 640psi at 134th day. However, at 175th day, the field bottomhole pressure is 1050psi. This increase in field pressure is a staggering 400psi. Another important observation is that the field injection pressure presents an consistently increasing trend. In most of the injector wells, the field injection pressures present an increasing trend until the available data. Although, one of the reasons is the increasing oil bank and injected slug size, but other reasons are suspected. Moreover, the fluctuation in the field injection rate is increased in some cases after slug injection.

It is interesting to compare the field and simulated results after surfactant slug injection. Clearly, in all the cases, the field pressures seem to be higher than expected by UTCHEM after the slug injection. Even though, in the simulated results the injection pressure rise is seen after slug injection, however, the field pressures show a much higher

rise. One of the reasons for this inconsistency could be due to a dynamic near wellbore skin.

This inconsistency between the simulated data and field data should be corrected. The next section presents some of the key parameters that could be changed to better predict the field performance of this chemical flood.

5.6 CONCLUSION AND SUGGESTED FUTURE WORK

A heterogeneous sandstone reservoir was successfully simulated in UTCHEM. The base case was simulated at reservoir conditions of porosity, permeability, expected initial water saturation etc. A surfactant slug with a chase polymer drive was injected as planned in the field. Various sensitivities were performed on the base case. The simulated results were compared to the available field data. A conscious effort is needed to better predict the field performance. The present comparison between the field and simulated has a lot of inconsistencies, hence, presents a scope of improvement. The suggested workflow and key parameters which can be changed for better prediction are as follows:

1. The first step should be to change the injector well block permeability. At present, all injector well block permeabilities are increased by a factor of 50 over the base reservoir permeability to simulate various stimulation techniques performed at all the injectors. Since the field injection pressure during the water flood is more than the simulated injection pressure, the simulated well block permeabilities could be increased by a factor lower than 50. This should increase the simulated bottomhole pressure, hence, bringing it closer to field data. Other parameters that could be tweaked are relative permeability end points and skin.
2. After a comfortable match with the injection rate and pressures of the field is obtained, sensitivity on initial oil saturation needs to be done to match field oil

production to that of UTCHEM. It is known that the present field oil production rate is 15 bpd. Simulated results predict 31 bpd in the same time frame. One of reasons for this inconsistency could be higher than actual initial mobile oil in simulation reservoir model. Another reason could be better sweep predicted by simulation model during the water pre-flush.

3. After a reasonable match between oil production rate is obtained, the tracer data from the field needs to be matched with the updated model of UTCHEM. Section 5.5 presented inconsistencies between breakthrough times and tracer concentration curves of field data and simulated result. A better conformance of both simulated and field data can be achieved by adjusting local permeabilities in-between the patterns.
4. Lastly, injection rates can be adjusted to optimize the sweep efficiency within the pattern and hence, increasing the oil recovery. Various sensitivity cases could be done to better understand the effectiveness of various parameters on fluid behavior and oil recovery. Sensitivities to the following parameters could be looked into: kv/kh ratio, dispersion coefficients, relative permeability, shear coefficient, effective well radius, capillary desaturation parameters and other reservoir realizations.

Table 5.1: JLSW brine composition (Softened Water)

anion	conc., mg/lt	MW	charge	conc., meq/ml
Cl	76.08	36	1	0.00214
SO4	37	98	2	0.00076
HCO3	439.92	61	1	0.00721
CO3	0	60	2	0.00000
Br	0	80	1	0.00000
I	0	127	1	0.00000
total anions	553	60.0		0.01011
divalent cations				
Mg	2.49	24	2	0.00020
Ca++	3.62	40	2	0.00005
Sr	0	88	2	0.00000
Ba (not analyzed)	0	137	2	0.00000
total Divalent cations	6.11	33.6		0.00025
Other Ions				
Na+	233	23	1	0.0101

Table 5.2: Reservoir Brine Composition

anion	conc., mg/lt	MW	charge	conc., meq/ml
Cl	11300	36	1	0.318
SO4	0	98	2	0
HCO3	1085	61	1	0.0178
CO3	0	60	2	0
Br	0	80	1	0
I	0	127	1	0
total anion	12385	37.7		0.336
divalent cation				
Mg	220	24	2	0.0181
Ca++	880	40	2	0.0440
Sr	0	88	2	0.0000
Ba	140	137	2	0.0020
total divalents	1240	48.2		0.0641
Other Ions				
Na+	233	23	1	0.0101

Table 5.3: Summary of simulation input parameters

Simulation model (pod) Volume, ft x ft x ft	2625 x 1715 x 16.11
Number of grid blocks in X, Y, Z	75 x 49 x 9
Pattern Pore Volume, bbls (1PV)	523,968.44
1.25 Pattern Pore Volume, bbls (1 PPV)	654960.55
Initial Reservoir Pressure, psi	75
Arithmetic Average porosity	0.19
Arithmetic Average Permeability, md	174.45
Initial water saturation, fraction	0.35
Reservoir Salinity, meq/ml	0.33
Water viscosity, cp	0.933
Oil viscosity, cp	10.9
Water Compressibility, psi^{-1}	0
Oil Compressibility, psi^{-1}	0.00001
Capillary desaturation parameter for water, oil, ME	1865, 10000, 364.2
Intercept of binodal curve at zero, OPT., and 2xOPT salinity	0.03, 0.015, 0.03
CMC, volume fraction	0.001
Type-III salinity window (CSEL, CSEU, COPT)	0.370, 0.541, 0.455
Interfacial Tension Parameters for Huh's model, CHUH,AHUH	0.3 , 10
Log10 of oil/water interfacial tension , XIFTW	1.3
Compositional phase viscosity parameters for microemulsion (ALPHAV1- ALPHAV5)	2.1 , 2.1 , 0.1 , 0.1 , 0.1
Parameters to calculate polymer viscosity at zero shear rate (AP1, AP2 , AP3), $wt\%^{-1}$	35, 30, 1000
Gamma C	4
Parameter for salinity dependence of polymer viscosity (SSLOPE), dimensionless	-0.5264
Parameter for shear rate dependence of polymer viscosity (POWN, GAMMAHF1)	1.7, 15
Permeability reduction factors, (BRK , CRK)	100 , 0.015

Table 5.3 Continued

Residual water saturation, fraction	0.28
Residual oil saturation, fraction	0.28
Endpoint relative permeability of water	0.268
Endpoint relative permeability of oil	0.788
Relative permeability exponent of water	2
Relative permeability exponent of oil	2
Physical Dispersion Coefficients for Water, Oil, ME (ALPHAL1-3, ALPHAT1-3)	3 , 1

Table 5.4: Layer properties within the pilot well pattern

Layer No.	Porosity	NTG	Pore Volume, ft3	Soi	Oil Present, ft^3
Layer 1	0.166	1.138	277,525	0.512	142,187
Layer 2	0.177	1.182	293,554	0.368	107,901
Layer 3	0.182	1.213	306,304	0.309	94,662
Layer 4	0.171	1.177	289,363	0.369	106,897
Layer 5	0.198	1.323	346,778	0.400	138,787
Layer 6	0.207	1.324	362,906	0.296	107,386
Layer 7	0.212	1.324	371,666	0.286	106,207
Layer 8	0.210	1.324	367,907	0.284	104,478
Layer 9	0.186	1.323	326,080	0.283	92,231
Sum (bbls)			523,968		178,226

Table 5.5: Surfactant slug size sensitivity

Surfactant Slug Size (PPV)	% Surfactant injected	Surf. Adsorption (mg/gm rock)	Surfactant Concentration (%)	Polymer Drive (PPV)	Oil Recovered, (Bbl)
0.5	1	0.25	2	0.70	156370
0.3	1	0.25	1.2	0.70	127640
0.25	1	0.25	1	0.70	117920
0.2	1	0.25	0.8	0.70	104950
0.1	1	0.25	0.4	0.70	70594

Table 5.6: Injection rate detail for all wells for various sensitivities

		Injection Rate Sensitivity, Section **Error! Reference source not found.**		Section **Error! Reference source not found.**
Well Name	Base case, bpd	Quarter Wise Injector Contribution, bpd	Field Injection Rates, bpd	Peripheral producer time optimization, bpd
Pattern Injectors				
BCF 01	125	62.5	110	110
BCF 02	125	125	125	125
BCF 03	125	125	125	125
BCF 04	125	62.5	110	110
BCF 05	125	125	120	120
BCF 06	125	250	150	150
BCF 07	125	250	150	150
BCF 08	125	125	110	110
BCF 09	125	62.5	120	120
BCF 10	125	125	130	130
BCF 11	125	125	130	130
BCF 12	125	62.5	120	120
Sum	**1500**	**1500**	**1500**	**1500**
Pattern Producers				
pM 31	250	250	250	250
pM 42	250	250	250	250
pM 44	250	250	250	250
pM 45	250	250	250	250
pM 46	250	250	250	250
pM 47	250	250	250	250
Peripheral Injectors				
DD 6	75	75	75	75
GG 7	75	75	75	75
D 7	50	50	50	50
Peripheral Producers				
pM 23	1	1	1	50
pM 28	1	1	1	50
pM 32	1	1	1	50

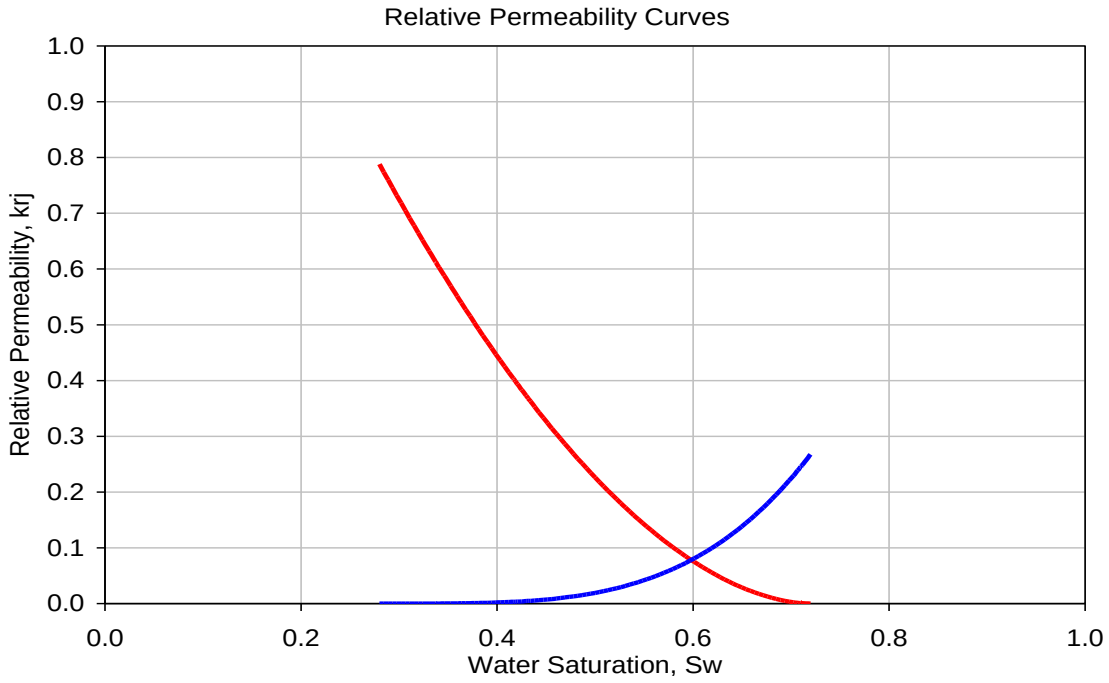

Figure 5.1: Oil/water relative permeability curves

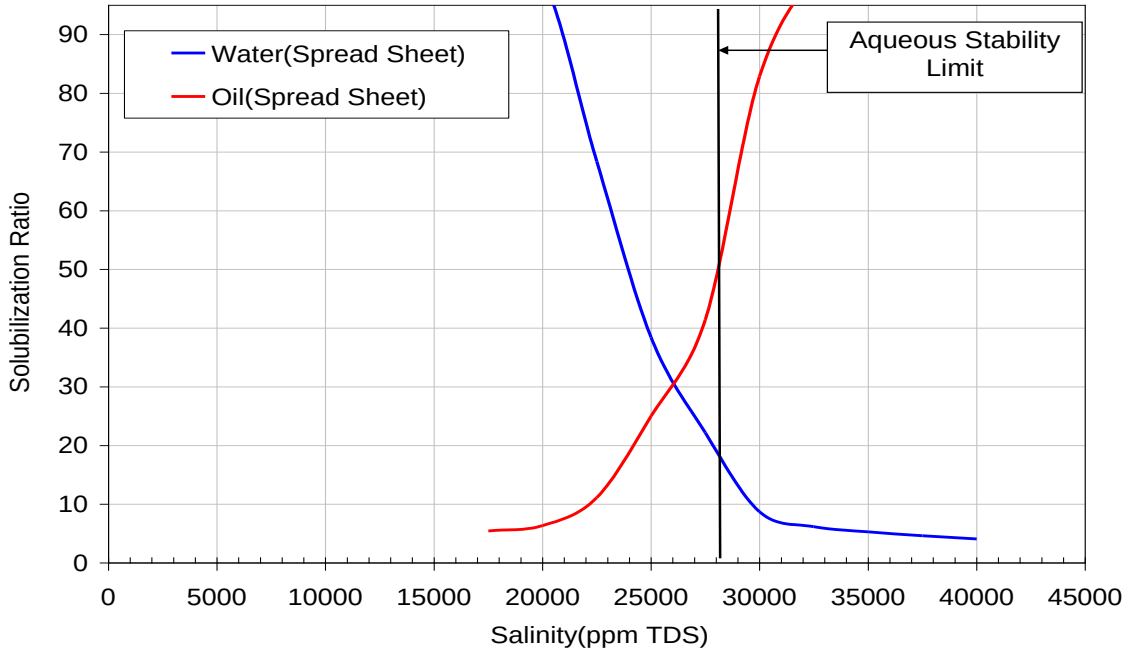

Figure 5.2: Phase behavior model for reservoir B simulation with 1%Surfactant

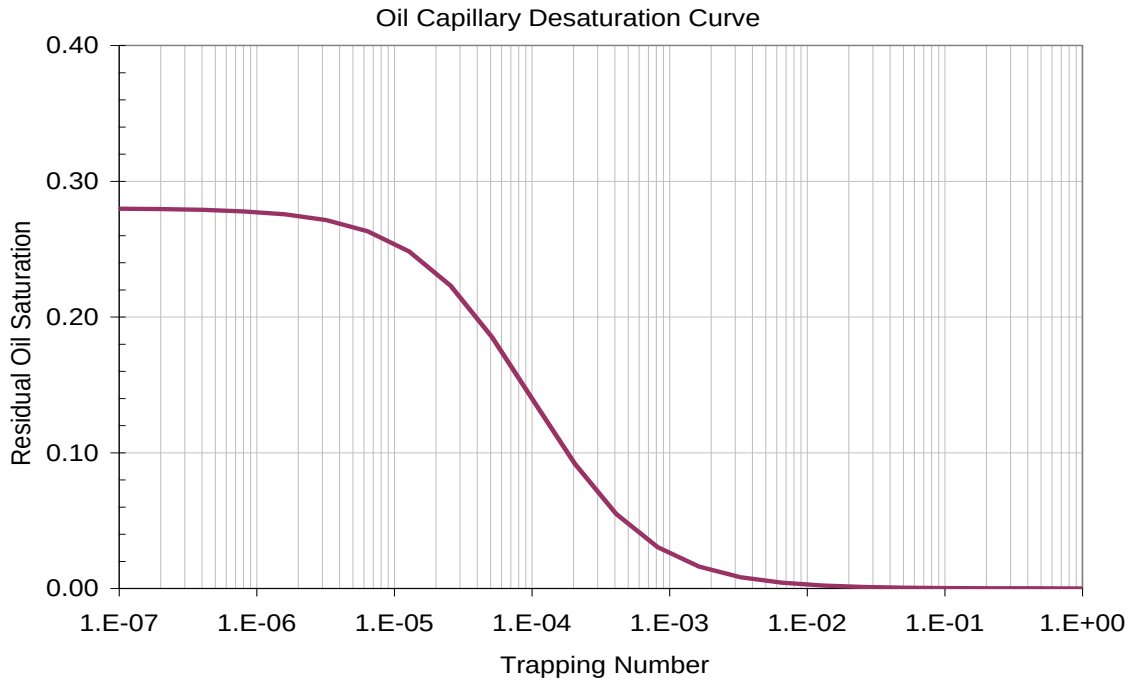

Figure 5.3: Capillary desaturation curve for oil in simulation model input

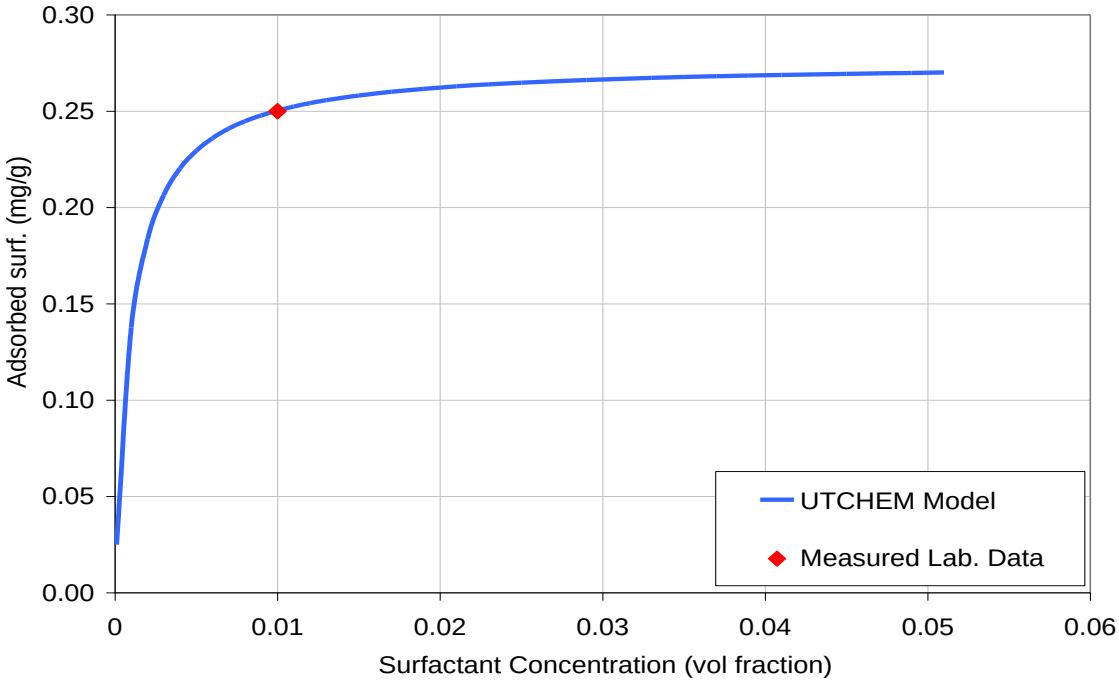

Figure 5.4: UTCHEM match with lab data of surfactant adsorption

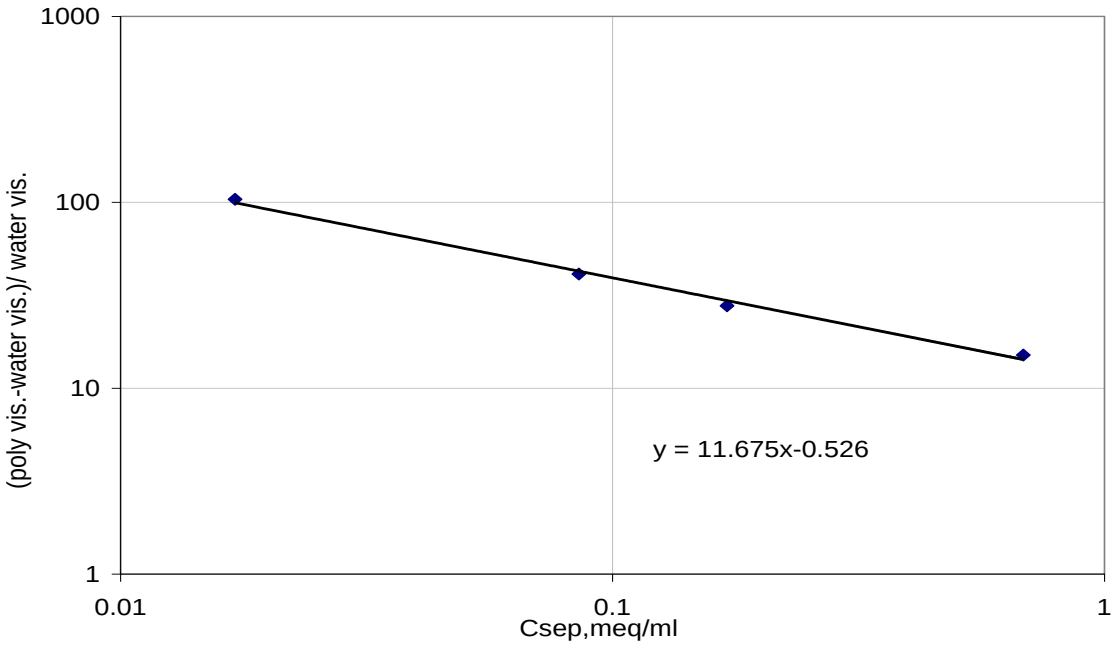

Figure 5.5: UTCHEM model fit to measured lab. data for Flopaam 3330S polymer viscosity vs. salinity (2200 ppm; 25degC)

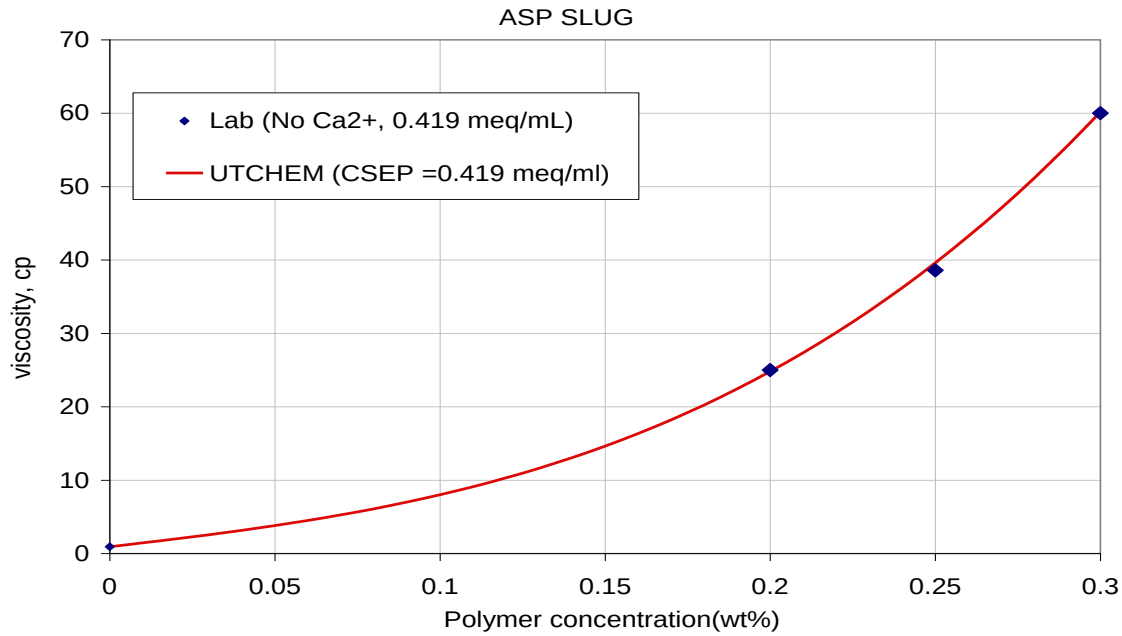

Figure 5.6: UTCHEM model fit to measured lab. data for Flopaam 3330S polymer viscosity vs. concentration (0.419 meq/ml; 25degC)

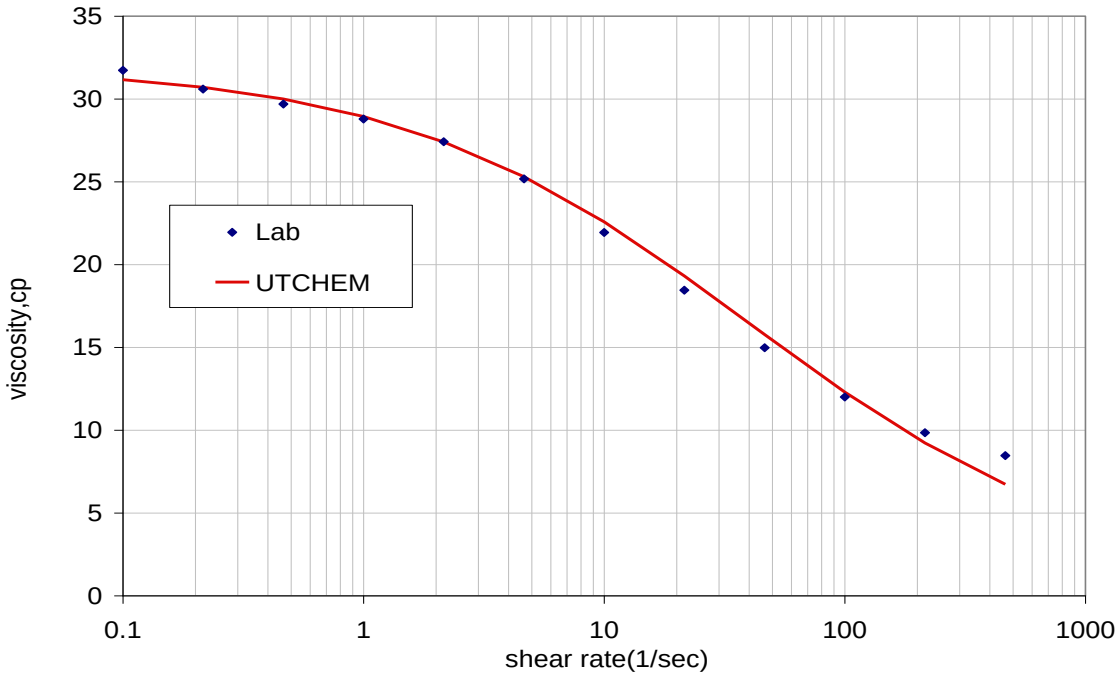

Figure 5.7: UTCHEM model fit to measured lab. data for Flopaam 3330S polymer viscosity vs. shear rate (2200 ppm; 1.6% NaCl;25degC)

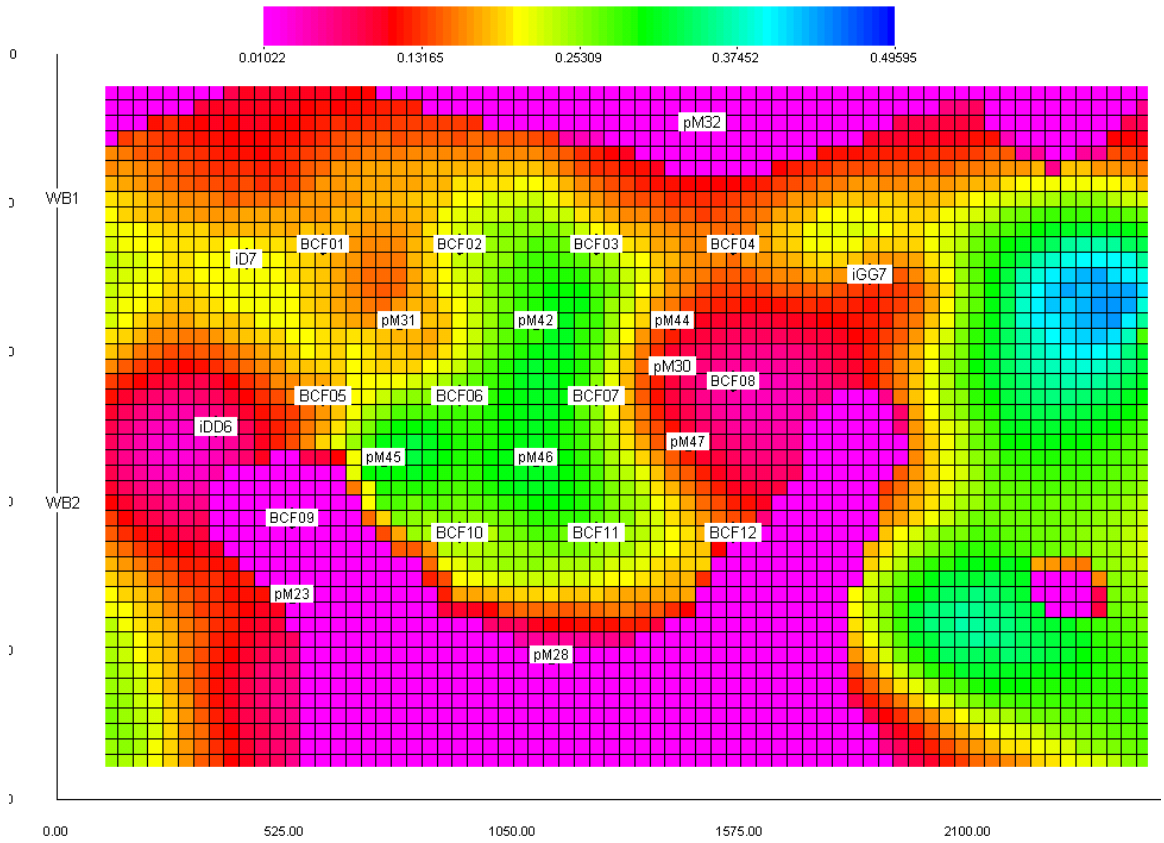

Figure 5.8: Areal view of porosity of layer 1 of the pod

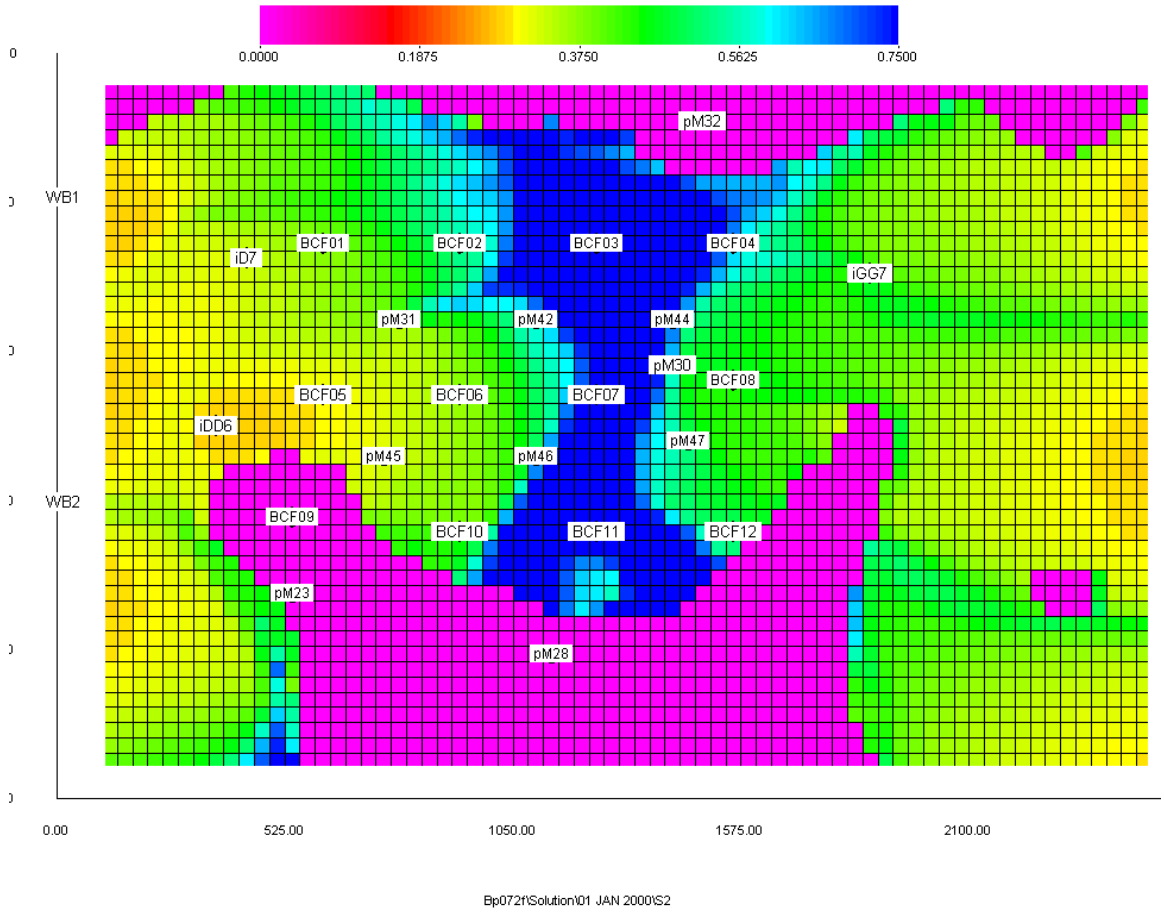

Figure 5.9: Areal view of initial oil saturation of layer 1 of the pod

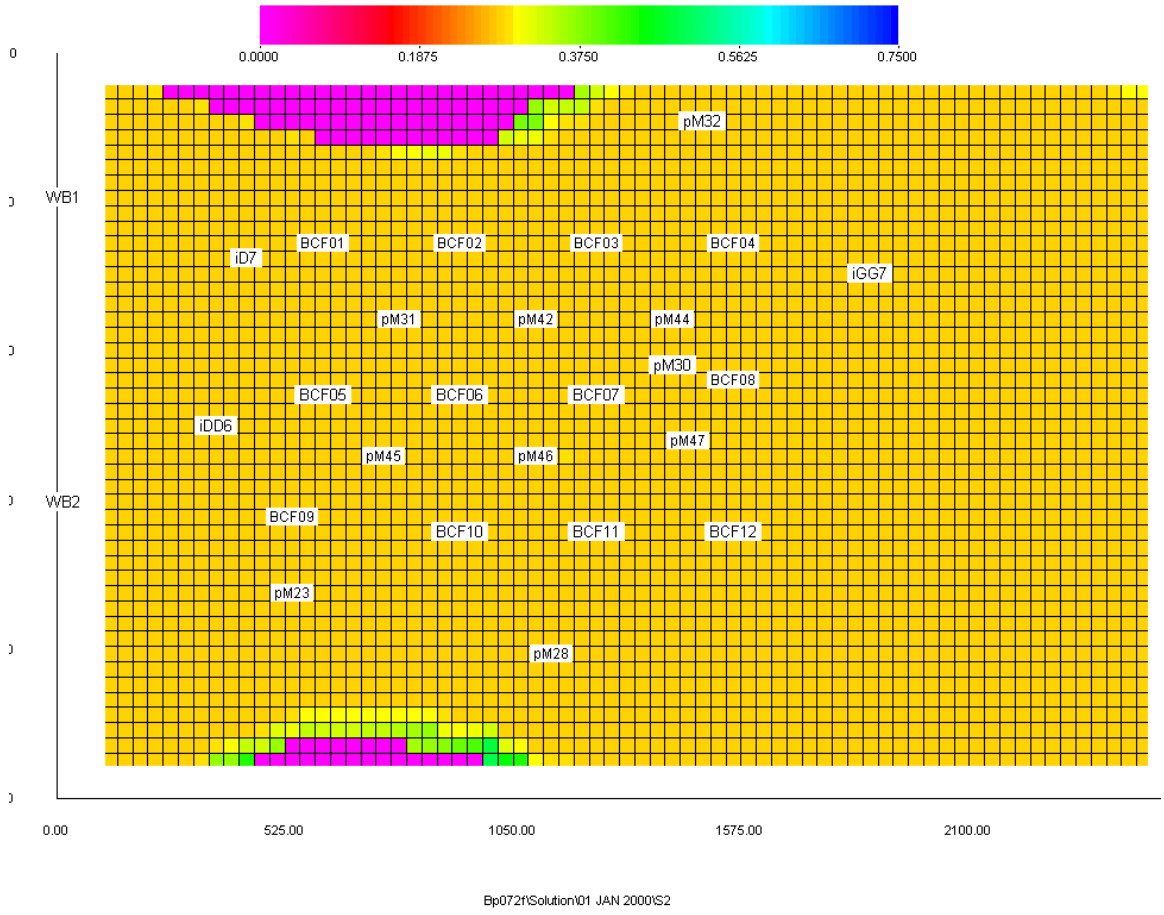

Figure 5.10: Areal view of initial oil saturation of layer 9 of the pod

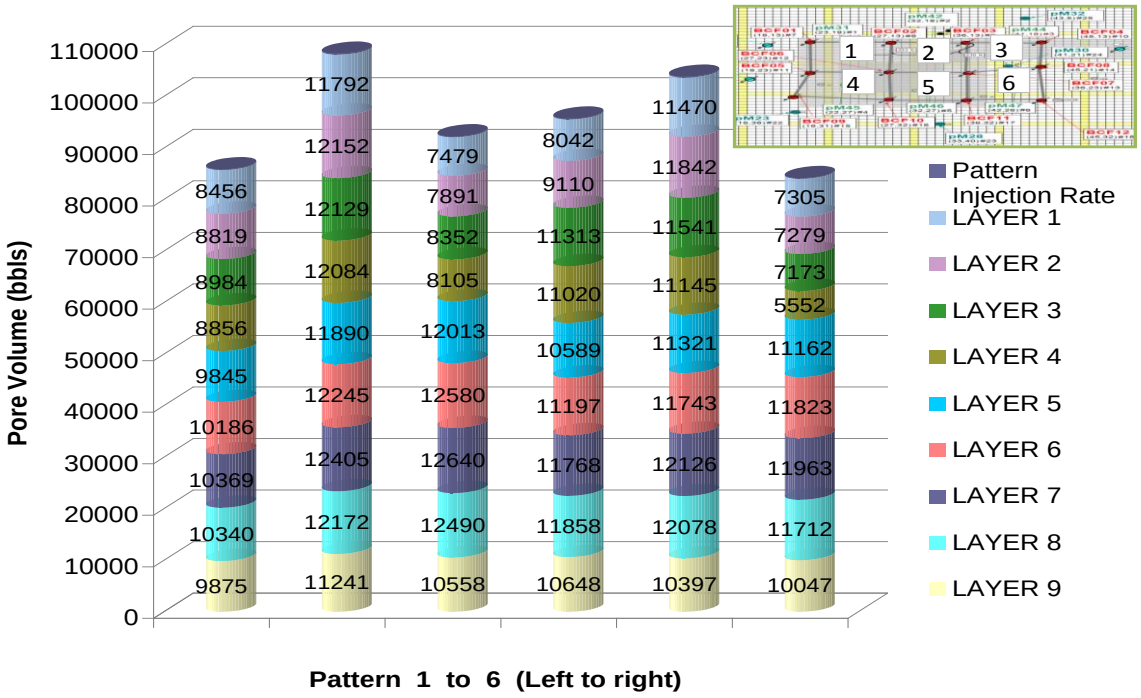

Figure 5.11: Layerwise pore volume distribution of five spots within the pattern

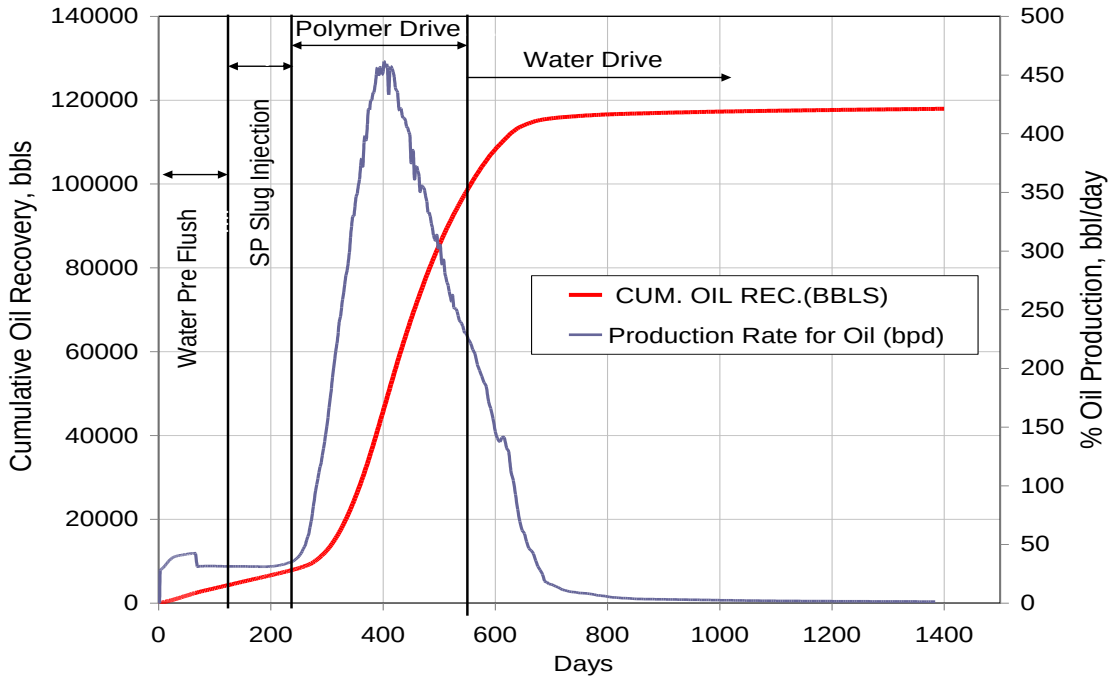

Figure 5.12: Cumulative oil recovery and oil cut for the simulated base case

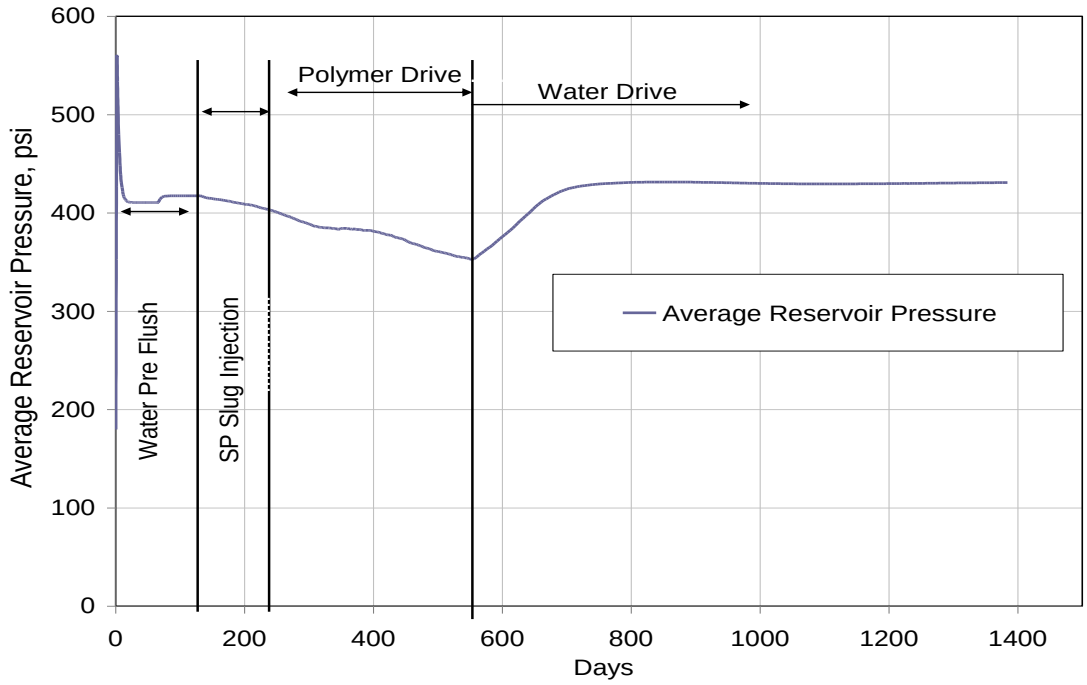

Figure 5.13: Reservoir pressure for the base case

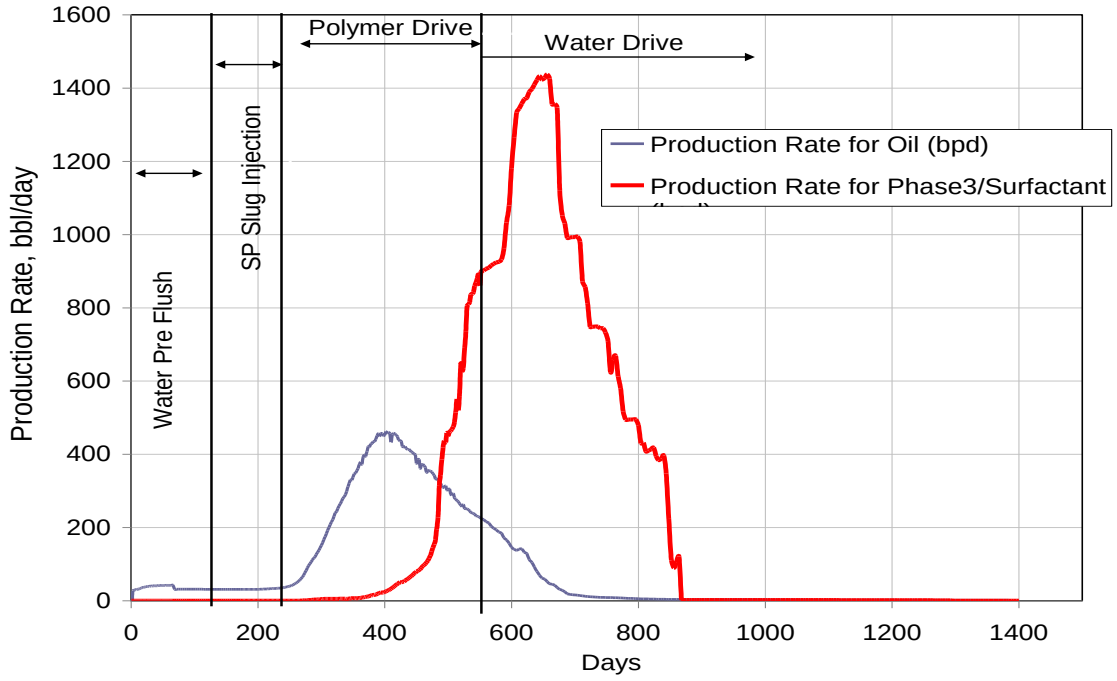

Figure 5.14: Oil and phase3 cut for the simulated base case

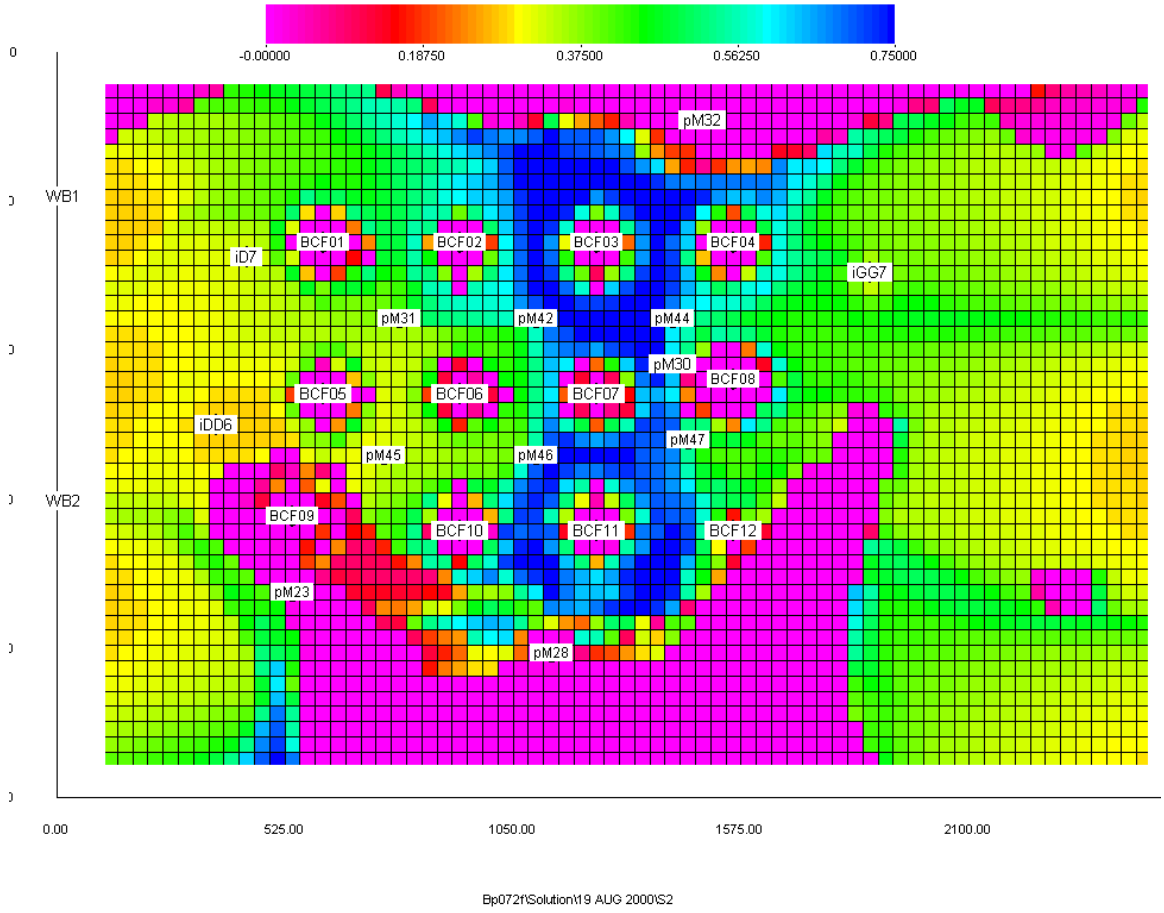

Figure 5.15: Oil saturation of layer 1 at 234th day (end of slug injection)

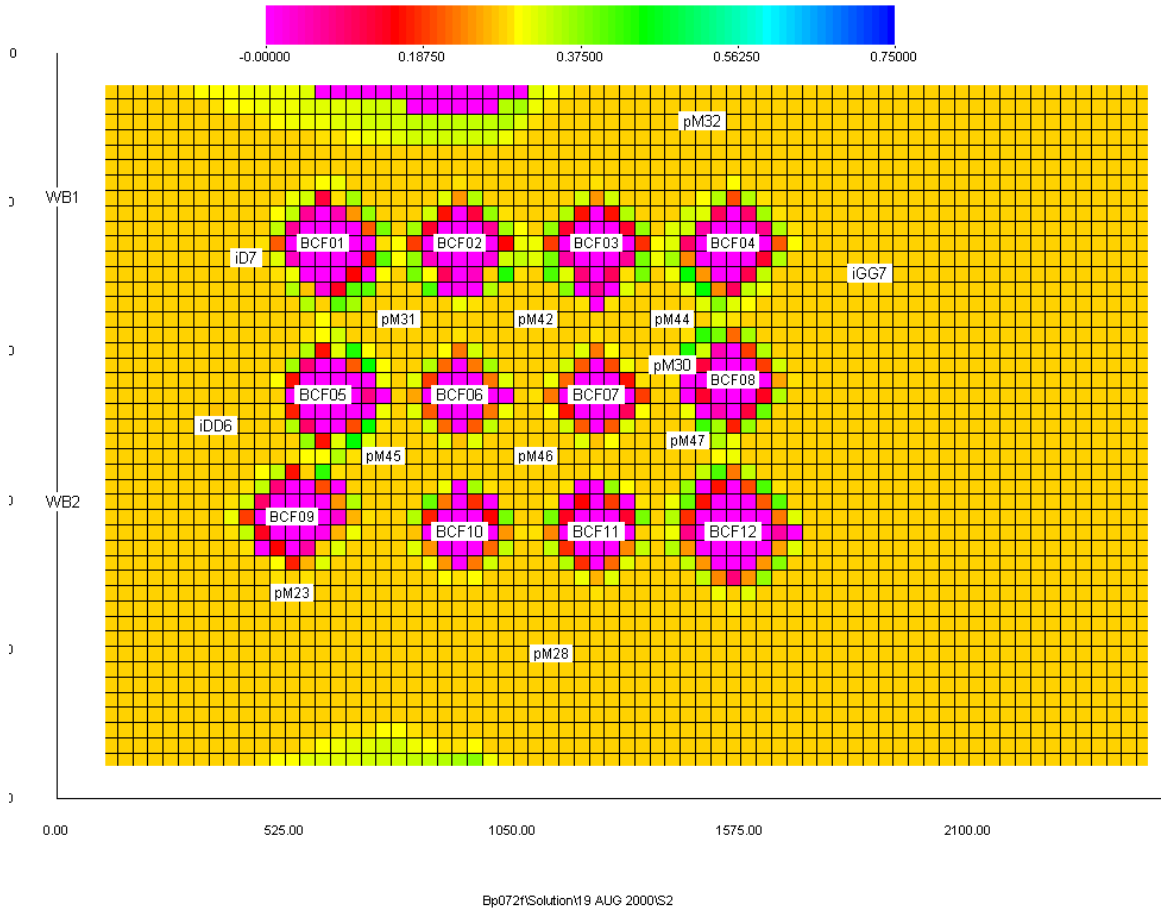

Figure 5.16: Oil saturation of layer 9 at 234th day (end of slug injection)

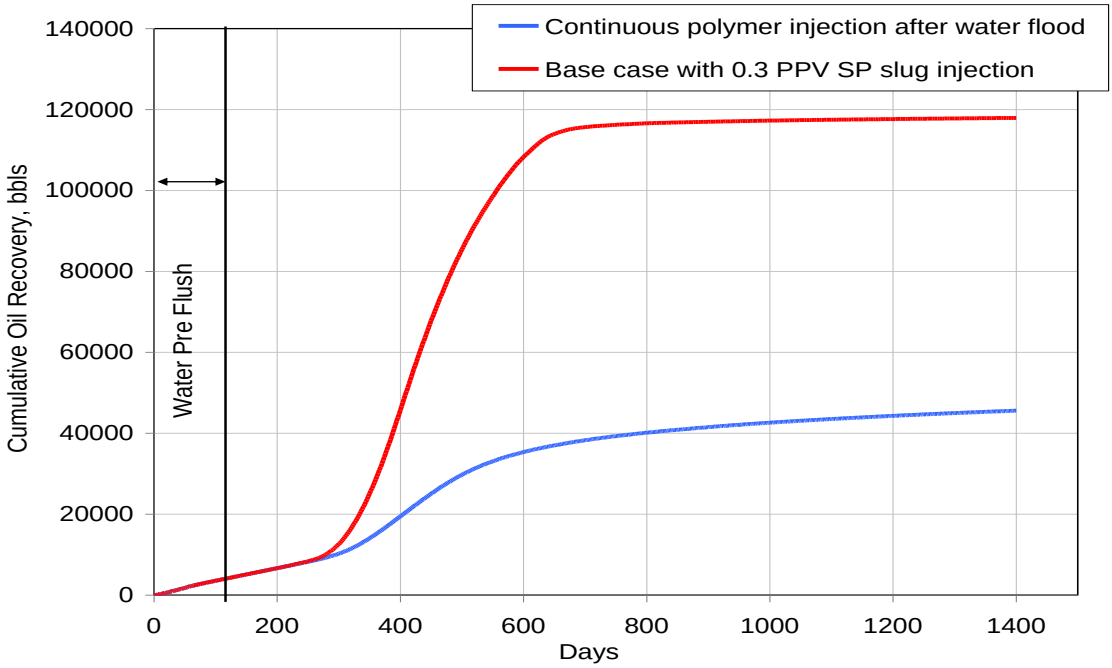

Figure 5.17: Comparison of incremental oil recovered by a surfactant flood over polymer flood

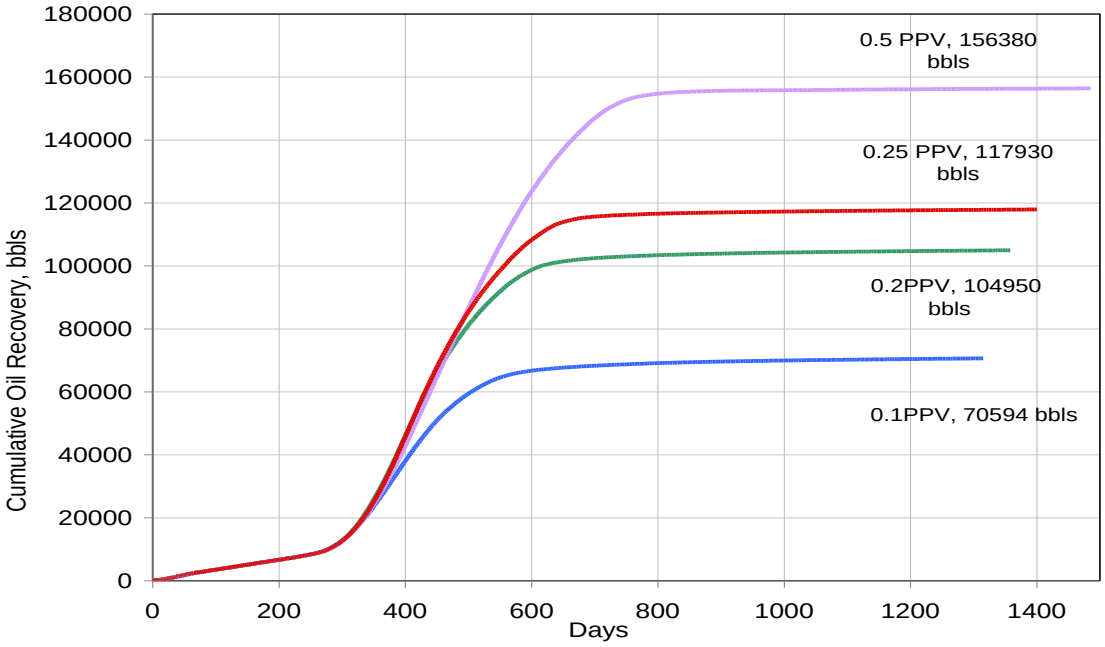

Figure 5.18: Comparison between various sensitivity cases of surfactant slug size Bp072c

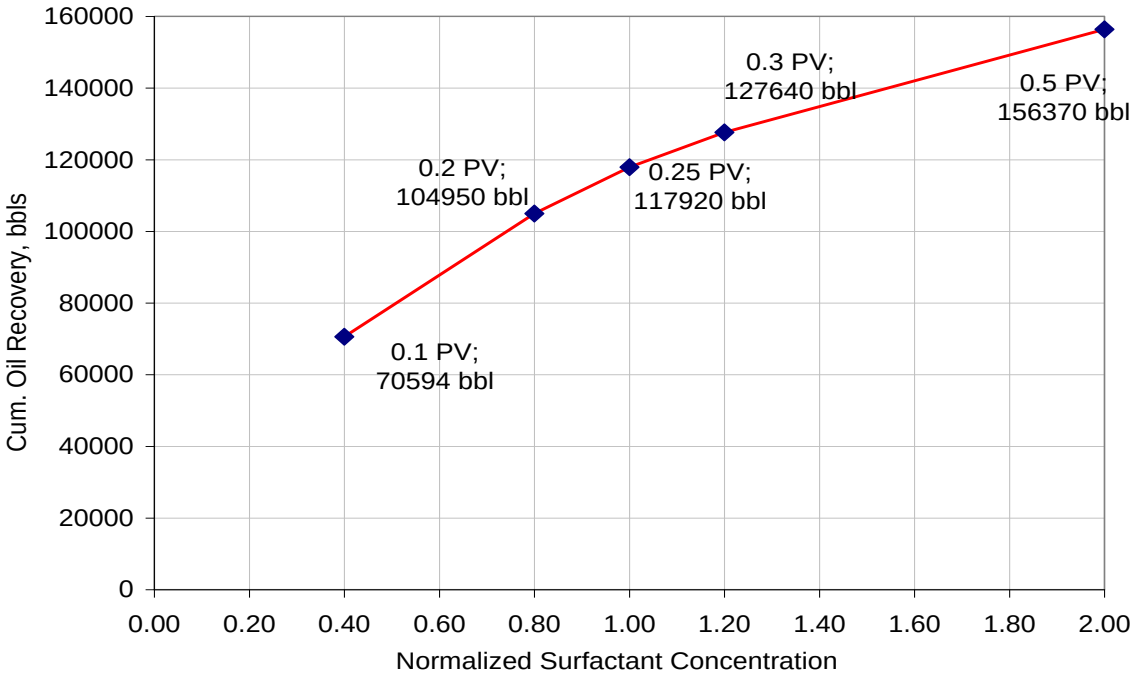

Figure 5.19: Cum. oil recovery vs. normalized surf. conc. for surfactant slug size sensitivity

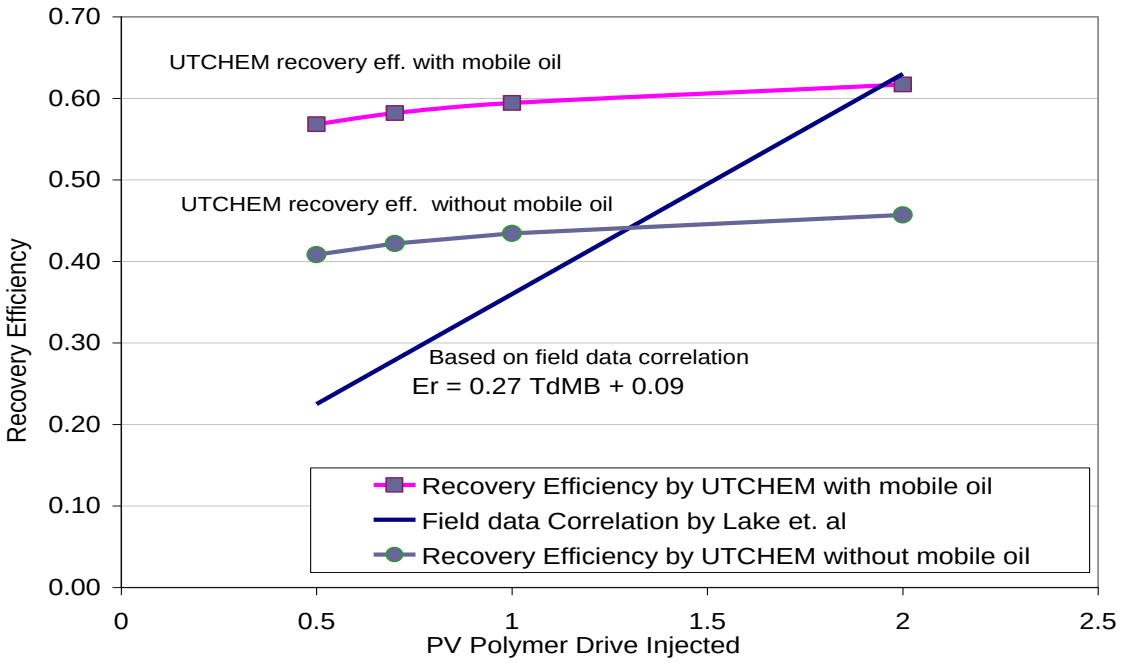

Figure 5.20: Recovery efficiency for polymer drive size sensitivity cases

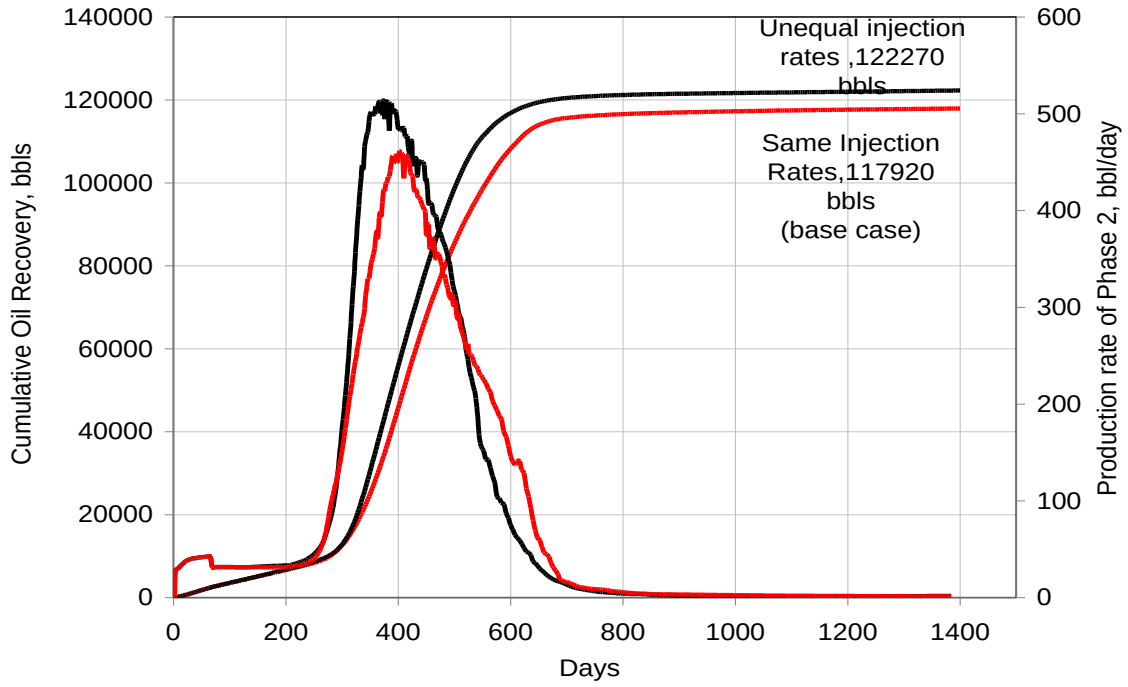

Figure 5.21: Cumulative oil recovery and oil cut for injection rate sensitivity

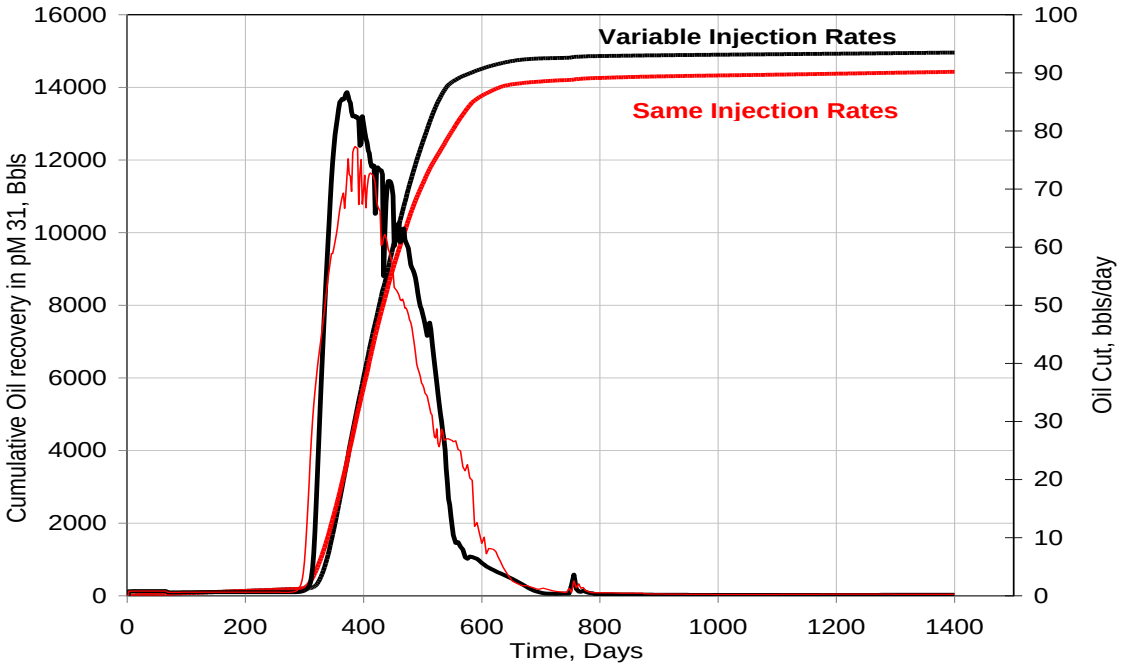

Figure 5.22: Oil recovery comparison for injection rate sensitivity for pM31

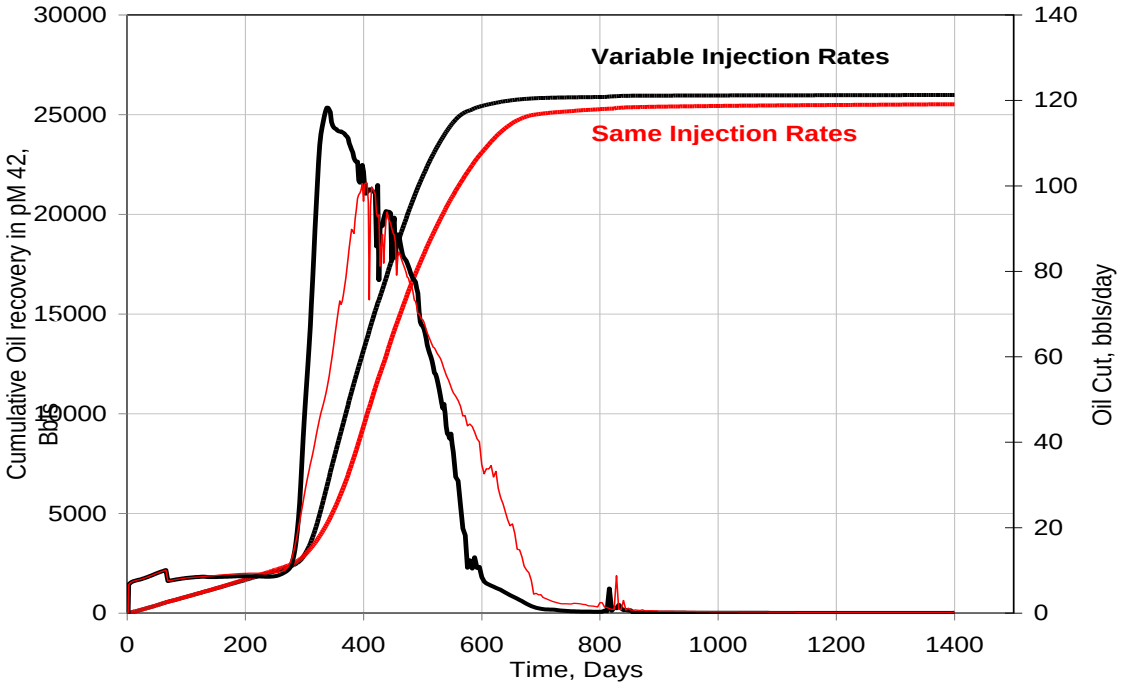

Figure 5.23: Oil recovery comparison for injection rate sensitivity for pM42

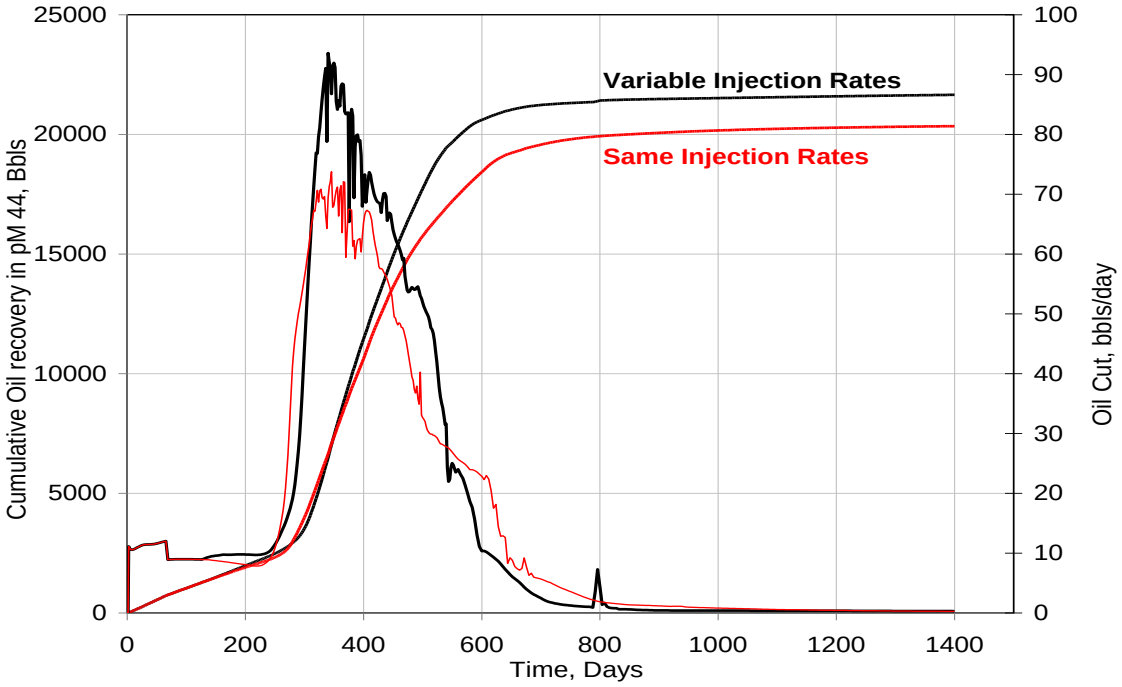

Figure 5.24: Oil recovery comparison for injection rate sensitivity for pM44

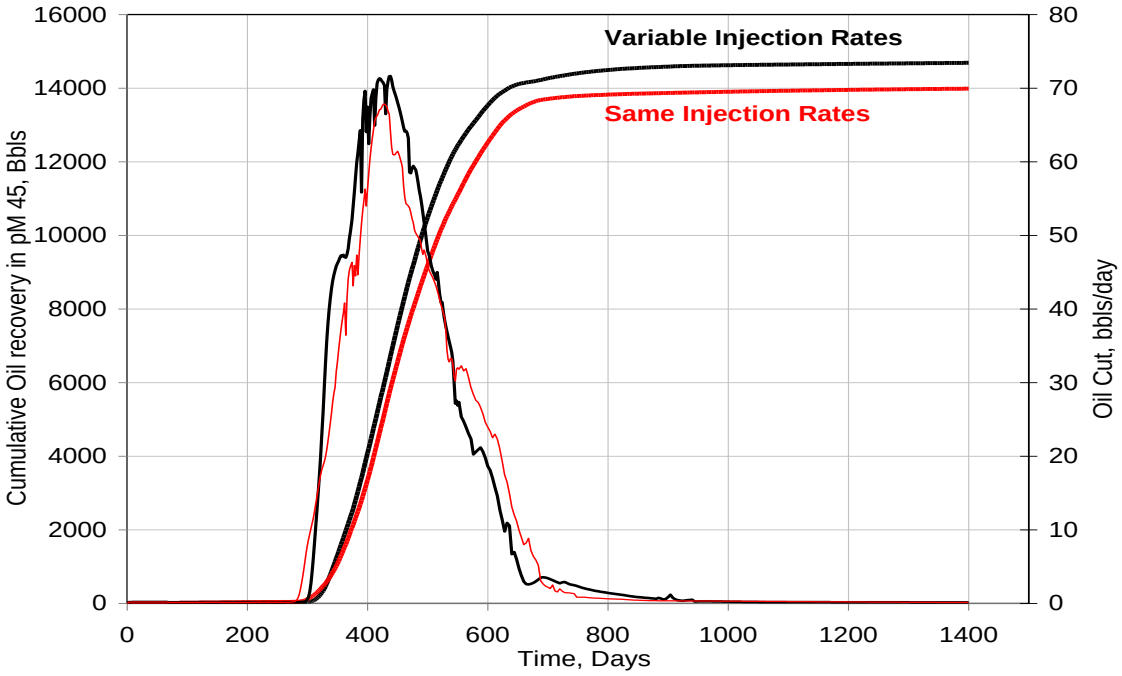

Figure 5.25: Oil recovery comparison for injection rate sensitivity for pM45

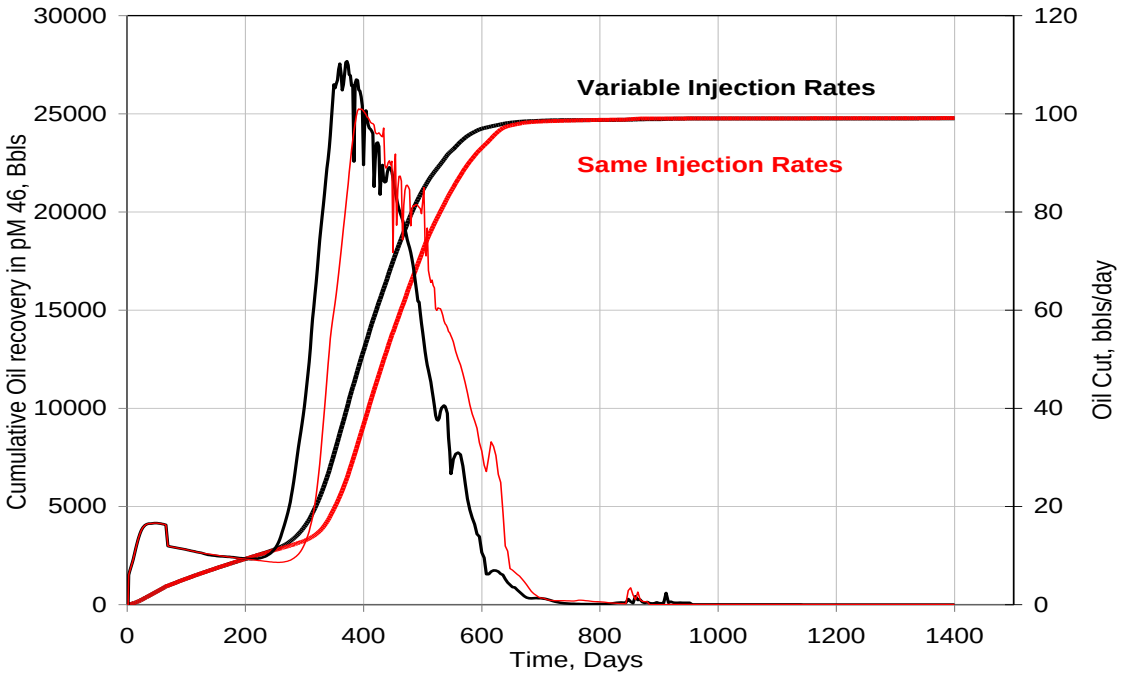

Figure 5.26: Oil recovery comparison for injection rate sensitivity for pM46

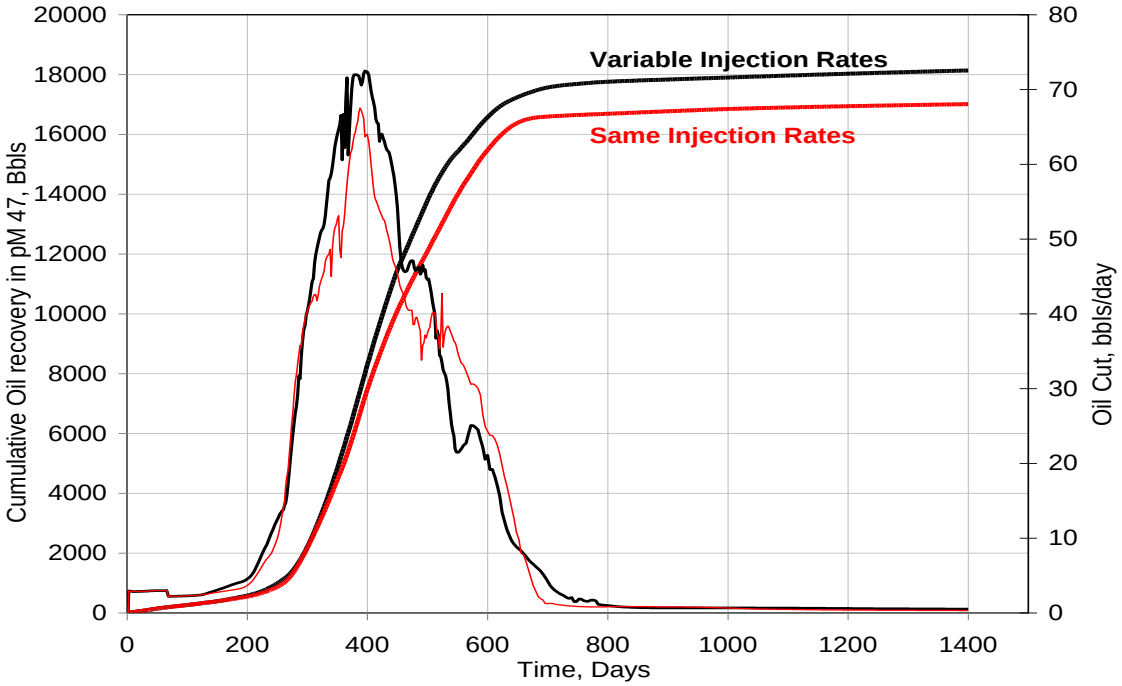

Figure 5.27: Oil recovery comparison for injection rate sensitivity for pM47

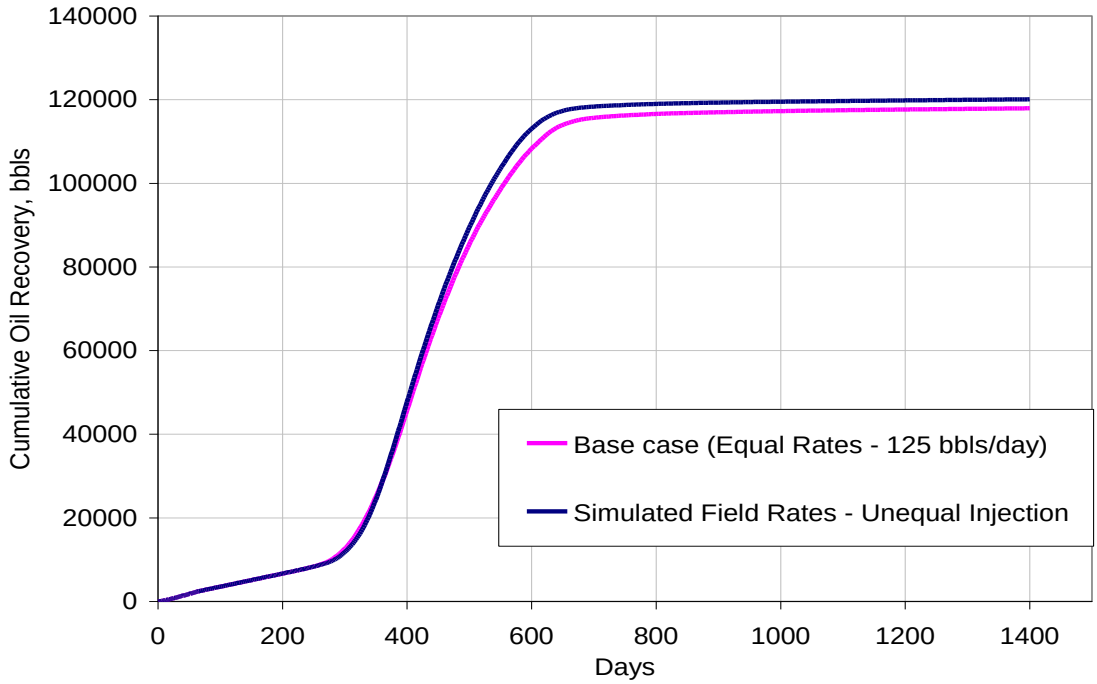

Figure 5.28: Oil recovery comparison between field and equal injection rate

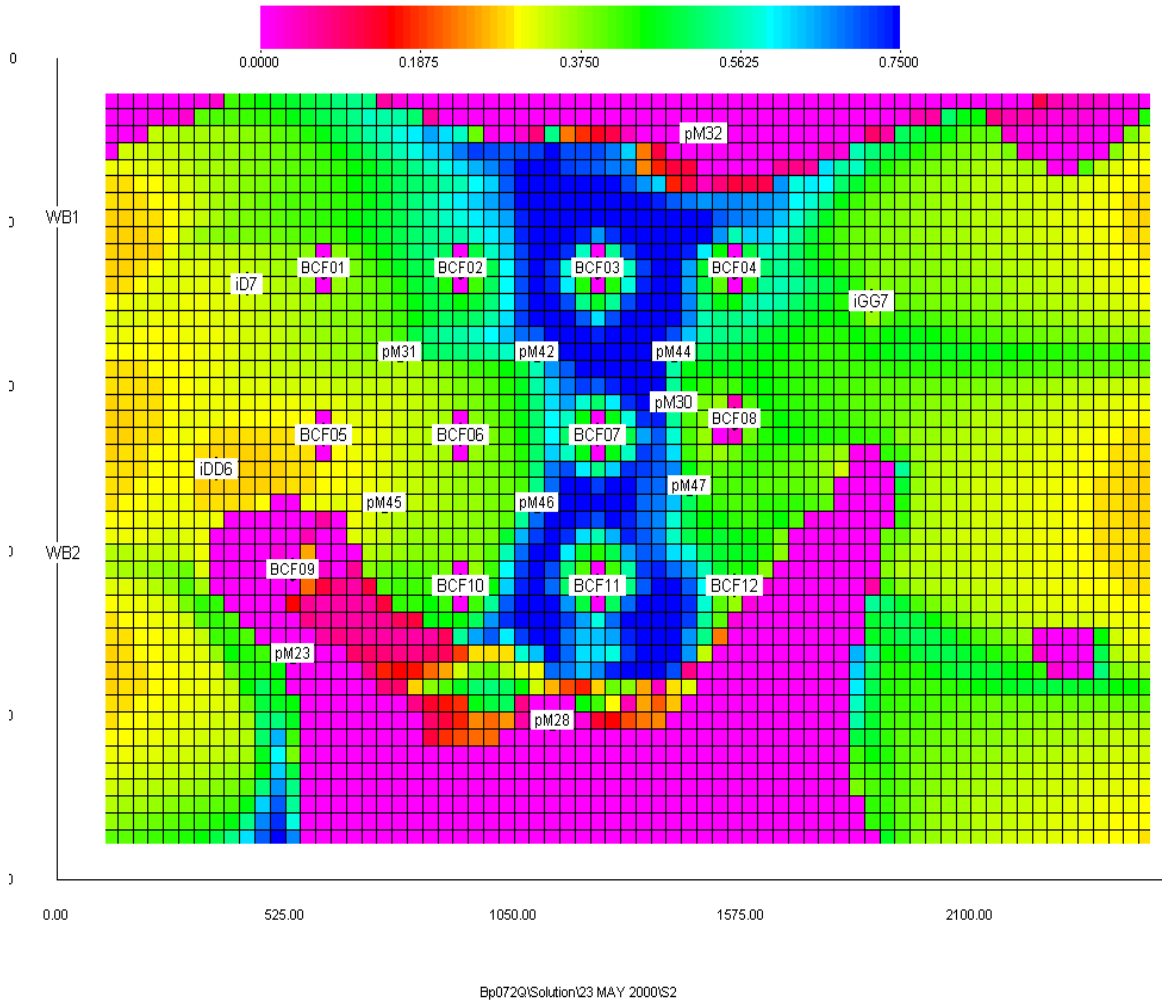

Figure 5.29: Oil saturation of layer 1 at 128th day i.e. 0th day of surfactant injection

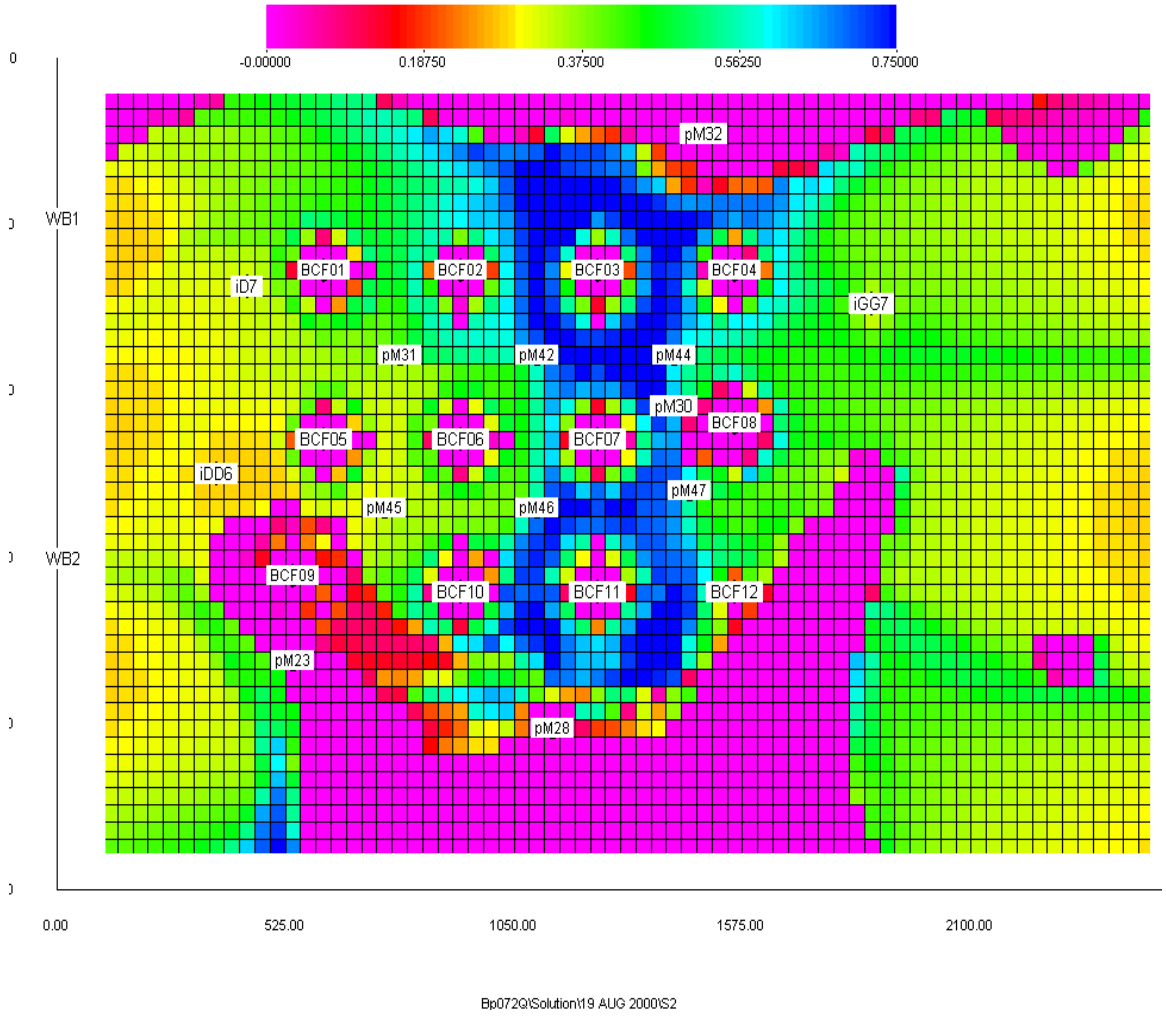

Figure 5.30: Oil saturation of layer 1 at 234th day i.e. 0th day of polymer drive injection

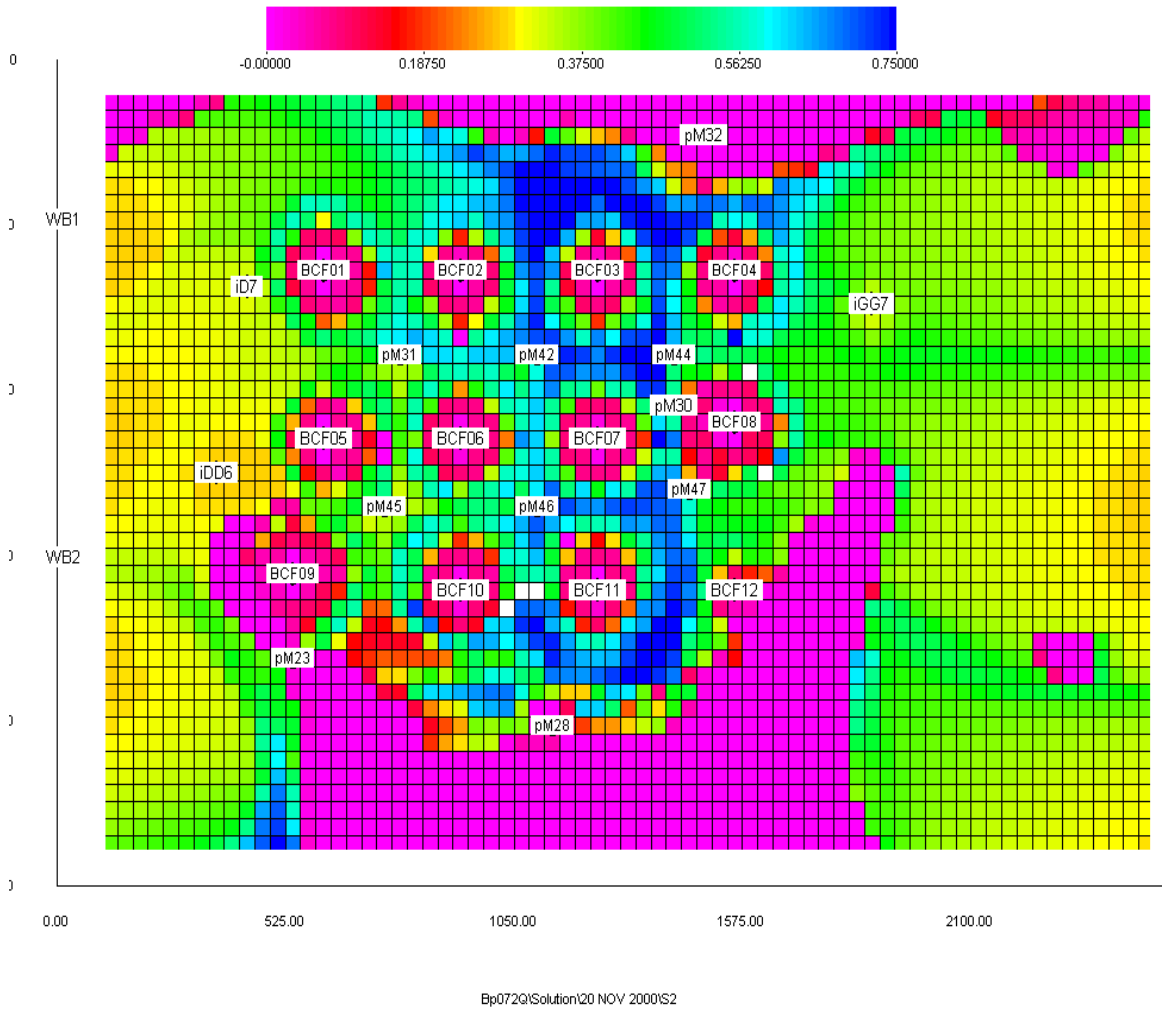

Figure 5.31: Oil saturation of layer 1 at 334th day i.e. 100th day after polymer drive injection

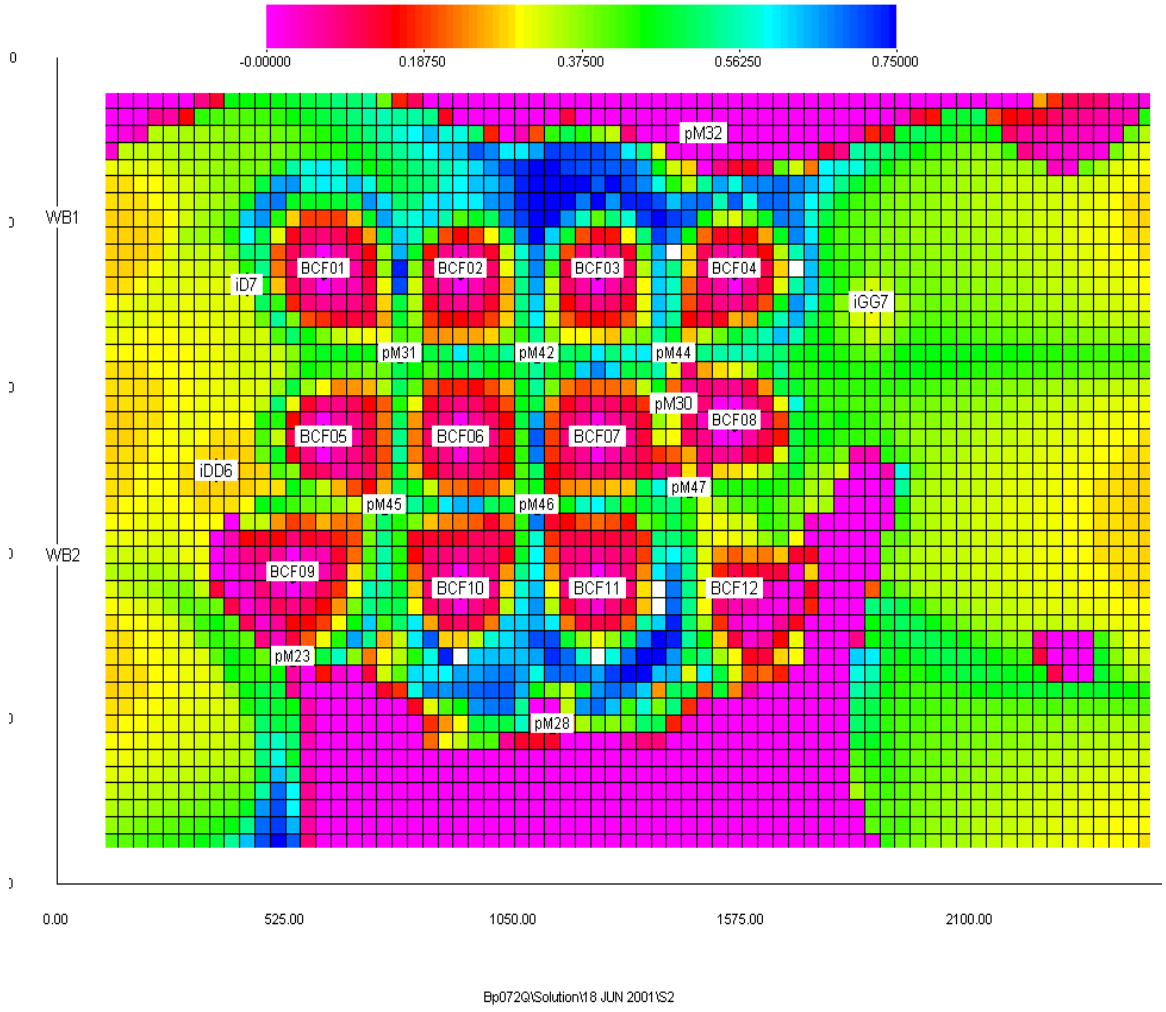

Figure 5.32: Oil saturation of layer 1 at 554th day i.e. 0th day of water drive injection

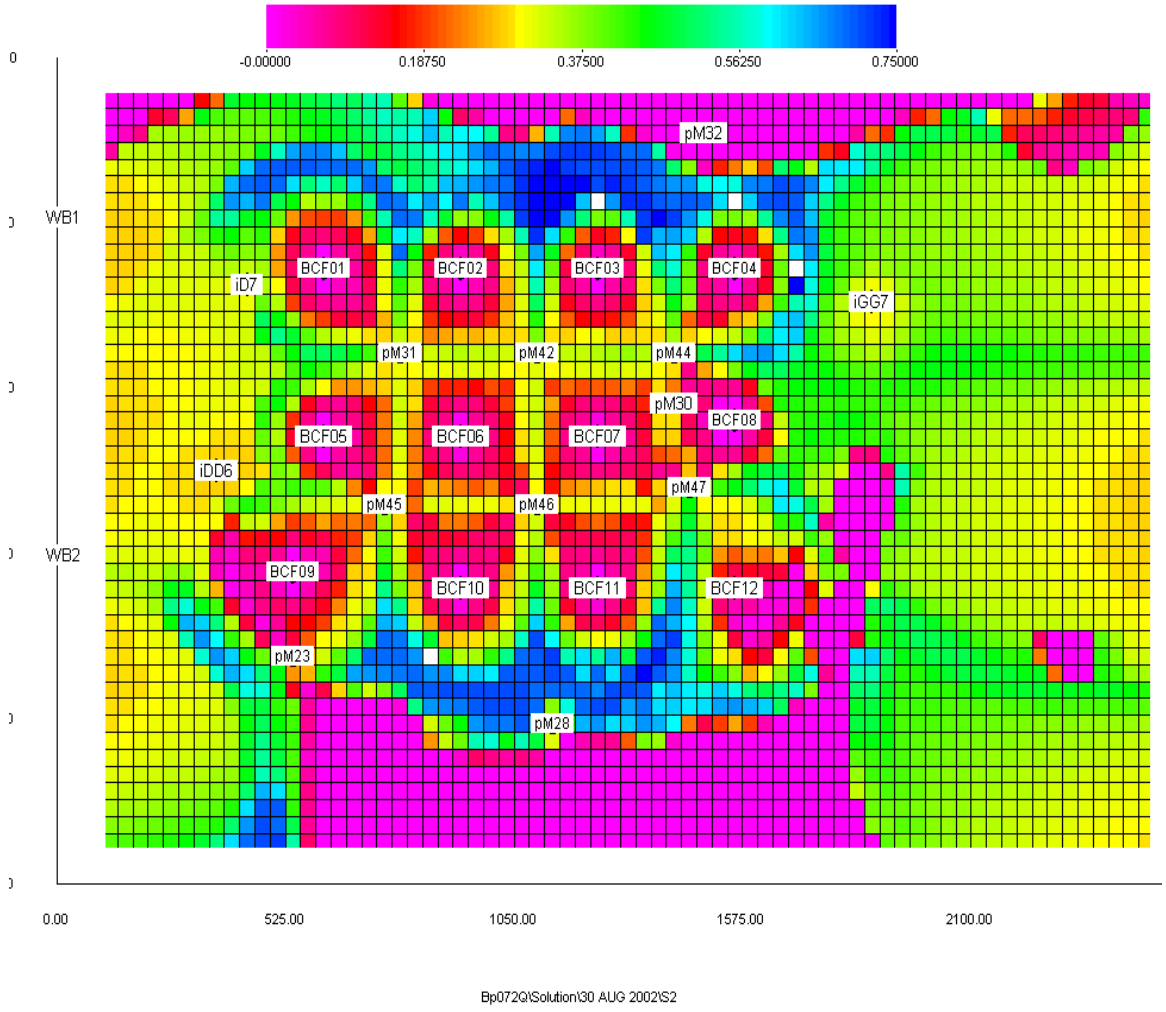

Figure 5.33: Oil saturation of layer 1 at 965th day i.e. 1PPV of water drive injection

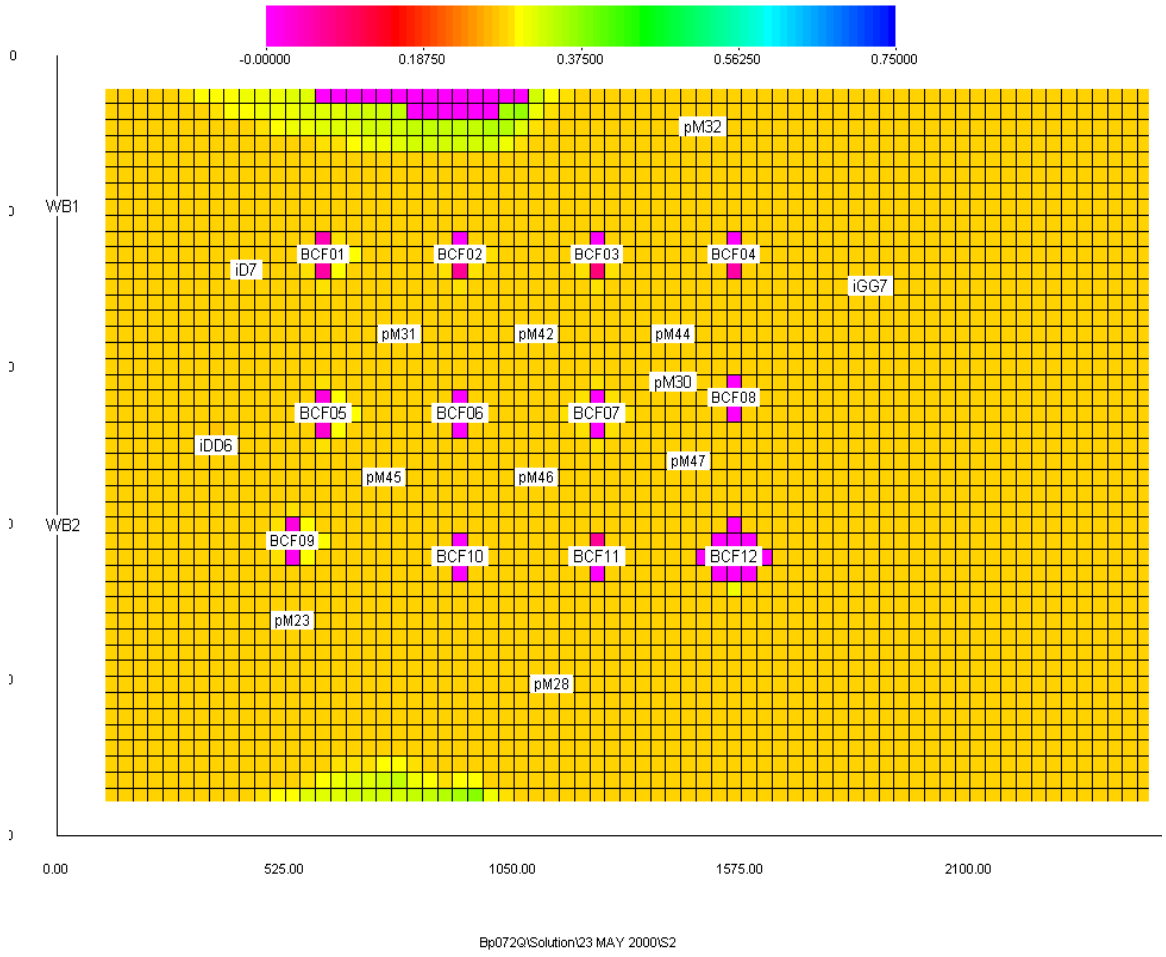

Figure 5.34: Oil saturation of layer 9 at 128th day i.e. 0th day of surfactant injection

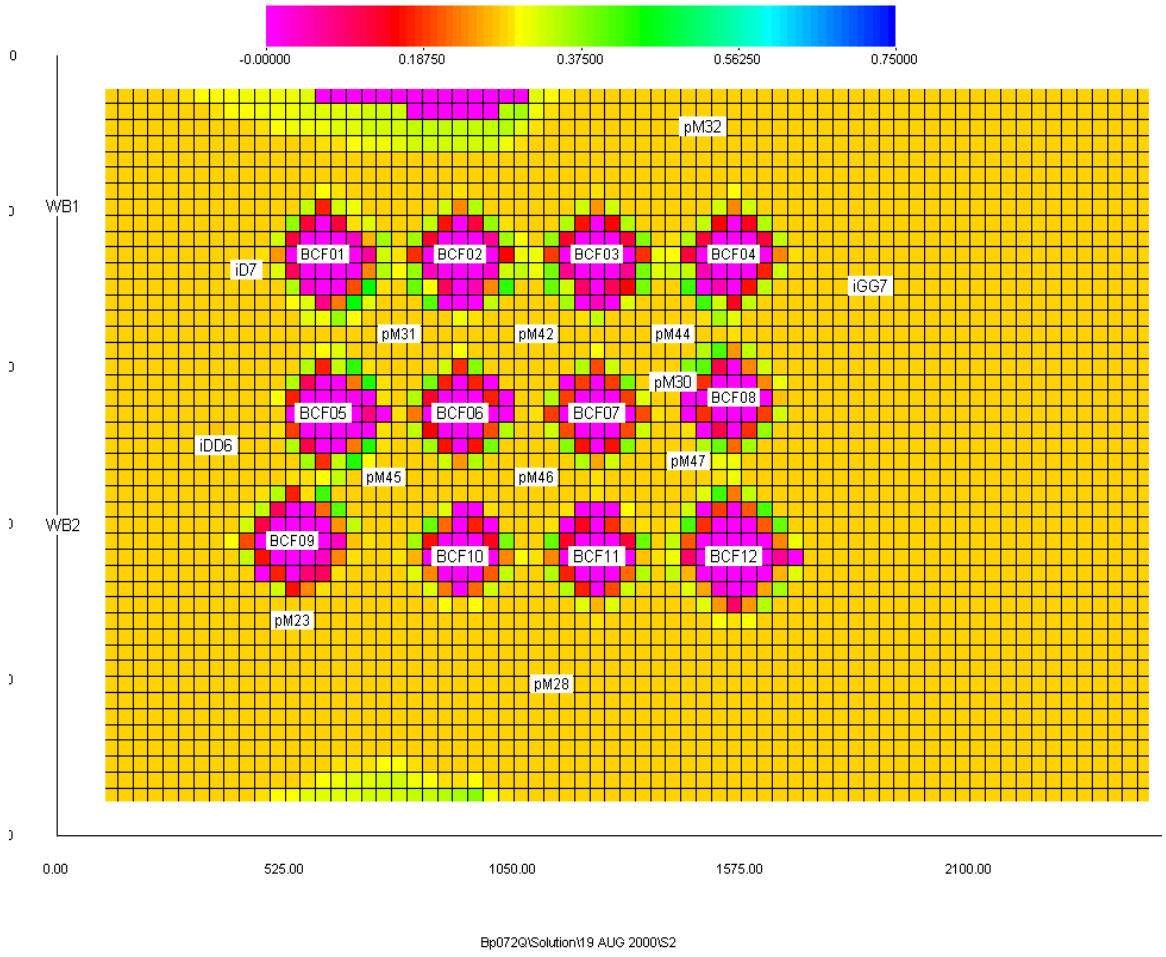

Figure 5.35: Oil saturation of layer 9 at 234th day i.e. 0th day of polymer drive injection

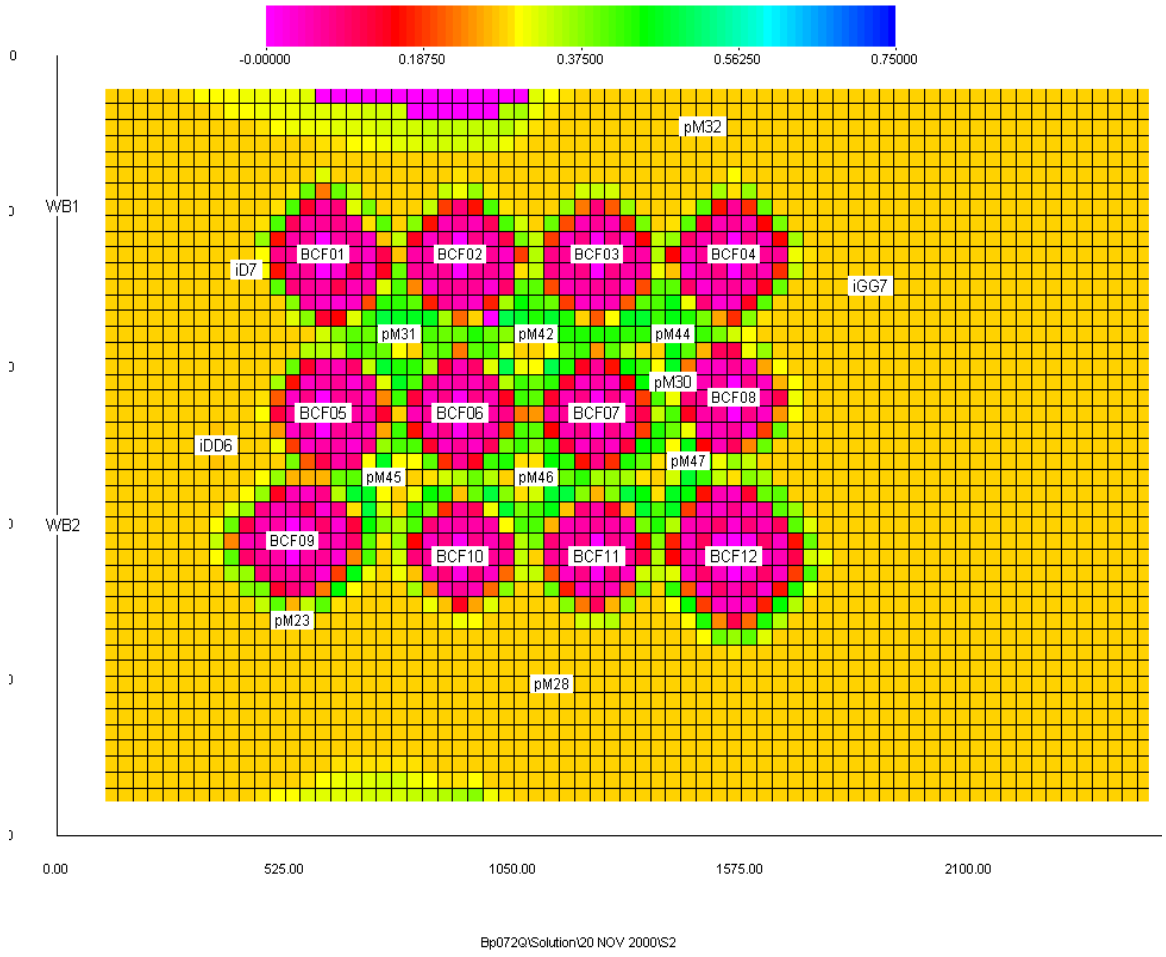

Figure 5.36: Oil saturation of layer 9 at 334th day i.e. 100th day after polymer drive injection

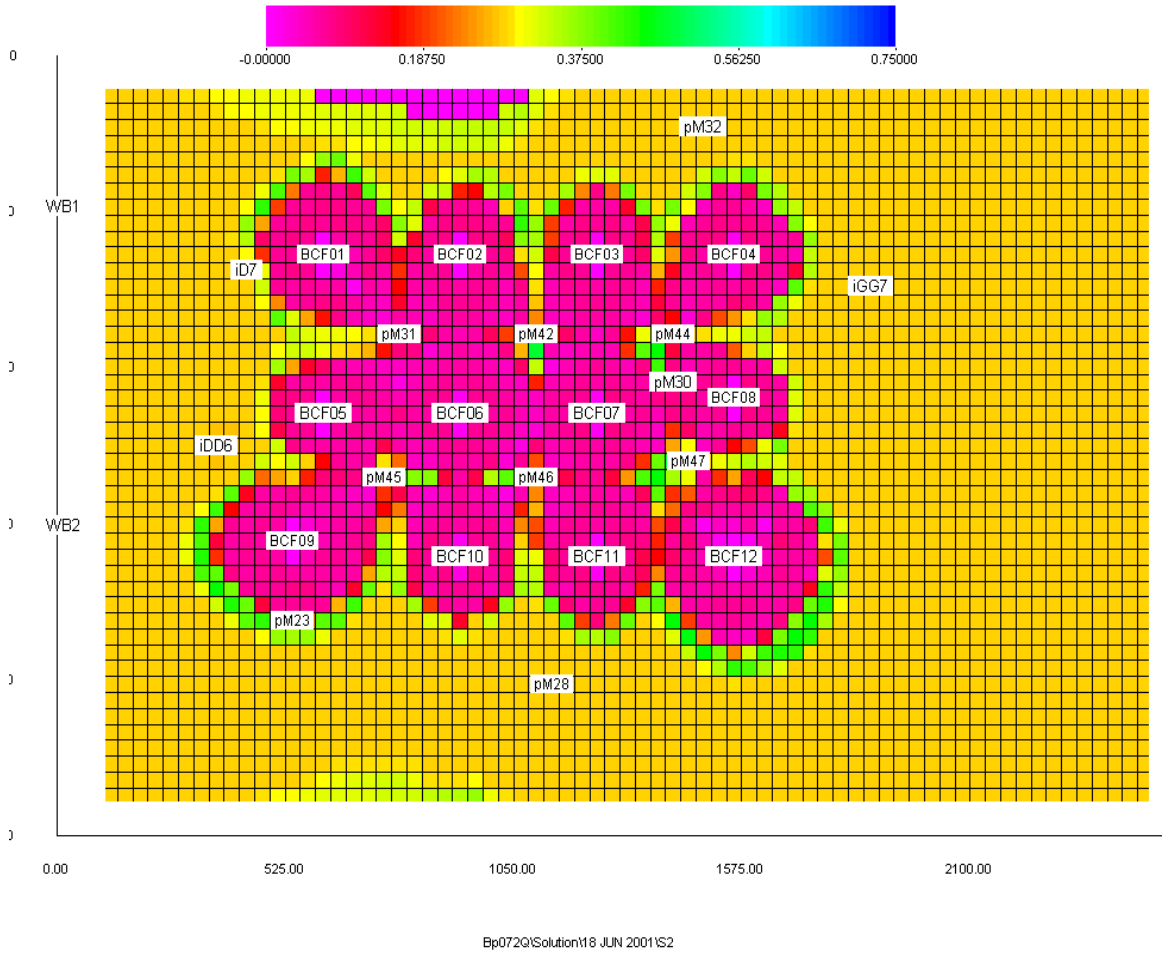

Figure 5.37: Oil saturation of layer 9 at 554th day i.e. 0th day of water drive injection

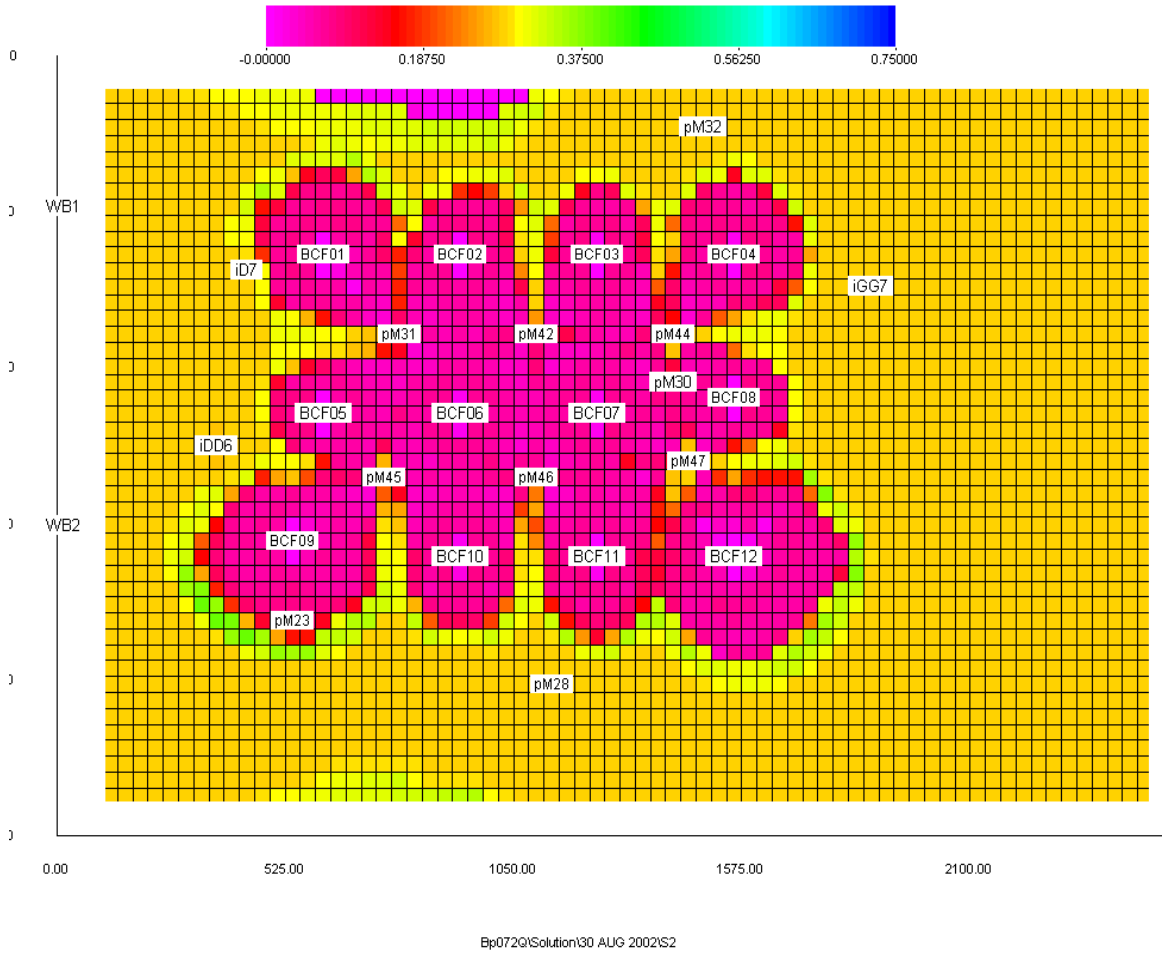

Figure 5.38: Oil saturation of layer 1 at 965th day i.e. 1PPV of water drive injection

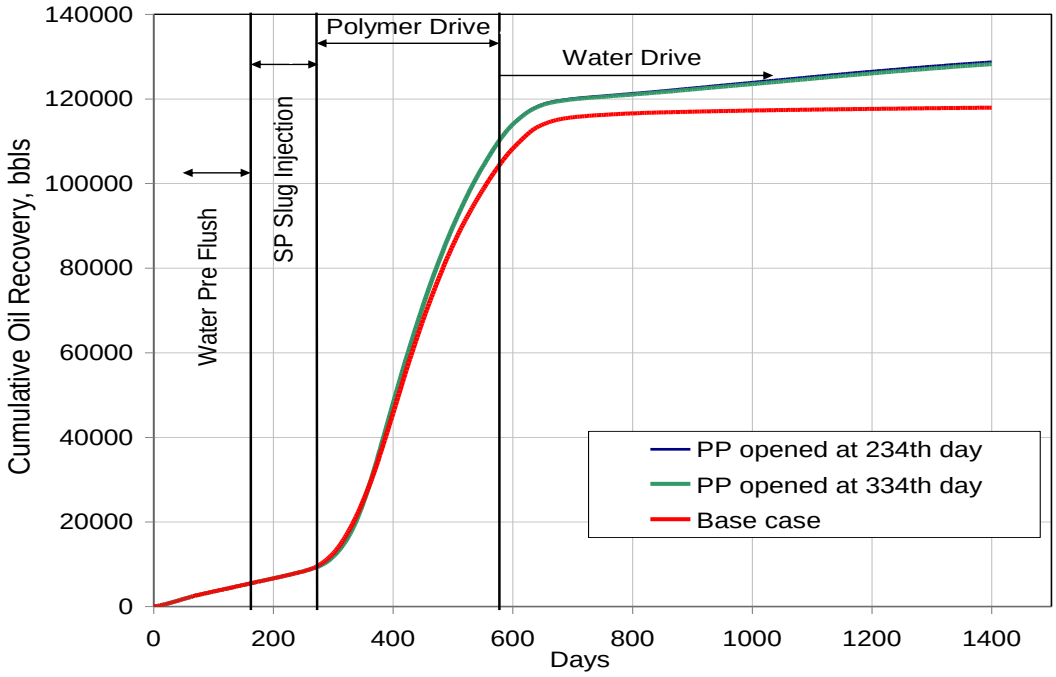

Figure 5.39: Oil recovery comparison at different opening times of peripheral producers

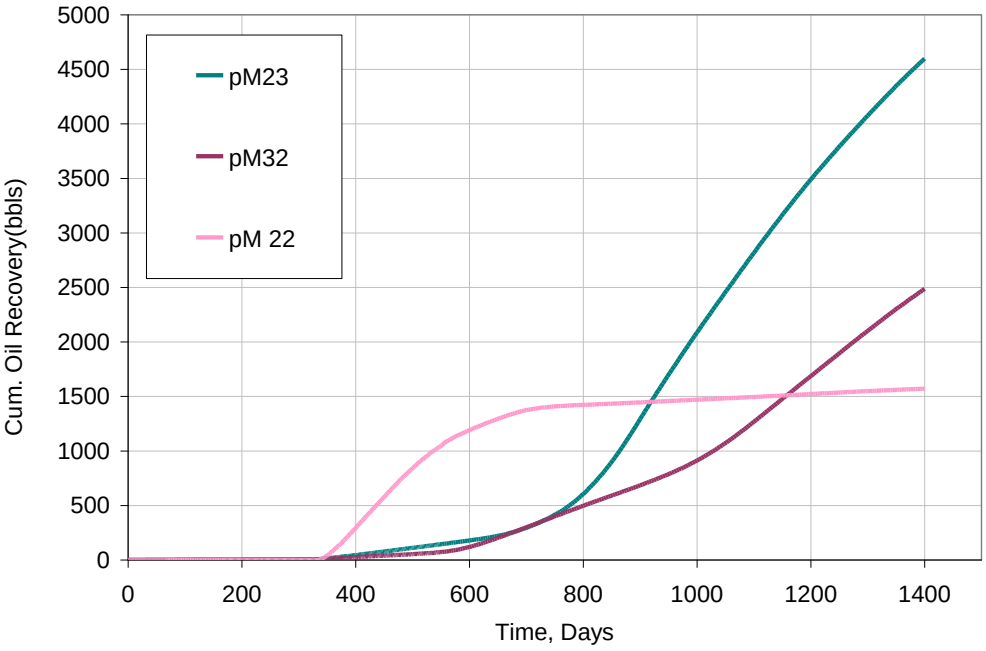

Figure 5.40: Cumulative oil recovery by peripheral producers opened at 334th day

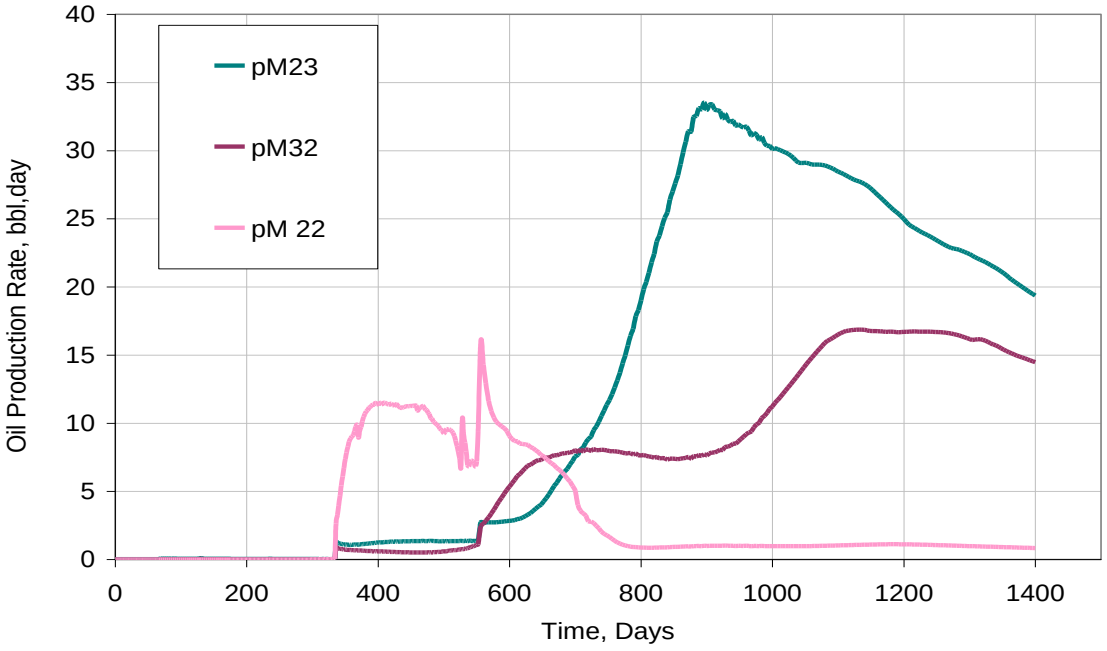

Figure 5.41: Oil production rate by peripheral producers opened at 334th day

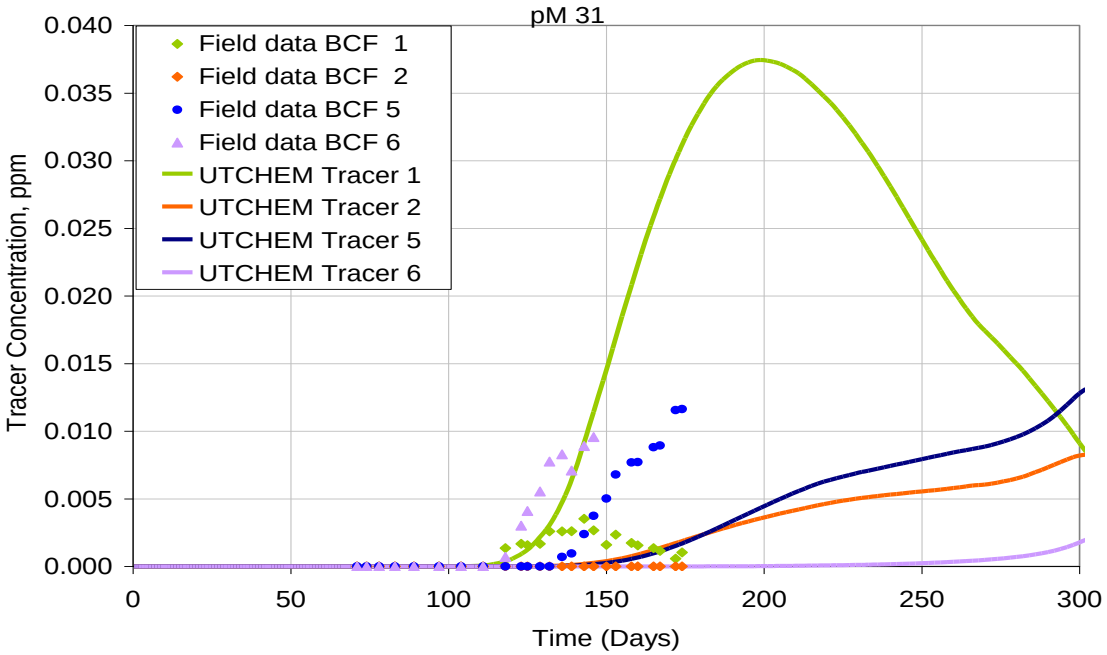

Figure 5.42: Tracer concentration history comparison between field and simulated result for pM31 producer

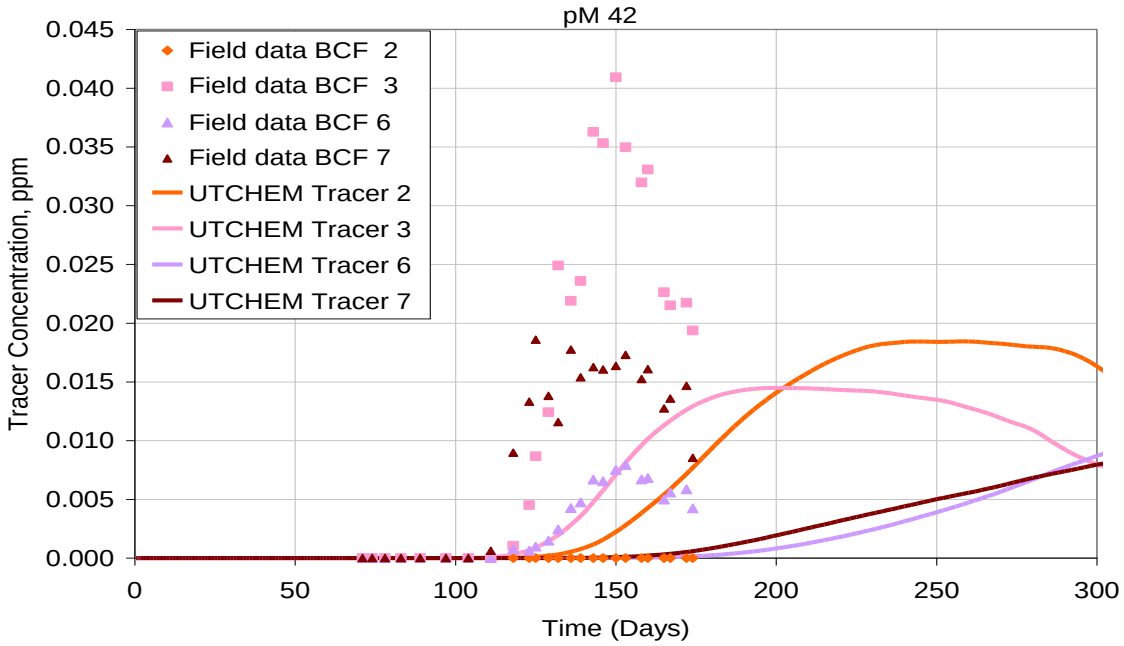

Figure 5.43: Tracer concentration history comparison between field and simulated result for pM42 producer

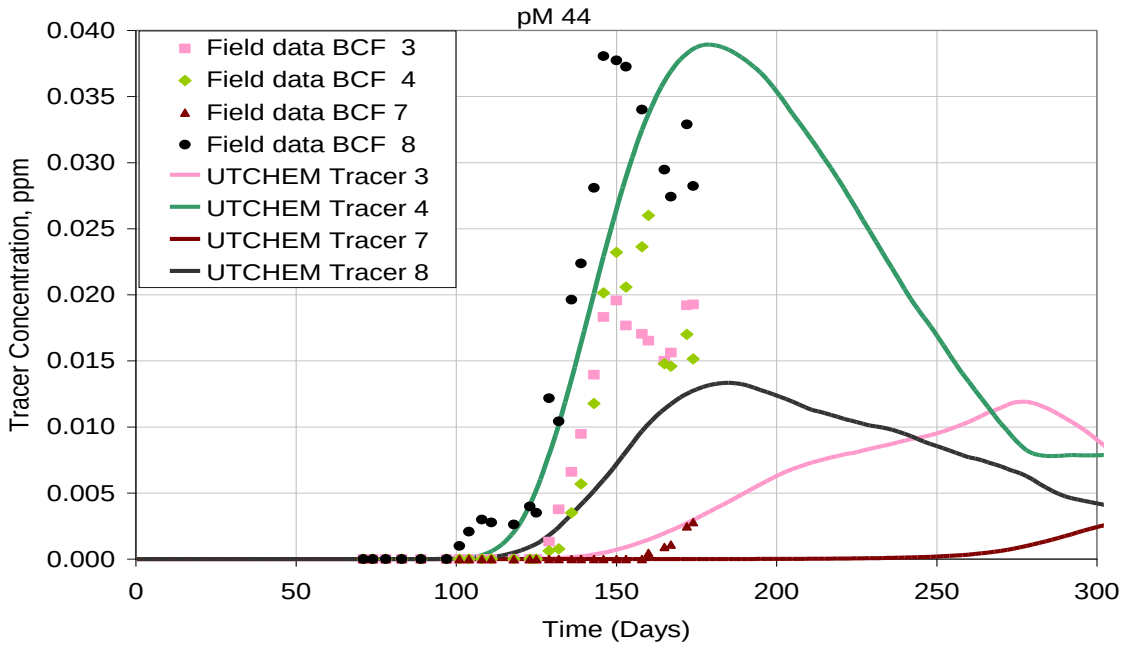

Figure 5.44: Tracer concentration history comparison between field and simulated result for pM44 producer

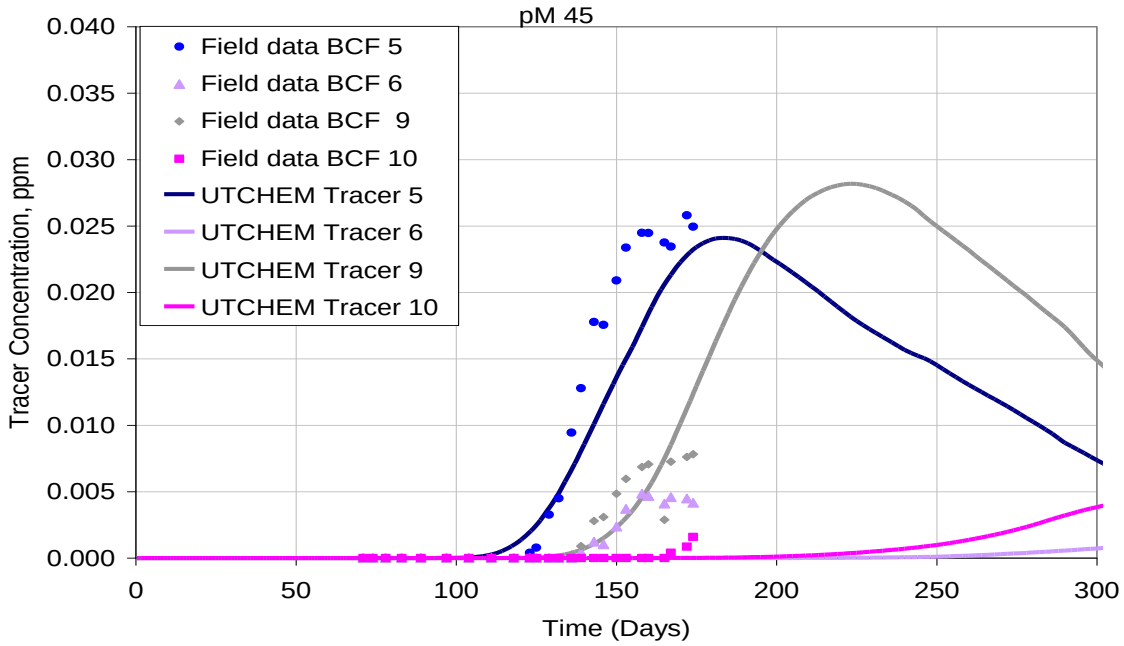

Figure 5.45: Tracer concentration history comparison between field and simulated result for pM45 producer

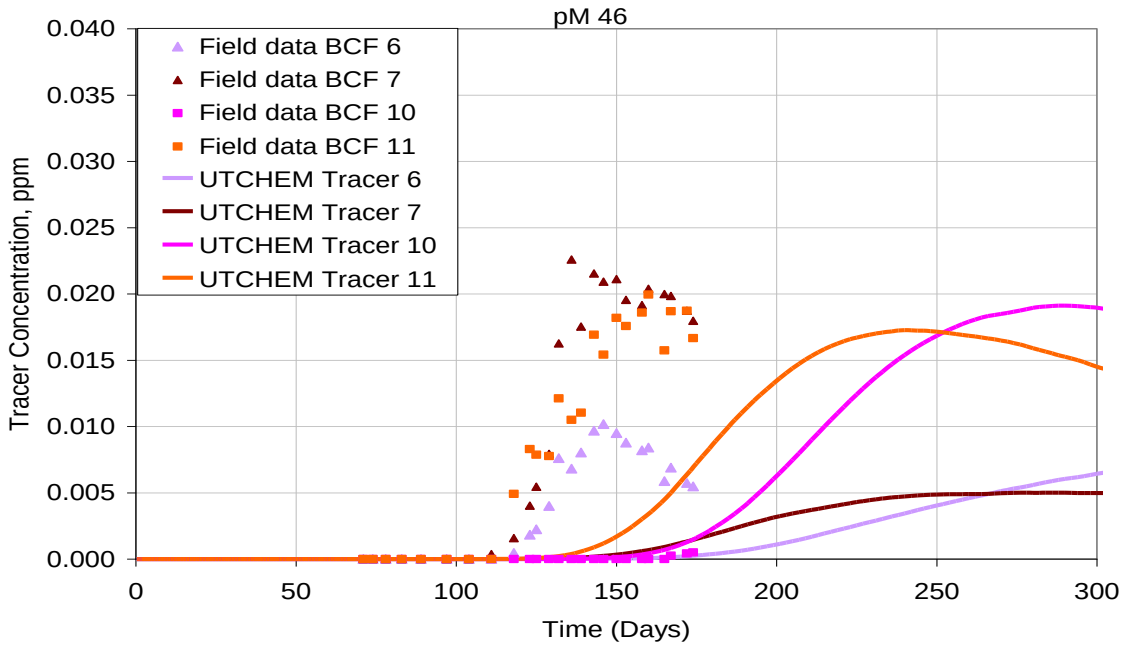

Figure 5.46: Tracer concentration history comparison between field and simulated result for pM46 producer

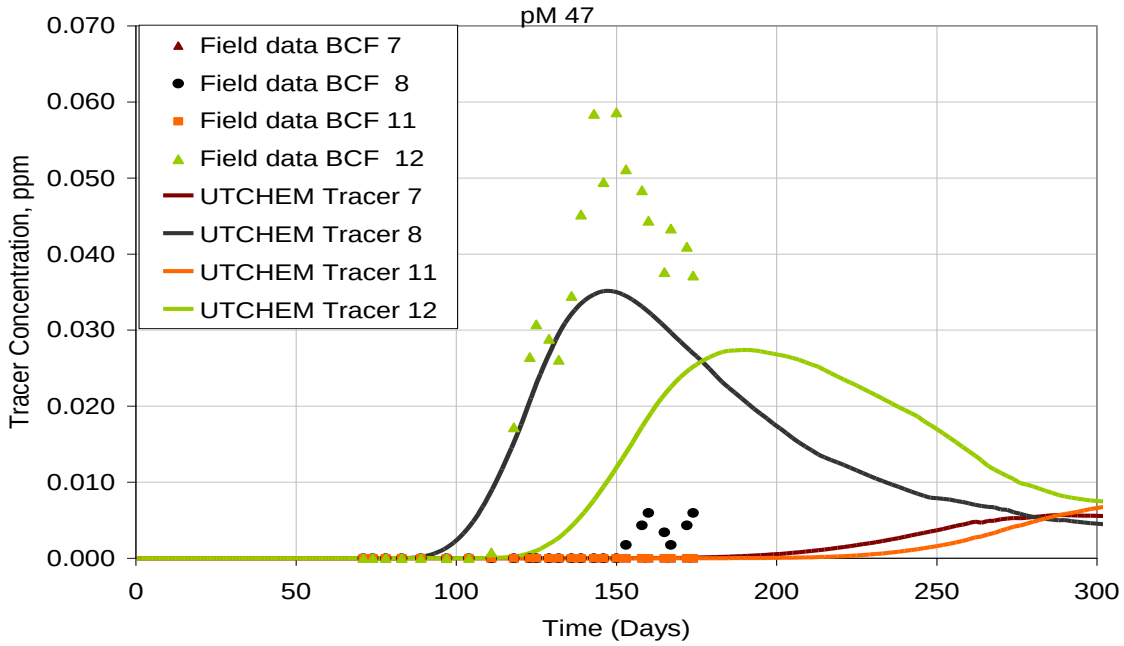

Figure 5.47: Tracer concentration history comparison between field and simulated result for pM47 producer

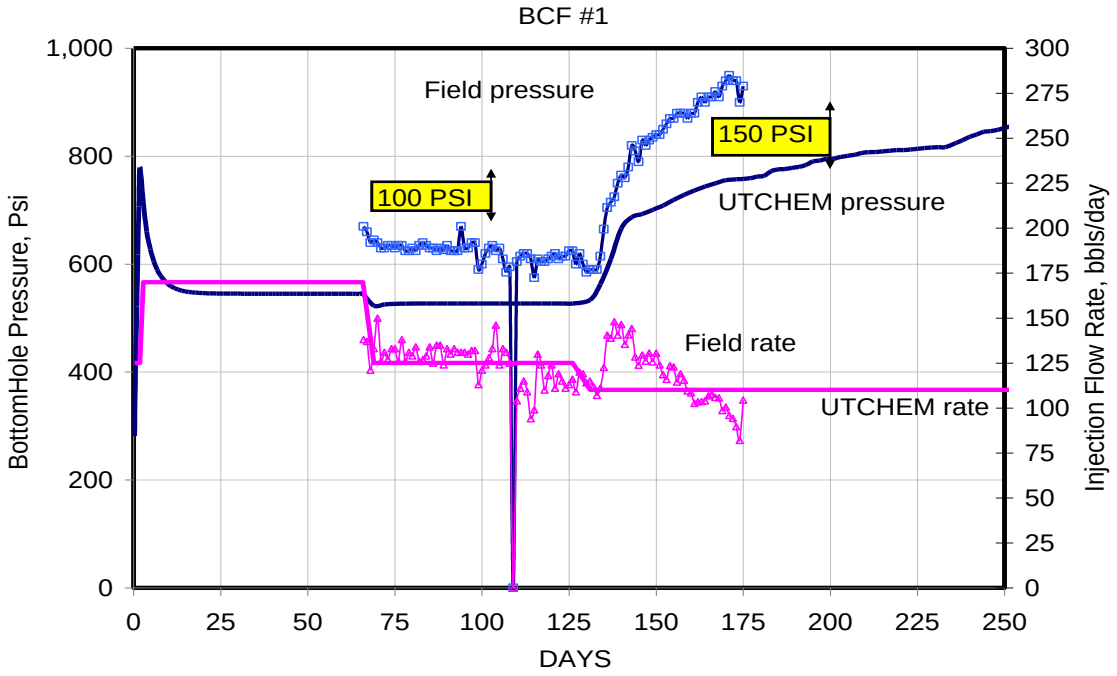

Figure 5.48: Field pressure & injection rate comparison with simulated results of BCF01

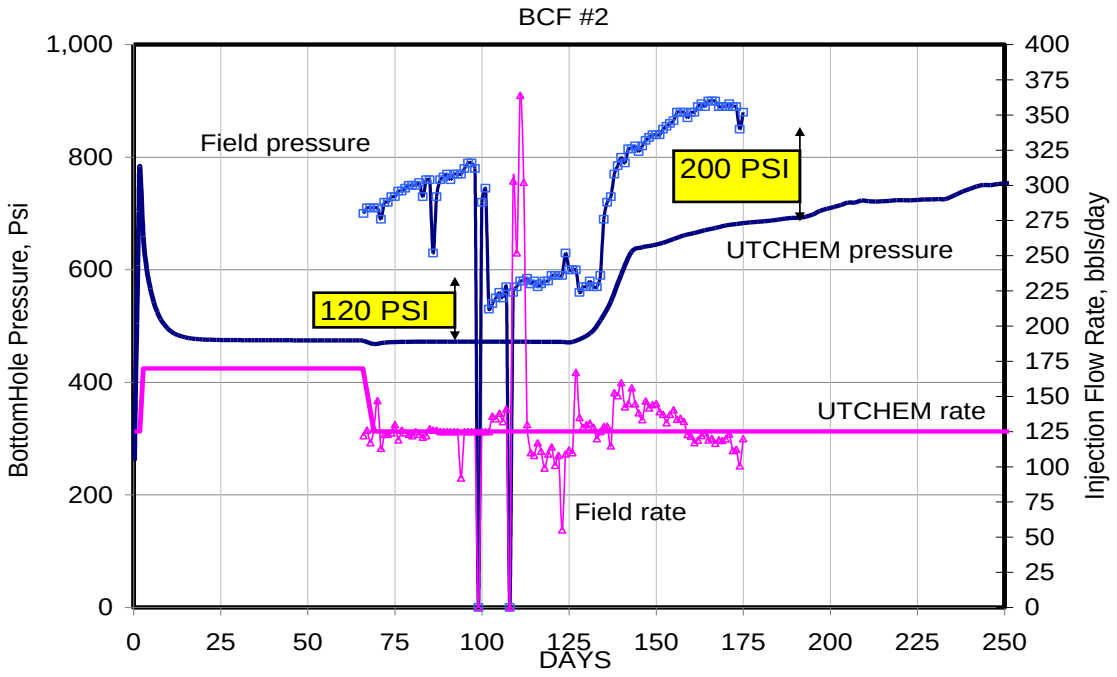

Figure 5.49: Field pressure & injection rate comparison with simulated results of BCF02

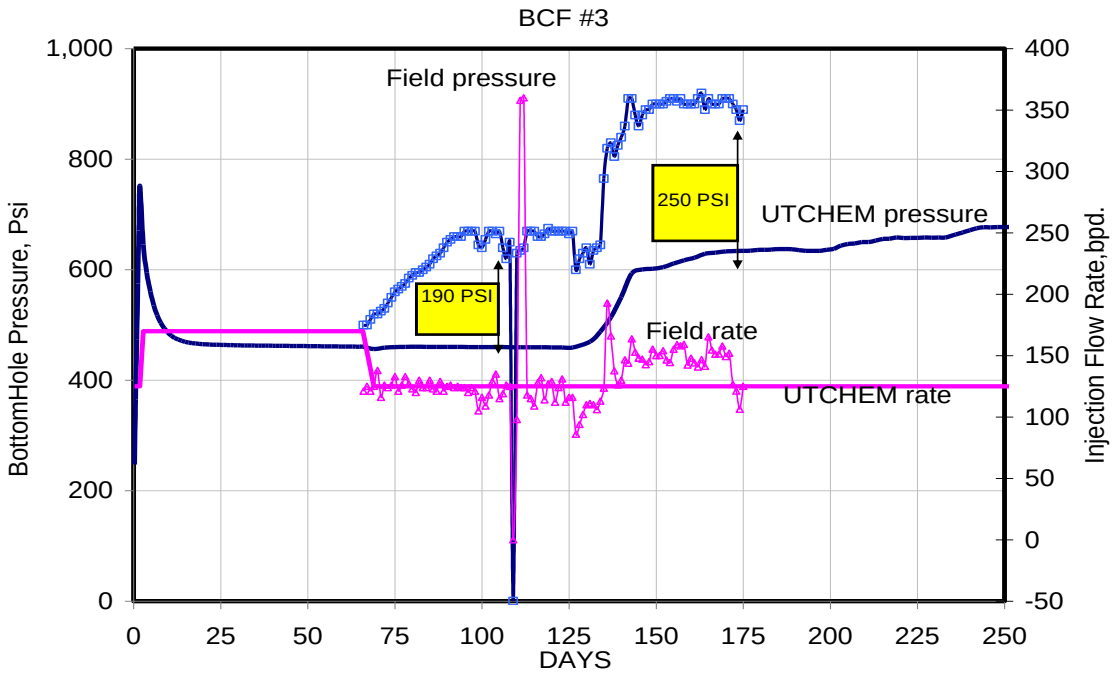

Figure 5.50: Field pressure & injection rate comparison with simulated results of BCF03

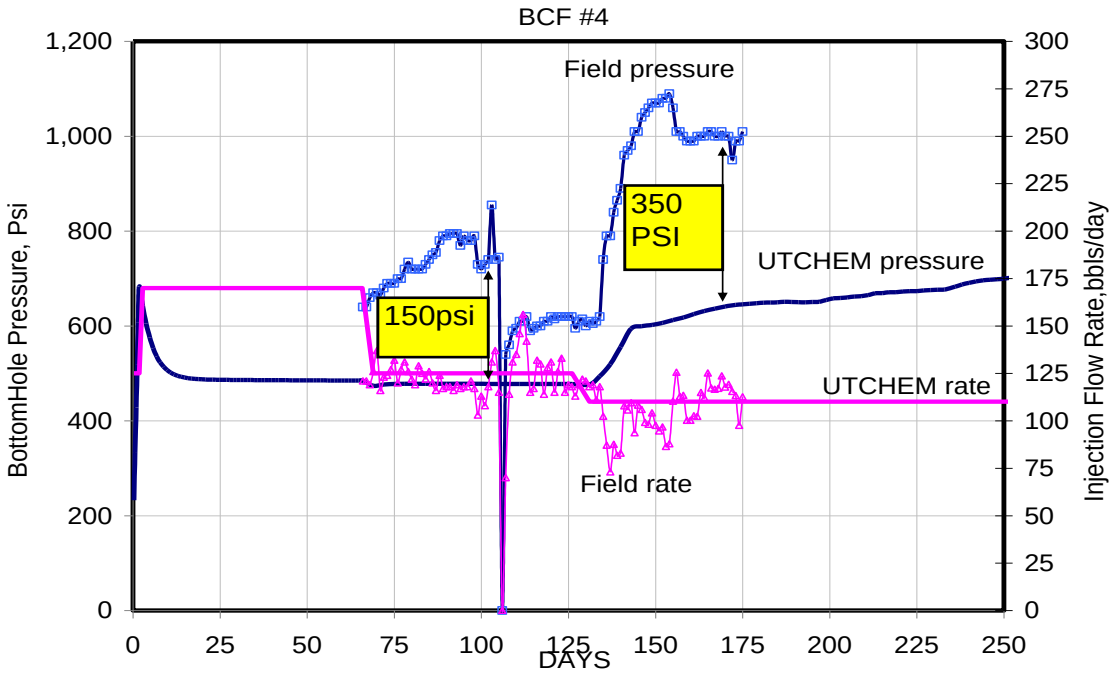

Figure 5.51: Field pressure & injection rate comparison with simulated results of BCF04

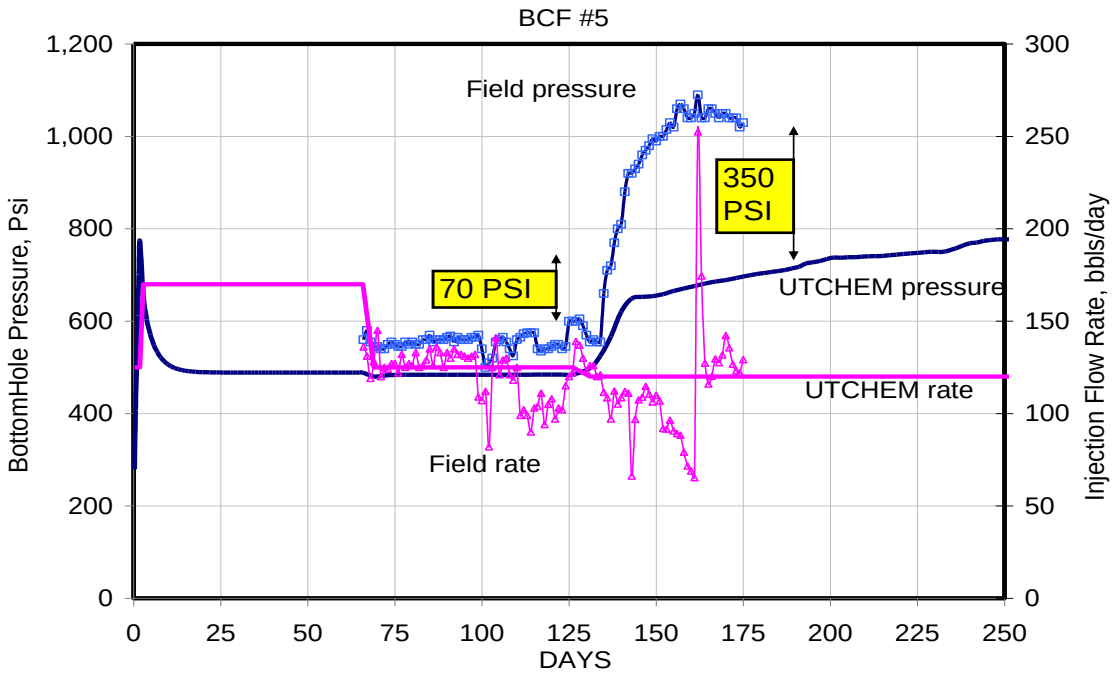

Figure 5.52: Field pressure & injection rate comparison with simulated results of BCF05

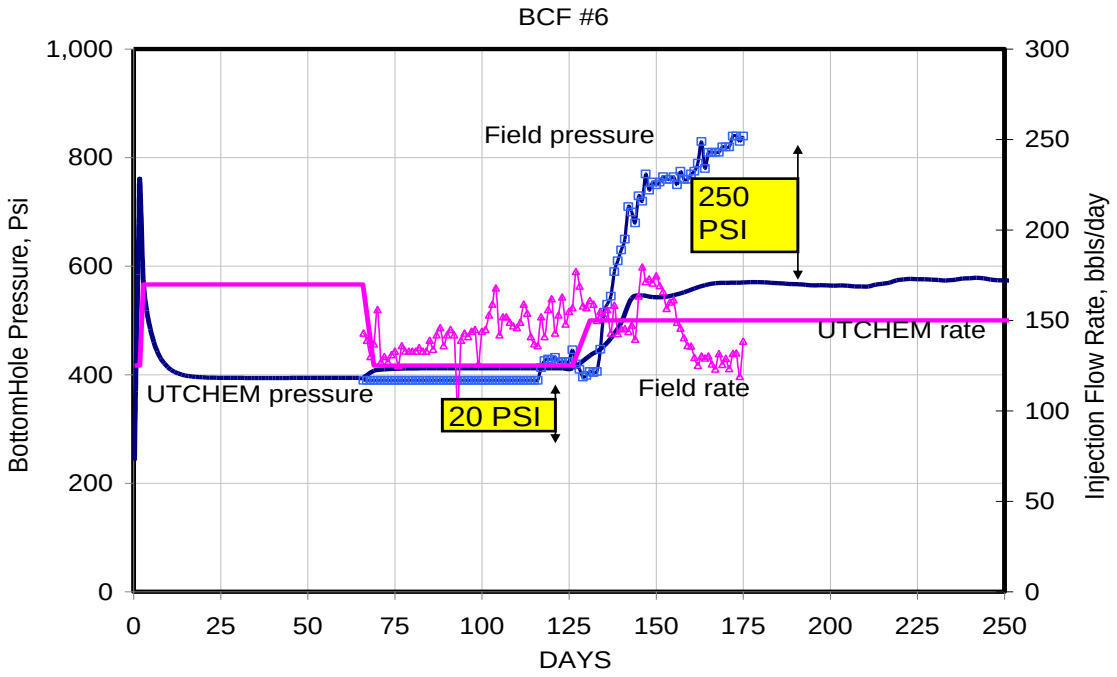

Figure 5.53: Field pressure & injection rate comparison with simulated results of BCF06

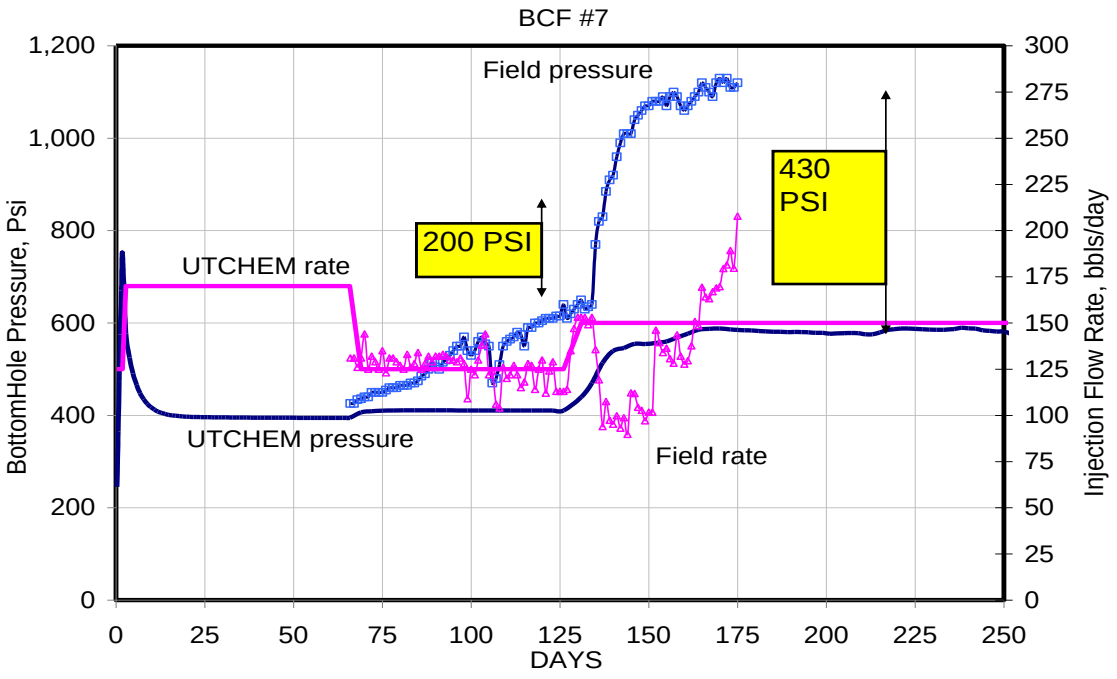

Figure 5.54: Field pressure & injection rate comparison with simulated results of BCF07

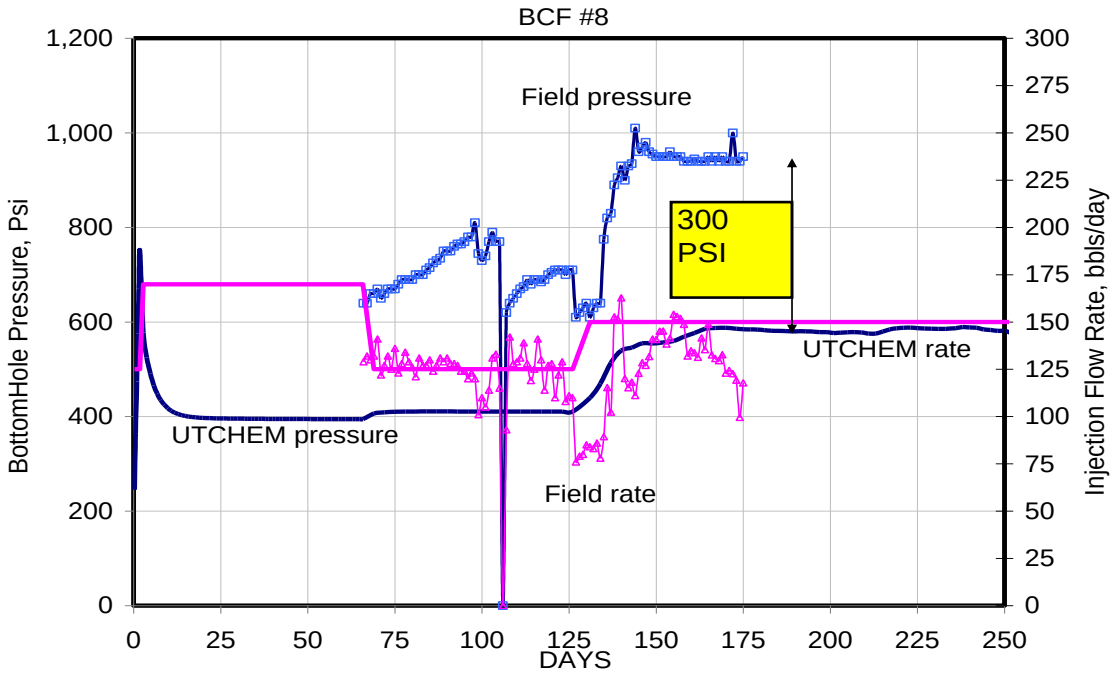

Figure 5.55: Field pressure & injection rate comparison with simulated results of BCF08

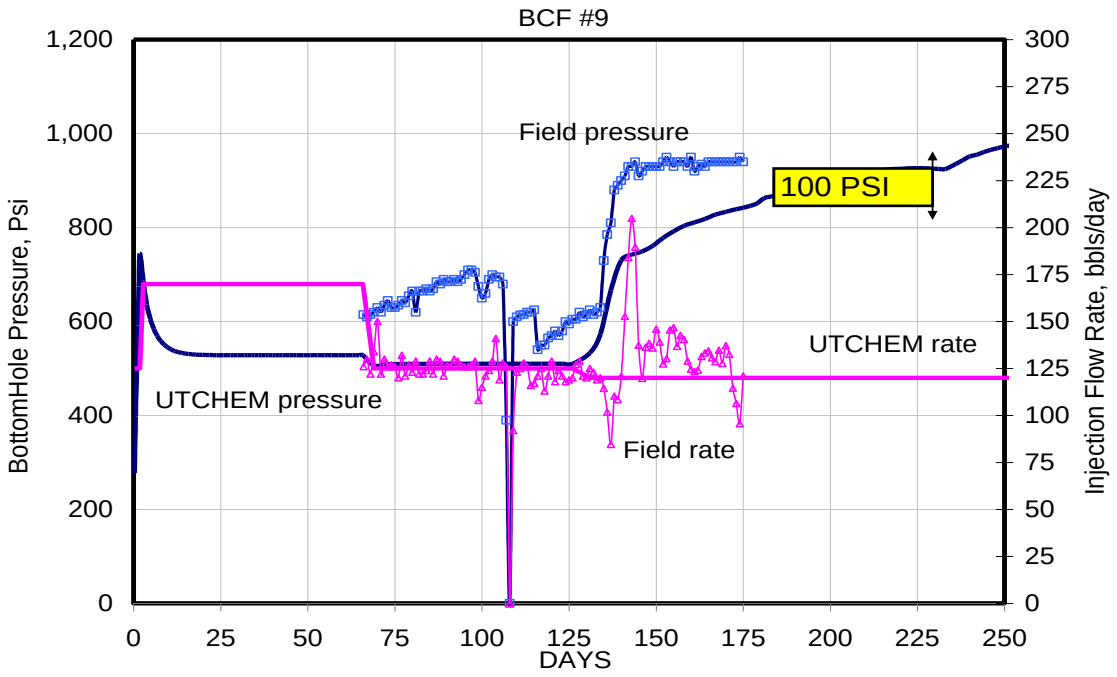

Figure 5.56: Field pressure & injection rate comparison with simulated results of BCF09

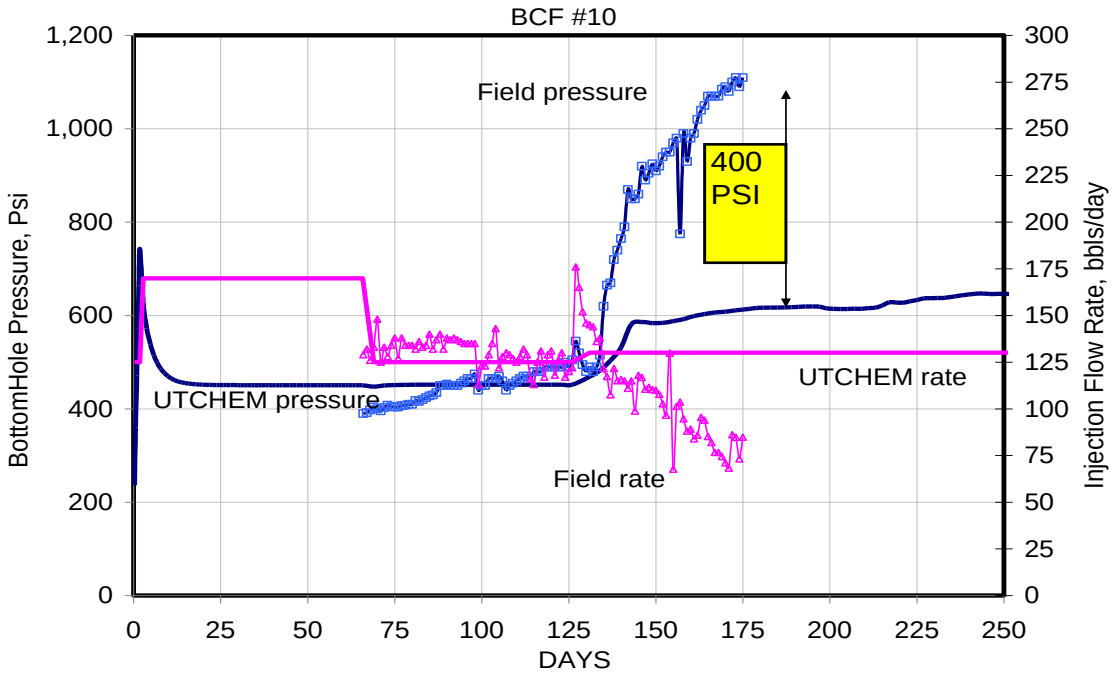

Figure 5.57: Field pressure & injection rate comparison with simulated results of BCF10

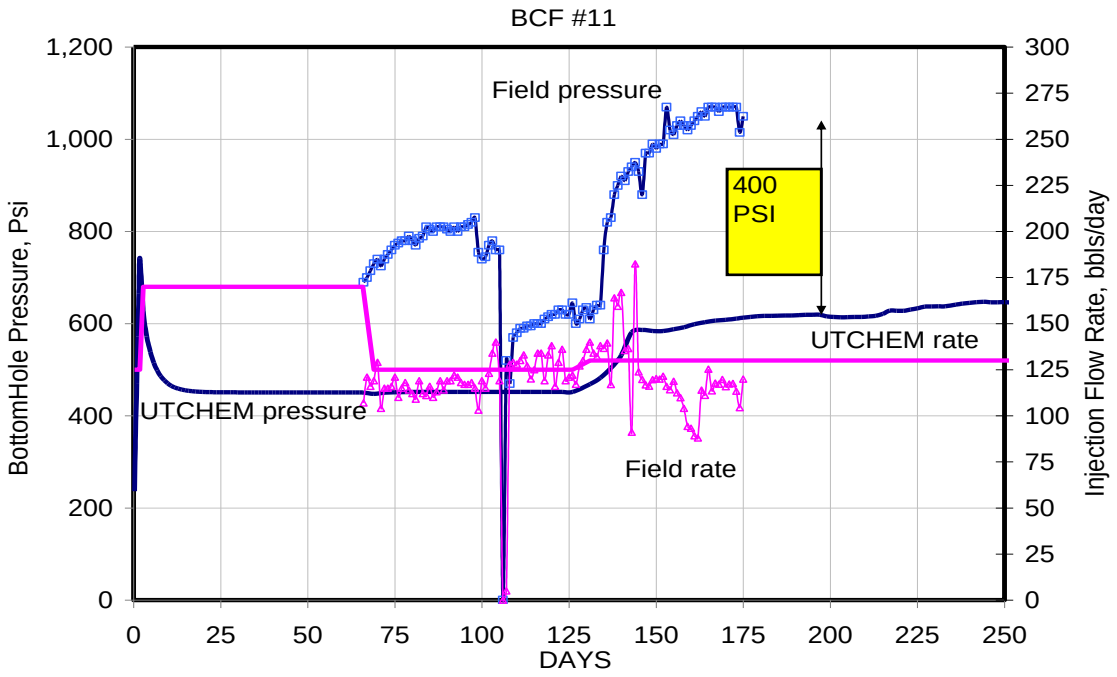

Figure 5.58: Field pressure & injection rate comparison with simulated results of BCF01

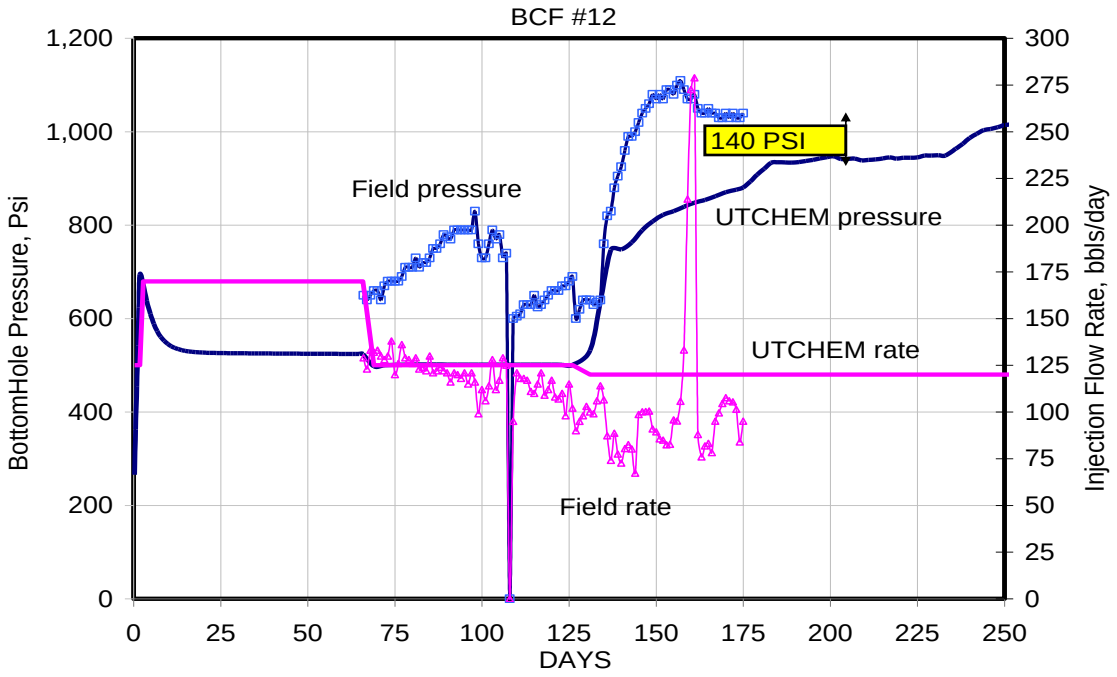

Figure 5.59: Field pressure & injection rate comparison with simulated results of BCF12

6 Summary and Conclusions

Polymer is an important component of various chemical EOR processes. Polymer is needed for mobility control to prevent fingering and channeling and to improve sweep efficiency. The polymer increases the viscosity of the injected fluid and hence reduces the injectivity, which affects project life and economics. Thus, it is important to be able to accurately predict its effect on injectivity. The use of large grid blocks in numerical simulations causes large errors in the shear rate calculations near the wellbore and thus the polymer viscosity and injectivity are not accurately calculated. In some cases, the error can be as much as 100%. This study focused on minimizing the error in the predicted polymer injectivity.

Chapter 2 presented the improvements in modeling of polymer rheology, both shear thinning and shear thickening. A better fit to the bulk (shear thinning) laboratory data was obtained after those improvements. Moreover, the Unified Viscosity Model was further enhanced to model polymer viscosity over a wider range of velocity and the improved model was implemented in UTCHEM.

Chapter 3 presented the use of effective well radius to reduce the effect of grid size on the injectivity calculations. First, simulation results were presented for a homogeneous reservoir to investigate the extent of the numerical error induced when different grid block sizes are used. The relationship between an effective well radius (Rweff) and grid block size and, the sensitivity of Rweff to various reservoir permeability were presented. These results show that very small grid blocks are needed for accurate simulations when the actual well radius is used. The fine-grid results can be approximated using a much coarser grid if an effective well radius is used. This is a very important result since it is not practical to use very small grid blocks for many large field

cases and the simulated injectivity is much too low when large grid blocks are used, so the only practical alternative is to use an effective well radius. However, more research is needed to further develop this approach since these preliminary results are based on single-phase flow in a homogeneous reservoir.

Chapter 4 discusses the effect of a fracture on polymer injectivity in a horizontal well. These results show that the impact of the fracture on injection rate and cumulative oil recovery decreases as the reservoir permeability increases. A better way of modeling well skin was also presented.

In Chapter 5, UTCHEM simulations were compared with incomplete field data from a surfactant-polymer flood pilot in progress. The field data included interwell tracer data from a tracer injection test started before the SP flood. Various sensitivities were also studied for this SP flood. The effect of the amount of polymer on the oil recovery was simulated and compared with field data from the literature. The literature data indicate increasing the total mass of injected polymer in an SP flood increases the oil recovery more than predicted by the simulator for this particular SP pilot. One explanation for this difference is related to reservoir heterogeneity. The more heterogeneous the reservoir, the more mass of polymer is needed. The predicted results are thus sensitive to the geological model used in the simulations. Another explanation for this difference is related to numerical accuracy of the simulations. The water pushing the polymer is less viscous and thus fingers into the polymer. This is difficult to simulate accurately unless very small grid blocks are used. .

This research both demonstrates the usefulness of current polymer simulations and the need for more research to improve the accuracy of the predictions.

Appendix

Input file for Chapter -5 base case simulation is presented below

```
**********************************************************************
**
CC
      *
CC    BRIEF DESCRIPTION OF DATA SET : UTCHEM (VERSION 9.97)
      *
CC
      *
CC*********************************************************************
**
CC
*
CC   ASP/SP Flood Pilot Evaluation              *
CC
*
CC  LENGTH (FT) : 2625'             PROCESS : SP
*
CC  THICKNESS (FT) : 16'            PRESSURE (i) CONSTRAINTS
*
CC  WIDTH (FT) : 1715'              COORDINATES : CARTESIAN
      *
CC  POROSITY : varies, 0.20 avg     DAY SPECIFICATION
      *
CC  GRID BLOCKS : 79x49x9=33,075    COURANT NUMBER SPECIFICATION
*
CC  UNIFORM GRIDBLOCK SIZES         WELL SKIN = 0
      *
CC
      *
CC*********************************************************************
**
CC
*
CC*********************************************************************
**
CC
      *
CC    RESERVOIR DESCRIPTION
      *
CC
      *
CC*********************************************************************
**
CC
CC Run number
*---- RUNNO
```

```
Bp072f
CC
CC Title and run description
*---- title(i)
Bp072f: (Ref. Bp070c) 0.25 pv surf slug; 0.25 mg/gm surf ads; 0.75 PD
Abhinav Sharma;1July 2010, 9:30 pm, 1219 day run, lower CNMAX, add EDTA
so beta6=0.00 and betap = 1
75x49 grid, realistic current So=0.31 (Sorw=0.28), delete old
POR,PERM,NTG files
CC
CC SIMULATION FLAGS: IMODE = 1 for new case, IMODE=2 for restart
*---- IMODE IMES IDISPC ICWM ICAP IREACT IBIO ICOORD ITREAC ITC  IGAS
IENG  idual  itens
        1    2     3     0    0     0     0     1      0     0    0
0      0       0
CC
CC no. of gridblocks,flag specifies constant or variable grid size,unit
*---- NX    NY    NZ  IDXYZ  IUNIT
      75    49     9     2      0
CC
CC VARIABLE GRID SIZE ON A REGIONAL BASIS IN X DIRECTION
*---- II1, II2, DX1
  75*35
CC
CC VARIABLE GRID SIZE ON A REGIONAL BASIS IN Y DIRECTION
*---- JJ1, JJ2, DY1
 49*35
CC
CC VARIABLE GRID SIZE ON A REGIONAL BASIS IN Z DIRECTION
*---- KK1, KK2, DZ1
4*1.84
5*1.75
CC
CC total no. of components,no. of tracers,no. of gel components
*----n    no    ntw    nta    ngc    ng    noth
     14    0      6     0      0      0       0
CC
CC Name of the components
*----spname(i) for i=1 to n
Water
Oil
Surf.
Polymer
Chloride
Calcium
Alcohol1
Alcohol2
Trace1
Trace2
Trace3
Trace4
Trace5
Trace6
```

```
CC
CC flag indicating if the component is included in calculations or not
*----icf(kc) for kc=1,n
      1  1  1  1  1  1  0 0 1 1 1 1 1 1
CC
CC*****************************************************************
CC                                                                 *
CC  3.2  OUTPUT OPTIONS                                            *
CC                                                                 *
CC*****************************************************************
CC  IOUTGMS = 2 to generate .case to run kraken
CC  ISTOP=0 for TMAX & TINJ in days, =1 for PV; ICUM=0 for output in
days, =1 for PV
CC 3.2.1 FLAG TO WRITE TO UNIT 3,FLAG FOR PV OR DAYS TO PRINT OR TO
STOP THE RUN
*---- ICUMTM  ISTOP  IOUTGMS
        0       0       0
CC
CC 3.2.2 FLAG INDICATING IF THE PROFILE OF KCTH COMPONENT SHOULD BE
WRITTEN
*---- IPRFLG(KC),KC=1,N
      1  1  1  1  1  1  0 0 1 1 1 1 1 1
CC
CC 3.2.3 FLAG FOR PRES.,SAT.,TOTAL CONC.,TRACER CONC.,CAP.,GEL,
ALKALINE PROFILES
*---- IPPRES IPSAT IPCTOT IPBIO IPCAP IPGEL IPALK IPTEMP IPOBS
        1      1      1      0     0     0     0     0      0
CC
CC 3.2.4 FLAG FOR WRITING SEVERAL PROPERTIES TO UNIT 4 (Prof)
*---- ICKL IVIS IPER ICNM ICSE IHYSTP IFOAMP INONEQ
       1    1    1    1    1    0    0    0
CC
CC 3.2.5 FLAG  for variables to PROF output file
*---- IADS IVEL IRKF IPHSE
       1    1    1    1
CC
CC*****************************************************************
CC                                                                 *
CC  3.3      RESERVOIR PROPERTIES                                  *
CC                                                                 *
CC*****************************************************************
CC
CC
CC 3.3.1 MAX. SIMULATION TIME (days)
*---- TMAX
      1401
CC
CC 3.3.2 ROCK COMPRESSIBILITY (1/PSI), STAND. PRESSURE(PSIA)
*---- COMPR                PSTAND
        0                   1270.
CC  value=0 for constant, =1 by layer, =2 for each gridblock, =3 ratio,
=4 for include file
```

```
CC 3.3.3 use EDITS to PERM,POR,NTG files to make all cells active, but
low perm&poros in formerly inactive cells.
*---- IPOR1  IPERMX IPERMY IPERMZ IMOD  ITRANZ  INTG INTG=1:read in NTG
file
       4      4      3      3     1        0      1
CC
CC 3.3.13 Y DIRECTION PERMEABILITY IS DEPENDENT ON X DIRECTION
PERMEABILITY
*---- FACTY,   CONSTANT PERMEABILITY MULTIPLIER FOR Y DIRECTION
PERMEABILITY
       1
CC
CC 3.3.17 Z DIRECTION PERMEABILITY IS DEPENDENT ON X DIRECTION
PERMEABILITY
*---- FACTZ, CONSTANT PERMEABILITY MULTIPLIER FOR Z DIRECTION
PERMEABILITY
       1.0
CC  =0 for constant, =1 by layer, =2 by gridblock, =4 separate file, =-
1 for backward compatbility
CC 3.3.18 FLAG FOR CONSTANT OR VARIABLE DEPTH, PRESSURE, WATER
SATURATION,INITIAL AQUEOUS PHASE cOMPOSITIONS
*----IDEPTH  IPRESS  ISWI  ICWI
       4       1      4     -1
CC
CC 3.3.23  INITIAL PRESSURE FOR A POINT AT A SPECIFIED DEPTH IS
SPECIFIED
*---- PINIT  HINIT
      75.    400.
CC
CC FLAG FOR RESERVOIR PROPERTY MODIFICATION
*----IMPOR  IMKX  IMKY  IMKZ  IMSW
       1     1     1     1     0
CC K=1.3 and 1.15 multipliers are to increase kh to adjust for constant
thickness constraint
CC NUMBER OF REGIONS WITH MODIFIED X PERMEABILITY
*---- NMOD1
       1
CC  if IFACT=1 then replace, =2 then multiply =3 add to current value
CC use EDITS to PERM,POR,NTG file to make all cells active, but low
perm in formerly inactive cells.
*---- IMIN    IMAX    JMIN    JMAX    KMIN     KMAX    IFACT    FACTX
       1       75     1        49        1       9       2         1.01
CC K=1.3 and 1.15 multipliers are to increase kh to adjust for constant
thickness constraint
CC NUMBER OF REGIONS WITH MODIFIED X PERMEABILITY
*---- NMOD1
       22
CC  if IFACT=1 then replace, =2 then multiply =3 add to current value
CC use EDITS to PERM,POR,NTG file to make all cells active, but low
perm in formerly inactive cells.
*---- IMIN    IMAX    JMIN    JMAX    KMIN     KMAX    IFACT    FACTX
       17      38     12       34        1       9       2         1.3
       39      55     12       18        1       9       2         1.3
```

```
       22      33      20       29        1       9       2         1.15
       30      36      16       19        1       9       2         1.15
       23      23      18       18        1       9       2         50.
       32      32      18       18        1       9       2         50.
       41      41      18       18        1       9       2         50.
       22      22      27       27        1       9       2         50.
       32      32      27       27        1       9       2         50.
       42      42      26       26        1       9       2         50.
       18      18      13       13        1       9       2         50.
       27      27      13       13        1       9       2         50.
       36      36      13       13        1       9       2         50.
       45      45      13       13        1       9       2         50.
       18      18      23       23        1       9       2         50.
       27      27      23       23        1       9       2         50.
       36      36      23       23        1       9       2         50.
       45      45      22       22        1       9       2         50.
       16      16      31       31        1       9       2         50.
       27      27      32       32        1       9       2         50.
       36      36      32       32        1       9       2         50.
       45      45      32       32        5       9       2         50.
CC
CC NUMBER OF REGIONS WITH MODIFIED Y PERMEABILITY
*---- NMOD2
       22
CC  if IFACT=1 then replace, =2 then multiply =3 add to current value
CC  use 50x perm mult. in well cells to account for ball frac jobs
*---- IMIN    IMAX    JMIN    JMAX    KMIN     KMAX    IFACT    FACTX
       17      38      12       34        1       9       2         1.3
       39      55      12       18        1       9       2         1.3
       22      33      20       29        1       9       2         1.15
       30      36      16       19        1       9       2         1.15
       23      23      18       18        1       9       2         50.
       32      32      18       18        1       9       2         50.
       41      41      18       18        1       9       2         50.
       22      22      27       27        1       9       2         50.
       32      32      27       27        1       9       2         50.
       42      42      26       26        1       9       2         50.
       18      18      13       13        1       9       2         50.
       27      27      13       13        1       9       2         50.
       36      36      13       13        1       9       2         50.
       45      45      13       13        1       9       2         50.
       18      18      23       23        1       9       2         50.
       27      27      23       23        1       9       2         50.
       36      36      23       23        1       9       2         50.
       45      45      22       22        1       9       2         50.
       16      16      31       31        1       9       2         50.
       27      27      32       32        1       9       2         50.
       36      36      32       32        1       9       2         50.
       45      45      32       32        5       9       2         50.
CC
CC NUMBER OF REGIONS WITH MODIFIED Z PERMEABILITY
*---- NMOD3
       25
```

```
CC  if IFACT=1 then replace, =2 then multiply =3 add to current value
CC FIRST AND LAST INDEX IN X,Y,Z DIRECTION,MODIFIED METHOD,CONSTANT
VALUE.
*---- IMIN    IMAX    JMIN    JMAX     KMIN     KMAX    IFACT    FACTX
       1       75       1      49        1        3       2        0.3
       1       75       1      49        4        4       2        0.01
       1       75       1      49        5        9       2        0.4
       17      38      12       34       1        9       2        1.3
       39      55      12       18       1        9       2        1.3
       22      33      20       29       1        9       2        1.15
       30      36      16       19       1        9       2        1.15
       23      23      18       18       1        9       2        50.
       32      32      18       18       1        9       2        50.
       41      41      18       18       1        9       2        50.
       22      22      27       27       1        9       2        50.
       32      32      27       27       1        9       2        50.
       42      42      26       26       1        9       2        50.
       18      18      13       13       1        9       2        50.
       27      27      13       13       1        9       2        50.
       36      36      13       13       1        9       2        50.
       45      45      13       13       1        9       2        50.
       18      18      23       23       1        9       2        50.
       27      27      23       23       1        9       2        50.
       36      36      23       23       1        9       2        50.
       45      45      22       22       1        9       2        50.
       16      16      31       31       1        9       2        50.
       27      27      32       32       1        9       2        50.
       36      36      32       32       1        9       2        50.
       45      45      32       32       5        9       2        50.
CC
CC 3.3.52 BRINE SALINITY AND DIVALENT CATION CONCENTRATION (MEQ/ML)
*---- C50       C60
       0.3362      0.0621
CC
CC*********************************************************************
CC                                                                     *
CC    3.4 PHYSICAL PROPERTY DATA                                       *
CC                                                                     *
CC*********************************************************************
CC
CC 3.4.1 OIL CONC. AT PLAIT POINT FOR TYPE II(+)AND TYPE II(-), CMC
CC                     CMC
*---- c2plc  c2prc   epsme   ihand
        0      1     0.0001     0
CC
CC 3.4.2 flag indicating type of phase behavior parameters
*---- ifghbn=0 for input height of binodal curve; =1 for input sol.
ratio
        0
CC 3.4.3 SLOPE AND INTERCEPT OF BINODAL CURVE AT ZERO, OPT., AND 2XOPT
SALINITY
CC FOR ALCOHOL 1
*---- hbns70   hbnc70   hbns71   hbnc71   hbns72   hbnc72
```

```
        0    0.03       0     0.015     0     0.03
CC 3.4.5 SLOPE AND INTERCEPT OF BINODAL CURVE AT ZERO, OPT., AND 2XOPT
SALINITY
CC FOR ALCOHOL 2
*---- hbns80  hbnc80  hbns81  hbnc81  hbns82  hbnc82
        0       0       0       0       0       0
CC
CC 3.4.6 LOWER AND UPPER EFFECTIVE SALINITY FOR ALCOHOL 1 AND ALCOHOL 2
*---- csel7   cseu7   csel8   cseu8
     0.370       0.541   0.     0.
CC 3.4.7 THE CSE SLOPE PARAMETER FOR CALCIUM AND ALCOHOL 1 AND ALCOHOL
2
CC    Ca     Alcohol#1  Alcohol#2
*---- beta6    beta7    beta8
        0.0        0       0
CC
CC 3.4.8 FLAG FOR ALCOHOL PART. MODEL AND PARTITION COEFFICIENTS
*---- ialc   opsk7o   opsk7s   opsk8o   opsk8s
        0      0        0        0        0
CC  these are used only for alcohol partitioning in a two alcohol
system:
CC 3.4.9 NO. OF ITERATIONS, AND TOLERANCE
*---- nalmax     epsalc
        20       0.0001
CC 3.4.10 ALCOHOL 1 PARTITIONING PARAMETERS IF IALC=1
CC   aq-oleic   aq-oleic  surf-oleic
*---- akwc7     akws7     akm7       ak7      pt7
       4.671    1.79       48       35.31    0.222
CC
CC 3.4.11 ALCOHOL 2 PARTITIONING PARAMETERS IF IALC=1
*---- akwc8     akws8    akm8    ak8     pt8
        0         0        0      0       0
CC
CC 3.4.22 ift model flag
*----  ift=0 for Healy&Reed; =1 for Chun Huh correl.
        1
CC 3.4.24 INTERFACIAL TENSION PARAMETERS
CC    typ=.1-.35   typ=5-20
*---- chuh         ahuh
      0.3           10
CC 3.4.25 LOG10 OF OIL/WATER INTERFACIAL TENSION
CC     units of log 10 dynes/cm = mN/m
*---- xiftw
       1.5
CC 3.4.26 ORGANIC MASS TRANSFER FLAG
CC    imass=0 for no oil sol. in water.  icorr=0 for constant MTC
*---- imass   icor
        0       0
cc
cc
*--- IWALT    IWALF
       0       0
CC 3.4.31 CAPILLARY DESATURATION PARAMETERS FOR PHASE 1, 2, AND 3
```

```
CC                AQ     OLEIC     ME
*---- itrap      t11      t22      t33
       2        1865    10000    364.2
CC    iperm=0 for constant; =1 varies by layer; =2 varies by gridblock
CC  3.4.32 FLAG FOR RELATIVE PERMEABILITY AND CAPILLARY PRESSURE MODEL
*---- iperm         irtype
       0             0
CC
CC 3.4.35 FLAG FOR CONSTANT OR VARIABLE REL. PERM. PARAMETERS
*---- isrw    iprw    iew
       0      0       0
CC
CC 3.4.37 CONSTANT RES. SATURATION OF PHASES 1,2,AND 3 AT LOW CAPILLARY
NO.
*---- s1rwc      s2rwc     s3rwc
      0.28      0.282      0.28
CC
CC 3.4.44 CONSTANT ENDPOINT REL. PERM. OF PHASES 1,2,AND 3 AT LOW
CAPILLARY NO.
*---- p1rwc     p2rwc    p3rwc
      0.268       0.788      0.268
CC
CC 3.4.51   CONSTANT REL. PERM. EXPONENT OF PHASES 1,2,AND 3 AT LOW
CAPILLARY NO.
*---- e1wc     e2wc       e3wc
     2.0        2.0      2.0
CC
CC 3.4.58 RES. SATURATION OF PHASES 1,2,AND 3 AT HIGH CAPILLARY NO.
*---- s1rc   s2rc   s3rc
      0      0.01       0
CC
CC 3.4.59 ENDPOINT REL. PERM. OF PHASES 1,2,AND 3 AT HIGH CAPILLARY NO.
*---- p1rc   p2rc   p3rc
      1      1      1
CC
CC 3.4.60 REL. PERM. EXPONENT OF PHASES 1,2,AND 3 AT HIGH CAPILLARY NO.
*---- e13c   e23c   e31c
      1      1      1
CC 3.4.61 WATER AND OIL VISCOSITY , RESERVOIR TEMPERATURE
CC   water     oil       =0 for isothermal modeling
*---- VIS1     VIS2   TSTAND
     0.933       10.9        0
CC
CC 3.4.80 COMPOSITIONAL PHASE VISCOSITY PARAMETERS for microemulsion
*----   ALPHAV1   ALPHAV2   ALPHAV3   ALPHAV4  ALPHAV5
         2.1         2.1         0.1         0.1       0.1
CC
CC 3.4.81 PARAMETERS TO CALCULATE POLYMER VISCOSITY AT ZERO SHEAR RATE
*---- AP1      AP2      AP3
      35       30      1000
CC
CC 3.4.82 PARAMETER TO COMPUTE CSEP,MIN. CSEP, AND SLOPE OF LOG VIS.
VS. LOG CSEP
```

```
*---- BETAP    CSE1     SSLOPE
       1       0.01        -0.5264
CC
CC 3.4.83 PARAMETER FOR SHEAR RATE DEPENDENCE OF POLYMER VISCOSITY
*---- GAMMAC   GAMHF   POWN   ipmod    ISHEAR   RWEFF  GAMHF2
       4        15      1.7      0       1       1.0    0.0
CC
CC 3.4.84  FLAG FOR POLYMER PARTITIONING, PERM. REDUCTION PARAMETERS
*---- IPOLYM    EPHI3    EPHI4    BRK     CRK   rkcut
       1         1         1      100    0.015      10
CC 3.4.85 SPECIFIC WEIGHT FOR COMPONENTS 1,2,3,7,8 ,Coeffient of oil
and GRAVITY FLAG
CC   if IDEN=1 ignore gravity effect; =2 then include gravity effect
*---- DEN1     DEN2      DEN23     DEN3      DEN7    DEN8    IDEN
      0.43     0.377     0.377      0.433     0.346    0        2
CC   ISTB=0:BOTTOMHOLE CONDITION , 1: STOCK TANK
CC 3.4.93 FLAG FOR CHOICE OF UNITS when printing
*----- ISTB
        0
CC
CC 3.4.95 COMPRESSIBILITY FOR VOL. OCCUPYING COMPONENTS 1,2,3,7,AND 8
*----   COMPC(1)          COMPC(2)     COMPC(3)  COMPC(7)  COMPC(8)
         0         0.00001         0         0         0
CC  IOW=0 water wet, =1 oil wet, =2 mixed wet
CC 3.4.99 CONSTANT OR VARIABLE PC PARAM., WATER-WET OR OIL-WET PC CURVE
FLAG
*---- ICPC    IEPC   IOW
       0       0      0
CC    CPC = 0 for no capillary pressure
CC 3.4.100 CAPILLARY PRESSURE PARAMETER, CPC0
*---- CPC0
       0
CC
CC 3.4.103 CAPILLARY PRESSURE PARAMETER, EPC0
*---- EPC0
       4.0
CC
CC 3.4.117 MOLECULAR DIFFUSION COEF. KCTH COMPONENT IN PHASE 1
*---- D(KC,1),KC=1,N
         0  0  0  0  0  0  0  0  0  0  0  0  0  0
CC
CC 3.4.118 MOLECULAR DIFFUSION COEF. KCTH COMPONENT IN PHASE 2
*---- D(KC,2),KC=1,N
         0  0  0  0  0  0  0  0  0  0  0  0  0  0
CC
CC 3.4.119 MOLECULAR DIFFUSION COEF. KCTH COMPONENT IN PHASE 3
*---- D(KC,3),KC=1,N
         0  0  0  0  0  0  0  0  0  0  0  0  0  0
CC
CC 3.4.121 LONGITUDINAL AND TRANSVERSE DISPERSIVITY OF PHASE 1
*---- ALPHAL(1)     ALPHAT(1)
         3            1
CC
```

```
CC 3.4.122 LONGITUDINAL AND TRANSVERSE DISPERSIVITY OF PHASE 2
*---- ALPHAL(2)     ALPHAT(2)
         3            1
CC
CC 3.4.124 LONGITUDINAL AND TRANSVERSE DISPERSIVITY OF PHASE 3
*---- ALPHAL(3)     ALPHAT(3)
         3            1
CC
CC 3.4.125 flag to specify organic adsorption calculation
*---- iadso=0 if organic adsorption is not considered
        0
CC
CC 3.4.130 SURFACTANT AND POLYMER ADSORPTION PARAMETERS
*---- AD31    AD32     B3D    AD41    AD42   B4D   IADK  IADS1   FADS
REFK
       2.7      0.1    1000.      2   0.    100.       0       0     0
00.
CC
CC 3.4.131 PARAMETERS FOR CATION EXCHANGE OF CLAY AND SURFACTANT
*---- QV      XKC     XKS     EQW
      0.12    0.25    0.20    400.
CC
CC 3.4.132 TRACER PARTITIONING COEFFICIENT (TK(IT),IT=1,NT)
*---- TK(1)
      0.0    0.0      0.8    0.0      0.0     0.3
CC
CC 3.4.133 SALINITY DEPENDENCE PART. COEFF.
*---- TKS(1) TKS(2) TKS(3) TKS(4)    TKS(5)   TKS(6)  c5ref
      0.0    0.0      0.0    0.0      0.0     0.0      0.0
CC
CC RADIACTIVE DECAY COEFFICIENT (RDC(IT),IT=1,NT)
*---- RDC(1)
         0  0  0  0  0  0
CC
CC TRACER RETARDATION COEFFICIENT (RET(IT),IT=1,NT)
*---- RET(1)
         0  0  0  0  0  0
CC
CC*****************************************************************
CC                                                                *
CC    3.7 WELL DATA                                               *
CC                                                                *
CC*****************************************************************
CC
CC
CC 3.7.1 FLAG FOR SPECIFIED BOUNDARY AND ZONE IS MODELED
*---- IBOUND     IZONE
        0      0
CC 3.7.5 TOTAL NUMBER OF WELLS, WELL RADIUS FLAG, FLAG FOR TIME OR
COURANT NO.
CC     IRO=2 for Peaceman.  ITIME=0 for days; =1 for CN for min&max
tstep size
*---- NWELL   IRO    ITIME    NWREL
```

```
        31      2       1        31
CC 3.7.6a WELL ID,LOCATIONS,AND FLAG FOR SPECIFYING WELL TYPE, WELL
RADIUS, SKIN
CC     IFLAG =1QInj,=2PresProd,=3PresInj=4Qprod,IDIR =3for vert. well
*---- IDW    IW    JW    IFLAG    RW     SWELL   IDIR   IFIRST   ILAST
IPRF
       1     23     18       4     0.3      -2      3         1      9
0
CC
CC 3.7.6c WELL NAME
*----  WELNAM
pM31
CC 3.7.6d ICHEK , MAX. AND MIN. ALLOWABLE BOTTOMHOLE PRESSURE AND RATE
CC  if ICHEK = 0 then no check for limits
*---- ICHEK     PWFMIN     PWFMAX    QTMIN    QTMAX
        0          0        9999.      0        -9999.
CC 3.7.6a WELL ID,LOCATIONS,AND FLAG FOR SPECIFYING WELL TYPE, WELL
RADIUS, SKIN
CC     IFLAG =1QInj,=2PresProd,=3PresInj=4Qprod,IDIR =3for vert. well
*---- IDW    IW    JW    IFLAG    RW     SWELL   IDIR   IFIRST   ILAST
IPRF
       2     32     18       4     0.3      -2      3         1      9
0
CC
CC 3.7.6c WELL NAME
*----  WELNAM
pM42
CC 3.7.6d ICHEK , MAX. AND MIN. ALLOWABLE BOTTOMHOLE PRESSURE AND RATE
CC  if ICHEK = 0 then no check for limits
*---- ICHEK     PWFMIN     PWFMAX    QTMIN    QTMAX
        0          0        9999.      0        -4492.
CC 3.7.6a WELL ID,LOCATIONS,AND FLAG FOR SPECIFYING WELL TYPE, WELL
RADIUS, SKIN
CC     IFLAG =1QInj,=2PresProd,=3PresInj=4Qprod,IDIR =3for vert. well
*---- IDW    IW    JW    IFLAG    RW     SWELL   IDIR   IFIRST   ILAST
IPRF
       3     41    18       4     0.3      -2      3         1      9
1
cc
cc  3.7.6.b =0 for not perforated, =1 for perforated in this layer
*----kprf
      1  1  1  1  1  1  1  1  1
CC
CC 3.7.6c WELL NAME
*----  WELNAM
pM44
CC 3.7.6d ICHEK , MAX. AND MIN. ALLOWABLE BOTTOMHOLE PRESSURE AND RATE
CC  if ICHEK = 0 then no check for limits
*---- ICHEK     PWFMIN     PWFMAX    QTMIN    QTMAX
        0          0        9999.      0        -4492.
CC 3.7.6a WELL ID,LOCATIONS,AND FLAG FOR SPECIFYING WELL TYPE, WELL
RADIUS, SKIN
CC     IFLAG =1QInj,=2PresProd,=3PresInj=4Qprod,IDIR =3for vert. well
```

```
*---- IDW    IW    JW    IFLAG    RW     SWELL   IDIR   ZFIRST   ZLAST
IPRF
      4      22    27    4     0.3      -2        3      1       9
0
CC
CC 3.7.6c WELL NAME
*----  WELNAM
pM45
CC  if ICHEK = 0 then no check for limits
CC 3.7.6d ICHEK , MAX. AND MIN. ALLOWABLE BOTTOMHOLE PRESSURE AND RATE
in CFD
*---- ICHEK     PWFMIN     PWFMAX    QTMIN       QTMAX
        0          0         6000.      0        3370.
CC 3.7.6a WELL ID,LOCATIONS,AND FLAG FOR SPECIFYING WELL TYPE, WELL
RADIUS, SKIN
CC     IFLAG =1QInj,=2PresProd,=3PresInj=4Qprod,IDIR =3for vert. well
*---- IDW    IW    JW    IFLAG    RW     SWELL   IDIR   ZFIRST   ZLAST
IPRF
      5      32    27     4     0.3      -2        3      1         9
0
CC
CC 3.7.6c WELL NAME
*----  WELNAM
pM46
CC  if ICHEK = 0 then no check for limits
CC 3.7.6d ICHEK , MAX. AND MIN. ALLOWABLE BOTTOMHOLE PRESSURE AND RATE
in CFD
*---- ICHEK     PWFMIN     PWFMAX    QTMIN       QTMAX
        0          0         6000.      0        3370.
CC 3.7.6a WELL ID,LOCATIONS,AND FLAG FOR SPECIFYING WELL TYPE, WELL
RADIUS, SKIN
CC     IFLAG =1QInj,=2PresProd,=3PresInj=4Qprod,IDIR =3for vert. well
*---- IDW    IW    JW    IFLAG    RW     SWELL   IDIR   ZFIRST   ZLAST
IPRF
      6      42    26    4     0.3      -2        3      1         9
1
cc
cc  3.7.6.b =0 for not perforated, =1 for perforated in this layer
*kpr  1  2  3  4  5  6  7  8  9
      1  1  1  1  1  1  1  1  1
CC
CC 3.7.6c WELL NAME
*----  WELNAM
pM47
CC  if ICHEK = 0 then no check for limits
CC 3.7.6d ICHEK , MAX. AND MIN. ALLOWABLE BOTTOMHOLE PRESSURE AND RATE
in CFD
*---- ICHEK     PWFMIN     PWFMAX    QTMIN       QTMAX
        0          0         6000.      0        3370.
CC 3.7.6a WELL ID,LOCATIONS,AND FLAG FOR SPECIFYING WELL TYPE, WELL
RADIUS, SKIN
CC     IFLAG =1QInj,=2PresProd,=3PresInj=4Qprod,IDIR =3for vert. well
```

```
*---- IDW    IW    JW    IFLAG    RW     SWELL   IDIR   ZFIRST   ZLAST
IPRF
      7      18    13    1        0.3      -2        3      1         9
1
cc
cc  3.7.6.b =0 for not perforated, =1 for perforated in this layer
*kpr  1  2  3  4  5  6  7  8  9
      1  1  1  1  1  1  1  1  1
CC
CC 3.7.6c WELL NAME
*----  WELNAM
BCF01
CC  if ICHEK = 0 then no check for limits
CC 3.7.6d ICHEK , MAX. AND MIN. ALLOWABLE BOTTOMHOLE PRESSURE AND RATE
in CFD
*---- ICHEK     PWFMIN     PWFMAX    QTMIN       QTMAX
        0          0         6000.      0        3370.
CC 3.7.6a WELL ID,LOCATIONS,AND FLAG FOR SPECIFYING WELL TYPE, WELL
RADIUS, SKIN
CC     IFLAG =1QInj,=2PresProd,=3PresInj=4Qprod,IDIR =3for vert. well
*---- IDW    IW    JW    IFLAG    RW     SWELL   IDIR   ZFIRST   ZLAST
IPRF
      8      27    13    1        0.3      -2        3      1         9
0
CC
CC 3.7.6c WELL NAME
*----  WELNAM
BCF02
CC  if ICHEK = 0 then no check for limits
CC 3.7.6d ICHEK , MAX. AND MIN. ALLOWABLE BOTTOMHOLE PRESSURE AND RATE
in CFD
*---- ICHEK     PWFMIN     PWFMAX    QTMIN       QTMAX
        0          0         6000.      0        3370.
CC 3.7.6a WELL ID,LOCATIONS,AND FLAG FOR SPECIFYING WELL TYPE, WELL
RADIUS, SKIN
CC     IFLAG =1QInj,=2PresProd,=3PresInj=4Qprod,IDIR =3for vert. well
*---- IDW    IW    JW    IFLAG    RW     SWELL   IDIR   ZFIRST   ZLAST
IPRF
      9      36    13    1        0.3      -2        3      1         9
1
cc
cc  3.7.6.b =0 for not perforated, =1 for perforated in this layer
*kpr  1  2  3  4  5  6  7  8  9
      1  1  1  1  1  1  1  1  1
CC
CC 3.7.6c WELL NAME
*----  WELNAM
BCF03
CC  if ICHEK = 0 then no check for limits
CC 3.7.6d ICHEK , MAX. AND MIN. ALLOWABLE BOTTOMHOLE PRESSURE AND RATE
in CFD
*---- ICHEK     PWFMIN     PWFMAX    QTMIN       QTMAX
        0          0         6000.      0        3370.
```

```
CC 3.7.6a WELL ID,LOCATIONS,AND FLAG FOR SPECIFYING WELL TYPE, WELL
RADIUS, SKIN
CC     IFLAG =1QInj,=2PresProd,=3PresInj=4Qprod,IDIR =3for vert. well
*---- IDW    IW    JW    IFLAG    RW     SWELL   IDIR   ZFIRST   ZLAST
IPRF
      10     45    13    1        0.3      -2        3      1         9
1
cc
cc  3.7.6.b =0 for not perforated, =1 for perforated in this layer
*kpr  1  2  3  4  5  6  7  8  9
      1  1  1  1  1  1  1  1  1
CC
CC 3.7.6c WELL NAME
*----  WELNAM
BCF04
CC  if ICHEK = 0 then no check for limits
CC 3.7.6d ICHEK , MAX. AND MIN. ALLOWABLE BOTTOMHOLE PRESSURE AND RATE
in CFD
*---- ICHEK     PWFMIN     PWFMAX    QTMIN       QTMAX
        0          0         6000.      0        3370.
CC 3.7.6a WELL ID,LOCATIONS,AND FLAG FOR SPECIFYING WELL TYPE, WELL
RADIUS, SKIN
CC     IFLAG =1QInj,=2PresProd,=3PresInj=4Qprod,IDIR =3for vert. well
*---- IDW    IW    JW    IFLAG    RW     SWELL   IDIR   ZFIRST   ZLAST
IPRF
      11     18    23    1        0.3      -2       3      1         9
1
cc
cc  3.7.6.b =0 for not perforated, =1 for perforated in this layer
*kpr  1  2  3  4  5  6  7  8  9
      1  1  1  1  1  1  1  1  1
CC
CC 3.7.6c WELL NAME
*----  WELNAM
BCF05
CC  if ICHEK = 0 then no check for limits
CC 3.7.6d ICHEK , MAX. AND MIN. ALLOWABLE BOTTOMHOLE PRESSURE AND RATE
in CFD
*---- ICHEK     PWFMIN     PWFMAX    QTMIN       QTMAX
        0          0         6000.      0        3370.
CC 3.7.6a WELL ID,LOCATIONS,AND FLAG FOR SPECIFYING WELL TYPE, WELL
RADIUS, SKIN
CC     IFLAG =1QInj,=2PresProd,=3PresInj=4Qprod,IDIR =3for vert. well
*---- IDW    IW    JW    IFLAG    RW     SWELL   IDIR   ZFIRST   ZLAST
IPRF
      12     27    23    1        0.3      -2        3      1         9
1
cc
cc  3.7.6.b =0 for not perforated, =1 for perforated in this layer
*kpr  1  2  3  4  5  6  7  8  9
      1  1  1  1  1  1  1  1  1
CC
CC 3.7.6c WELL NAME
```

```
*----  WELNAM
BCF06
CC  if ICHEK = 0 then no check for limits
CC 3.7.6d ICHEK , MAX. AND MIN. ALLOWABLE BOTTOMHOLE PRESSURE AND RATE
in CFD
*---- ICHEK     PWFMIN     PWFMAX    QTMIN       QTMAX
        0          0         6000.      0        3370.
CC 3.7.6a WELL ID,LOCATIONS,AND FLAG FOR SPECIFYING WELL TYPE, WELL
RADIUS, SKIN
CC     IFLAG =1QInj,=2PresProd,=3PresInj=4Qprod,IDIR =3for vert. well
*---- IDW    IW    JW    IFLAG    RW     SWELL   IDIR   ZFIRST   ZLAST
IPRF
      13     36    23    1        0.3      -2        3      6         9
0
CC
CC 3.7.6c WELL NAME
*----  WELNAM
BCF07
CC  if ICHEK = 0 then no check for limits
CC 3.7.6d ICHEK , MAX. AND MIN. ALLOWABLE BOTTOMHOLE PRESSURE AND RATE
in CFD
*---- ICHEK     PWFMIN     PWFMAX    QTMIN       QTMAX
        0          0         6000.      0        3370.
CC 3.7.6a WELL ID,LOCATIONS,AND FLAG FOR SPECIFYING WELL TYPE, WELL
RADIUS, SKIN
CC     IFLAG =1QInj,=2PresProd,=3PresInj=4Qprod,IDIR =3for vert. well
*---- IDW    IW    JW    IFLAG    RW     SWELL   IDIR   ZFIRST   ZLAST
IPRF
      14     45    22    1        0.3      -2        3      1         9
1
cc
cc  3.7.6.b =0 for not perforated, =1 for perforated in this layer
*kpr  1  2  3  4  5  6  7  8  9
      1  1  1  1  1  1  1  1  1
CC
CC 3.7.6c WELL NAME
*----  WELNAM
BCF08
CC  if ICHEK = 0 then no check for limits
CC 3.7.6d ICHEK , MAX. AND MIN. ALLOWABLE BOTTOMHOLE PRESSURE AND RATE
in CFD
*---- ICHEK     PWFMIN     PWFMAX    QTMIN       QTMAX
        0          0         6000.      0        3370.
CC 3.7.6a WELL ID,LOCATIONS,AND FLAG FOR SPECIFYING WELL TYPE, WELL
RADIUS, SKIN
CC     IFLAG =1QInj,=2PresProd,=3PresInj=4Qprod,IDIR =3for vert. well
*---- IDW    IW    JW    IFLAG    RW     SWELL   IDIR   ZFIRST   ZLAST
IPRF
      15     16    31    1        0.3      -2        3      1         9
1
cc
cc  3.7.6.b =0 for not perforated, =1 for perforated in this layer
*kpr  1  2  3  4  5  6  7  8  9
```

```
      0  1  1  1  0  1  1  1  1
CC
CC 3.7.6c WELL NAME
*----  WELNAM
BCF09
CC  if ICHEK = 0 then no check for limits
CC 3.7.6d ICHEK , MAX. AND MIN. ALLOWABLE BOTTOMHOLE PRESSURE AND RATE
in CFD
*---- ICHEK     PWFMIN     PWFMAX    QTMIN       QTMAX
        0          0         6000.      0        3370.
CC 3.7.6a WELL ID,LOCATIONS,AND FLAG FOR SPECIFYING WELL TYPE, WELL
RADIUS, SKIN
CC     IFLAG =1QInj,=2PresProd,=3PresInj=4Qprod,IDIR =3for vert. well
*---- IDW    IW    JW    IFLAG    RW     SWELL   IDIR   ZFIRST   ZLAST
IPRF
      16     27    32    1        0.3      -2        3      1         9
1
cc
cc  3.7.6.b =0 for not perforated, =1 for perforated in this layer
*kpr  1  2  3  4  5  6  7  8  9
      1  1  1  1  1  1  1  1  1
CC
CC 3.7.6c WELL NAME
*----  WELNAM
BCF10
CC  if ICHEK = 0 then no check for limits
CC 3.7.6d ICHEK , MAX. AND MIN. ALLOWABLE BOTTOMHOLE PRESSURE AND RATE
in CFD
*---- ICHEK     PWFMIN     PWFMAX    QTMIN       QTMAX
        0          0         6000.      0        3370.
CC 3.7.6a WELL ID,LOCATIONS,AND FLAG FOR SPECIFYING WELL TYPE, WELL
RADIUS, SKIN
CC     IFLAG =1QInj,=2PresProd,=3PresInj=4Qprod,IDIR =3for vert. well
*---- IDW    IW    JW    IFLAG    RW     SWELL   IDIR   ZFIRST   ZLAST
IPRF
      17     36    32    1        0.3      -2       3      1         9
1
cc
cc  3.7.6.b =0 for not perforated, =1 for perforated in this layer
*kpr  1  2  3  4  5  6  7  8  9
      1  1  1  1  1  1  1  1  1
CC
CC 3.7.6c WELL NAME
*----  WELNAM
BCF11
CC  if ICHEK = 0 then no check for limits
CC 3.7.6d ICHEK , MAX. AND MIN. ALLOWABLE BOTTOMHOLE PRESSURE AND RATE
in CFD
*---- ICHEK     PWFMIN     PWFMAX    QTMIN       QTMAX
        0          0         6000.      0        3370.
CC 3.7.6a WELL ID,LOCATIONS,AND FLAG FOR SPECIFYING WELL TYPE, WELL
RADIUS, SKIN
CC     IFLAG =1QInj,=2PresProd,=3PresInj=4Qprod,IDIR =3for vert. well
```

```
*---- IDW    IW    JW    IFLAG    RW     SWELL   IDIR   ZFIRST   ZLAST
IPRF
      18     45    32    1        0.3      -2        3      6         9
0
CC
CC 3.7.6c WELL NAME
*----  WELNAM
BCF12
CC  if ICHEK = 0 then no check for limits
CC 3.7.6d ICHEK , MAX. AND MIN. ALLOWABLE BOTTOMHOLE PRESSURE AND RATE
in CFD
*---- ICHEK     PWFMIN     PWFMAX    QTMIN       QTMAX
        0          0         6000.      0        3370.
CC 3.7.6a WELL ID,LOCATIONS,AND FLAG FOR SPECIFYING WELL TYPE, WELL
RADIUS, SKIN
CC     IFLAG =1QInj,=2PresProd,=3PresInj=4Qprod,IDIR =3for vert. well
*---- IDW    IW    JW    IFLAG    RW     SWELL   IDIR   ZFIRST   ZLAST
IPRF
      19     11    25    1        0.3      -2        3      1         9
1
cc
cc  3.7.6.b =0 for not perforated, =1 for perforated in this layer
*kpr  1  2  3  4  5  6  7  8  9
      1  0  0  0  1  1  1  1  1
CC
CC 3.7.6c WELL NAME
*----  WELNAM
iDD6
CC  if ICHEK = 0 then no check for limits
CC 3.7.6d ICHEK , MAX. AND MIN. ALLOWABLE BOTTOMHOLE PRESSURE AND RATE
in CFD
*---- ICHEK     PWFMIN     PWFMAX    QTMIN       QTMAX
        0          0         6000.      0        3370.
CC 3.7.6a WELL ID,LOCATIONS,AND FLAG FOR SPECIFYING WELL TYPE, WELL
RADIUS, SKIN
CC     IFLAG =1QInj,=2PresProd,=3PresInj=4Qprod,IDIR =3for vert. well
*---- IDW    IW    JW    IFLAG    RW     SWELL   IDIR   ZFIRST   ZLAST
IPRF
      20     54    15    1        0.3      -2        3      1         9
1
cc
cc  3.7.6.b =0 for not perforated, =1 for perforated in this layer
*kpr  1  2  3  4  5  6  7  8  9
      1  1  1  1  0  1  1  1  1
CC
CC 3.7.6c WELL NAME
*----  WELNAM
iGG7
CC  if ICHEK = 0 then no check for limits
CC 3.7.6d ICHEK , MAX. AND MIN. ALLOWABLE BOTTOMHOLE PRESSURE AND RATE
in CFD
*---- ICHEK     PWFMIN     PWFMAX    QTMIN       QTMAX
        0          0         6000.      0        3370.
```

```
CC 3.7.6a WELL ID,LOCATIONS,AND FLAG FOR SPECIFYING WELL TYPE, WELL
RADIUS, SKIN
CC     IFLAG =1QInj,=2PresProd,=3PresInj=4Qprod,IDIR =3for vert. well
*---- IDW    IW    JW    IFLAG    RW     SWELL   IDIR   ZFIRST   ZLAST
IPRF
      21     13    14    1        0.3      -2        3      1         9
1
cc
cc  3.7.6.b =0 for not perforated, =1 for perforated in this layer
*kpr  1  2  3  4  5  6  7  8  9
      1  1  1  1  1  1  1  1  1
CC
CC 3.7.6c WELL NAME
*----  WELNAM
iD7
CC  if ICHEK = 0 then no check for limits
CC 3.7.6d ICHEK , MAX. AND MIN. ALLOWABLE BOTTOMHOLE PRESSURE AND RATE
in CFD
*---- ICHEK     PWFMIN     PWFMAX    QTMIN       QTMAX
        0          0         6000.      0        3370.
CC 3.7.6a WELL ID,LOCATIONS,AND FLAG FOR SPECIFYING WELL TYPE, WELL
RADIUS, SKIN
CC     IFLAG =1QInj,=2PresProd,=3PresInj=4Qprod,IDIR =3for vert. well
*---- IDW    IW    JW    IFLAG    RW     SWELL   IDIR   IFIRST   ILAST
IPRF
       22    16    36       4     0.3      -2      3         1      9
1
cc
cc  3.7.6.b =0 for not perforated, =1 for perforated in this layer
*kpr  1  2  3  4  5  6  7  8  9
      0  0  0  0  1  1  1  1  1
CC
CC 3.7.6c WELL NAME
*----  WELNAM
pM23
CC 3.7.6d ICHEK , MAX. AND MIN. ALLOWABLE BOTTOMHOLE PRESSURE AND RATE
CC  if ICHEK = 0 then no check for limits
*---- ICHEK     PWFMIN     PWFMAX    QTMIN    QTMAX
        0          0        9999.      0        -9999.
CC 3.7.6a WELL ID,LOCATIONS,AND FLAG FOR SPECIFYING WELL TYPE, WELL
RADIUS, SKIN
CC     IFLAG =1QInj,=2PresProd,=3PresInj=4Qprod,IDIR =3for vert. well
*---- IDW    IW    JW    IFLAG    RW     SWELL   IDIR   IFIRST   ILAST
IPRF
       23    33    40       4     0.3      -2      3         1      9
1
cc
cc  3.7.6.b =0 for not perforated, =1 for perforated in this layer
*kpr  1  2  3  4  5  6  7  8  9
      0  0  0  0  1  1  1  1  1
CC
CC 3.7.6c WELL NAME
*----  WELNAM
```

```
pM28
CC 3.7.6d ICHEK , MAX. AND MIN. ALLOWABLE BOTTOMHOLE PRESSURE AND RATE
CC  if ICHEK = 0 then no check for limits
*---- ICHEK     PWFMIN     PWFMAX    QTMIN    QTMAX
        0          0        9999.      0        -9999.
CC 3.7.6a WELL ID,LOCATIONS,AND FLAG FOR SPECIFYING WELL TYPE, WELL
RADIUS, SKIN
CC     IFLAG =1QInj,=2PresProd,=3PresInj=4Qprod,IDIR =3for vert. well
*---- IDW    IW    JW    IFLAG    RW     SWELL   IDIR   IFIRST   ILAST
IPRF
       24    41    21       4     0.3      -2      3         1      9
0
CC
CC 3.7.6c WELL NAME
*----  WELNAM
pM30
CC 3.7.6d ICHEK , MAX. AND MIN. ALLOWABLE BOTTOMHOLE PRESSURE AND RATE
CC  if ICHEK = 0 then no check for limits
*---- ICHEK     PWFMIN     PWFMAX    QTMIN    QTMAX
        0          0        9999.      0        -9999.
CC 3.7.6a WELL ID,LOCATIONS,AND FLAG FOR SPECIFYING WELL TYPE, WELL
RADIUS, SKIN
CC     IFLAG =1QInj,=2PresProd,=3PresInj=4Qprod,IDIR =3for vert. well
*---- IDW    IW    JW    IFLAG    RW     SWELL   IDIR   IFIRST   ILAST
IPRF
       25    43    5        4     0.3      -2      3         1      9
1
cc
cc  3.7.6.b =0 for not perforated, =1 for perforated in this layer
*kpr  1  2  3  4  5  6  7  8  9
      0  0  0  0  1  1  1  1  1
CC
CC 3.7.6c WELL NAME
*----  WELNAM
pM32
CC 3.7.6d ICHEK , MAX. AND MIN. ALLOWABLE BOTTOMHOLE PRESSURE AND RATE
CC  if ICHEK = 0 then no check for limits
*---- ICHEK     PWFMIN     PWFMAX    QTMIN    QTMAX
        0          0        9999.      0        -9999.
CC 3.7.6a WELL ID,LOCATIONS,AND FLAG FOR SPECIFYING WELL TYPE, WELL
RADIUS, SKIN
CC     IFLAG =1QInj,=2PresProd,=3PresInj=4Qprod,IDIR =3for vert. well
*---- IDW    IW    JW    IFLAG    RW     SWELL   IDIR   ZFIRST   ZLAST
IPRF
      26     1    10    2        0.3      0        3      1         9
0
CC
CC 3.7.6c WELL NAME
*----  WELNAM
WB1
CC  if ICHEK = 0 then no check for limits
CC 3.7.6d ICHEK , MAX. AND MIN. ALLOWABLE BOTTOMHOLE PRESSURE AND RATE
in CFD
```

```
*---- ICHEK     PWFMIN     PWFMAX    QTMIN       QTMAX
        0          0         6000.      0        3370.
CC 3.7.6a WELL ID,LOCATIONS,AND FLAG FOR SPECIFYING WELL TYPE, WELL
RADIUS, SKIN
CC     IFLAG =1QInj,=2PresProd,=3PresInj=4Qprod,IDIR =3for vert. well
*---- IDW    IW    JW    IFLAG    RW     SWELL   IDIR   ZFIRST   ZLAST
IPRF
      27     1    30    2        0.3      0        3      1         9
1
cc
cc  3.7.6.b =0 for not perforated, =1 for perforated in this layer
*kpr  1  2  3  4  5  6  7  8  9
      1  1  1  1  1  1  1  1  1
CC
CC 3.7.6c WELL NAME
*----  WELNAM
WB2
CC  if ICHEK = 0 then no check for limits
CC 3.7.6d ICHEK , MAX. AND MIN. ALLOWABLE BOTTOMHOLE PRESSURE AND RATE
in CFD
*---- ICHEK     PWFMIN     PWFMAX    QTMIN       QTMAX
        0          0         6000.      0        3370.
CC 3.7.6a WELL ID,LOCATIONS,AND FLAG FOR SPECIFYING WELL TYPE, WELL
RADIUS, SKIN
CC     IFLAG =1QInj,=2PresProd,=3PresInj=4Qprod,IDIR =3for vert. well
*---- IDW    IW    JW    IFLAG    RW     SWELL   IDIR   ZFIRST   ZLAST
IPRF
      28    1     40    2        0.3      0        3      1         9
0
CC
CC 3.7.6c WELL NAME
*----  WELNAM
WB3
CC  if ICHEK = 0 then no check for limits
CC 3.7.6d ICHEK , MAX. AND MIN. ALLOWABLE BOTTOMHOLE PRESSURE AND RATE
in CFD
*---- ICHEK     PWFMIN     PWFMAX    QTMIN       QTMAX
        0          0         6000.      0        3370.
CC 3.7.6a WELL ID,LOCATIONS,AND FLAG FOR SPECIFYING WELL TYPE, WELL
RADIUS, SKIN
CC     IFLAG =1QInj,=2PresProd,=3PresInj=4Qprod,IDIR =3for vert. well
*---- IDW    IW    JW    IFLAG    RW     SWELL   IDIR   ZFIRST   ZLAST
IPRF
      29     75    20    2        0.3      0        3      1         9
1
cc
cc  3.7.6.b =0 for not perforated, =1 for perforated in this layer
*kpr  1  2  3  4  5  6  7  8  9
      1  1  1  1  0  1  1  1  1
CC
CC 3.7.6c WELL NAME
*----  WELNAM
EB1
```

```
CC  if ICHEK = 0 then no check for limits
CC 3.7.6d ICHEK , MAX. AND MIN. ALLOWABLE BOTTOMHOLE PRESSURE AND RATE
in CFD
*---- ICHEK     PWFMIN     PWFMAX    QTMIN       QTMAX
        0          0         6000.      0        3370.
CC 3.7.6a WELL ID,LOCATIONS,AND FLAG FOR SPECIFYING WELL TYPE, WELL
RADIUS, SKIN
CC     IFLAG =1QInj,=2PresProd,=3PresInj=4Qprod,IDIR =3for vert. well
*---- IDW    IW    JW    IFLAG    RW     SWELL   IDIR   ZFIRST   ZLAST
IPRF
      30     75    36    2        0.3      0        3      1         9
1
cc
cc  3.7.6.b =0 for not perforated, =1 for perforated in this layer
*kpr  1  2  3  4  5  6  7  8  9
      1  1  1  1  1  1  1  1  1
CC
CC 3.7.6c WELL NAME
*----  WELNAM
EB2
CC  if ICHEK = 0 then no check for limits
CC 3.7.6d ICHEK , MAX. AND MIN. ALLOWABLE BOTTOMHOLE PRESSURE AND RATE
in CFD
*---- ICHEK     PWFMIN     PWFMAX    QTMIN       QTMAX
        0          0         6000.      0        3370.
CC 3.7.6a WELL ID,LOCATIONS,AND FLAG FOR SPECIFYING WELL TYPE, WELL
RADIUS, SKIN
CC     IFLAG =1QInj,=2PresProd,=3PresInj=4Qprod,IDIR =3for vert. well
*---- IDW    IW    JW    IFLAG    RW     SWELL   IDIR   ZFIRST   ZLAST
IPRF
      31     73    49    2        0.3      0        3      1         9
1
cc
cc  3.7.6.b =0 for not perforated, =1 for perforated in this layer
*kpr  1  2  3  4  5  6  7  8  9
      0  1  1  1  1  1  1  1  1
CC
CC 3.7.6c WELL NAME
*----  WELNAM
EB3
CC  if ICHEK = 0 then no check for limits
CC 3.7.6d ICHEK , MAX. AND MIN. ALLOWABLE BOTTOMHOLE PRESSURE AND RATE
in CFD
*---- ICHEK     PWFMIN     PWFMAX    QTMIN       QTMAX
        0          0         6000.      0        3370.
CC
CC 3.7.7b ID, RATE FOR RATE CONSTRAINT WELL (IFLAG=1 OR 4)
*----  ID      For IFLAG =4, specified RATE in CFD, negative for
prodcution
       1        0.
CC
CC 3.7.7b ID, RATE FOR RATE CONSTRAINT WELL (IFLAG=1 OR 4)
```

```
*----  ID      For IFLAG =4, specified RATE in CFD, negative for
prodcution
       2        0.
CC
CC 3.7.7b ID, RATE FOR RATE CONSTRAINT WELL (IFLAG=1 OR 4)
*----  ID      For IFLAG =4, specified RATE in CFD, negative for
prodcution
       3        0.
CC
CC 3.7.7b ID, RATE FOR RATE CONSTRAINT WELL (IFLAG=1 OR 4)
*----  ID      For IFLAG =4, specified RATE in CFD, negative for
prodcution
       4        0.
CC
CC 3.7.7b ID, RATE FOR RATE CONSTRAINT WELL (IFLAG=1 OR 4)
*----  ID      For IFLAG =4, specified RATE in CFD, negative for
prodcution
       5        0.
CC
CC 3.7.7b ID, RATE FOR RATE CONSTRAINT WELL (IFLAG=1 OR 4)
*----  ID      For IFLAG =4, specified RATE in CFD, negative for
prodcution
       6       0.
CC    FOR IFLAG = 3, pressure controlled injector
CC  3.7.7a ID,INJ. RATE AND INJ. COMP. FOR RATE CONS. WELLS FOR EACH
PHASE (L=1,3)
*----  ID     QI(M,L) water oil  surf  polymer Chlor  divalent   al1
al2  tr1 tr2 tr3 tr4   tr5   tr6
       7    702.     1.0      0    0.     0.    0.6084  0.00       0
0    0.  0   0   0    0.    0.
       7      0      0       0    0      0      0       0          0
0    0   0   0   0    0     0
       7      0      0       0    0      0      0       0          0
0    0   0   0   0    0     0
CC    FOR IFLAG = 3, pressure controlled injector
CC  3.7.7a ID,INJ. RATE AND INJ. COMP. FOR RATE CONS. WELLS FOR EACH
PHASE (L=1,3)
*----  ID     QI(M,L) water oil  surf  polymer Chlor  divalent   al1
al2  tr1 tr2 tr3 tr4   tr5   tr6
       8   702.    1.0      0    0.     0.    0.6084    0.00       0
0    0.  0   0   0    0.    0.
       8      0      0       0    0      0      0       0          0
0    0   0   0   0    0     0
       8      0      0       0    0      0      0       0          0
0    0   0   0   0    0     0
CC    FOR IFLAG = 3, pressure controlled injector
CC  3.7.7a ID,INJ. RATE AND INJ. COMP. FOR RATE CONS. WELLS FOR EACH
PHASE (L=1,3)
*----  ID     QI(M,L) water oil  surf  polymer Chlor  divalent   al1
al2  tr1 tr2 tr3 tr4   tr5   tr6
       9      702.    1.0      0    0.     0.   0.6084    0.00     0
0    0.  0.  0   0    0.    0.
```

```
       9      0      0       0    0      0      0       0          0
0    0   0   0   0    0     0
       9      0      0       0    0      0      0       0          0
0    0   0   0   0    0     0
CC    FOR IFLAG = 3, pressure controlled injector
CC  3.7.7a ID,INJ. RATE AND INJ. COMP. FOR RATE CONS. WELLS FOR EACH
PHASE (L=1,3)
*----  ID     QI(M,L) water oil  surf  polymer Chlor  divalent   al1
al2  tr1 tr2 tr3 tr4   tr5   tr6
       10      702.  1.0      0    0.     0.    0.6084   0.00       0
0    0.  0   0.  0    0.    0.
       10      0      0       0    0      0      0       0          0
0    0   0   0   0    0     0
       10      0      0       0    0      0      0       0          0
0    0   0   0   0    0     0
CC    FOR IFLAG = 3, pressure controlled injector
CC  3.7.7a ID,INJ. RATE AND INJ. COMP. FOR RATE CONS. WELLS FOR EACH
PHASE (L=1,3)
*----  ID     QI(M,L) water oil  surf  polymer Chlor  divalent   al1
al2  tr1 tr2 tr3 tr4   tr5   tr6
       11      702.  1.0      0    0.     0.   0.6084    0.00       0
0    0.  0   0.  0    0.    0.
       11      0      0       0    0      0      0       0          0
0    0   0   0   0    0     0
       11      0      0       0    0      0      0       0          0
0    0   0   0   0    0     0
CC    FOR IFLAG = 3, pressure controlled injector
CC  3.7.7a ID,INJ. RATE AND INJ. COMP. FOR RATE CONS. WELLS FOR EACH
PHASE (L=1,3)
*----  ID     QI(M,L) water oil  surf  polymer Chlor  divalent   al1
al2  tr1 tr2 tr3 tr4   tr5   tr6
       12      702. 1.0      0    0.     0.    0.6084    0.00       0
0    0.  0   0   0.   0.    0.
       12      0      0       0    0      0      0       0          0
0    0   0   0   0    0     0
       12      0      0       0    0      0      0       0          0
0    0   0   0   0    0     0
CC    FOR IFLAG = 3, pressure controlled injector
CC  3.7.7a ID,INJ. RATE AND INJ. COMP. FOR RATE CONS. WELLS FOR EACH
PHASE (L=1,3)
*----  ID     QI(M,L) water oil  surf  polymer Chlor  divalent   al1
al2  tr1 tr2 tr3 tr4   tr5   tr6
       13      702. 1.0      0    0.     0.    0.6084    0.00       0
0    0.  0   0.  0    0.    0.
       13      0      0       0    0      0      0       0          0
0    0   0   0   0    0     0
       13      0      0       0    0      0      0       0          0
0    0   0   0   0    0     0
CC    FOR IFLAG = 3, pressure controlled injector
CC  3.7.7a ID,INJ. RATE AND INJ. COMP. FOR RATE CONS. WELLS FOR EACH
PHASE (L=1,3)
*----  ID     QI(M,L) water oil  surf  polymer Chlor  divalent   al1
al2  tr1 tr2 tr3 tr4   tr5   tr6
```

```
       14      702.    1.0      0    0.     0.    0.6084   0.00     0
0    0.  0   0.  0    0.    0.
       14      0       0       0    0      0      0       0          0
0    0   0   0   0    0     0
       14      0       0       0    0      0      0       0          0
0    0   0   0   0    0     0
CC    FOR IFLAG = 3, pressure controlled injector
CC  3.7.7a ID,INJ. RATE AND INJ. COMP. FOR RATE CONS. WELLS FOR EACH
PHASE (L=1,3)
*----  ID     QI(M,L) water oil  surf  polymer Chlor  divalent   al1
al2  tr1 tr2 tr3 tr4   tr5   tr6
       15      702.   1.0     0    0.     0.    0.6084   0.00       0
0    0.  0   0.  0    0.    0.
       15      0       0       0    0      0      0       0          0
0    0   0   0   0    0     0
       15      0       0       0    0      0      0       0          0
0    0   0   0   0    0     0
CC    FOR IFLAG = 3, pressure controlled injector
CC  3.7.7a ID,INJ. RATE AND INJ. COMP. FOR RATE CONS. WELLS FOR EACH
PHASE (L=1,3)
*----  ID     QI(M,L) water oil  surf  polymer Chlor  divalent   al1
al2  tr1 tr2 tr3 tr4   tr5   tr6
       16    702.    1.0      0    0.     0.    0.6084   0.00       0
0    0.  0   0.  0    0.    0.
       16      0       0       0    0      0      0       0          0
0    0   0   0   0    0     0
       16      0       0       0    0      0      0       0          0
0    0   0   0   0    0     0
CC    FOR IFLAG = 3, pressure controlled injector
CC  3.7.7a ID,INJ. RATE AND INJ. COMP. FOR RATE CONS. WELLS FOR EACH
PHASE (L=1,3)
*----  ID     QI(M,L) water oil  surf  polymer Chlor  divalent   al1
al2  tr1 tr2 tr3 tr4   tr5   tr6
       17    702.    1.0      0    0.     0.    0.6084   0.00       0
0    0.  0   0.  0    0.    0.
       17      0       0       0    0      0      0       0          0
0    0   0   0   0    0     0
       17      0       0       0    0      0      0       0          0
0    0   0   0   0    0     0
CC    FOR IFLAG = 3, pressure controlled injector
CC  3.7.7a ID,INJ. RATE AND INJ. COMP. FOR RATE CONS. WELLS FOR EACH
PHASE (L=1,3)
*----  ID     QI(M,L) water oil  surf  polymer Chlor  divalent   al1
al2  tr1 tr2 tr3 tr4   tr5   tr6
       18    702.    1.0      0    0.     0.    0.6084   0.00       0
0    0.  0   0.  0    0.    0.
       18      0       0       0    0      0      0       0          0
0    0   0   0   0    0     0
       18      0       0       0    0      0      0       0          0
0    0   0   0   0    0     0
CC    FOR IFLAG = 3, pressure controlled injector
CC  3.7.7a ID,INJ. RATE AND INJ. COMP. FOR RATE CONS. WELLS FOR EACH
PHASE (L=1,3)
```

```
*----  ID     QI(M,L) water oil  surf  polymer Chlor  divalent   al1
al2  tr1 tr2 tr3 tr4   tr5   tr6
       19    421.    1.0      0    0.     0.    0.336   0.0641       0
0    0.  0   0.  0    0.    0.
       19      0      0       0    0      0      0       0          0
0    0   0   0   0    0     0
       19      0      0       0    0      0      0       0          0
0    0   0   0   0    0     0
CC    FOR IFLAG = 3, pressure controlled injector
CC  3.7.7a ID,INJ. RATE AND INJ. COMP. FOR RATE CONS. WELLS FOR EACH
PHASE (L=1,3)
*----  ID     QI(M,L) water oil  surf  polymer Chlor  divalent   al1
al2  tr1 tr2 tr3 tr4   tr5   tr6
       20    421.    1.0      0    0.     0.    0.336   0.0641       0
0    0.  0   0.  0    0.    0.
       20      0      0       0    0      0      0       0          0
0    0   0   0   0    0     0
       20      0      0       0    0      0      0       0          0
0    0   0   0   0    0     0
CC    FOR IFLAG = 3, pressure controlled injector
CC  3.7.7a ID,INJ. RATE AND INJ. COMP. FOR RATE CONS. WELLS FOR EACH
PHASE (L=1,3)
*----  ID     QI(M,L) water oil  surf  polymer Chlor  divalent   al1
al2  tr1 tr2 tr3 tr4   tr5   tr6
       21    281.    1.0      0    0.     0.    0.336   0.0641       0
0    0.  0   0.  0    0.    0.
       21      0      0       0    0      0      0       0          0
0    0   0   0   0    0     0
       21      0      0       0    0      0      0       0          0
0    0   0   0   0    0     0
CC
CC 3.7.7b ID, RATE FOR RATE CONSTRAINT WELL (IFLAG=4)
*----  ID      For IFLAG =4, specified RATE in CFD, negative for
prodcution
       22        -5.6
CC
CC 3.7.7b ID, RATE FOR RATE CONSTRAINT WELL (IFLAG=4)
*----  ID      For IFLAG =4, specified RATE in CFD, negative for
prodcution
       23        -5.6
CC
CC 3.7.7b ID, RATE FOR RATE CONSTRAINT WELL (IFLAG=4)
*----  ID      For IFLAG =4, specified RATE in CFD, negative for
prodcution
       24        -5.6
CC
CC 3.7.7b ID, RATE FOR RATE CONSTRAINT WELL (IFLAG=4)
*----  ID      For IFLAG =4, specified RATE in CFD, negative for
prodcution
       25        -5.6
CC   IFLAG = 2
CC 3.7.7b ID, Pressure constrained boundary well
*----  ID      pressure in psi
```

```
       26      350.
CC   IFLAG = 2
CC 3.7.7b ID, Pressure constrained boundary well
*----  ID      pressure in psi
       27      370.
CC   IFLAG = 2
CC 3.7.7b ID, Pressure constrained boundary well
*----  ID      pressure in psi
       28      350.
CC   IFLAG = 2
CC 3.7.7b ID, Pressure constrained boundary well
*----  ID      pressure in psi
       29      320.
CC   IFLAG = 2
CC 3.7.7b ID, Pressure constrained boundary well
*----  ID      pressure in psi
       30      340.
CC   IFLAG = 2
CC 3.7.7b ID, Pressure constrained boundary well
*----  ID      pressure in psi
       31      320.
CC 3.7.8 CUM. INJ. TIME , AND INTERVALS (PV OR DAY) FOR WRITING TO
OUTPUT FILES
CC          profilesPROF    prodPROF    prodHIST    maps
recovery
*---- TINJ     CUMPR1     CUMHI1          WRHPV      WRPRF        RSTC
       1.8          7.        7.0            0.3          7.
10.
CC**************  injection only for 2 days to pressure up depleted
reservoir**************
CC 3.7.11 FOR IMES=2 ,THE INI. TIME STEP,CONC. TOLERANCE,MAX.,MIN.
courant numbers
*----  DT            DCLIM      CNMAX         CNMIN
       0.00001       0.001       0.01         0.001
CC**************  injection and production of water t0 66 days at 2000
bbl/day  ************************************************************
CC FLAG FOR INDICATING BOUNDARY CHANGE
*---- IBMOD
        0
CC
CC  IRO, ITIME, NEW FLAGS FOR ALL THE WELLS
*----  IRO    ITIME     IFLAG
        2       1        6*4 15*1 4*4 6*2
CC
CC  NUMBER OF WELLS CHANGES IN LOCATION OR SKIN OR PWF
*----  NWEL1
         0
CC
CC  NUMBER OF WELLS WITH RATE CHANGES, ID
*---- NWEL2     ID
        18     1  2  3  4  5  6  7 8 9  10  11  12  13 14 15  16   17
18
CC
```

```
CC 3.7.7b ID, RATE FOR RATE CONSTRAINT WELL (IFLAG=1 OR 4)
*----  ID      For IFLAG =4, specified RATE in CFD, negative for
prodcution
       1         -1909.
CC
CC 3.7.7b ID, RATE FOR RATE CONSTRAINT WELL (IFLAG=1 OR 4)
*----  ID      For IFLAG =4, specified RATE in CFD, negative for
prodcution
       2         -1909.
CC
CC 3.7.7b ID, RATE FOR RATE CONSTRAINT WELL (IFLAG=1 OR 4)
*----  ID      For IFLAG =4, specified RATE in CFD, negative for
prodcution
       3         -1909.
CC
CC 3.7.7b ID, RATE FOR RATE CONSTRAINT WELL (IFLAG=1 OR 4)
*----  ID      For IFLAG =4, specified RATE in CFD, negative for
prodcution
       4         -1909.
CC
CC 3.7.7b ID, RATE FOR RATE CONSTRAINT WELL (IFLAG=1 OR 4)
*----  ID      For IFLAG =4, specified RATE in CFD, negative for
prodcution
       5         -1909.
CC
CC 3.7.7b ID, RATE FOR RATE CONSTRAINT WELL (IFLAG=1 OR 4)
*----  ID      For IFLAG =4, specified RATE in CFD, negative for
prodcution
       6         -1909.
CC    FOR IFLAG = 3, pressure controlled injector
CC  3.7.7a ID,INJ. RATE AND INJ. COMP. FOR RATE CONS. WELLS FOR EACH
PHASE (L=1,3)
*----  ID     QI(M,L) water oil  surf  polymer Chlor  divalent   al1
al2  tr1 tr2 tr3 tr4   tr5   tr6
       7    954.     1.0      0    0.     0.    0.6084  0.00       0
0    0.  0   0   0    0.    0.
       7      0      0       0    0      0      0       0          0
0    0   0   0   0    0     0
       7      0      0       0    0      0      0       0          0
0    0   0   0   0    0     0
CC    FOR IFLAG = 3, pressure controlled injector
CC  3.7.7a ID,INJ. RATE AND INJ. COMP. FOR RATE CONS. WELLS FOR EACH
PHASE (L=1,3)
*----  ID     QI(M,L) water oil  surf  polymer Chlor  divalent   al1
al2  tr1 tr2 tr3 tr4   tr5   tr6
       8   954.    1.0      0    0.     0.    0.6084    0.00       0
0    0.  0   0   0    0.    0.
       8      0      0       0    0      0      0       0          0
0    0   0   0   0    0     0
       8      0      0       0    0      0      0       0          0
0    0   0   0   0    0     0
CC    FOR IFLAG = 3, pressure controlled injector
```

```
CC  3.7.7a ID,INJ. RATE AND INJ. COMP. FOR RATE CONS. WELLS FOR EACH
PHASE (L=1,3)
*----  ID     QI(M,L) water oil  surf  polymer Chlor  divalent   al1
al2  tr1 tr2 tr3 tr4   tr5   tr6
       9      954.  1.0      0    0.     0.   0.6084    0.00       0
0    0.  0.  0   0    0.    0.
       9      0      0       0    0      0      0       0          0
0    0   0   0   0    0     0
       9      0      0       0    0      0      0       0          0
0    0   0   0   0    0     0
CC    FOR IFLAG = 3, pressure controlled injector
CC  3.7.7a ID,INJ. RATE AND INJ. COMP. FOR RATE CONS. WELLS FOR EACH
PHASE (L=1,3)
*----  ID     QI(M,L) water oil  surf  polymer Chlor  divalent   al1
al2  tr1 tr2 tr3 tr4   tr5   tr6
       10      954. 1.0      0    0.     0.    0.6084    0.00       0
0    0.  0   0.  0    0.    0.
       10      0      0       0    0      0      0       0          0
0    0   0   0   0    0     0
       10      0      0       0    0      0      0       0          0
0    0   0   0   0    0     0
CC    FOR IFLAG = 3, pressure controlled injector
CC  3.7.7a ID,INJ. RATE AND INJ. COMP. FOR RATE CONS. WELLS FOR EACH
PHASE (L=1,3)
*----  ID     QI(M,L) water oil  surf  polymer Chlor  divalent   al1
al2  tr1 tr2 tr3 tr4   tr5   tr6
       11      954.  1.0      0    0.     0.   0.6084    0.00       0
0    0.  0   0.  0    0.    0.
       11      0      0       0    0      0      0       0          0
0    0   0   0   0    0     0
       11      0      0       0    0      0      0       0          0
0    0   0   0   0    0     0
CC    FOR IFLAG = 3, pressure controlled injector
CC  3.7.7a ID,INJ. RATE AND INJ. COMP. FOR RATE CONS. WELLS FOR EACH
PHASE (L=1,3)
*----  ID     QI(M,L) water oil  surf  polymer Chlor  divalent   al1
al2  tr1 tr2 tr3 tr4   tr5   tr6
       12      954.  1.0      0    0.     0.    0.6084    0.00      0
0    0.  0   0   0.   0.    0.
       12      0      0       0    0      0      0       0          0
0    0   0   0   0    0     0
       12      0      0       0    0      0      0       0          0
0    0   0   0   0    0     0
CC    FOR IFLAG = 3, pressure controlled injector
CC  3.7.7a ID,INJ. RATE AND INJ. COMP. FOR RATE CONS. WELLS FOR EACH
PHASE (L=1,3)
*----  ID     QI(M,L) water oil  surf  polymer Chlor  divalent   al1
al2  tr1 tr2 tr3 tr4   tr5   tr6
       13      954.  1.0      0    0.     0.    0.6084    0.00      0
0    0.  0   0.  0    0.    0.
       13      0      0       0    0      0      0       0          0
0    0   0   0   0    0     0
```

```
       13      0      0       0    0      0      0       0          0
0    0   0   0   0    0     0
CC    FOR IFLAG = 3, pressure controlled injector
CC  3.7.7a ID,INJ. RATE AND INJ. COMP. FOR RATE CONS. WELLS FOR EACH
PHASE (L=1,3)
*----  ID     QI(M,L) water oil  surf  polymer Chlor  divalent   al1
al2  tr1 tr2 tr3 tr4   tr5   tr6
       14      954.  1.0      0    0.     0.    0.6084   0.00       0
0    0.  0   0.  0    0.    0.
       14      0      0       0    0      0      0       0          0
0    0   0   0   0    0     0
       14      0      0       0    0      0      0       0          0
0    0   0   0   0    0     0
CC    FOR IFLAG = 3, pressure controlled injector
CC  3.7.7a ID,INJ. RATE AND INJ. COMP. FOR RATE CONS. WELLS FOR EACH
PHASE (L=1,3)
*----  ID     QI(M,L) water oil  surf  polymer Chlor  divalent   al1
al2  tr1 tr2 tr3 tr4   tr5   tr6
       15      954.  1.0      0    0.     0.    0.6084   0.00       0
0    0.  0   0.  0    0.    0.
       15      0      0       0    0      0      0       0          0
0    0   0   0   0    0     0
       15      0      0       0    0      0      0       0          0
0    0   0   0   0    0     0
CC    FOR IFLAG = 3, pressure controlled injector
CC  3.7.7a ID,INJ. RATE AND INJ. COMP. FOR RATE CONS. WELLS FOR EACH
PHASE (L=1,3)
*----  ID     QI(M,L) water oil  surf  polymer Chlor  divalent   al1
al2  tr1 tr2 tr3 tr4   tr5   tr6
       16      954.  1.0      0    0.     0.    0.6084   0.00       0
0    0.  0   0.  0    0.    0.
       16      0      0       0    0      0      0       0          0
0    0   0   0   0    0     0
       16      0      0       0    0      0      0       0          0
0    0   0   0   0    0     0
CC    FOR IFLAG = 3, pressure controlled injector
CC  3.7.7a ID,INJ. RATE AND INJ. COMP. FOR RATE CONS. WELLS FOR EACH
PHASE (L=1,3)
*----  ID     QI(M,L) water oil  surf  polymer Chlor  divalent   al1
al2  tr1 tr2 tr3 tr4   tr5   tr6
       17      954.  1.0      0    0.     0.    0.6084   0.00       0
0    0.  0   0.  0    0.    0.
       17      0      0       0    0      0      0       0          0
0    0   0   0   0    0     0
       17      0      0       0    0      0      0       0          0
0    0   0   0   0    0     0
CC    FOR IFLAG = 3, pressure controlled injector
CC  3.7.7a ID,INJ. RATE AND INJ. COMP. FOR RATE CONS. WELLS FOR EACH
PHASE (L=1,3)
*----  ID     QI(M,L) water oil  surf  polymer Chlor  divalent   al1
al2  tr1 tr2 tr3 tr4   tr5   tr6
       18      954.  1.0      0    0.     0.    0.6084   0.00       0
0    0.  0   0.  0    0.    0.
```

```
       18      0      0       0    0      0      0       0          0
0    0   0   0   0    0     0
       18      0      0       0    0      0      0       0          0
0    0   0   0   0    0     0
CC 3.7.8 CUM. INJ. TIME , AND INTERVALS (PV OR DAY) FOR WRITING TO
OUTPUT FILES
CC          profilesPROF    prodPROF    prodHIST    maps
recovery
*---- TINJ     CUMPR1     CUMHI1         WRHPV      WRPRF        RSTC
       66.      33.        33.0             1.          33.
64.
CC*************************************************************************
*******************************
CC 3.7.11 FOR IMES=2 ,THE INI. TIME STEP,CONC. TOLERANCE,MAX.,MIN.
courant numbers
*----  DT            DCLIM      CNMAX         CNMIN
       0.00001       0.001       0.01         0.001
CC**************  inject water @ 1500 bbl/day + tracer preflush for 30
days, 96 days cumul) ************  ************
CC FLAG FOR INDICATING BOUNDARY CHANGE
*---- IBMOD
        0
CC
CC  IRO, ITIME, NEW FLAGS FOR ALL THE WELLS
*----  IRO    ITIME     IFLAG
        2       1        6*4 15*1 4*4 6*2
CC
CC  NUMBER OF WELLS CHANGES IN LOCATION OR SKIN OR PWF
*----  NWEL1
         0
CC
CC  NUMBER OF WELLS WITH RATE CHANGES, ID
*---- NWEL2     ID
        18     1  2  3  4  5  6  7 8 9  10  11  12  13 14 15  16   17
18
CC
CC 3.7.7b ID, RATE FOR RATE CONSTRAINT WELL (IFLAG=1 OR 4)
*----  ID      For IFLAG =4, specified RATE in CFD, negative for
prodcution
       1         -1404.
CC
CC 3.7.7b ID, RATE FOR RATE CONSTRAINT WELL (IFLAG=1 OR 4)
*----  ID      For IFLAG =4, specified RATE in CFD, negative for
prodcution
       2         -1404.
CC
CC 3.7.7b ID, RATE FOR RATE CONSTRAINT WELL (IFLAG=1 OR 4)
*----  ID      For IFLAG =4, specified RATE in CFD, negative for
prodcution
       3         -1404.
CC
CC 3.7.7b ID, RATE FOR RATE CONSTRAINT WELL (IFLAG=1 OR 4)
```

```
*----  ID      For IFLAG =4, specified RATE in CFD, negative for
prodcution
       4         -1404.
CC
CC 3.7.7b ID, RATE FOR RATE CONSTRAINT WELL (IFLAG=1 OR 4)
*----  ID      For IFLAG =4, specified RATE in CFD, negative for
prodcution
       5         -1404.
CC
CC 3.7.7b ID, RATE FOR RATE CONSTRAINT WELL (IFLAG=1 OR 4)
*----  ID      For IFLAG =4, specified RATE in CFD, negative for
prodcution
       6         -1404.
CC    FOR IFLAG = 3, pressure controlled injector
CC  3.7.7a ID,INJ. RATE AND INJ. COMP. FOR RATE CONS. WELLS FOR EACH
PHASE (L=1,3)
*----  ID     QI(M,L) water oil  surf  polymer Chlor  divalent   al1
al2  tr1 tr2 tr3 tr4   tr5   tr6
       7    702.     1.0      0    0.    0   0.6084  0.00       0    0
1.  1   1   0    0.    0.
       7      0      0       0    0      0      0       0          0
0    0   0   0   0    0     0
       7      0      0       0    0      0      0       0          0
0    0   0   0   0    0     0
CC    FOR IFLAG = 3, pressure controlled injector
CC  3.7.7a ID,INJ. RATE AND INJ. COMP. FOR RATE CONS. WELLS FOR EACH
PHASE (L=1,3)
*----  ID     QI(M,L) water oil  surf  polymer Chlor  divalent   al1
al2  tr1 tr2 tr3 tr4   tr5   tr6
       8     702.   1.0       0    0.    0   0.6084  0.00       0    0
1.  1   1   0    0.    0.
       8      0      0       0    0      0      0       0          0
0    0   0   0   0    0     0
       8      0      0       0    0      0      0       0          0
0    0   0   0   0    0     0
CC    FOR IFLAG = 3, pressure controlled injector
CC  3.7.7a ID,INJ. RATE AND INJ. COMP. FOR RATE CONS. WELLS FOR EACH
PHASE (L=1,3)
*----  ID     QI(M,L) water oil  surf  polymer Chlor  divalent   al1
al2  tr1 tr2 tr3 tr4   tr5   tr6
       9      702.    1.0    0    0.     0   0.6084  0.00       0    0
1.  1   1   0    0.    0.
       9      0      0       0    0      0      0       0          0
0    0   0   0   0    0     0
       9      0      0       0    0      0      0       0          0
0    0   0   0   0    0     0
CC    FOR IFLAG = 3, pressure controlled injector
CC  3.7.7a ID,INJ. RATE AND INJ. COMP. FOR RATE CONS. WELLS FOR EACH
PHASE (L=1,3)
*----  ID     QI(M,L) water oil  surf  polymer Chlor  divalent   al1
al2   tr1 tr2 tr3 tr4   tr5   tr6
       10      702.    1.0    0    0.     0   0.6084  0.00       0    0
1.  1   1   0    0.    0.
```

```
       10      0      0       0    0      0      0       0          0
0    0   0   0   0    0     0
       10      0      0       0    0      0      0       0          0
0    0   0   0   0    0     0
CC    FOR IFLAG = 3, pressure controlled injector
CC  3.7.7a ID,INJ. RATE AND INJ. COMP. FOR RATE CONS. WELLS FOR EACH
PHASE (L=1,3)
*----  ID     QI(M,L) water oil  surf  polymer Chlor  divalent   al1
al2   tr1 tr2 tr3 tr4   tr5   tr6
       11      702.    1.0    0    0.     0   0.6084  0.00       0    0
1.  1   1   0    0.    0.
       11      0      0       0    0      0      0       0          0
0    0   0   0   0    0     0
       11      0      0       0    0      0      0       0          0
0    0   0   0   0    0     0
CC    FOR IFLAG = 3, pressure controlled injector
CC  3.7.7a ID,INJ. RATE AND INJ. COMP. FOR RATE CONS. WELLS FOR EACH
PHASE (L=1,3)
*----  ID     QI(M,L) water oil  surf  polymer Chlor  divalent   al1
al2   tr1 tr2 tr3 tr4   tr5   tr6
       12      702.    1.0    0    0.     0   0.6084  0.00       0    0
1.  1   1   0    0.    0.
       12      0      0       0    0      0      0       0          0
0    0   0   0   0    0     0
       12      0      0       0    0      0      0       0          0
0    0   0   0   0    0     0
CC    FOR IFLAG = 3, pressure controlled injector
CC  3.7.7a ID,INJ. RATE AND INJ. COMP. FOR RATE CONS. WELLS FOR EACH
PHASE (L=1,3)
*----  ID     QI(M,L) water oil  surf  polymer Chlor  divalent    al1
al2  tr1 tr2 tr3 tr4   tr5   tr6
       13      702.    1.0    0    0.     0   0.6084  0.00       0    0
1.  1   1   0    0.    0.
       13      0      0       0    0      0      0       0          0
0    0   0   0   0    0     0
       13      0      0       0    0      0      0       0          0
0    0   0   0   0    0     0
CC    FOR IFLAG = 3, pressure controlled injector
CC  3.7.7a ID,INJ. RATE AND INJ. COMP. FOR RATE CONS. WELLS FOR EACH
PHASE (L=1,3)
*----  ID     QI(M,L) water oil  surf  polymer Chlor  divalent    al1
al2  tr1 tr2 tr3 tr4   tr5   tr6
       14      702.    1.0    0    0.     0   0.6084  0.00       0    0
1.  1   1   0    0.    0.
       14      0      0       0    0      0      0       0          0
0    0   0   0   0    0     0
       14      0      0       0    0      0      0       0          0
0    0   0   0   0    0     0
CC    FOR IFLAG = 3, pressure controlled injector
CC  3.7.7a ID,INJ. RATE AND INJ. COMP. FOR RATE CONS. WELLS FOR EACH
PHASE (L=1,3)
*----  ID     QI(M,L) water oil  surf  polymer Chlor  divalent    al1
al2  tr1 tr2 tr3 tr4   tr5   tr6
```

```
       15      702.    1.0    0    0.     0   0.6084  0.00       0    0
1.  1   1   0    0.    0.
       15      0       0       0    0      0      0       0          0
0    0   0   0   0    0     0
       15      0       0       0    0      0      0       0          0
0    0   0   0   0    0     0
CC    FOR IFLAG = 3, pressure controlled injector
CC  3.7.7a ID,INJ. RATE AND INJ. COMP. FOR RATE CONS. WELLS FOR EACH
PHASE (L=1,3)
*----  ID     QI(M,L) water oil  surf  polymer Chlor  divalent    al1
al2  tr1 tr2 tr3 tr4   tr5   tr6
       16      702.    1.0    0    0.     0   0.6084  0.00       0    0
1.  1   1   0    0.    0.
       16      0       0       0    0      0      0       0          0
0    0   0   0   0    0     0
       16      0       0       0    0      0      0       0          0
0    0   0   0   0    0     0
CC    FOR IFLAG = 3, pressure controlled injector
CC  3.7.7a ID,INJ. RATE AND INJ. COMP. FOR RATE CONS. WELLS FOR EACH
PHASE (L=1,3)
*----  ID     QI(M,L) water oil  surf  polymer Chlor  divalent    al1
al2  tr1 tr2 tr3 tr4   tr5   tr6
       17      702.    1.0    0    0.     0   0.6084  0.00       0    0
1.  1   1   0    0.    0.
       17      0       0       0    0      0      0       0          0
0    0   0   0   0    0     0
       17      0       0       0    0      0      0       0          0
0    0   0   0   0    0     0
CC    FOR IFLAG = 3, pressure controlled injector
CC  3.7.7a ID,INJ. RATE AND INJ. COMP. FOR RATE CONS. WELLS FOR EACH
PHASE (L=1,3)
*----  ID     QI(M,L) water oil  surf  polymer Chlor  divalent    al1
al2  tr1 tr2 tr3 tr4   tr5   tr6
       18      702.    1.0    0    0.     0   0.6084  0.00       0    0
1.  1   1   0    0.    0.
       18      0       0       0    0      0      0       0          0
0    0   0   0   0    0     0
       18      0       0       0    0      0      0       0          0
0    0   0   0   0    0     0
CC 3.7.8 CUM. INJ. TIME , AND INTERVALS (PV OR DAY) FOR WRITING TO
OUTPUT FILES
CC          profilesPROF    prodPROF    prodHIST    maps
recovery
*---- TINJ     CUMPR1     CUMHI1         WRHPV      WRPRF        RSTC
       128.      35.        35.0            3.          30.
45.
CC*****************************************************************
*******************************
CC 3.7.11 FOR IMES=2 ,THE INI. TIME STEP,CONC. TOLERANCE,MAX.,MIN.
courant numbers
*----  DT            DCLIM      CNMAX         CNMIN
       0.00001       0.001       0.02         0.001
CC**************  inject ASP + tracer 30 days, 171 cumul.
```

```
CC FLAG FOR INDICATING BOUNDARY CHANGE
*---- IBMOD
        0
CC
CC  IRO, ITIME, NEW FLAGS FOR ALL THE WELLS
*----  IRO    ITIME     IFLAG
        2       1        6*4 15*1 4*4 6*2
CC
CC  NUMBER OF WELLS CHANGES IN LOCATION OR SKIN OR PWF
*----  NWEL1
         0
CC
CC  NUMBER OF WELLS WITH RATE CHANGES, ID
*---- NWEL2     ID
        12     7 8 9  10  11  12  13 14 15  16  17  18
CC    FOR IFLAG = 1, rate controlled injector
CC  3.7.7a ID,INJ. RATE AND INJ. COMP. FOR RATE CONS. WELLS FOR EACH
PHASE (L=1,3)
*----  ID     QI(M,L) water oil  surf  polymer Chlor  divalent   al1
al2  tr1 tr2 tr3 tr4   tr5   tr6
       7    702.    0.99     0   0.01    0.22   0.455 0.00         0
0    1.  0   0   1    0.    0.
       7      0      0       0    0      0      0       0          0
0    0   0   0   0    0     0
       7      0      0       0    0      0      0       0          0
0    0   0   0   0    0     0
CC    FOR IFLAG = 1, rate controlled injector
CC  3.7.7a ID,INJ. RATE AND INJ. COMP. FOR RATE CONS. WELLS FOR EACH
PHASE (L=1,3)
*----  ID     QI(M,L) water oil  surf  polymer Chlor  divalent   al1
al2  tr1 tr2 tr3 tr4   tr5   tr6
       8    702.    0.99     0   0.01    0.22   0.455 0.00         0
0    1.  0   0   1    0.    0.
       8      0      0       0    0      0      0       0          0
0    0   0   0   0    0     0
       8      0      0       0    0      0      0       0          0
0    0   0   0   0    0     0
CC    FOR IFLAG = 1, rate controlled injector
CC  3.7.7a ID,INJ. RATE AND INJ. COMP. FOR RATE CONS. WELLS FOR EACH
PHASE (L=1,3)
*----  ID     QI(M,L) water oil  surf  polymer Chlor  divalent   al1
al2  tr1 tr2 tr3 tr4   tr5   tr6
       9    702.    0.99     0   0.01    0.22   0.455 0.00         0
0    1.  0   0   1    0.    0.
       9      0      0       0    0      0      0       0          0
0    0   0   0   0    0     0
       9      0      0       0    0      0      0       0          0
0    0   0   0   0    0     0
CC    FOR IFLAG = 1, rate controlled injector
CC  3.7.7a ID,INJ. RATE AND INJ. COMP. FOR RATE CONS. WELLS FOR EACH
PHASE (L=1,3)
*----  ID     QI(M,L) water oil  surf  polymer Chlor  divalent   al1
al2    tr1 tr2 tr3 tr4   tr5   tr6
```

```
       10    702.    0.99     0   0.01    0.22   0.455 0.00         0
0    1.  0   0   1    0.    0.
       10      0      0       0    0      0      0       0          0
0    0   0   0   0    0     0
       10      0      0       0    0      0      0       0          0
0    0   0   0   0    0     0
CC    FOR IFLAG = 1, rate controlled injector
CC  3.7.7a ID,INJ. RATE AND INJ. COMP. FOR RATE CONS. WELLS FOR EACH
PHASE (L=1,3)
*----  ID     QI(M,L) water oil  surf  polymer Chlor  divalent   al1
al2  tr1 tr2 tr3 tr4   tr5   tr6
       11    702.    0.99     0   0.01    0.22   0.455 0.00         0
0    1.  0   0   1    0.    0.
       11      0      0       0    0      0      0       0          0
0    0   0   0   0    0     0
       11      0      0       0    0      0      0       0          0
0    0   0   0   0    0     0
CC    FOR IFLAG = 1, rate controlled injector
CC  3.7.7a ID,INJ. RATE AND INJ. COMP. FOR RATE CONS. WELLS FOR EACH
PHASE (L=1,3)
*----  ID     QI(M,L) water oil  surf  polymer Chlor  divalent   al1
al2   tr1 tr2 tr3 tr4   tr5   tr6
       12    702.    0.99     0   0.01    0.22   0.455 0.00         0
0    1.  0   0   1    0.    0.
       12      0      0       0    0      0      0       0          0
0    0   0   0   0    0     0
       12      0      0       0    0      0      0       0          0
0    0   0   0   0    0     0
CC    FOR IFLAG = 1, rate controlled injector
CC  3.7.7a ID,INJ. RATE AND INJ. COMP. FOR RATE CONS. WELLS FOR EACH
PHASE (L=1,3)
*----  ID     QI(M,L) water oil  surf  polymer Chlor  divalent   al1
al2  tr1 tr2 tr3 tr4   tr5   tr6
       13    702.    0.99     0   0.01    0.22   0.455 0.00         0
0    1.  0   0   1    0.    0.
       13      0      0       0    0      0      0       0          0
0    0   0   0   0    0     0
       13      0      0       0    0      0      0       0          0
0    0   0   0   0    0     0
CC    FOR IFLAG = 1, rate controlled injector
CC  3.7.7a ID,INJ. RATE AND INJ. COMP. FOR RATE CONS. WELLS FOR EACH
PHASE (L=1,3)
*----  ID     QI(M,L) water oil  surf  polymer Chlor  divalent   al1
al2  tr1 tr2 tr3 tr4   tr5   tr6
       14    702.    0.99     0   0.01    0.22   0.455 0.00         0
0    1.  0   0   1    0.    0.
       14      0      0       0    0      0      0       0          0
0    0   0   0   0    0     0
       14      0      0       0    0      0      0       0          0
0    0   0   0   0    0     0
CC    FOR IFLAG = 1, rate controlled injector
CC  3.7.7a ID,INJ. RATE AND INJ. COMP. FOR RATE CONS. WELLS FOR EACH
PHASE (L=1,3)
```

```
*----  ID     QI(M,L) water oil  surf  polymer Chlor  divalent   al1
al2  tr1 tr2 tr3 tr4   tr5   tr6
       15    702.    0.99     0   0.01    0.22   0.455 0.00         0
0    1.  0   0   1    0.    0.
       15      0       0       0    0      0      0       0          0
0    0   0   0   0    0     0
       15      0       0       0    0      0      0       0          0
0    0   0   0   0    0     0
CC    FOR IFLAG = 1, rate controlled injector
CC  3.7.7a ID,INJ. RATE AND INJ. COMP. FOR RATE CONS. WELLS FOR EACH
PHASE (L=1,3)
*----  ID     QI(M,L) water oil  surf  polymer Chlor  divalent   al1
al2  tr1 tr2 tr3 tr4   tr5   tr6
       16    702.    0.99     0   0.01    0.22   0.455 0.00         0
0    1.  0   0   1    0.    0.
       16      0       0       0    0      0      0       0          0
0    0   0   0   0    0     0
       16      0       0       0    0      0      0       0          0
0    0   0   0   0    0     0
CC    FOR IFLAG = 1, rate controlled injector
CC  3.7.7a ID,INJ. RATE AND INJ. COMP. FOR RATE CONS. WELLS FOR EACH
PHASE (L=1,3)
*----  ID     QI(M,L) water oil  surf  polymer Chlor  divalent   al1
al2  tr1 tr2 tr3 tr4   tr5   tr6
       17    702.    0.99     0   0.01    0.22   0.455 0.00         0
0    1.  0   0   1    0.    0.
       17      0       0       0    0      0      0       0          0
0    0   0   0   0    0     0
       17      0       0       0    0      0      0       0          0
0    0   0   0   0    0     0
CC    FOR IFLAG = 1, rate controlled injector
CC  3.7.7a ID,INJ. RATE AND INJ. COMP. FOR RATE CONS. WELLS FOR EACH
PHASE (L=1,3)
*----  ID     QI(M,L) water oil  surf  polymer Chlor  divalent   al1
al2  tr1 tr2 tr3 tr4   tr5   tr6
       18    702.    0.99     0   0.01    0.22   0.455 0.00         0
0    1.  0   0   1    0.    0.
       18      0       0       0    0      0      0       0          0
0    0   0   0   0    0     0
       18      0       0       0    0      0      0       0          0
0    0   0   0   0    0     0
CC 3.7.8 CUM. INJ. TIME , AND INTERVALS (DAY) FOR WRITING TO OUTPUT
FILES
CC          profilesPROF    prodPROF    prodHIST    maps
recovery
*---- TINJ     CUMPR1     CUMHI1          WRHPV      WRPRF        RSTC
      171.      30.        30.0            3.          15.         30.
CC*****************************************************************
**************************************
CC 3.7.11 FOR IMES=2 ,THE INI. TIME STEP,CONC. TOLERANCE,MAX.,MIN.
courant numbers
*----  DT            DCLIM      CNMAX         CNMIN
       0.00001       0.001       0.01         0.001
```

```
CC**************  inject ASP w/o tracer 82 days, 112 total, 253 cumul.
(0.30 ppv, 0.68 cum ppv)*****************************
CC FLAG FOR INDICATING BOUNDARY CHANGE
*---- IBMOD
        0
CC
CC  IRO, ITIME, NEW FLAGS FOR ALL THE WELLS
*----  IRO    ITIME     IFLAG
        2       1        6*4 15*1 4*4 6*2
CC
CC  NUMBER OF WELLS CHANGES IN LOCATION OR SKIN OR PWF
*----  NWEL1
         0
CC
CC  NUMBER OF WELLS WITH RATE CHANGES, ID
*---- NWEL2     ID
        12     7 8 9  10  11  12  13 14 15  16  17  18
CC    FOR IFLAG = 1, rate controlled injector
CC  3.7.7a ID,INJ. RATE AND INJ. COMP. FOR RATE CONS. WELLS FOR EACH
PHASE (L=1,3)
*----  ID     QI(M,L) water oil  surf  polymer Chlor  divalent   al1
al2  tr1 tr2 tr3 tr4   tr5   tr6
       7    702.    0.99     0   0.01    0.22   0.455 0.00         0
0    1.  0   0   0    0.    0.
       7      0      0       0    0      0      0       0          0
0    0   0   0   0    0     0
       7      0      0       0    0      0      0       0          0
0    0   0   0   0    0     0
CC    FOR IFLAG = 1, rate controlled injector
CC  3.7.7a ID,INJ. RATE AND INJ. COMP. FOR RATE CONS. WELLS FOR EACH
PHASE (L=1,3)
*----  ID     QI(M,L) water oil  surf  polymer Chlor  divalent   al1
al2  tr1 tr2 tr3 tr4   tr5   tr6
       8    702.    0.99     0   0.01    0.22   0.455 0.00         0
0    1.  0   0   0    0.    0.
       8      0      0       0    0      0      0       0          0
0    0   0   0   0    0     0
       8      0      0       0    0      0      0       0          0
0    0   0   0   0    0     0
CC    FOR IFLAG = 1, rate controlled injector
CC  3.7.7a ID,INJ. RATE AND INJ. COMP. FOR RATE CONS. WELLS FOR EACH
PHASE (L=1,3)
*----  ID     QI(M,L) water oil  surf  polymer Chlor  divalent   al1
al2  tr1 tr2 tr3 tr4   tr5   tr6
       9    702.    0.99     0   0.01    0.22   0.455 0.00         0
0    1.  0   0   0    0.    0.
       9      0      0       0    0      0      0       0          0
0    0   0   0   0    0     0
       9      0      0       0    0      0      0       0          0
0    0   0   0   0    0     0
CC    FOR IFLAG = 1, rate controlled injector
CC  3.7.7a ID,INJ. RATE AND INJ. COMP. FOR RATE CONS. WELLS FOR EACH
PHASE (L=1,3)
```

```
*----  ID     QI(M,L) water oil  surf  polymer Chlor  divalent   al1
al2    tr1 tr2 tr3 tr4   tr5   tr6
       10    702.    0.99     0   0.01    0.22   0.455 0.00         0
0    1.  0   0   0    0.    0.
       10      0      0       0    0      0      0       0          0
0    0   0   0   0    0     0
       10      0      0       0    0      0      0       0          0
0    0   0   0   0    0     0
CC    FOR IFLAG = 1, rate controlled injector
CC  3.7.7a ID,INJ. RATE AND INJ. COMP. FOR RATE CONS. WELLS FOR EACH
PHASE (L=1,3)
*----  ID     QI(M,L) water oil  surf  polymer Chlor  divalent   al1
al2  tr1 tr2 tr3 tr4   tr5   tr6
       11    702.    0.99     0   0.01    0.22   0.455 0.00         0
0    1.  0   0   0    0.    0.
       11      0      0       0    0      0      0       0          0
0    0   0   0   0    0     0
       11      0      0       0    0      0      0       0          0
0    0   0   0   0    0     0
CC    FOR IFLAG = 1, rate controlled injector
CC  3.7.7a ID,INJ. RATE AND INJ. COMP. FOR RATE CONS. WELLS FOR EACH
PHASE (L=1,3)
*----  ID     QI(M,L) water oil  surf  polymer Chlor  divalent   al1
al2   tr1 tr2 tr3 tr4   tr5   tr6
       12    702.    0.99     0   0.01    0.22   0.455 0.00         0
0    1.  0   0   0    0.    0.
       12      0      0       0    0      0      0       0          0
0    0   0   0   0    0     0
       12      0      0       0    0      0      0       0          0
0    0   0   0   0    0     0
CC    FOR IFLAG = 1, rate controlled injector
CC  3.7.7a ID,INJ. RATE AND INJ. COMP. FOR RATE CONS. WELLS FOR EACH
PHASE (L=1,3)
*----  ID     QI(M,L) water oil  surf  polymer Chlor  divalent   al1
al2  tr1 tr2 tr3 tr4   tr5   tr6
       13    702.    0.99     0   0.01    0.22   0.455 0.00         0
0    1.  0   0   0    0.    0.
       13      0      0       0    0      0      0       0          0
0    0   0   0   0    0     0
       13      0      0       0    0      0      0       0          0
0    0   0   0   0    0     0
CC    FOR IFLAG = 1, rate controlled injector
CC  3.7.7a ID,INJ. RATE AND INJ. COMP. FOR RATE CONS. WELLS FOR EACH
PHASE (L=1,3)
*----  ID     QI(M,L) water oil  surf  polymer Chlor  divalent   al1
al2  tr1 tr2 tr3 tr4   tr5   tr6
       14    702.    0.99     0   0.01    0.22   0.455 0.00         0
0    1.  0   0   0    0.    0.
       14      0      0       0    0      0      0       0          0
0    0   0   0   0    0     0
       14      0      0       0    0      0      0       0          0
0    0   0   0   0    0     0
CC    FOR IFLAG = 1, rate controlled injector
```

```
CC  3.7.7a ID,INJ. RATE AND INJ. COMP. FOR RATE CONS. WELLS FOR EACH
PHASE (L=1,3)
*----  ID     QI(M,L) water oil  surf  polymer Chlor  divalent   al1
al2  tr1 tr2 tr3 tr4   tr5   tr6
       15    702.    0.99     0   0.01    0.22   0.455 0.00         0
0    1.  0   0   0    0.    0.
       15      0      0       0    0      0      0       0          0
0    0   0   0   0    0     0
       15      0      0       0    0      0      0       0          0
0    0   0   0   0    0     0
CC    FOR IFLAG = 1, rate controlled injector
CC  3.7.7a ID,INJ. RATE AND INJ. COMP. FOR RATE CONS. WELLS FOR EACH
PHASE (L=1,3)
*----  ID     QI(M,L) water oil  surf  polymer Chlor  divalent   al1
al2  tr1 tr2 tr3 tr4   tr5   tr6
       16    702.    0.99     0   0.01    0.22   0.455 0.00         0
0    1.  0   0   0    0.    0.
       16      0      0       0    0      0      0       0          0
0    0   0   0   0    0     0
       16      0      0       0    0      0      0       0          0
0    0   0   0   0    0     0
CC    FOR IFLAG = 1, rate controlled injector
CC  3.7.7a ID,INJ. RATE AND INJ. COMP. FOR RATE CONS. WELLS FOR EACH
PHASE (L=1,3)
*----  ID     QI(M,L) water oil  surf  polymer Chlor  divalent   al1
al2  tr1 tr2 tr3 tr4   tr5   tr6
       17    702.    0.99     0   0.01    0.22   0.455 0.00         0
0    1.  0   0   0    0.    0.
       17      0      0       0    0      0      0       0          0
0    0   0   0   0    0     0
       17      0      0       0    0      0      0       0          0
0    0   0   0   0    0     0
CC    FOR IFLAG = 1, rate controlled injector
CC  3.7.7a ID,INJ. RATE AND INJ. COMP. FOR RATE CONS. WELLS FOR EACH
PHASE (L=1,3)
*----  ID     QI(M,L) water oil  surf  polymer Chlor  divalent   al1
al2  tr1 tr2 tr3 tr4   tr5   tr6
       18    702.    0.99     0   0.01    0.22   0.455 0.00         0
0    1.  0   0   1    0.    0.
       18      0      0       0    0      0      0       0          0
0    0   0   0   0    0     0
       18      0      0       0    0      0      0       0          0
0    0   0   0   0    0     0
CC 3.7.8 CUM. INJ. TIME , AND INTERVALS (DAY) FOR WRITING TO OUTPUT
FILES
CC          profilesPROF    prodPROF    prodHIST    maps
recovery
*---- TINJ     CUMPR1     CUMHI1          WRHPV      WRPRF         RSTC
       234.      41.        41.0             2.          20.
82.
CC*********************************************************************
************************************
```

```
CC 3.7.11 FOR IMES=2 ,THE INI. TIME STEP,CONC. TOLERANCE,MAX.,MIN.
courant numbers
*----  DT            DCLIM      CNMAX         CNMIN
       0.00001       0.001       0.01         0.001
CC**************  inject Polymer Drive 262 days, 515 cumul. (0.70 ppv,
1.38 cum ppv)************************************
CC FLAG FOR INDICATING BOUNDARY CHANGE
*---- IBMOD
        0
CC
CC  IRO, ITIME, NEW FLAGS FOR ALL THE WELLS
*----  IRO    ITIME     IFLAG
        2       1        6*4 15*1 4*4 6*2
CC
CC  NUMBER OF WELLS CHANGES IN LOCATION OR SKIN OR PWF
*----  NWEL1
         0
CC
CC  NUMBER OF WELLS WITH RATE CHANGES, ID
*---- NWEL2     ID
        12     7 8 9  10  11  12  13 14 15  16  17  18
CC    FOR IFLAG = 1, rate controlled injector
CC  3.7.7a ID,INJ. RATE AND INJ. COMP. FOR RATE CONS. WELLS FOR EACH
PHASE (L=1,3)
*----  ID     QI(M,L) water oil  surf  polymer Chlor  divalent   al1
al2  tr1 tr2 tr3 tr4   tr5   tr6
       7    702.    1.0      0    0.     0.21   0.2665  0.00       0
0    1.  0   0   0    0.    0.
       7      0      0       0    0      0      0       0          0
0    0   0   0   0    0     0
       7      0      0       0    0      0      0       0          0
0    0   0   0   0    0     0
CC    FOR IFLAG = 1, rate controlled injector
CC  3.7.7a ID,INJ. RATE AND INJ. COMP. FOR RATE CONS. WELLS FOR EACH
PHASE (L=1,3)
*----  ID     QI(M,L) water oil  surf  polymer Chlor  divalent   al1
al2  tr1 tr2 tr3 tr4   tr5   tr6
       8    702.    1.0      0    0.     0.21   0.2665  0.00       0
0    1.  0   0   0    0.    0.
       8      0      0       0    0      0      0       0          0
0    0   0   0   0    0     0
       8      0      0       0    0      0      0       0          0
0    0   0   0   0    0     0
CC    FOR IFLAG = 1, rate controlled injector
CC  3.7.7a ID,INJ. RATE AND INJ. COMP. FOR RATE CONS. WELLS FOR EACH
PHASE (L=1,3)
*----  ID     QI(M,L) water oil  surf  polymer Chlor  divalent   al1
al2  tr1 tr2 tr3 tr4   tr5   tr6
       9    702.    1.0      0    0.     0.21   0.2665  0.00       0
0    1.  0   0   0    0.    0.
       9      0      0       0    0      0      0       0          0
0    0   0   0   0    0     0
```

```
       9      0      0       0    0      0      0       0          0
0    0   0   0   0    0     0
CC    FOR IFLAG = 1, rate controlled injector
CC  3.7.7a ID,INJ. RATE AND INJ. COMP. FOR RATE CONS. WELLS FOR EACH
PHASE (L=1,3)
*----  ID     QI(M,L) water oil  surf  polymer Chlor  divalent   al1
al2    tr1 tr2 tr3 tr4   tr5   tr6
       10    702.    1.0      0    0.     0.21   0.2665  0.00       0
0    1.  0   0   0    0.    0.
       10      0      0       0    0      0      0       0          0
0    0   0   0   0    0     0
       10      0      0       0    0      0      0       0          0
0    0   0   0   0    0     0
CC    FOR IFLAG = 1, rate controlled injector
CC  3.7.7a ID,INJ. RATE AND INJ. COMP. FOR RATE CONS. WELLS FOR EACH
PHASE (L=1,3)
*----  ID     QI(M,L) water oil  surf  polymer Chlor  divalent   al1
al2  tr1 tr2 tr3 tr4   tr5   tr6
       11    702.    1.0      0    0.     0.21   0.2665  0.00       0
0    1.  0   0   0    0.    0.
       11      0      0       0    0      0      0       0          0
0    0   0   0   0    0     0
       11      0      0       0    0      0      0       0          0
0    0   0   0   0    0     0
CC    FOR IFLAG = 1, rate controlled injector
CC  3.7.7a ID,INJ. RATE AND INJ. COMP. FOR RATE CONS. WELLS FOR EACH
PHASE (L=1,3)
*----  ID     QI(M,L) water oil  surf  polymer Chlor  divalent   al1
al2   tr1 tr2 tr3 tr4   tr5   tr6
       12    702.    1.0      0    0.     0.21   0.2665  0.00       0
0    1.  0   0   0    0.    0.
       12      0      0       0    0      0      0       0          0
0    0   0   0   0    0     0
       12      0      0       0    0      0      0       0          0
0    0   0   0   0    0     0
CC    FOR IFLAG = 1, rate controlled injector
CC  3.7.7a ID,INJ. RATE AND INJ. COMP. FOR RATE CONS. WELLS FOR EACH
PHASE (L=1,3)
*----  ID     QI(M,L) water oil  surf  polymer Chlor  divalent   al1
al2  tr1 tr2 tr3 tr4   tr5   tr6
       13    702.    1.0      0    0.     0.21   0.2665  0.00       0
0    1.  0   0   0    0.    0.
       13      0      0       0    0      0      0       0          0
0    0   0   0   0    0     0
       13      0      0       0    0      0      0       0          0
0    0   0   0   0    0     0
CC    FOR IFLAG = 1, rate controlled injector
CC  3.7.7a ID,INJ. RATE AND INJ. COMP. FOR RATE CONS. WELLS FOR EACH
PHASE (L=1,3)
*----  ID     QI(M,L) water oil  surf  polymer Chlor  divalent   al1
al2  tr1 tr2 tr3 tr4   tr5   tr6
       14    702.    1.0      0    0.     0.21   0.2665  0.00       0
0    1.  0   0   0    0.    0.
```

```
       14      0      0       0    0      0      0       0          0
0    0   0   0   0    0     0
       14      0      0       0    0      0      0       0          0
0    0   0   0   0    0     0
CC    FOR IFLAG = 1, rate controlled injector
CC  3.7.7a ID,INJ. RATE AND INJ. COMP. FOR RATE CONS. WELLS FOR EACH
PHASE (L=1,3)
*----  ID     QI(M,L) water oil  surf  polymer Chlor  divalent   al1
al2  tr1 tr2 tr3 tr4   tr5   tr6
       15    702.    1.0      0    0.     0.21   0.2665  0.00       0
0    1.  0   0   0    0.    0.
       15      0      0       0    0      0      0       0          0
0    0   0   0   0    0     0
       15      0      0       0    0      0      0       0          0
0    0   0   0   0    0     0
CC    FOR IFLAG = 1, rate controlled injector
CC  3.7.7a ID,INJ. RATE AND INJ. COMP. FOR RATE CONS. WELLS FOR EACH
PHASE (L=1,3)
*----  ID     QI(M,L) water oil  surf  polymer Chlor  divalent   al1
al2  tr1 tr2 tr3 tr4   tr5   tr6
       16    702.    1.0      0    0.     0.21   0.2665  0.00       0
0    1.  0   0   0    0.    0.
       16      0      0       0    0      0      0       0          0
0    0   0   0   0    0     0
       16      0      0       0    0      0      0       0          0
0    0   0   0   0    0     0
CC    FOR IFLAG = 1, rate controlled injector
CC  3.7.7a ID,INJ. RATE AND INJ. COMP. FOR RATE CONS. WELLS FOR EACH
PHASE (L=1,3)
*----  ID     QI(M,L) water oil  surf  polymer Chlor  divalent   al1
al2  tr1 tr2 tr3 tr4   tr5   tr6
       17    702.    1.0      0    0.     0.21   0.2665  0.00       0
0    1.  0   0   0    0.    0.
       17      0      0       0    0      0      0       0          0
0    0   0   0   0    0     0
       17      0      0       0    0      0      0       0          0
0    0   0   0   0    0     0
CC    FOR IFLAG = 1, rate controlled injector
CC  3.7.7a ID,INJ. RATE AND INJ. COMP. FOR RATE CONS. WELLS FOR EACH
PHASE (L=1,3)
*----  ID     QI(M,L) water oil  surf  polymer Chlor  divalent   al1
al2  tr1 tr2 tr3 tr4   tr5   tr6
       18    702.    1.0      0    0.     0.21   0.2665  0.00       0
0    1.  0   0   0    0.    0.
       18      0      0       0    0      0      0       0          0
0    0   0   0   0    0     0
       18      0      0       0    0      0      0       0          0
0    0   0   0   0    0     0
CC 3.7.8 CUM. INJ. TIME , AND INTERVALS (DAY) FOR WRITING TO OUTPUT
FILES
CC          profilesPROF    prodPROF    prodHIST    maps
recovery
*---- TINJ     CUMPR1     CUMHI1          WRHPV      WRPRF        RSTC
```

```
       552.      131.        131.0            2.          30.
262.
CC*************************************************************************
************************************
CC 3.7.11 FOR IMES=2 ,THE INI. TIME STEP,CONC. TOLERANCE,MAX.,MIN.
courant numbers
*----  DT            DCLIM      CNMAX         CNMIN
       0.00001       0.001       0.015         0.002
CC**************  inject Post-Water Flush for 747 days 1262 cumul., 2
ppv, 3.38 ppv cumul***********************
CC FLAG FOR INDICATING BOUNDARY CHANGE
*---- IBMOD
        0
CC
CC  IRO, ITIME, NEW FLAGS FOR ALL THE WELLS
*----  IRO    ITIME     IFLAG
        2       1        6*4 15*1 4*4 6*2
CC
CC  NUMBER OF WELLS CHANGES IN LOCATION OR SKIN OR PWF
*----  NWEL1
         0
CC
CC  NUMBER OF WELLS WITH RATE CHANGES, ID
*---- NWEL2     ID
        25    1  2  3  4  5  6 7 8 9  10  11  12  13 14 15  16  17  18
19  20  21  22  23  24   25
CC
CC 3.7.7b ID, RATE FOR RATE CONSTRAINT WELL (IFLAG=1 OR 4)
*----  ID      For IFLAG =4, specified RATE in CFD, negative for
prodcution
       1         -1404.
CC
CC 3.7.7b ID, RATE FOR RATE CONSTRAINT WELL (IFLAG=1 OR 4)
*----  ID      For IFLAG =4, specified RATE in CFD, negative for
prodcution
       2         -1404.
CC
CC 3.7.7b ID, RATE FOR RATE CONSTRAINT WELL (IFLAG=1 OR 4)
*----  ID      For IFLAG =4, specified RATE in CFD, negative for
prodcution
       3         -1404.
CC
CC 3.7.7b ID, RATE FOR RATE CONSTRAINT WELL (IFLAG=1 OR 4)
*----  ID      For IFLAG =4, specified RATE in CFD, negative for
prodcution
       4         -1404.
CC
CC 3.7.7b ID, RATE FOR RATE CONSTRAINT WELL (IFLAG=1 OR 4)
*----  ID      For IFLAG =4, specified RATE in CFD, negative for
prodcution
       5         -1404.
CC
CC 3.7.7b ID, RATE FOR RATE CONSTRAINT WELL (IFLAG=1 OR 4)
```

```
*----  ID      For IFLAG =4, specified RATE in CFD, negative for
prodcution
       6         -1404.
CC    FOR IFLAG = 3, pressure controlled injector
CC  3.7.7a ID,INJ. RATE AND INJ. COMP. FOR RATE CONS. WELLS FOR EACH
PHASE (L=1,3)
*----  ID     QI(M,L) water oil  surf  polymer Chlor  divalent   al1
al2  tr1 tr2 tr3 tr4   tr5   tr6
       7    702.    1.0      0    0.     0.    0.1811   0.00       0
0    1.  0   0   0    0.    0.
       7      0      0       0    0      0      0       0          0
0    0   0   0   0    0     0
       7      0      0       0    0      0      0       0          0
0    0   0   0   0    0     0
CC    FOR IFLAG = 3, pressure controlled injector
CC  3.7.7a ID,INJ. RATE AND INJ. COMP. FOR RATE CONS. WELLS FOR EACH
PHASE (L=1,3)
*----  ID     QI(M,L) water oil  surf  polymer Chlor  divalent   al1
al2  tr1 tr2 tr3 tr4   tr5   tr6
       8    702.    1.0      0    0.     0.    0.1811   0.00       0
0    1.  0   0   0    0.    0.
       8      0      0       0    0      0      0       0          0
0    0   0   0   0    0     0
       8      0      0       0    0      0      0       0          0
0    0   0   0   0    0     0
CC    FOR IFLAG = 3, pressure controlled injector
CC  3.7.7a ID,INJ. RATE AND INJ. COMP. FOR RATE CONS. WELLS FOR EACH
PHASE (L=1,3)
*----  ID     QI(M,L) water oil  surf  polymer Chlor  divalent   al1
al2  tr1 tr2 tr3 tr4   tr5   tr6
       9    702.    1.0      0    0.     0.    0.1811   0.00       0
0    1.  0   0   0    0.    0.
       9      0      0       0    0      0      0       0          0
0    0   0   0   0    0     0
       9      0      0       0    0      0      0       0          0
0    0   0   0   0    0     0
CC    FOR IFLAG = 3, pressure controlled injector
CC  3.7.7a ID,INJ. RATE AND INJ. COMP. FOR RATE CONS. WELLS FOR EACH
PHASE (L=1,3)
*----  ID     QI(M,L) water oil  surf  polymer Chlor  divalent   al1
al2  tr1 tr2 tr3 tr4   tr5   tr6
       10    702.    1.0      0    0.     0.    0.1811   0.00       0
0    1.  0   0   0    0.    0.
       10      0      0       0    0      0      0       0          0
0    0   0   0   0    0     0
       10      0      0       0    0      0      0       0          0
0    0   0   0   0    0     0
CC    FOR IFLAG = 3, pressure controlled injector
CC  3.7.7a ID,INJ. RATE AND INJ. COMP. FOR RATE CONS. WELLS FOR EACH
PHASE (L=1,3)
*----  ID     QI(M,L) water oil  surf  polymer Chlor  divalent   al1
al2  tr1 tr2 tr3 tr4   tr5   tr6
```

```
       11    702.    1.0      0    0.     0.    0.1811   0.00       0
0    1.  0   0   0    0.    0.
       11      0      0       0    0      0      0       0          0
0    0   0   0   0    0     0
       11      0      0       0    0      0      0       0          0
0    0   0   0   0    0     0
CC    FOR IFLAG = 3, pressure controlled injector
CC  3.7.7a ID,INJ. RATE AND INJ. COMP. FOR RATE CONS. WELLS FOR EACH
PHASE (L=1,3)
*----  ID     QI(M,L) water oil  surf  polymer Chlor  divalent   al1
al2  tr1 tr2 tr3 tr4   tr5   tr6
       12    702.    1.0      0    0.     0.    0.1811   0.00       0
0    1.  0   0   0    0.    0.
       12      0      0       0    0      0      0       0          0
0    0   0   0   0    0     0
       12      0      0       0    0      0      0       0          0
0    0   0   0   0    0     0
CC    FOR IFLAG = 3, pressure controlled injector
CC  3.7.7a ID,INJ. RATE AND INJ. COMP. FOR RATE CONS. WELLS FOR EACH
PHASE (L=1,3)
*----  ID     QI(M,L) water oil  surf  polymer Chlor  divalent   al1
al2  tr1 tr2 tr3 tr4   tr5   tr6
       13    702.    1.0      0    0.     0.    0.1811   0.00       0
0    1.  0   0   0    0.    0.
       13      0      0       0    0      0      0       0          0
0    0   0   0   0    0     0
       13      0      0       0    0      0      0       0          0
0    0   0   0   0    0     0
CC    FOR IFLAG = 3, pressure controlled injector
CC  3.7.7a ID,INJ. RATE AND INJ. COMP. FOR RATE CONS. WELLS FOR EACH
PHASE (L=1,3)
*----  ID     QI(M,L) water oil  surf  polymer Chlor  divalent   al1
al2  tr1 tr2 tr3 tr4   tr5   tr6
       14    702.    1.0      0    0.     0.    0.1811   0.00       0
0    1.  0   0   0    0.    0.
       14      0      0       0    0      0      0       0          0
0    0   0   0   0    0     0
       14      0      0       0    0      0      0       0          0
0    0   0   0   0    0     0
CC    FOR IFLAG = 3, pressure controlled injector
CC  3.7.7a ID,INJ. RATE AND INJ. COMP. FOR RATE CONS. WELLS FOR EACH
PHASE (L=1,3)
*----  ID     QI(M,L) water oil  surf  polymer Chlor  divalent   al1
al2  tr1 tr2 tr3 tr4   tr5   tr6
       15    702.    1.0      0    0.     0.    0.1811   0.00       0
0    1.  0   0   0    0.    0.
       15      0      0       0    0      0      0       0          0
0    0   0   0   0    0     0
       15      0      0       0    0      0      0       0          0
0    0   0   0   0    0     0
CC    FOR IFLAG = 3, pressure controlled injector
CC  3.7.7a ID,INJ. RATE AND INJ. COMP. FOR RATE CONS. WELLS FOR EACH
PHASE (L=1,3)
```

```
*----  ID     QI(M,L) water oil  surf  polymer Chlor  divalent   al1
al2  tr1 tr2 tr3 tr4   tr5   tr6
       16    702.    1.0      0    0.     0.    0.1811   0.00       0
0    1.  0   0   0    0.    0.
       16      0       0       0    0      0      0       0          0
0    0   0   0   0    0     0
       16      0       0       0    0      0      0       0          0
0    0   0   0   0    0     0
CC    FOR IFLAG = 3, pressure controlled injector
CC  3.7.7a ID,INJ. RATE AND INJ. COMP. FOR RATE CONS. WELLS FOR EACH
PHASE (L=1,3)
*----  ID     QI(M,L) water oil  surf  polymer Chlor  divalent   al1
al2  tr1 tr2 tr3 tr4   tr5   tr6
       17    702.    1.0      0    0.     0.    0.1811   0.00       0
0    1.  0   0   0    0.    0.
       17      0       0       0    0      0      0       0          0
0    0   0   0   0    0     0
       17      0       0       0    0      0      0       0          0
0    0   0   0   0    0     0
CC    FOR IFLAG = 3, pressure controlled injector
CC  3.7.7a ID,INJ. RATE AND INJ. COMP. FOR RATE CONS. WELLS FOR EACH
PHASE (L=1,3)
*----  ID     QI(M,L) water oil  surf  polymer Chlor  divalent   al1
al2  tr1 tr2 tr3 tr4   tr5   tr6
       18    702.    1.0      0    0.     0.    0.1811   0.00       0
0    1.  0   0   0    0.    0.
       18      0       0       0    0      0      0       0          0
0    0   0   0   0    0     0
       18      0       0       0    0      0      0       0          0
0    0   0   0   0    0     0
CC    FOR IFLAG = 3, pressure controlled injector
CC  3.7.7a ID,INJ. RATE AND INJ. COMP. FOR RATE CONS. WELLS FOR EACH
PHASE (L=1,3)
*----  ID     QI(M,L) water oil  surf  polymer Chlor  divalent   al1
al2  tr1 tr2 tr3 tr4   tr5   tr6
       19    421.    1.0      0    0.     0.    0.336   0.06       0
0    0.  0   0   0    0.    0.
       19      0       0       0    0      0      0       0          0
0    0   0   0   0    0     0
       19      0       0       0    0      0      0       0          0
0    0   0   0   0    0     0
CC    FOR IFLAG = 3, pressure controlled injector
CC  3.7.7a ID,INJ. RATE AND INJ. COMP. FOR RATE CONS. WELLS FOR EACH
PHASE (L=1,3)
*----  ID     QI(M,L) water oil  surf  polymer Chlor  divalent   al1
al2  tr1 tr2 tr3 tr4   tr5   tr6
       20     421.    1.0      0    0.     0.    0.336   0.06       0
0    0.  0   0   0    0.    0.
       20      0       0       0    0      0      0       0          0
0    0   0   0   0    0     0
       20      0       0       0    0      0      0       0          0
0    0   0   0   0    0     0
CC    FOR IFLAG = 3, pressure controlled injector
```

```
CC  3.7.7a ID,INJ. RATE AND INJ. COMP. FOR RATE CONS. WELLS FOR EACH
PHASE (L=1,3)
*----  ID     QI(M,L) water oil  surf  polymer Chlor  divalent   al1
al2  tr1 tr2 tr3 tr4   tr5   tr6
       21    281.    1.0       0    0.     0.    0.336   0.06       0
0    0.  0   0   0    0.    0.
       21      0      0       0    0      0      0       0          0
0    0   0   0   0    0     0
       21      0      0       0    0      0      0       0          0
0    0   0   0   0    0     0
CC    Convert observation well to production well after polymer drive
is complete
CC 3.7.7b ID, RATE FOR RATE CONSTRAINT WELL (IFLAG=4)
*----  ID      For IFLAG =4, specified RATE in CFD, negative for
prodcution
       22        -5.615
CC    Convert observation well to production well after polymer drive
is complete
CC 3.7.7b ID, RATE FOR RATE CONSTRAINT WELL (IFLAG=4)
*----  ID      For IFLAG =4, specified RATE in CFD, negative for
prodcution
       23        -5.615
CC    Convert observation well to production well after polymer drive
is complete
CC 3.7.7b ID, RATE FOR RATE CONSTRAINT WELL (IFLAG=4)
*----  ID      For IFLAG =4, specified RATE in CFD, negative for
prodcution
       24        -5.615
CC    Convert observation well to production well after polymer drive
is complete
CC 3.7.7b ID, RATE FOR RATE CONSTRAINT WELL (IFLAG=4)
*----  ID      For IFLAG =4, specified RATE in CFD, negative for
prodcution
       25        -5.615
CC 3.7.8 CUM. INJ. TIME , AND INTERVALS (DAY) FOR WRITING TO OUTPUT
FILES
CC          profilesPROF    prodPROF    prodHIST    maps
recovery
*---- TINJ     CUMPR1     CUMHI1          WRHPV      WRPRF         RSTC
      1401     180.        180.0           4.          60.           747.
CC*****************************************************************
************************************
CC 3.7.11 FOR IMES=2 ,THE INI. TIME STEP,CONC. TOLERANCE,MAX.,MIN.
courant numbers
*----  DT            DCLIM      CNMAX         CNMIN
       0.00001       0.001       0.03         0.003
```

References

Bird, R. B., Armstrong R. C., and Hassanger, O., Dynamics of Polymeric Liquids, Wiley, N.Y., 1987.

Bragg, J.R. et al.: "Loudon Surfactant Flood Pilot Test," paper SPE 10862 presented at 1982 SPE/DOE Enhanced Oil Recovery Symposium, Tulsa, April 4-7.

Cannella, W. J., Huh, C., and Seright, R. S., "Prediction of Xanthan Rheology in Porous Media", SPE 18089, presented at 63rd Annual Tech. Conf. SPE, Houston, TX, Oct. 2-5, 1988.

Chauveteau, G.: "Molecular Interpretation Of Several Different Properties Of Flow Of Coiled Polymer Solutions Through Porous Media In Oil Recovery Conditions," paper SPE 10060 presented in ATCE, San Antonio, Texas, USA October 1981

Delshad, M., Kim, D. H., Magbagbeola, O. A., Huh, C., Pope, G. A., and Tarahhom, F., "Mechanistic Interpretation and utilization of Viscoelastic Behavior of Polymer Solutions for Improved Polymer-Flood Efficiency", SPE 113620 presented at SPE Improved Oil Recovery Symposium, Tulsa, OK, Apr. 19-23, 2008.

Green, D.W., Willhite, G.P.: "Enhanced Oil Recovery," SPE Textbook Series Volume 6

Hirasaki, G.J., Pope, G.A.: "Analysis of Factors Influencing Mobility and Adsorption in the Flow of Polymer Solution Through Porous Media," paper SPE 4026 presented in SPE-AIME, San Antonio, Texas, Oct. 8-11, 1972.

Huh, C., and Pope, G. A., "Residual Oil Saturation from Polymer Floods: Laboratory measurements and Theoretical Interpretation", SPE 113417 presented at SPE Improved Oil Recovery Symposium, Tulsa, OK, Apr. 19-23, 2008.

Kim, D.H., Lee S., Huh C., Pope G.A.: "Development of a Viscoelastic Property Database for EOR Polymers," SPE 129971presented in SPE Improved Oil Recovery Symposium, Tulsa, Oklahoma, USA, April 2010.

Lake, L., Pope, G.A.: "Status of Micellar-Polymer Field Tests," presented in Petroleum Engineer International, November 1979

Levitt, D.B., Pope, G.A., Jouenne, S.: "Chemical Degradation of Polyacrylamide Polymers Under Alkaline Conditions", SPE 129879 presented SPE in Improved Oil Recovery Symposium, Tulsa, Oklahoma, USA, April 2010.

Magbagbeola, O. A.,: "Quantification of the Viscoelastic Behavior of High Molecular Weight Polymers used for Chemical Enhanced Oil Recovery,"MS Thesis, The University of Texas at Austin, 2008

Masuda, Y., Tang, K., Mlyazawa, M., Tanaka, S.: "1D Simulation of Polymer Flooding Including the Viscoelastic Effect of Polymer Solution," SPE 19499 presented in SPE Reservoir Engineering, May, 1992

Pope, G.A.: “The Application of Fractional Flow Theory to Enhanced Oil Recovery,” SPEJ, June 1980, 191-205.

Putz, A., Lecourtier, J. and Bruckert, L.: "Interpretation of High Recovery Obtained in a New Polymer Flood in the Chateaurenard Field" SPE 18093 presented at the 63rd SPE ATCE, Houston Texas, USA October 1988

Serigth, R.S., Seheult,M. and Talashek, T.:"Injectivity Characteristics of EOR Polymers," SPE 115142 ATCE, Denver 2008

Sorbie, Kenneth “Polymer Improved Oil Recovery,” Blackie and Son Ltd, Glasgow, 1991

Wang, D., Xia, H., Liu, Z., and Yang, Q., “Study of the Mechanism of Polymer Solution with Visco-Elastic Behavior Increasing Microscopic Oil Displacement Efficiency and the Forming of Steady ‘Oil Thread’ Flow Channel”, SPE 68723, presented at SPE Asia Pacific Oil Gas Conf., Jakarta, Indonesia, April 17-19, 2001

Wreath, D., Pope, G. A., and Sepehnoori, K., “Dependence of polymer apparent viscosity on the permeable media and flow conditions”, *In Situ*, 14(3), 263-284, 1990.

Takagi, S., Pope, G.A., Sepehrnoori, K.: "Simulation of a Successful Polymer Flood in the Chateaurenard Field"

Yuan, M.: "A Rheological Study of Polymer and Microemulsion in Porous Media", MS Thesis, University of Texas at Austin, May 1981.

Vita

Abhinav Sharma, the son of Ashwani Sharma and Neena Sharma was born in Chandigarh, India. After completing his high school studies from Apeejay School, Noida, India, he earned his Bachelor of Engineering degree in Chemical Engineering in May 2006 from Panjab University, India. Subsequently he worked as a Process Engineer in Technip KT India. In January 2008, he entered the Graduate School at the University of Texas at Austin for Petroleum Engineering.

Email Address: abhicoool1@gmail.com

This thesis was typed by the author.